

WestminsterResearch

<http://www.westminster.ac.uk/westminsterresearch>

**The Role of the RNA-binding Protein ZFP36L1 in Suppression of
Replication Stress-induced Genomic Instability**

Shaikh Solaiman, N.

This is an electronic version of a PhD thesis awarded by the University of Westminster.

© Ms Nadeen Shaikh Solaiman, 2021.

The WestminsterResearch online digital archive at the University of Westminster aims to make the research output of the University available to a wider audience. Copyright and Moral Rights remain with the authors and/or copyright owners.

The Role of the RNA-binding Protein ZFP36L1 in Suppression of Replication Stress-induced Genomic Instability

Nadeen Shaikh Solaiman



A thesis submitted in partial fulfilment of the requirements of the University of
Westminster for the degree of Doctor of Philosophy

June 2021

Genome Engineering Laboratory
Department of Life Sciences
University of Westminster

Abstract

Replication stress, a hallmark of pre-cancerous and cancerous lesions, is characterised by the slowing or stalling in replication fork progression and the consequent failure to preserve genomic stability. ZFP36L1, a member of the ZFP36 family of CCCH tandem zinc finger (ZF) proteins, is an RNA-binding protein that plays a crucial role in the post-transcriptional regulation of gene expression underlying physiological processes and pathological diseases. Recent evidence has revealed that *ZFP36L1*, is significantly mutated or downregulated in certain human cancers, and exhibits tumour-suppressive properties across various cancer cell types. However, the precise molecular link between ZFP36L1 and cancer, particularly from the angle of genomic stability, remains poorly elucidated. Here, we report a novel role for ZFP36L1, characterised in human U2OS and U2OS H2B-GFP osteosarcoma cells, in suppressing replication stress-induced genomic instability. We found that, CRISPR/Cas9-mediated knockout of ZFP36L1 resulted in increased chromosome segregation defects including anaphase bridges, chromosome laggards and micronuclei formation, even in the absence of exogenous replication stress. Moreover, ZFP36L1-deficient cells exhibited an elevated accumulation of γ H2AX, 53BP1 nuclear bodies (NBs) and RPA, which indicated an active role for ZFP36L1 in limiting replication stress-induced DNA damage. Furthermore, we demonstrated an unanticipated function for ZFP36L1 in potentially suppressing the expression of common fragile sites (CFSs) in response to replication stress, reflected by the increased mitotic CFS-characteristic chromosomal aberrations and MiDAS events at CFS loci observed in cells deficient in ZFP36L1. Finally, we also showed that a CRISPR/Cas9-mediated truncation in ZFP36L1, carrying a compromised lead-in

sequence to its first ZF-domain, resulted in increased replication stress-associated phenotypes, similar to that of a ZFP36L1-knockout. Taken together, our data reveal, for the first time, a role for ZFP36L1 in contributing to the protection of genomic integrity against replication stress.

Table of Contents

Abstract	II
Table of Contents	IV
List of Figures	IX
List of Tables	XII
Acknowledgments	XIII
Declaration	XV
1 Introduction	1
1.1 RNA-binding Proteins	2
1.2 RBPs in Controlling Key Physiological Processes	5
1.3 The ZFP36 Family of RBPs	7
1.3.1 Identification of Human ZFP36 Family Members.....	7
1.3.2 Structure of the ZFP36 Family Members	11
1.3.3 The ZFP36 Family in Post-transcriptional Gene Regulation.....	14
1.3.4 Post-translational Regulation of ZFP36 Proteins Via Phosphorylation	17
1.3.5 Subcellular Localisation of the ZFP36 Family Members.....	20
1.3.6 Physiological Roles and mRNA Targets	25
1.3.7 The ZFP36 Family in Inflammatory Disease.....	28
1.3.8 The Role of ZFP36 Family Members in Cancer.....	30
1.4 Replication stress-induced Genomic Instability	39
1.4.1 DNA Replication and Associated Inhibitors	41
1.4.2 The Replication Stress Response.....	45
1.4.3 The DNA Damage Response	47
1.4.4 The Pathways of DSB repair.....	51
1.5 RBPs in the Maintenance of Genomic Stability	57

1.5.1	RBP Regulation of DDR-related mRNA Targets.....	57
1.5.2	Direct Roles of RBPs in the DDR.....	59
1.5.3	Post-translational Modification of RBPs in Response to DNA Damage.....	61
1.5.4	The Functional Roles of RBPs in R-loop Stability.....	64
1.6	The Emerging Role of the ZFP36 Family of RBPs in the Maintenance of Genomic Stability.....	68
1.7	Study Aims.....	70
2	Materials and Methods.....	71
2.1	CRISPR gRNA Cloning into pSpCas9(BB)-2A-Puro (PX459) Plasmid.....	71
2.1.1	Target Selection for gRNA Design.....	71
2.1.2	gRNA design and oligo annealing.....	71
2.1.3	Restriction digestion of pSpCas9(BB)-2A-Puro (PX459) plasmid.....	72
2.1.4	Cloning gRNAs into pSpCas9(BB)-2A-Puro (PX459) plasmid vector.....	73
2.1.5	PCR screen for bacterial colonies harbouring sgRNA-pSpCas9(BB).....	74
2.1.6	Sequence validation of pSpCas9(BB)-sgRNAs constructs.....	75
2.1.7	gRNA-containing pSpCas9(BB) plasmid amplification by Midiprep.....	76
2.2	Cell Line Manipulation and Generation.....	76
2.2.1	Cell lines and culture conditions.....	76
2.2.2	Delivery of gRNA-expressed pSp(Cas9) plasmid into U2OS cell lines.....	77
2.2.3	Puromycin selection of transfected cell lines.....	78
2.2.4	Clonal isolation and expansion.....	78
2.3	Screening and Validation of ZFP36L1-targeted Monoclones.....	80
2.3.1	Genomic DNA isolation.....	80
2.3.2	PCR genotyping screens of ZFP36L1-targeted monoclones.....	81
2.3.3	Immunoblotting.....	82
2.3.4	Sequence analysis of ZFP36L1 monoclonal lines.....	83
2.4	Functional Characterisation of ZFP36L1-edited Cell lines.....	84

2.4.1	Growth curve analysis.....	84
2.4.2	Immunofluorescence.....	84
2.4.3	Micronucleus formation assay	85
2.4.4	Analysis of chromosome segregation	86
2.4.5	Metaphase spreads preparation	86
2.4.6	5-ethynyl-2'-deoxyuridine (EdU) labelling in mitotic cells.....	87
2.5	Statistical Analysis	88
3	CRISPR/Cas9-mediated Generation of ZFP36L1-knockout and ZFP36L1-mutant Cell lines.....	89
3.1	Introduction	89
3.2	Cloning of gRNA oligos into pSpCas9(BB)-2A-Puro Plasmid	93
3.3	Validation of gRNA oligo expression in pSpCas9(BB) Plasmid	96
3.4	Cell line Manipulation and Generation	99
3.5	Screening for On-target Mutations/Indels	101
3.6	CRISPR/Cas9-mediated deletion of ZFP36L1 in U2OS Cells Compromises Cell Growth	109
3.7	Discussion.....	111
4	Loss of ZFP36L1 Leads to Replication Stress-induced Chromosomal Instability.....	115
4.1	Introduction	115
4.2	ZFP36L1 Facilitates Faithful Chromosome Segregation	118
4.3	Mitotic Defects in ZFP36L1-deficient Cells are Mediated by the Formation of UFBs.....	122
4.4	Loss of ZFP36L1 Increases Micronuclei Formation.....	124
4.5	Discussion.....	126

5	ZFP36L1 Suppresses Replication Stress-induced DNA	
	Damage.....	129
5.1	Introduction	129
5.2	ZFP36L1 Limits Replication Stress-induced DSB Formation	132
5.3	Loss of ZFP36L1 Increases Micronuclei Positive for γ H2AX.....	134
5.4	Deletion of ZFP36L1 Induces DSBs Sequestered into 53BP1 NBs	136
5.5	ZFP36L1 Deficiency Triggers the Recruitment of RPA During G1-phase and S/G2-phase.....	138
5.6	Discussion.....	141
6	Loss of ZFP36L1 Promotes the Expression of CFSs.....	143
6.1	Introduction	143
6.2	Loss of ZFP36L1 Leads to Increased Chromosomal Fragility	145
6.3	ZFP36L1 Suppresses MiDAS at CFSs during Early Mitosis.....	147
6.4	Discussion.....	149
7	General Discussion.....	152
8	Conclusions.....	166
	Appendices.....	168
	Appendix A- related to section 1.3.4.....	168
	Appendix B- pSpCas9(BB)-2A-Puro (PX459) plasmid-related to Chapter 3.	169
	Appendix C- related to Figure 3.8 and Figure 3.10.	170
	Appendix D- related to Figure 4.1 (D.1), 4.2 (D.2) and 4.3 (D.3)	172
	Appendix E- related to Figure 4.4.....	173
	Appendix F- related to Figure 5.1 (F.1) and 5.2 (F.2)	174
	Appendix G- related to Figure 5.3.....	175
	Appendix H- related to Figure 5.4.....	177
	Appendix I- related to Figure 6.2.....	179

Glossary.....	180
Bibliography.....	184

List of Figures

Figure 1.1. Modular Structure of RNA-binding Proteins (RBPs).....	4
Figure 1.2. Expression levels of mRNA transcripts of members of the ZFP36 family of RBPs extracted from normal human tissues.....	10
Figure 1.3. Schematic representation of the zinc finger domains of members of the ZFP36 family.	12
Figure 1.4. Structural similarities in the zinc finger binding domains of the ZFP36 family.	14
Figure 1.5. Schematic on the mechanism of post-transcriptional ARE-mRNA decay mediated by the ZFP36 family.....	17
Figure 1.6. Phosphorylation of ZFP36 family members impairs mRNA degradation through the inhibition of deadenylase recruitment.....	20
Figure 1.7. The ZFP36 family exhibit nuclear-cytoplasmic shuttling properties.	24
Figure 1.8. Schematic illustration of various cancer-related targeted mRNA transcripts regulated by the ZFP36 family.....	38
Figure 1.9. Schematic overview of the first steps of DNA replication initiation.....	44
Figure 1.10. Schematic of the basic framework of the DDR signalling pathway.	48
Figure 1.11. The replication stress-induced DNA damage response (DDR).....	50
Figure 1.12. Classical Non-homologous end join binding (C-NHEJ) of DSB repair.	54
Figure 1.13. DSB repair by Homologous Recombination (HR)	56
Figure 1.14. Post-translational modification of RBPs in response to DNA Damage.....	63
Figure 1.15. RBPs contribute to the prevention of R-loop structure formation.....	67
Figure 2.1. Experimental workflow of CRISPR-mediated genome-editing in U2OS cells.	79

Figure 3.1. Schematic of the mechanism underlying the Type II <i>Streptococcus pyogenes</i> -derived CRISPR/Cas9 system.....	92
Figure 3.2. Architecture of <i>ZFP36L1</i> gene and gRNA targeted genomic sequences.	94
Figure 3.3. Schematic for gRNA design and scarless cloning into pSpCas9(BB)....	95
Figure 3.4. Gel electrophoresis of colony PCR screen of gRNA oligos ligated in pSpCas9(BB)-2A-Puro plasmid.....	96
Figure 3.5. Sequence validation of sgRNA-expressed pSpCas9(BB)-2A-Puro plasmid.	98
Figure 3.6. Experimental workflow of CRISPR-mediated gene-editing of <i>ZFP36L1</i> in U2OS and U2OS H2B-GFP cells.	100
Figure 3.7. Genomic PCR products of <i>ZFP36L1</i> -targeted region in U2OS cells....	101
Figure 3.8. DNA sequence analysis of CRISPR/Cas9-mediated <i>ZFP36L1</i> mutants in U2OS cells.	103
Figure 3.9. Predicted amino acid translation of open reading frames identified in <i>ZFP36L1</i> -mutants in U2OS cells.....	105
Figure 3.10. Western blot analysis of <i>ZFP36L1</i> from whole-cell extracts of U2OS cells.	107
Figure 3.11. Characterisation of CRISPR/Cas9-mediated <i>ZFP36L1</i> knockout in U2OS H2B-GFP cells.....	108
Figure 3.12. Loss of <i>ZFP36L1</i> results in a slower growth rate in U2OS cells.....	110
Figure 4.1. Loss of <i>ZFP36L1</i> results in increased chromosome laggard formation.	119
Figure 4.2. Loss of <i>ZFP36L1</i> induces the formation of DNA bulky bridges.....	121
Figure 4.3. Loss of <i>ZFP36L1</i> induces PICH-positive UFB formation.....	123

Figure 4.4. Loss of ZFP36L1 induces micronuclei formation in U2OS cells.....	125
Figure 5.1. Deletion of ZFP36L1 induces DSBs in the form of γ H2AX.	133
Figure 5.2. ZFP36L1 deficiency induces micronuclei positive for γ H2AX.....	135
Figure 5.3. Loss of ZFP36L1 induces the accumulation of 53BP1 nuclear bodies (NBs).	137
Figure 5.4. RPA is recruited to G1 and S/G2 in response to ZFP36L1 deletion....	139
Figure 6.1. Deletion of ZFP36L1 triggers chromosome fragility.....	146
Figure 6.2. ZFP36L1 suppresses replication stress-induced CFS expression.....	148
Figure 7.1. Comprehensive model depicting replication stress-related phenotypic consequences associated with ZFP36L1 deficiency in human osteosarcoma cells.....	154

List of Tables

Table 1. The ZFP36 family of RBPs.....	8
Table 2. Examples of reported cancer hallmark-related mRNA targets of the ZFP36 family.....	31
Table 3. Selected gRNA sequences.....	71
Table 4. Modified gRNA oligos... ..	72
Table 5. Primer sequences used for colony PCR screens	75
Table 6. Primer sequences used for screening ZFP36L1 clones.....	81
Table 7. Primary and secondary antibodies used for immunoblots.....	83
Table 8. Primary and secondary antibodies used for immunofluorescence.....	85

Acknowledgments

Firstly, praises and thanks to God, Al Mighty, whose infinite blessings and love has granted me solace and strength throughout my PhD journey and the opportunity to complete this thesis.

I would like to express my deep and sincere gratitude to my PhD research supervisors, Dr John Murphy and Dr Kalpana Surendranath, for their invaluable guidance, support, patience and immense knowledge. I whole-heartedly appreciate Dr John Murphy for his constant encouragement and enthusiasm, and Dr Kalpana Surendranath for going above and beyond for the completion of this work and for being a constant source of inspiration. My genuine appreciation to Dr Kalpana Surendranath for all the unforgettable measures she has taken for me to reach this stage. I would like to extend my heartfelt thanks to our collaborator, Dr Kanagaraj Radhakrishnan at the Francis Crick Institute, whose unparalleled knowledge and support was a milestone for the completion of this project. Without this collective contribution and unwavering involvement in every step of this project, this thesis would not have been materialised.

I would like to gratefully acknowledge Dr Emanuela Volpi, for her encouragement and valuable assistance in microscopy. Special regards to the technical staff at the University of Westminster who have always done their best to assist me during my studies. I am also extremely grateful to my PhD colleagues, Ahmed Sidali and Varsha Teotia, for their unsurpassed friendship, discussions and fun! A special thank you to Ahmed Sidali for his boundless emotional support, insightful input and contribution. It has been a great pleasure and I am forever grateful. Thank you to Dr Amy Maclatchy and Dr Moonisah Usman for their consistent kind words of encouragement.

Most of all, I am completely indebted to my beloved parents, Mahmoud and Eman, for their unconditional love, support, and sacrifices. Without them, I would have never arrived to where I am today. To my sisters & brother, thank you for your consistent love, kindness and support.

Last but not least, my sincere love and thanks to my best friends, Rabab, Farida, Nawar, all of my soul sisters and of course my London family, Fabio, Axana, Meriam and Shehrazad, for their endless emotional support and understanding. Lots of love to all of you.

Declaration

I hereby declare that all the material presented in this thesis is my own work, except where indicated otherwise, and that it has not been previously submitted, in whole or part, for any other degree or qualification at this or any other University.

Signature:

Nadeen Shaikh Solaiman

Date:

28th February 2021

1 Introduction

The central dogma of molecular biology describes the basic framework by which genetic information is converted from DNA to RNA (mRNA), and from RNA into a functional protein, which ultimately dictates the function of living cells (Crick, 1970). This biological process, denoted as gene expression, is tightly regulated at every stage by a diverse range of cellular pathways and regulatory proteins that control the nature and amount of proteins expressed. RNA-binding proteins (RBPs) comprise a large class of more than 1,500 proteins that potently and ubiquitously control all aspects of mRNA biology, and are critical effectors of gene expression (reviewed in, Corley, Burns and Yeo, 2020). RBPs play crucial roles in regulating RNAs at the post-transcriptional level, by binding to mRNA transcripts using their characteristic RNA binding domains (Gerstberger, Hafner and Tuschl, 2014). The ZFP36 family is one class of RBPs that tightly regulates mRNA stability as part of their post-transcriptional control function (Blackshear, 2002; Murphy, Baou and Jewell, 2009). The functional role of the ZFP36 family members has been widely implicated in a numerous range of physiological and pathological processes. Recently, various RBPs including, members of the ZFP36 family, have emerged as key players in the preservation of genomic integrity. Failure of these pathways contributes to the development of genomic instability, a hallmark of cancer (Hanahan and Weinberg, 2011).

1.1 RNA-binding Proteins

Gene regulation control by transcriptional and post-transcriptional mechanisms is crucial to sustaining RNA processing at multiple levels including maturation, stability, transport, cellular localisation and translation efficiency. At a molecular level, these processes are mediated by the formation of large multimeric ribonucleoprotein (RNP) complexes coalesced by RNA-binding proteins (RBPs) (Gerstberger, Hafner and Tuschl, 2014). The dynamic formation of these mRNA-coated RBPs structures determines all aspects of RNA fate by regulating transcription, splicing, 5' capping, polyadenylation, decay and in turn, protein turnover (Müller-Mcnicoll and Neugebauer, 2013). Developments in cell biological research complemented by high-throughput genome-wide studies have uncovered diverse binding ranges of RBPs and revealed that RBPs could also act as scaffold proteins that recruit additional proteins to modify RNP composition in accordance with nascent mRNAs stage and locale (Keene, 2007; Änkö and Neugebauer, 2012; Ascano et al., 2012). By associating with different complexes, RBPs can therefore critically modulate gene expression in a spatial and temporal-based manner throughout the life-cycle of mRNA transcripts.

It is estimated that out of the 20,000 mammalian protein-coding genes, over 1,500 (7.5% of the proteome) have been curated as RBPs that encompass canonical RNA-binding domains (RBDs) or characteristic domains with RNA-related functions (Gerstberger, Hafner and Tuschl, 2014). RBPs have been categorised into different families based on their evolutionarily conserved RNA-binding motifs that enable them to bind to RNAs in a sequence or structure-specific manner (Ray et al., 2009, 2013). A limited set of well-defined structural motifs have been reported to orchestrate this interaction and accommodate large structural diversity, allowing broader interactions

of these proteins. Among them are included, the RNA recognition motif (RRM), double-stranded RNA binding motif (dsRBM), K-homology (KH) domain, cold-shock domain (CSD), DEAD-box helicase motif, RGG (Arg-Gly-Gly) box and Zinc Finger (ZF) domain ([Figure 1.1](#)) (Lunde, Moore and Varani, 2007). Through the use of these RNA-binding motifs, RBPs can interact with target mRNAs at 5' and 3' untranslated regions (UTRs) as well as coding and non-coding regions (Lunde, Moore and Varani, 2007). Furthermore, RBPs can embody combinations of multiple RBDs, conferring additional expansion and flexibility for mRNA interaction and specificity (Corcoran et al., 2011). In addition, RBDs from multiple proteins can cooperate through weak protein-protein interactions and define their RNA specificity (Glisovic et al., 2008). Interestingly, several candidate RBPs, particularly with zinc finger binding domains, have been shown to recognise both RNA and DNA through similar residues, but with different structural interactions formed on the nucleic acid template (Lu, Searles and Klug, 2003). These observations suggested that in addition to mRNA binding, RBPs can, in certain circumstances, also exert DNA-binding activities, further emphasising their versatile nature.

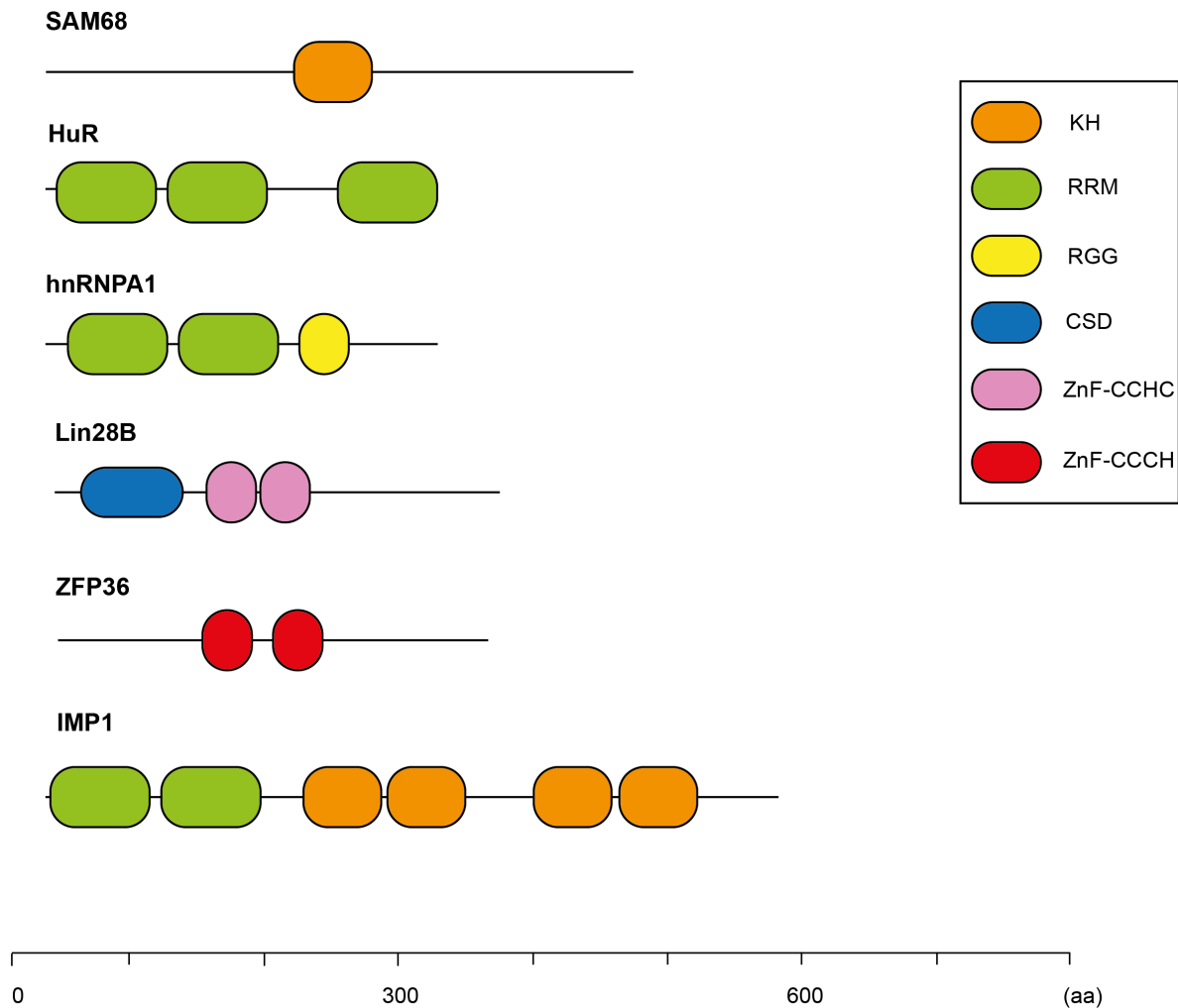


Figure 1.1. Modular structure of RNA-binding proteins (RBPs).

Representative examples of some of the most common RNA-binding domains (RBDs) present in various RBPs. RBDs mediate the interaction between RBPs and RNAs in a sequence-specific manner. The combination of different RBDs in a single RBP confers further expansion and flexibility for RBP-mRNA association and promotes a myriad of various regulatory events. Different domains are schematically illustrated in coloured boxes and include: KH (K-Homology) domain, orange; RNA-recognition motif (RRM, the most common RBD), green; RGG (Arginine-glycine-glycine) motif, yellow; CSD (Cold-Shock-Domain), blue; Zinc Finger (ZF) domain of the CCHC type, pink; ZF of the CCCH type, red. Different RBPs conferring various RBDs are represented according to their aa (amino acid) length. Adapted from Pereira, Billaud and Almeida (2017).

1.2 RBPs in Controlling Key Physiological Processes

Due to their abundance and diverse interactions, RBPs can exert a multitude of functional roles in the control of gene expression and other physiological processes. Thus, appropriate function of RBPs is vital for the coordination of these intricate dynamic complexes, and perturbation in their regulation has been implicated in a wide range of diseases and disorders (Gerstberger, Hafner and Tuschl, 2014). Due to their high expression in the brain, altered levels of RBPs that impact RNA metabolism in motor neurons have been frequently demonstrated to result in neurodegenerative and neuromuscular diseases (Lukong et al., 2008; Cooper, Wan and Dreyfuss, 2009). For example, mutations in heterogeneous nuclear RNPs (hnRNPs; hnRNPA2 and hnRNPA1) have been implicated in the degenerative disease amyotrophic lateral sclerosis (ALS) (Kim et al., 2013). Aberration in the splicing pattern of snRNP assembly factor survival motor neuron 1 (SMN1) was shown to be directly linked to muscular diseases such as myotonic dystrophy (Cooper, Wan and Dreyfuss, 2009). Additionally, modifications in splicing patterns have been revealed to disrupt cardiomyocyte function. For example, suppressed levels of several splicing factors such as SRSF4 and SRSF5 were found to be correlated with high levels of ejection fraction (EF), the volumetric fraction of blood ejected from the heart chambers in each contraction, which could precede heart dysfunction (De Bruin et al., 2017). Moreover, the importance of RBPs in immune cell development and function has also been well-described (reviewed in, Turner and Hodson, 2012; Newman, McHugh and Turner, 2016; Díaz-Muñoz and Turner, 2018). To name a few, the RBP ELVAL1 (also known as HuR) facilitates B-cell antibody response and T-cell development in the bone marrow and thymus, respectively (Papadaki et al., 2009; Diaz-Muñoz et al., 2015). Loss of function in selected members of the hnRNP and SRSF RBP family was

revealed to be associated with significant deficiencies in haematopoiesis and myelodysplastic syndromes (Komeno et al., 2015; Fang et al., 2017). Furthermore, RBPs have also been shown to majorly contribute to pleiotropic functions (Van Nostrand et al., 2017) as well as autoimmune and inflammatory-related diseases (reviewed in, Newman, McHugh and Turner, 2016). Lastly, but importantly, RBPs are currently emerging as fundamental players in the development and progression of tumourigenesis (reviewed in, Pereira, Billaud and Almeida, 2017). Indeed, aberrant expression of several RBPs has been widely detected in a variety of cancers including breast, prostate and colorectal cancer (Kechavarzi and Janga, 2014). Since their function is associated with a plethora of mRNA targets and various biological processes, RBPs can therefore impact all aspects of cancer development and progression including, but not limited to, sustained cell growth and proliferation, evasion of apoptosis, stimulating invasion and metastasis and evading immune surveillance (reviewed in, Pereira, Billaud and Almeida, 2017).

The abundance of RBPs and their scaffolding ability to form a vast intricate network of interactions between targeted mRNAs and proteins provide them with an exquisite capacity to mediate a myriad of biological processes. This incredible functional repertoire reflects the significance of furthering our understanding of the global regulatory network governed by RBPs. Despite the increasing data collected on RBPs, many questions, particularly concerning their molecular roles in human disease, remain to be answered.

1.3 The ZFP36 Family of RBPs

The 12-O-tetradecanoylphorbol-13-acetate (TPA) inducible sequence 11 (TIS11) family of proteins consist of four RBPs which tightly regulate mRNA stability as part of their post-transcriptional control function (reviewed in, Murphy, Baou and Jewell, 2009). These include ZFP36 (TIS11, TTP, Nup475, GOS24), ZFP36L1 (Tis11b, Berg36, ERF-1, BRF-1), and ZFP36L2 (Tis11d, ERF-2, BRF-2) (Table 1) (reviewed in, Blackshear, 2002; Murphy, Baou and Jewell, 2009). A fourth family member, ZFP36L3, has been identified in mouse placenta and yolk sac but not in human placenta or other human tissues (Blackshear et al., 2005). ZFP36 homologues have also been described in drosophila and yeast (Ma et al., 1994; Ma and Herschman, 1995). The ZFP36 family of proteins display a high level of conservation across species with direct orthologues reported in all vertebrates with the single exception of birds, which appeared to lack a sequence that corresponded to ZFP36 (Lai et al., 2013; Blackshear and Perera, 2014).

1.3.1 Identification of Human ZFP36 Family Members

Located on chromosome 19q13.1, the prototype Tristetrapolin (TTP) encoded by the ZFP36 (zinc finger protein 36) gene in humans was originally described as an immediate early-response gene induced by tumour-promoting phorbol esters (TPA) and by growth factors; insulin and serum, in fibroblasts and other cell types (DuBois et al., 1990; Lai, Stumpo and Blackshear, 1990; Ma and Herschman, 1991). Its function remained ambiguous until a study on a ZFP36 knockout (KO) mouse model was conducted (Carballo et al., 1996). ZFP36-deficient mice were found to exhibit severe inflammatory syndromes characterised by myeloid hyperplasia, erosive arthritis and autoimmunity, caused by excess tumour necrosis factor (TNF) (Carballo et al., 1996). Further ZFP36-KO mice-based studies subsequently showed ZFP36

deficiency to be associated with increased levels of macrophage-derived TNF mRNA and protein in response to lipopolysaccharide treatment (Carballo et al., 1997). Elevated TNF mRNA and protein levels were later found to result as a consequence of increased TNF mRNA stability, and ZFP36 was revealed to directly bind to TNF mRNA and promote mRNA destabilisation (Carballo, Lai and Blackshear, 1998).

The second member of the human ZFP36 family, zinc finger protein 36-like 1 (ZFP36L1) is located on chromosome 14q24.1 (Pospisilova et al., 2007). ZFP36L1 was initially isolated from chronic lymphocytic leukaemia (CLL) B cells that were stimulated by TPA to undergo plasmacytoid differentiation, from human cDNA libraries, and was described to function as an early-response gene to stimulated B cells (Murphy and Norton, 1990; Bustin et al., 1994; Ning et al., 1996). As for the third member, human zinc finger protein 36-like 2 (ZFP36L2) is positioned on chromosome 2 p22.3-p21. ZFP36L2 was first identified in murine cells also as an early-response gene and was later isolated from cDNA libraries probed with the mouse ZFP36L2 mRNA (Varnum et al., 1991; Nie et al., 1995; Maclean, McKay and Bustin, 1998).

Table 1. The ZFP36 family of RBPs.

Gene	Other Names	Chr. Location	Size (kDa)
ZFP36	TIS11, TTP, Nup475, GOS24	19q13.1	34
ZFP36L1	Tis11b, Berg36, ERF-1, BRF-1	14q24.1	36.3
ZFP36L2	Tis11d, ERF-2, BRF-2	2p22.3-p21	51

Sequence analysis of each of the ZFP36 members displays minimal variation between human individuals, with the majority of polymorphisms identified in the promoter, intron and 3' untranslated regions (UTR) (Blackshear et al., 2003). Initial work had detected thirteen polymorphisms in the protein-coding regions of all members of the ZFP36 genes, and six of these led to amino acid changes (Blackshear et al., 2003). A single nucleotide polymorphism (SNP) in ZFP36L1 was found to generate a dinucleotide substitution that prevented complete splicing within the protein-coding region of ZFP36L1 (Blackshear et al., 2003). Although this had resulted in a 50% decrease in ZFP36L1 mRNA expression in lymphoblasts, most of these gene variants' functional implications are not yet known (Blackshear et al., 2003). Further studies identified additional polymorphisms in the protein-coding domain of ZFP36, whereby a single SNP (C to T modification), was found to be associated with rheumatoid arthritis in African-Americans (Carrick et al., 2006). Another gene polymorphism (A>G; ZFP36*2) detected in ZFP36, was shown to be significantly associated with poor prognosis of breast cancer in Caucasian patients (Upadhyay et al., 2013). Further, a C/T SNP in ZFP36L1 was also linked to multiple sclerosis (Gourraud et al., 2012).

Human ZFP36, ZFP36L1 and ZFP36L2 are all widely expressed across normal tissue types. Comparative analysis of quantitated endogenous mRNA levels of the human ZFP36 family members showed all three members to be differentially expressed in a variety of human tissues ([Figure 1.2](#)) (Carrick and Blackshear, 2007). ZFP36 (TTP) and its variants were reported to be expressed at low levels in testicles, stomach, liver and spleen, with higher levels detected in ovary, bladder, lung and cervical tissues (Carrick and Blackshear, 2007). Further, mRNA levels were also found to vary in expression between the three individual members in specific tissue types. For

example, ZFP36 transcript was expressed in lower levels in the thymus compared to the higher levels expressed by ZFP36L1 and ZFP36L2 mRNA transcripts. The highest level of ZFP36 transcript was found in cervical tissue, while ZFP36L1 and ZFP36L2 transcripts exhibited the highest levels in the lung and thymus, respectively (Carrick and Blackshear, 2007). Interestingly, immunoblot analysis from our laboratory has also showed differential expression of ZFP36L1 protein across human cancer cell lines. Indeed, we observed ZFP36L1 protein to be least expressed in cervical cancer cells (HeLa) compared to its moderate and high expression in breast (MCF-7) and osteosarcoma (U2OS) human cancer cell lines, respectively (conducted by Dr Kalpana Surendranath (2016), University of Westminster; unpublished data).

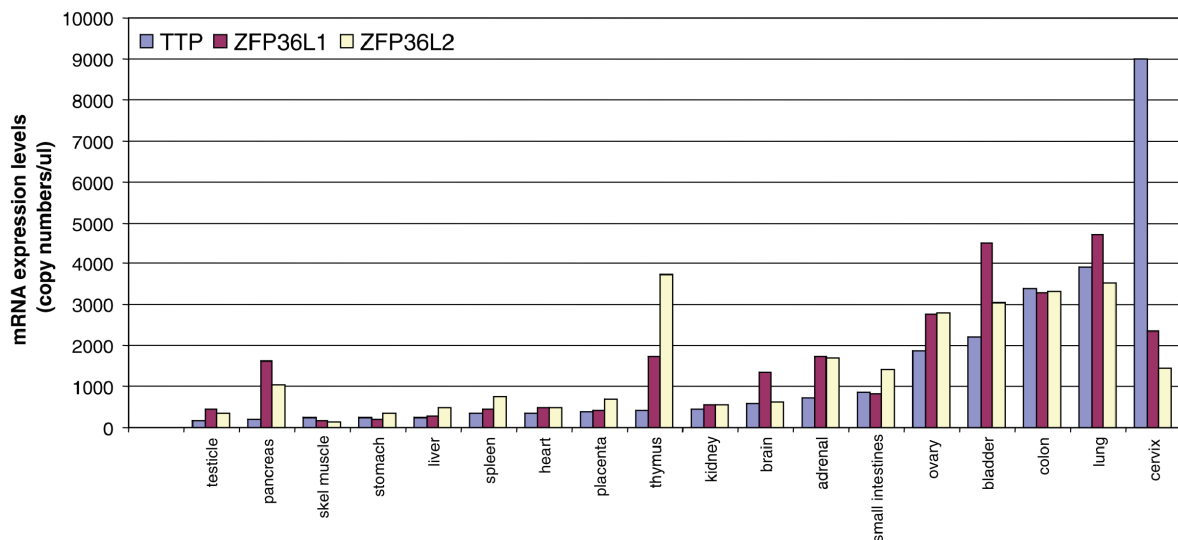


Figure 1.2. Expression levels of mRNA transcripts of members of the ZFP36 family of RBPs extracted from normal human tissues.

Level of mRNA transcripts was measured using Real-time PCR of cDNAs from the indicated human tissues samples. Expression of mRNA transcripts varies amongst individual members of the ZFP36 family of RBPs, and is presented in ascending order. Figure is adapted from Carrick and Blackshear (2007). TTP: ZFP36.

1.3.2 Structure of the ZFP36 Family Members

A defining characteristic shared between members of the ZFP36 family proteins is the presence of two putative tandem zinc finger (ZF) domains, consisting of a 64-amino acid sequence, which has been established as the structural motif that mediates direct binding to mRNA transcripts ([Figure 1.3](#)) (Lai, Kennington and Blackshear, 2002; Blackshear et al., 2003; Brewer et al., 2004). All three members of the ZFP36 family contain two highly-conserved tandemly repeated ZF domains of the CCCH class, characterised by strict internal spacing between the cysteines and histidines in the zinc-binding residues (CX8CX5CX3H; X represents variable amino acid) that are preceded by a (R/K) YKTEL motif and connected by an 18- amino acid residue linker ([Figure 1.4](#)) (Lai et al., 2000). The binding of ZFP36 proteins to their target mRNA transcripts stringently relies on the integrity of the CCCH residues of the two ZF domains, which correspond to the critical function of these RBPs (Lai et al., 2000). In this regard, a single-point mutation of any of the eight cysteines or histidines responsible for coordinating the zinc ions in either of the two ZFDs completely abrogates RNA binding (Lai et al., 2000). This was initially described in ZFP36, where a single mutation (cysteine to arginine) in any of the ZFDs completely attenuated ZFP36 binding to the mRNA transcript of tumour necrosis-alpha (TNF- α), a major target of ZFP36 (Lai et al., 1999). More recent studies reported similar effects in ZFP36L1 and ZFP36L2 in which mutations in the ZF domains appeared to negatively affect the proteins destabilising activity on its mRNA targets (Iwanaga et al., 2011; Suk et al., 2018).

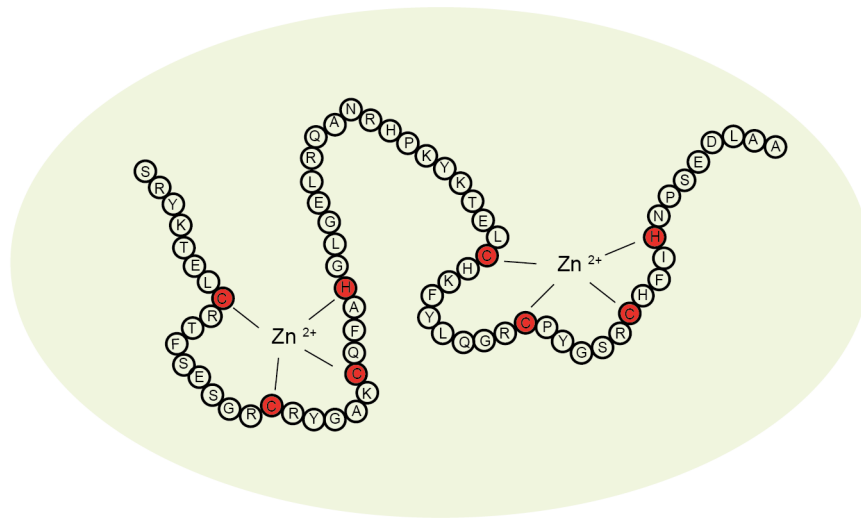
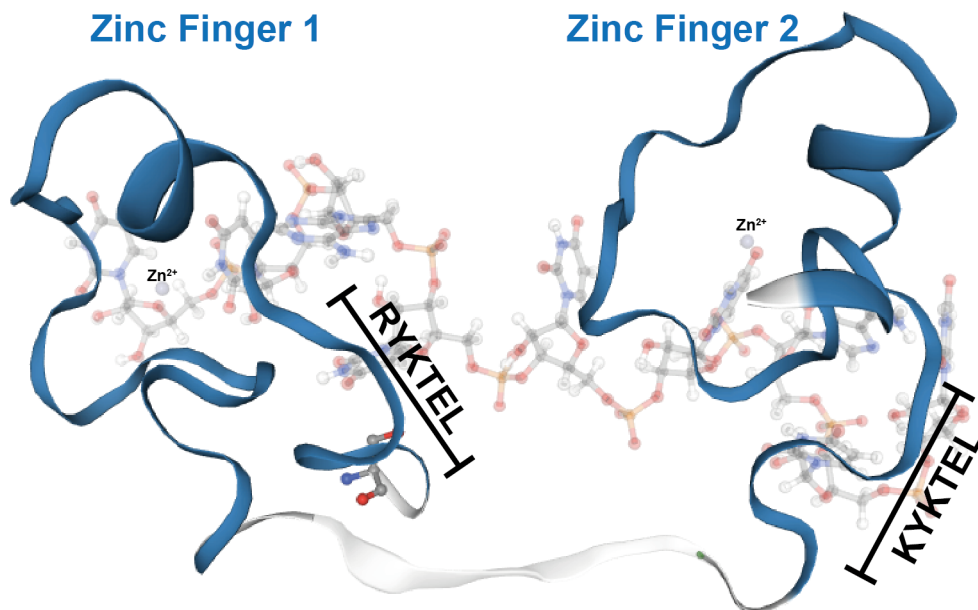
A**B**

Figure 1.3. Schematic representation of the zinc finger domains of members of the ZFP36 family.

All three members of the ZFP36 family of RBPs contain two putative zinc finger domains that mediate ZFP36 family-binding to mRNA transcripts. **(A)** The ZF domains of the CCCH class, consists of 64 amino acids with cysteines and histidines residues (red) contributing to the coordination of the Zn^{2+} ions in each ZF. Schematic adapted from Brewer et al. (2004). **(B)** 3D amino acid structure of ZFP36L1 showing the highly conserved ZFD 1 and 2 (blue) with its lead-in RYKTEL and KYKTEL sequences indicated. Adapted from Swiss Model Repository; A0A024R658.

The ZF-binding domains shared amongst these proteins share a high sequence identity; ZFP36L1 and ZFP36L2 ZF domains are 91% identical, while ZFP36L1 ZF domain is 71% identical to that of ZFP36 ([Figure 1.4](#)) (Morgan, Deveau and Massi, 2015). Thus, the structures within the motifs are preserved between the ZFP36 family members and the surface residues involved in interactions with other molecules contribute to individual variability. In addition to the shared tandem ZF binding-domains, ZFP36 proteins also have other characteristics in common; leucine-rich nuclear export sequences, which allow shuttling of the proteins out of the nucleus; subject to post-translational modification via high levels of phosphorylation; and similar mechanisms in their post-transcriptional control of target mRNA stability (Carrick and Blackshear, 2007). Although these proteins encompass key differences in their cell and tissue-specific regulated expression pattern or interactions with different proteins, ZFP36 and its two related proteins may sometimes overlap in their functions due to these similarities (Carrick and Blackshear, 2007).

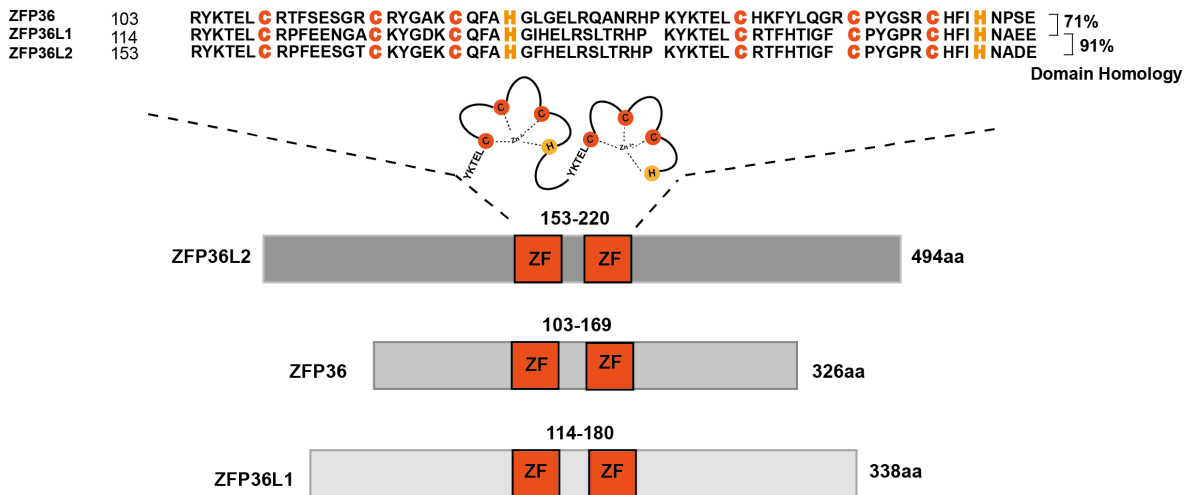


Figure 1.4. Structural similarities in the zinc finger binding domains of the ZFP36 family.

Amino acid sequence of the highly-conserved tandem ZF domains of the CCCH-class of each of the ZFP36 family members. The ZF domains are characterised by highly strict internal spacing between the cysteines and histidines in the zinc binding residues, that are preceded by a (R/K) YKTEL motif and connected by an 18- amino acid residue linker. The ZFP36 ZF domain shares a 71% sequence identity with that of ZFP36L1, while ZFP36L1 ZF domain sequence is 91% identical to that of ZFP36L2. Schematic adapted from Ciais, Cherradi and Feige (2013).

1.3.3 The ZFP36 Family in Post-transcriptional Gene Regulation

Post-transcriptional control of mRNA stability is vital for the regulation of gene expression and protein turnover. Using their ZF structural motifs, the ZFP36 family of RBPs bind to *cis*-acting Adenine-Uridine rich elements (ARE) in the 3' untranslated regions (UTR) of sets of mRNAs and subsequently mediate mRNA decay (reviewed in, Murphy, Baou and Jewell, 2009; Baou, Norton and Murphy, 2011). This preference of ARE-binding was first described from work that showed the prototype ZFP36 to prevent TNF- α production from macrophages via mRNA degradation by direct binding to the ARE region in TNF- α transcript (Carballo, Lai and Blackshear, 1998). Later studies found that the optimal nonameric consensus sequence required for mRNA binding by the ZFs is; UUAUUUAUU, though a few variations of this RNA sequence

can also allow strong affinity binding (Worthington et al., 2002; Blackshear et al., 2003; Brewer et al., 2004; Lai, Carrick and Blackshear, 2005).

The significance of these ARE regions in the 3' UTR of certain mRNAs is apparent in their prevalence, which is currently estimated to occur in up to 10% of the human transcriptome (Bakheet, Williams and Khabar, 2006). Following their interaction with AREs, ZFP36 proteins mediate their effect on mRNA degradation first by promoting mRNA deadenylation (poly-A shortening) through the recruitment of mRNA decay enzyme complexes (reviewed in, Murphy, Baou and Jewell, 2009; Khabar, 2017). Although the precise molecular mechanisms with respect to how these proteins interact with the deadenylase machinery are not yet fully understood, several transacting elements involved in this process have been reported (Lai, Kennington and Blackshear, 2003; Fenger-Grøn et al., 2005; Lykke-Andersen and Wagner, 2005). ZFP36 and ZFP36L1 were shown to associate with the Ccr4/Caf1/Not deadenylase (CCR4-NOT) complex and recruit decapping enzymes (hDcp1 and hDcp2), 5'-3' exonuclease (hXrn1) and exosome element (hRrp4) through the N-terminal domain, and this interaction results in the decay of mRNA targets (Lykke-Andersen and Wagner, 2005). The interaction of ZFP36 with hDcp1 and XRN1 was also consistently shown in a separate study (Hau et al., 2007). ZFP36-dependent deadenylation was also described to occur through the activity of PolyA specific ribonuclease (PARN) complex in an indirect manner (Chen et al., 2001). In this study, ZFP36 was shown to recruit a multicomponent exosome complex with 3'-5' exonuclease activity to promote mRNA degradation in ARE-containing poly-deadenylated mRNAs (Chen et al., 2001). Exosome components involved in this process were also reported and included hRrp4, hRrp40, hRrp41 hRrp43, hRrp46, hCsl4 and hMtr3 (Chen et al., 2001). In a simplified outline, the ZFP36 family of proteins are proposed to mediate their destabilising effect

on mRNAs firstly through deadenylation directly or indirectly by recruiting NOT1 or PARN, respectively. Deadenylated-mRNAs can then take the route of 3'- 5' or 5'- 3' decay pathway facilitated by exonuclease activity via exosome or XRN1 recruitment, respectively (Figure 1.5). Altogether, the ZFP36 family of proteins serve as a molecular link between ARE-containing targeted mRNAs and decay pathways, implicating their importance in post-transcriptional gene regulation.

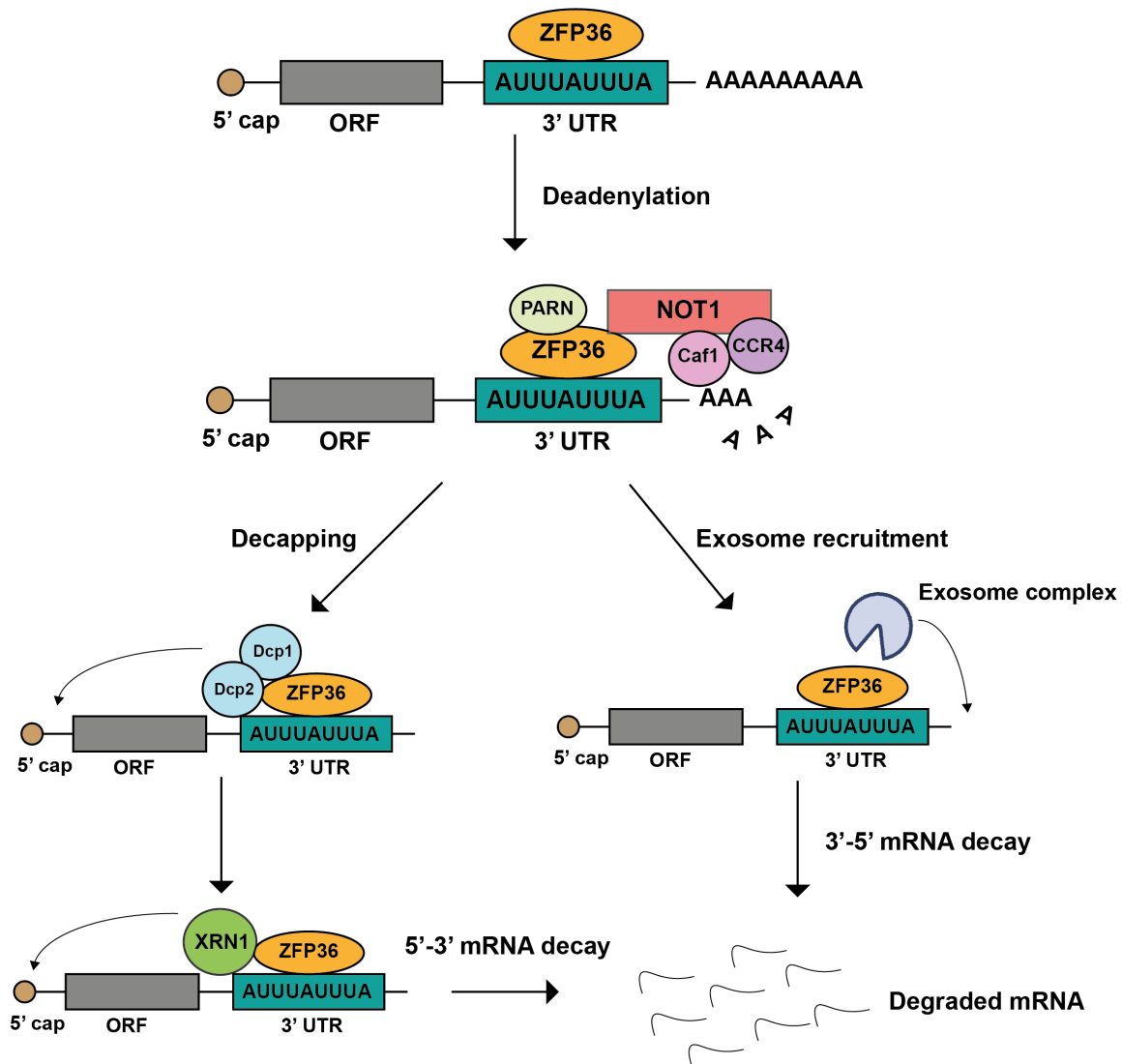


Figure 1.5. Schematic on the mechanism of post-transcriptional ARE-mRNA decay mediated by the ZFP36 family.

ZFP36 protein binds to AU-rich sequence in the 3'-UTR of targeted mRNA transcripts and triggers mRNA deadenylation through the recruitment of deadenylases directly (CCR4-NOT complex) or indirectly (PARN). Deadenylated mRNA transcripts can be degraded via the recruitment of a multiprotein exosome complex that facilitates 3' to 5' mRNA decay. Alternatively, deadenylated mRNA transcripts can undergo decapping, catalysed by decapping enzymes such as Dcp1 and Dcp2, which promotes 5' to 3' mRNA decay catalysed by XRN1 exonuclease. ORF, Open Reading Frame. Figure adapted from Murphy, Baou and Jewell (2009).

1.3.4 Post-translational Regulation of ZFP36 Proteins Via Phosphorylation

Post-translational control through phosphorylation of the ZFP36 family members is a crucial feature that enables these proteins to function as mRNA decay factors. Multiple studies have demonstrated that this post-translational modification can affect various

aspects of their RBP function (reviewed in, Brooks and Blackshear, 2013). A critical factor in which phosphorylation regulates the activity of the ZFP36 family members is through a multifunctional protein complex (14-3-3) that consists of a set of functionally diverse adaptor proteins that interact with other partner proteins containing phosphorylated residues, facilitating changes to RBP expression, function and localisation (reviewed in, Mackintosh, 2004). ZFP36 activity was shown to be controlled by phosphorylation on a number of residues including two conserved serine residues (Ser52 and Ser178 in mouse and Ser60 and Ser180 in human) by p38-MAPK2-activated protein kinase 2 (MK2) (Chrestensen et al., 2004). Upon phosphorylation, these serine residues act as substrates and recruit 14-3-3 adaptor proteins that bind to ZFP36 and inhibits its mRNA decay destabilising effects (Chrestensen et al., 2004; Stoecklin et al., 2004). In fact, phosphorylation of ZFP36 by p38-MK2 was also shown to impair its mRNA decay function by preventing the recruitment of CCR4-NOT deadenylase complex ([Figure 1.6](#)) (Clement et al., 2011). Based on these findings, binding of the 14-3-3 protein complex to ZFP36 was postulated to impair deadenylation by inhibiting the recruitment of deadenylase (Clement et al., 2011). ZFP36 was also identified as a downstream target of phosphorylation by a number of other major signalling pathways such as ERK MAPK, GSK3 β , JNK, PKA, PKB/AKT, and PKC pathways (Carballo et al., 2001; Mahtani et al., 2001; Cao, Dzineku and Blackshear, 2003; Cao, 2004; Chrestensen et al., 2004; Cao, Deterding and Blackshear, 2007).

Moreover, several phosphorylation sites located within the conserved sequence regions in ZFP36L1 and ZFP36L2 have also been reported (Appendix A) (reviewed in, Cao, Deterding and Blackshear, 2007). Accordingly, ZFP36L1 was revealed to be phosphorylated by MK2 and protein kinase B (PKB/AKT) signalling pathways

(Schmidlin et al., 2004; Benjamin et al., 2006; Maitra et al., 2008). ZFP36L1 was demonstrated to undergo phosphorylation by the MK2 pathway at serine residues, Ser54, Ser92 and Ser203 and at an unidentified site at the C-terminus, which subsequently resulted in the inhibition of its mRNA decay activity (Maitra et al., 2008). However, this did not appear to affect the ability of ZFP36L1 to bind to mRNA-AREs and recruit mRNA decay enzymes (Maitra et al., 2008). Additionally, phosphorylation of ZFP36L1 at Ser92 was shown to be mediated by the protein kinase B (PKB/AKT) pathway which resulted in ZFP36L1 binding to the 14-3-3 protein complex and impairment of ZFP36L1 mRNA decay activity on one of its ARE-containing mRNA targets (IL-3), also without affecting its ARE-binding activity (Schmidlin et al., 2004). In cooperation with Ser92, another regulatory site at Ser203 of ZFP36L1 was additionally reported to be phosphorylated by the PKB pathway, which abrogated mRNA degradation (Benjamin et al., 2006). Further, the C-terminal regions of ZFP36L1 and ZFP36L2 were reported to be directly phosphorylated by p90 ribosomal S6 kinase, a kinase downstream of MAPK/ERK pathway, which prevented the recruitment of the CCR4-NOT-deadenylase complex and inhibited the proteins destabilizing activity on low-density lipoprotein receptor (LDLR) target mRNA (Adachi et al., 2014).

While the signal-dependent activation of the p38-MAPK pathway inhibits ZFP36 family-mediated mRNA decay, the serine-threonine phosphatase, PP2A, was shown to contrastingly facilitate the de-phosphorylation of ZFP36 (Sun et al., 2007). In turn, this activity permits ZFP36 to resume its function in targeting mRNA transcripts for degradation and limiting mRNA expression levels ([Figure 1.6](#)) (Sun et al., 2007). Thus, post-translational modification of the ZFP36 proteins through phosphorylation can

greatly impact their RBP function at multiple levels, indicating the significance of such processes.

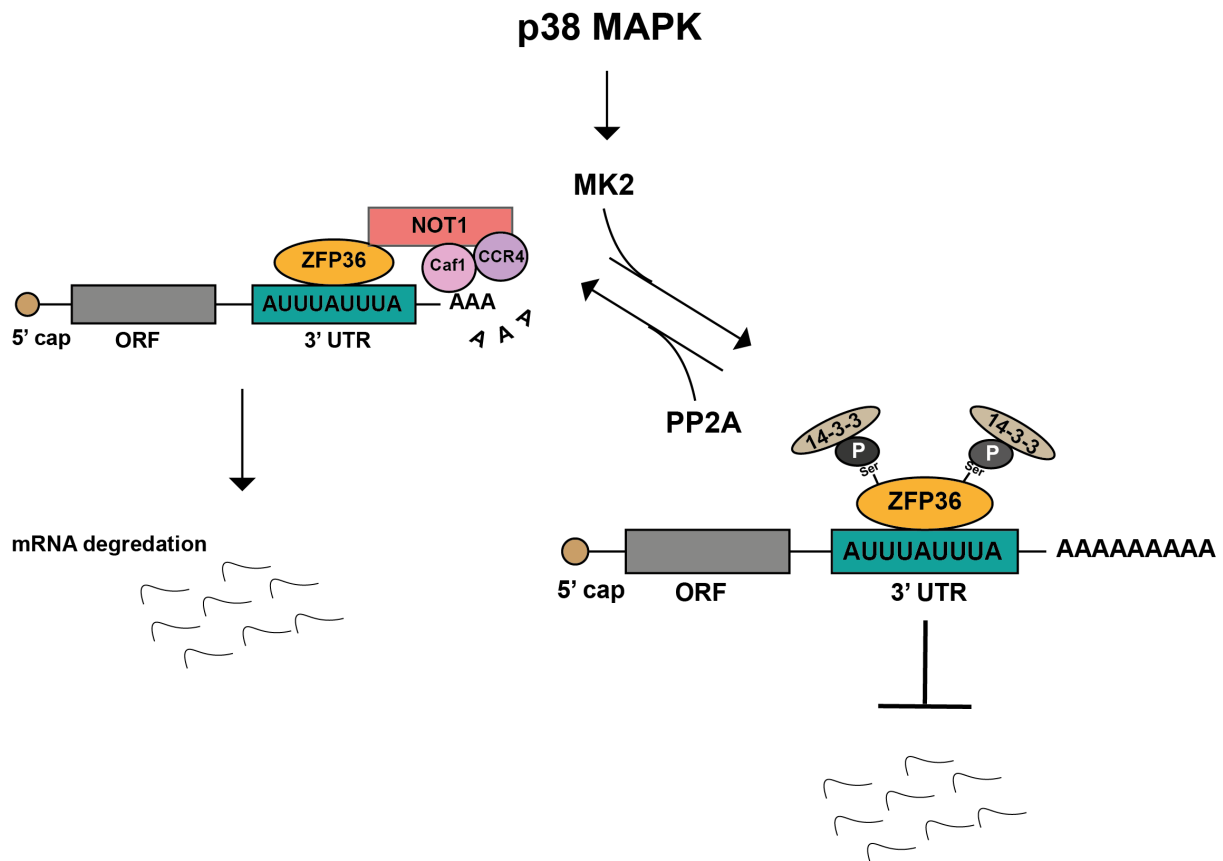


Figure 1.6. Phosphorylation of ZFP36 family members impairs mRNA degradation through the inhibition of deadenylase recruitment.

Phosphorylation of ZFP36 at Serine (Ser) residues by p38-MAPK2-activated protein kinase 2 (MK2) triggers the recruitment of the 14-3-3 protein complex. 14-3-3 adaptor proteins bind to ZFP36 and prevent the downstream recruitment of CCR4-NOT complex deadenylase, inhibiting ZFP36-mediated mRNA decay. In contrast, PP2A phosphatase promotes dephosphorylation of ZFP36, allowing it to resume its regulatory role in post-transcriptional mRNA destabilisation.

1.3.5 Subcellular Localisation of the ZFP36 Family Members

All three members of the ZFP36 family contain a nuclear localisation signal and nuclear export sequences between the two tandem ZF domains and N-terminus (ZFP36) or C-terminal (ZFP36L1 and ZFP36L2), respectively, which enable them to

shuttle between the nucleus and the cytoplasm (Phillips, Ramos and Blackshear, 2002). Initial studies had identified ZFP36 as a nuclear protein in fibroblasts and that its nuclear export to the cytosol was stimulated by serum and other mitogen factors (DuBois et al., 1990; Taylor et al., 1995; Taylor et al., 1996). Later studies with contrasting observations then demonstrated ZFP36's subcellular localisation to be in the cytosol in multiple cell types including, macrophages and leukocytes, and defined ZFP36 as an almost exclusively cytoplasmic protein (Carballo, Lai and Blackshear, 1998; Brooks et al., 2002; Fairhurst et al., 2003). However, parallel work described ZFP36 to encompass nucleocytoplasmic shuttling properties as it was detected in the nucleus as well as in the cytoplasm of COS-7 cells (Murata et al., 2002). This nuclear export activity of ZFP36 was also found to be mediated by CRM1 (nuclear export receptor) and was dependent on a Leucine-rich N-terminal region that appeared to serve as an LMB-sensitive nuclear export signal (NES) (Murata et al., 2002; Phillips, Ramos and Blackshear, 2002). Thus, this indicated that ZFP36 could shuttle between the nucleus and cytoplasm under certain circumstances (Figure 1.7). Nucleocytoplasmic shuttling by a CRM1-facilitated and NES-dependent pathway was also consistently shown in ZFP36L1 and ZFP36L2 (Phillips, Ramos and Blackshear, 2002). Unpublished observations from our laboratory also indicated ZFP36L1 to exhibit differential localisation patterns in various human cancer cell types. Nucleocytoplasmic shuttling of the ZFP36 family members is extensively regulated through phosphorylation of specific conserved serine residues within ZFP36 proteins (reviewed in, Clark and Dean, 2016).

Further, increasing evidence has suggested ZFP36 to target the Nuclear Kappa B (NF- κ B) signalling pathway and consequently alter its downstream cytokine

expression in an ARE-mediated decay-independent manner (Liang et al., 2009; Schichl et al., 2009). Intriguingly, ZFP36 was shown to inhibit NF- κ B signalling at the transcriptional co-repressor level through the recruitment of HDAC1 and HDAC3 to the NF- κ B p65 subunit (Liang et al., 2009), resulting in the suppression of NF- κ B /p65 nuclear import by a mechanism that is yet to be determined (Schichl et al., 2009). Accordingly, these findings suggested a possible function for ZFP36 in the nucleus.

Notably, the nuclear accumulation of ZFP36L1 in cervical cancer cells (HeLa) was recently reported to be regulated in a cell cycle-dependent manner, a process that was shown to be essentially controlled by a serine-rich cluster within the C-terminus of the ZFP36L1 protein (Matsuura et al., 2020). In particular, ZFP36L1 protein accumulation in the nucleus was prominent in G1/S-phase in HeLa cells, while it was greatly eliminated in S-phase cells and practically disappeared from the nucleus in G2-phase arrested cells (Matsuura et al., 2020). This fluctuation pattern interestingly indicated that ZFP36L1 probably encompasses specific nuclear physiological roles that are distinct from its cytoplasmic function, and provided novel clues to the mechanism controlling this nuclear accumulation (Matsuura et al., 2020). Prior to this study, however, nuclear to cytoplasmic translocation of the ZFP36 family members in murine cells has been shown to be modulated through the phosphorylation of Ser52 and Ser178 (Ser60 and Ser186 in human) by the p38-MAPK pathway using both, 14-3-3-dependent and independent mechanisms, to maintain protein localisation in the cytoplasm (Johnson et al., 2002; Brook et al., 2006). Moreover, unpublished observations from our laboratory have also suggested ZFP36L1 to potentially incorporate nuclear functions in certain human cancer cell lines. Indeed, isolated

chromatin fractions from U2OS, HeLa and HCTT16 cells revealed ZFP36L1 to be bound to the chromatin.

Lastly, ZFP36 family members can also localise to granular cytoplasmic structures known as stress granules (SGs) and processing bodies (P-bodies) (Kedersha and Anderson, 2002; Stoecklin et al., 2004; Kedersha et al., 2005). Environmental stresses such as heat shock, glucose deprivation and other stresses stimulate mRNA translation arrest, resulting in the accretion of SGs and P-bodies containing untranslated mRNA transcripts and stalled translational pre-initiation complexes (Anderson and Kedersha, 2002). SGs are cytoplasmic aggregates comprised of components of the translation machinery and are suggested to be formed through the accumulation of translationally repressed messenger RNAs, and are associated with RNA translational silencing and storage (reviewed in, Decker and Parker, 2012; Protter and Parker, 2016; Khong et al., 2017). In contrast, P-bodies are distinct cytoplasmic sites of mRNA turnover and harbour several components of mRNA decay machinery, including the CCR4-NOT complex (Hubstenberger et al., 2017; Youn et al., 2018). These two cytoplasmic structures are dynamically connected and can sometimes transiently interact with one another (reviewed in, Decker and Parker, 2012).

Under conditions of stress, ZFP36 and ZFP36L1 have been shown to localise to SGs to bind and sequester ARE-containing mRNAs, and deliver these targeted mRNAs to P-bodies for mRNA degradation (Kedersha et al., 2005). This suggested that the dynamic interaction between SGs and P-bodies relies on the ZFP36 family members where they play an active role in tethering SGs to P-bodies (Franks and Lykke-Andersen, 2007). In P-bodies on the other hand, ZFP36 for example, associates with

decapping enzymes including Dcp1 and Dcp2, and XRN1 exonuclease to stimulate 5'-3' exonuclease decay of the targeted ARE-containing mRNAs (Figure 1.7) (Fenger-Grøn et al., 2005; Hau et al., 2007). Furthermore, localisation of ZFP36 to SGs is post-translationally directed by the MK2 pathway in a 14-3-3 protein complex formation-dependent manner (Stoecklin et al., 2004). Indeed, MK2 phosphorylation of ZFP36 specifically at Ser52 and Ser178, was demonstrated to promote the assembly of MK2-14-3-3 complexes, which resulted in the exclusion of ZFP36 from SGs (Kedersha et al., 2005). This was in contrast to the observation in P-bodies, where ZFP36 was found to localise these cytoplasmic structures irrespective of its phosphorylation status (Kedersha et al., 2005).

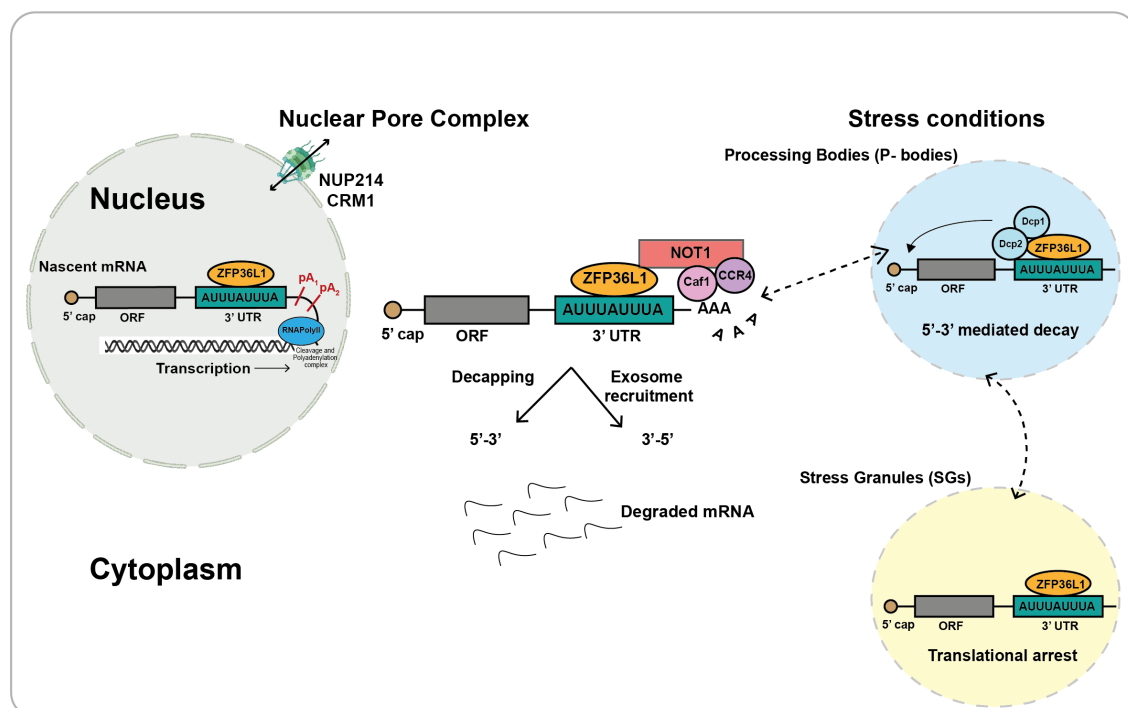


Figure 1.7. The ZFP36 family exhibit nuclear-cytoplasmic shuttling properties.

The ZFP36 family of proteins can shuttle between the nucleus and the cytoplasm to perform post-transcriptional regulatory functions on targeted mRNA transcripts. Nuclear export activity of ZFP36L1, for example, is mediated in a CRM1-dependent manner. After the deadenylation of mRNA transcripts, AU-rich mRNA undergoes 5' to 3' or 3' to 5' decay. ZFP36 proteins can also localise to processing bodies (P-bodies, blue) and stress granules (SGs, yellow) under stressed conditions, which are dynamically connected, and promote 5'-3' mRNA decay and translational arrest, respectively. Adapted from Ciaia, Cherradi and Feige (2013).

1.3.6 Physiological Roles and mRNA Targets

The post-transcriptional regulatory function of the human ZFP36 family of proteins in controlling the stability of ARE-bearing mRNAs is a crucial process required for the control of gene expression, and has been implicated in numerous physiological and pathological processes. Each of the three members of the ZFP36 family contains an extensive repertoire of distinct targeted mRNAs that may sometimes overlap with the other member-specific mRNA targets and are also cell type-specific (reviewed in, Murphy, Baou and Jewell, 2009). To date, ZFP36 is the best characterised of the ZFP36 protein family. The physiological role of ZFP36 was initially studied by Carballo et al. (1998) using a ZFP36-deficient mouse model. ZFP36-knockout mice displayed elevated macrophage-derived TNF- α mRNA production levels and therefore, increased TNF- α mRNA stability, as previously mentioned (Carballo, Lai and Blakeshear, 1998). Since this initial finding, ZFP36 family members have been described to bind ARE-containing mRNAs present in several mediators of immunity, inflammation, apoptosis, proliferation, and cancer-related hallmarks (reviewed in, Sanduja et al., 2012; Guo et al., 2017; Saini, Chen and Patial, 2020).

ZFP36 proteins can regulate the mRNA stability of various cytokines including several types of interleukins (IL); IL-2, IL-3, IL-6 and IL-10, IL-12 and IL-17 (Stoecklin et al., 2000, 2001, 2008; Ogilvie et al., 2005; Jalonen et al., 2006; Lee et al., 2012). Other reported mRNA targets include granulocyte macrophage colony-stimulating factor (GM-CSF), vascular endothelial growth factor (VEGF), and cyclooxygenase 2 (COX-2) (Carballo, Lai and Blakeshear, 2000; Boutaud et al., 2003; Essafi-Benkhadir et al., 2007). ZFP36 also mediates mRNA decay of IL-10 via deadenylation and destabilises GM-CSF mRNA through poly-A shortening (Lai et al., 1999; Tudor et al., 2009). ZFP36

proteins are also involved in the regulation of key transcription factors and cell cycle regulators such as BLIMP1, STAT5b, c-Myc and Cyclin D1 mRNA (Marderosian et al., 2006; Vignudelli et al., 2010; Nasir et al., 2012). Strikingly, ZFP36 protein members can negatively regulate their own expression by binding to the 3' UTR regions of their own ARE-containing mRNA (Brooks, Connolly and Rigby, 2004; Lin et al., 2007). Further, ZFP36 and ZFP36L1 have been shown to interact with BCL2 mRNA and promote mRNA degradation, resulting in apoptosis (Zekavati et al., 2014; Park et al., 2015). Additionally, ZFP36 can also induce apoptosis through the destabilisation of TNF- α mRNA transcripts (Johnson, Geha and Blackwell, 2000; Johnson and Blackwell, 2002).

All three members of the ZFP36 family are widely expressed throughout the early stages of lymphocyte development and exert their regulatory functions on several cyclins and cyclin-dependent kinases (CDKs), controlling mRNA expression at distinct stages of B and T-cell development (reviewed in, Galloway and Turner, 2017). The regulatory function of ZFP36L1 and ZFP36L2 was linked to the maintenance of cell quiescence in the critical stages of developing B lymphocytes (Galloway et al., 2016). ZFP36L1 and ZFP36L2 were shown to repress cell cycle regulators such as CyclinD1 and Cyclin D3, modulating key recombination processes in developing B cells (Galloway et al., 2016). ZFP36L1 was also demonstrated to regulate the differentiation, appropriate localisation, and survival of B cells in the mouse BCL1 cell line via the destabilisation of the transcription factor, BLIMP1 mRNA (Nasir et al., 2012). Moreover, an indispensable role for ZFP36L1 as a regulator for the proper localisation and survival of marginal zone (MZ) B cells was also reported (Newman et al., 2017). In this study, ZFP36L1 was found to post-transcriptionally control the

expression of transcription factors KLF2 and IRF8, which promote the follicular B-cell phenotype (Newman et al., 2017). Furthermore, it was also shown that loss of ZFP36L1 and ZFP36L2 results in perturbed thymic development and T-cell leukaemia in murine cells, indicating an active role for ZFP36L1 and ZFP36L2 in the prevention of malignant transformation (Hodson et al., 2010). More recently, ZFP36L1 was reported to promote potent antiviral activity against influenza A virus (IAV) infection via cytoplasmic mRNA binding to non-structural protein 1 (NS1), a protein known to enhance viral replication (Lin et al., 2020). Accordingly, knockdown of ZFP36L1 was found to be associated with a significant increase in IAV replication. In addition, overexpression of ZFP36L1 was described to translationally repress several IAV mRNA transcripts including hemagglutinin (HA), protein matrix (M1) and NS1, and reduce IAV replication (Lin et al., 2020). Interestingly, in the same study, a mutation of the ZFs of ZFP36L1 was also shown to restrict NS1 mRNA binding and therefore, reduce antiviral activity exerted by ZFP36L1 (Lin et al., 2020).

Owing to their ability to bind to a vast diversity of ARE-containing mRNA transcripts, ZFP36 family members' can concurrently mediate rapid mRNA decay on numerous tumour-related genes and cancer-related cytokines and thus, can extensively participate in regulatory networks for tumour suppression (reviewed in, Park, Lee and Kang, 2018). To name a few, several mRNA-encoding oncogenes including BCL2, MYC, NOTCH1 and COX-2 have been reported as direct targets for the ZFP36 family of RBPs (Sawaoka et al., 2003; Hodson et al., 2010; Rounbehler et al., 2012; Zekavati et al., 2014). Moreover, ZFP36 family members have been shown to inhibit malignant proliferation by suppressing the expression of genes associated with cell cycle progression and proliferation. Among these targets include, mRNA transcripts

encoding for oncogenic drivers Cyclin B1 and Cyclin D1; whose overexpression is linked with chronic tumour progression, E2F1; a key contributor to proper cell cycle transition and PIM-1; a facilitator of cell cycle progression (Diehl, 2002; Yuan et al., 2006; Mahat et al., 2012). Further, ZFP36 family members can also directly bind to mRNA-encoding tumour suppressor genes. For example, ZFP36 was evidenced to directly bind to the mRNA of the putative tumour suppressor, LATS2, whose function is associated with the control of the cell cycle, and promote its mRNA degradation in lung cancer cells (Lee et al., 2010). The ZFP36 family of proteins' physiological roles and the consequences associated with their dysregulation in tumourigenesis have been extensively studied and will be discussed in more detail in subsequent sections of this report.

1.3.7 The ZFP36 Family in Inflammatory Disease

As previously mentioned, the ZFP36 family members can impact the stability of a large repertoire of mRNA targets and are involved in numerous physiological processes. As such, dysregulation of their expression can cause changes in the levels of specific mRNAs, which is consequently associated with several established diseases including immune-related disorders and cancer (reviewed in, Sanduja et al., 2012; Guo et al., 2017). As demonstrated in the knockout mouse model, ZFP36 was initially found to function as a crucial post-transcriptional regulator of TNF- α and other pro-inflammatory cytokines, and abrogation of its expression can impact the onset and severity of several inflammatory diseases such as myeloid hyperplasia, rheumatoid arthritis (RA), dermatitis and systemic lupus erythematosus (SLE) (Carballo et al., 1996; Carballo, Lai and Blackshear, 1998). Following this study, loss of ZFP36 expression was evidenced to be linked with elevated levels of GM-CSF transcripts

from bone marrow stromal cells, which reinforced the key role of ZFP36 in physiologically regulating the inflammatory response (Carballo, Lai and Blakeshear, 2000). TNF- α and GM-CSF transcripts were also identified as mRNA targets for ZFP36L1 and ZFP36L2 (Lai et al., 2000; Lai and Blakeshear, 2001). Moreover, although the ZFP36 family members share similar RNA-binding specificities and encompass overlapping mRNA targets, the consequential phenotypes associated with loss of individual expression can differ between the three protein variants. For example, while loss of ZFP36 is functionally linked with pro-inflammatory effects in murine cells, disruption of ZFP36L1 was shown to be embryonically lethal due to defective placental development during gestation (Stumpo et al., 2004), and was associated with intraembryonic and extraembryonic vascular abnormalities and heart defects (Bell et al., 2006). On the other hand, disruption of ZFP36L2 was associated with defective haematopoiesis and resulted in complete female infertility (Stumpo et al., 2009).

Since these initial studies, the function of the ZFP36 family of proteins has been connected to the regulation of a diverse range of inflammatory and anti-inflammatory factors such as TNFs, interleukins (ILs) and interferons (IFNs) that play key roles in the immune response (reviewed in, Guo et al., 2017). In addition to the modulation of TNF- α transcript, ZFP36 has also been functionally connected to IL-6, IL-17, and IFN γ (Ogilvie et al., 2009; Zhao et al., 2011; Lee et al., 2012). More recently, the regulatory role of ZFP36L1 was shown to be functionally linked to the protection against osteoarthritis (OA), demonstrated in OA chondrocytes and OA cartilage of humans and mice (Son et al., 2019). Although the overexpression of ZFP36L1 did not appear to exert a protective role against OA pathogenesis, silencing of ZFP36L1 was

associated with a significant increase in the mRNA expression of two heat shock proteins (HSP70 family members), which resulted in the prevention of chondrocyte apoptosis and hence, protection against OA pathogenesis (Son et al., 2019). Thus, these crucial studies signified the involvement of the ZFP36 family members in the direct regulation of immune-related processes and that aberration of their expression results in enhanced inflammation.

1.3.8 The Role of ZFP36 Family Members in Cancer

Over the past decade, the ZFP36 family of RBPs have emerged as crucial regulators of several cancer-related hallmarks, and alterations in their expression/activity have been described to be affiliated with multiple cancer types (reviewed in, Saini, Chen and Patial, 2020). Mechanistically, these RBPs regulate the development and progression of cancer at three levels; *at the posttranscriptional level, transcriptional level and at the translation level* (Wang et al., 2016). Several studies have particularly reported a loss of ZFP36 family of RBP expression in multiple types of human cancers including breast, cervical, prostate and colorectal cancers (reviewed in, Guo et al., 2017). Loss of ZFP36 family members' expression was found to be functionally linked to inflammation-mediated cancer, dysregulation of the cell cycle, cancer cell proliferation, apoptosis, angiogenesis and metastasis (Table 2) (reviewed in, Wang et al., 2016; Guo et al., 2017; Saini, Chen and Patial, 2020).

Table 2. Examples of reported cancer hallmark-related mRNA targets of the ZFP36 family. Compiled and adapted from (Khabar, 2017; Park, Lee and Kang, 2018).

Gene	mRNA target	Cancer Hallmark	Reference
ZFP36, ZFP36L1, ZFP36L2	TNF- α	Angiogenesis, Invasion, Metastasis	(Carballo, Lai and Blackshear, 1998; Lai et al., 2000).
ZFP36, ZFP36L1, ZFP36L2	GM-CSF	Angiogenesis	(Carballo, Lai and Blackshear, 2000; Lai and Blackshear, 2001).
ZFP36	PD-L1	Evading Immunity	(Guo et al., 2018)
ZFP36	IL-33	Invasion and Metastasis	(Deng et al., 2016)
ZFP36	PIM-1, PIM-2	Invasion	(Selmi et al., 2012)
ZFP36, ZFP36L1	VEGF	Angiogenesis	(Ciais et al., 2004; Essafi-Benkhadir et al., 2007)
ZFP36	IL-8	Proliferation	(Bourcier et al., 2011)
ZFP36	COX-2	Anti-apoptosis	(Young et al., 2009)
ZFP36, ZFP36L1	IL-3	Angiogenesis	(Stoecklin et al., 2003)
ZFP36	IL-6	Proliferation	(Wei et al., 2016)
ZFP36	MMP2, MMP9	Invasion	(Van Tubergen et al., 2013)
ZFP36, ZFP36L1, ZFP36L2	Cyclin D1	Proliferation	(Al-Khalaf et al., 2011; Suk et al., 2018)

ZFP36, ZFP36L1	E2F1	Migration	(Lee, Lee and Leem, 2014; Loh et al., 2020)
ZFP36	IL-10	Evading Immunity	(Stoecklin et al., 2008)
ZFP36	IL-16	Invasion, Metastasis	(Milke et al., 2013)
ZFP36	IL-17	Pro-inflammatory	(Yang et al., 2014; Qian et al., 2017)
ZFP36	MYC	Proliferation, Anti-apoptosis	(Pandiri et al., 2016)
ZFP36	Snai1	Metastasis	(Montorsi et al., 2016)
ZFP36	Twist 1	Metastasis	(Montorsi et al., 2016)
ZFP36	Cyclin B1	Proliferation	(Mukherjee et al., 2014)
ZFP36	c-Jun	Proliferation	(Marderosian et al., 2006)
ZFP36L1	HIF1A	Angiogenesis	(Chen et al., 2015)
ZFP36L1	BCL-2	Anti-apoptosis	(Zekavati et al., 2014)
ZFP36, ZFP36L1	clAP2	Anti-apoptosis	(Lee et al., 2005; Kim et al., 2010)

(Continued)

Numerous studies have reported that persistent inflammation plays a vital and complex role in promoting carcinogenesis, and many tumours are known to originate at tissue sites undergoing chronic inflammation (reviewed in, Kundu and Surh, 2008; Mantovani et al., 2008; Crusz and Balkwill, 2015). The complex network of cancer-mediated inflammation is generally attributed to the presence of dysregulated pro-inflammatory factors and subsequent aberration in gene expression, both of which consequently drive the tumour microenvironment (Grivennikov, Greten and Karin, 2010). Since the ZFP36 family of proteins are well-established post-transcriptional mediators of many pro-inflammatory and anti-inflammatory cytokines and chemokines, dysregulation of these RBPs is tightly connected to the development and progression of inflammation-associated cancer (Anderson, 2010). This is mainly due to the many downstream targets of the ZFP36 family, that encode for key factors that play crucial roles in inflammation and tumourigenesis. For instance, ZFP36 was demonstrated to play a potent tumour suppressive role in a v-H-ras-dependent manner in a mast cell tumour model by suppressing interleukin-3 (IL-3) mRNA levels (Stoecklin et al., 2003). In this tumour model, cells exhibited elevated levels of IL-3 as part of an oncogenic autocrine loop, and ZFP36 expression was found to interfere with this loop, delaying tumour progression by enhancing mRNA decay of IL-3 (Stoecklin et al., 2003). Another example of a cancer-related inflammatory downstream target of ZFP36 is IL-17, a cytokine that is usually elevated in chronic inflammatory diseases and is associated with cancer progression (Yang et al., 2014; Qian et al., 2017). ZFP36 was evidenced to directly bind to IL-17 mRNA and facilitate the destabilisation of its transcripts (Lee et al., 2012). Further pro-tumourigenic inflammatory mediators of the ZFP36 family have also been identified and include IL-6, IL-8 and COX-2 (reviewed in, Sanduja et al., 2012).

Dysregulation of the cell cycle and sustenance of chronic proliferative signalling are two essential features of cancer cells. As previously mentioned, the regulatory role of the ZFP36 family is physiologically connected to several critical cell cycle regulators that are specifically involved in cell cycle progression and cellular proliferation such as cyclin B1, cyclin D1, E2F1 and PIM-1 (Diehl, 2002; Yuan et al., 2006; Mahat et al., 2012). ZFP36 has also been shown to modulate mRNA levels of c-Myc, an oncogene that regulates cellular proliferation and differentiation and one that is commonly dysregulated in human cancers (Marderosian et al., 2006). Moreover, ZFP36 was reported to inhibit cellular proliferation in breast cancer cells by suppressing the expression of the proto-oncogene c-Jun, an established accelerator of the cell cycle (Xu et al., 2015). By selectively blocking the NF- κ B pathway, ZFP36 was found to inhibit c-Jun expression at the transcriptional level, resulting in an increased expression of Wee1, which subsequently caused cell cycle arrest at the S-phase (Xu et al., 2015). Furthermore, ZFP36L1 was demonstrated to promote monocyte/macrophage differentiation by repressing mRNA levels of cyclin-dependent kinase 6 (CDK6) (Chen et al., 2015). Consequently, ZFP36L1 expression was significantly decreased in acute myeloid leukaemia (AML) patients (Chen et al., 2015). In a recent study, ZFP36L1 was found to serve as a safeguard against aberrant cell cycle progression by regulating the expression of key oncogenic transcripts; HIF1A, CCND1, and E2F1, in bladder and breast cancer cell lines (Loh et al., 2020). Lastly, forced expression of ZFP36L1 and ZFP36L2 was evidenced to inhibit cellular proliferation, mediated by downregulation in cyclin-D expression, in human colorectal cancer cell lines (Suk et al., 2018). Collectively, these studies indicated that the ZFP36 family of proteins could function as potential potent tumour suppressors by

destabilising mRNA transcripts whose over-expression is associated with tumour malignancy.

One of the hallmarks of cancer cells involves their ability to evade apoptosis or resist cell death (Hanahan and Weinberg, 2011). Due to the presence of many ARE-containing mRNAs encoding for gene products that allow cancer cells to evade programmed cell death, the ZFP36 family members can modulate tumour cell apoptosis through several downstream effectors. Indeed, overexpression of the ZFP36 protein family has been shown to induce apoptosis in multiple cell lines including HeLa (human cervical cancer cells), U2OS (osteosarcoma cells), SAOS2 (sarcoma osteogenic), 3T3 (mouse fibroblast cells) and B-lymphoma cells through direct regulation of mRNA targets (Johnson, Geha and Blackwell, 2000; Johnson and Blackwell, 2002; Baou et al., 2009). Moreover, ZFP36L1 was demonstrated to exert a pro-apoptotic function in Ramos Burkitt B lymphoma cells as well as in B-chronic lymphocytic leukaemia cells (Ning et al., 1996; Zekavati et al., 2014). ZFP36 can also, synergistically with TNF- α , sensitise cells to TNF-induced apoptosis in 3T3 cells (Johnson and Blackwell, 2002). More recently, ZFP36 was revealed to sensitise head and neck squamous cell carcinoma cell lines to cisplatin-induced apoptosis, by deregulating the expression of BCL-2 mRNA (Park et al., 2015). This was similarly shown for ZFP36L1, except that it was found to induce apoptosis by inhibiting mRNA expression of apoptotic protein-2 (CIAP2), in response to cisplatin treatment (Lee et al., 2005). Therefore, loss of members of ZFP36 expression can facilitate resistance to cell death and enhance tumour progression.

Consistent with their tumour suppressive role, members of the ZFP36 family have been implicated as key repressors of a subset of mRNA transcripts involved in angiogenesis and metastasis (reviewed in, Saini, Chen and Patial, 2020). Tumour cells require a continuous supply of oxygen and nutrients from blood vessels to support their development and growth (Neufeld et al., 1999). One of the critical modulators of tumour angiogenesis and vasculogenesis is vascular endothelial growth factor (VEGF) (Neufeld et al., 1999). Importantly, ZFP36 and ZFP36L1 have both been shown to post-transcriptionally destabilise VEGF mRNA transcripts or inhibit VEGF translation and hence, suppress tumour progression (Ciais et al., 2004; Bell et al., 2006; Essafi-Benkhadir et al., 2007). Another critical regulator of angiogenesis whose mRNA levels is mediated by ZFP36 is cyclooxygenase 2 (COX-2); a facilitator of the production of VEGF and BCL2 (Boutaud et al., 2003; Gately and Li, 2004). Functionally, reduced expression of ZFP36 was found to be directly correlated to increased expression of COX-2 and VEGF in human colon cancer cells (Cha et al., 2011). Further, potent factors associated with tumour angiogenesis such as hypoxia-inducible factor 1 (HIF-1), IL-6, IL-1 α and IL-8 are additionally controlled by members of the ZFP36 family (Planel et al., 2010; Chang and Hla, 2011; Griseri and Pagès, 2014).

Further, deficiency in the expression of the ZFP36 proteins also contributes to cancer invasion and metastasis. A compendium of studies has identified several mRNA targets involved in cancer malignancy that are regulated by this family of RBPs (reviewed in, Park, Lee and Kang, 2018). In addition to VEGF, COX-2 and IL-6 transcripts, members of ZFP36 proteins were revealed to destabilise ARE-containing mRNAs of MMP-1 (matrix metalloproteinase), MMP-2, MMP-9, and invasive factor

uPA (urokinase plasminogen activator), which functionally correlate with cancer metastasis (Al-Souhibani et al., 2010; Al-Ahmadi et al., 2013; Van Tubergen et al., 2013). Based on gene expression profiles from 80 patient samples, reduced ZFP36 expression was detected in metastatic tumours relative to primary tumours, which suggested that loss of ZFP36 can contribute to epithelial-mesenchymal transition (EMT) (Montorsi et al., 2016). In line with these findings, ZFP36 was reported to repress EMT progression through mRNA degradation of EMT marker genes including snail1 (zinc finger protein snail 1) and twist1 (twist-related protein 1) (Yoon et al., 2016). Recently, ZFP36L1 was found to be significantly downregulated in breast cancer cells and was associated with reduced mRNA levels of EMT markers (Rataj et al., 2019). In another study, ZFP36L2 expression was interestingly shown to be regulated by the metastatic suppressor gene, NME1, in melanoma and thyroid carcinoma cell lines (McCorkle et al., 2014). In a double conditional knockout-based study, mice that were depleted of ZFP36L1 and ZFP36L2 were observed to mature with a perturbation in thymic development, which in turn resulted in the development of T-cell acute lymphoblastic leukaemia (T-ALL) (Hodson et al., 2010). This phenotype was directly associated with ZFP36L1 and ZFP36L2 post-transcriptional regulatory role on the oncogenic transcription factor, NOTCH1, which suggested a role for ZFP36L1 and ZFP36L2 in the prevention of malignant transformation (Hodson et al., 2010). In the same study, ZFP36L1 was further shown to negatively regulate cell cycle progression, by targeting mRNA targets encoding for crucial cell cycle genes, during murine lymphocyte development (Hodson et al., 2010). Consistently, loss of ZFP36L1 function can facilitate cell cycle progression in tumourigenesis in various cancer cell types (Suk et al., 2018; Loh et al., 2020). A summary of the various cancer-related mRNAs by which the ZFP36 family of proteins regulate is illustrated in [Figure 1.8](#).

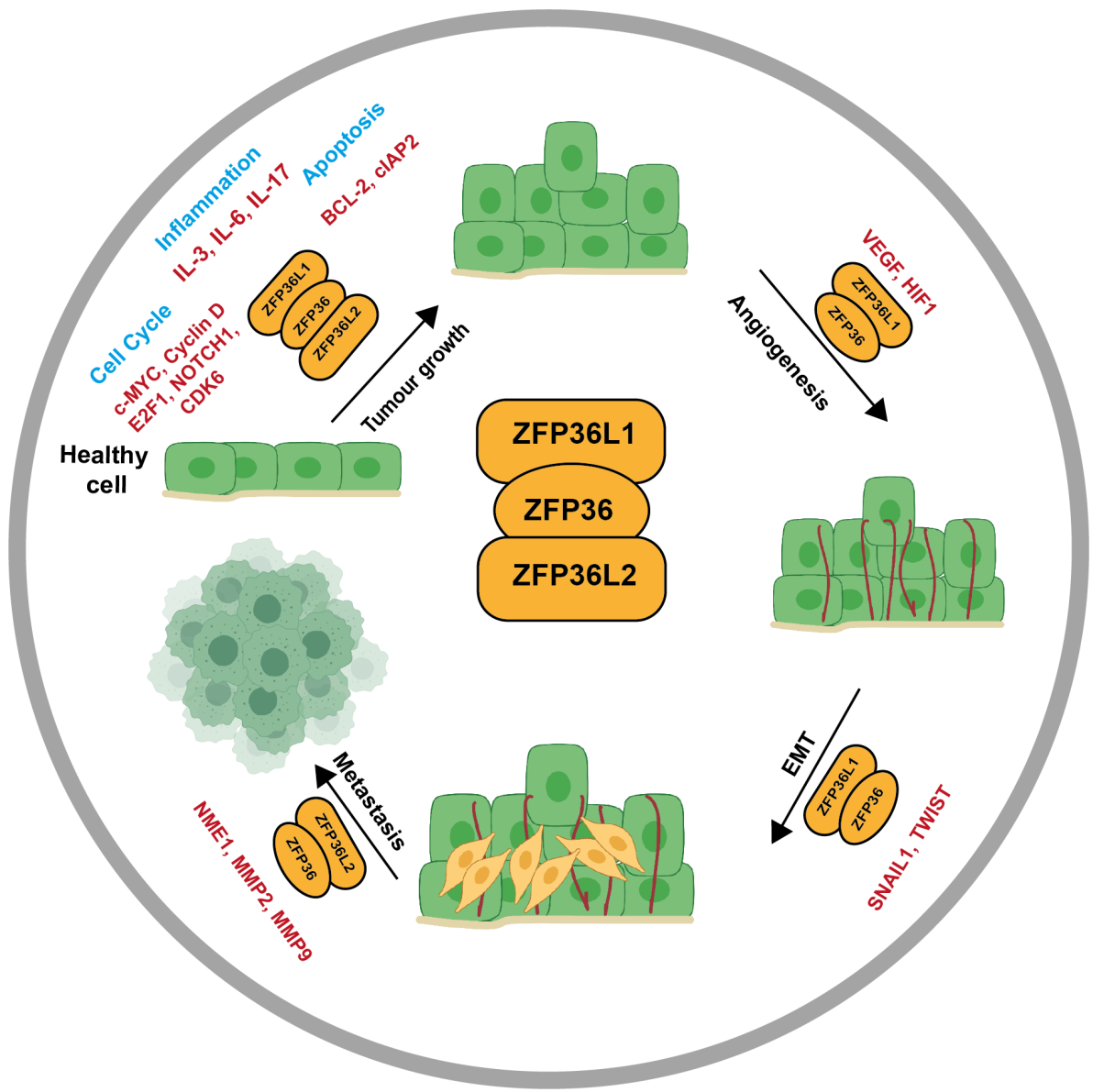


Figure 1.8. Schematic illustration of various cancer-related targeted mRNA transcripts regulated by the ZFP36 family.

Members of the ZFP36 family (yellow) regulate several mRNA transcripts (red) that are involved in carcinogenesis, at multiple stages during the process of tumourigenesis. The targeted mRNA transcripts encode for key proteins involved in tumour growth, angiogenesis, epithelial-mesenchymal transition (EMT) and metastasis. Dysregulation of ZFP36 proteins promotes tumourigenesis and drives tumour progression. Adapted from Saini, Chen and Sonika (2020).

In addition to the observations on its post-transcriptional regulatory role of key cell cycle and oncogenic-encoding mRNA targets (reviewed in, Khabar, 2017; Saini, Chen and Patial, 2020), recent systematic analysis of AU-rich element expression in cancers has also shed light on ZFP36L1's potential role as a tumour suppressor in human cancers, supported by the finding that ZFP36L1 expression was observed to be mutated or down-regulated in various cancer cell types compared to normal cells (Hitti et al., 2016). A recent landmark study that conducted whole-genome and exome sequencing of breast cancer patient genomes has identified *ZFP36L1* as a novel cancer driver gene in breast cancer (Nik-Zainal et al., 2016). This was consistently observed in a Capture-HiC-based study that annotated breast cancer risk loci to identify breast cancer-related driver genes, whereby *ZFP36L1* was identified as one of the putative target genes associated with breast cancer (Baxter et al., 2018). *ZFP36L1* was further identified as a novel cancer candidate gene in other cancer cell types due to the observation of its significant mutated expression in certain tumours (Martincorena et al., 2017; Priestley et al., 2019). In addition, a genome-scale CRISPR/Cas9 screen-based study had also importantly listed *ZFP36L1* among one of the prioritized candidates/targets for future cancer therapeutics (Behan et al., 2019).

1.4 Replication stress-induced Genomic Instability

Genomic instability (GIN) is a common feature observed in most cancers and can result as a consequence of various molecular incidents such as chromosomal instability, micro and mini-satellite instability and DNA mutations (reviewed in, Negrini, Gorgoulis and Halazonetis, 2010). Chromosomal instability (CIN), a phenomenon denoted by changes in chromosome number and structure, is the most common form of genomic instability in human cancers. Micro and mini-satellite instability (MIN),

characterised by repetitive-DNA expansions or contractions within microsatellite sequences, is caused by erroneous DNA synthesis, defective mismatch repair (MMR) or base excision repair (BER) (Fishel et al., 1993; Leach et al., 1993). Dysregulated MMR and BER can also lead to increased mutations such as base substitutions, micro-deletions and micro-insertions (Al-Tassan et al., 2002). Furthermore, dysfunctional mitotic checkpoints and telomere abrasion have also been proposed to induce genomic instability in cancer (Artandi et al., 2000; Kops, Weaver and Cleveland, 2005). Defects in mitotic checkpoints, which guard cells against chromosome mis-segregation during anaphase, drives CIN phenotypes and facilitates cancer development (Michel et al., 2001; Jeganathan et al., 2007; Ritchie et al., 2009). Finally, telomere erosion can also lead to GIN (Artandi et al., 2000). In healthy cells, telomeres protect chromosome ends from deleterious processing and unscheduled DNA recombination and repair (reviewed in, Blasco, 2005). Dysregulation of this process, however, can cause CIN thereby driving tumourigenesis (Artandi et al., 2000; Rudolph et al., 2001; Davoli, Denchi and de Lange, 2010). Despite the fact that such forms of instability can be detrimental for cells, these processes also simultaneously drive molecular evolution through genetic variation. Accordingly, genomic instability can also contribute to the generation of genetic variability within developmental processes, such as immunoglobulin (Ig) diversification (Maizels, 2005). Nonetheless, genomic instability in humans is typically affiliated with cellular pathologies and is a hallmark of tumour development and progression (Hanahan and Weinberg, 2011).

The efficient and faithful transmission of genetic material in every cell division is a critical determinant of genomic stability and cancer predisposition in human tissues, reflecting that our genomes are most vulnerable during DNA replication (Tomasetti and Vogelstein, 2015). Coordination of DNA replication with cell cycle progression,

DNA-damage sensing and DNA-repair pathways preserve genomic stability during cell divisions, preventing DNA mutations and rearrangements (reviewed in, Aguilera and Gómez-González, 2008). Perturbations in DNA replication dynamics such as replication stress, have emerged as a major source of genomic instability and are often increased in the initial stages of carcinogenesis (Gorgoulis et al., 2005; Shen and Ro, 2006). Despite the wide range of proteins and pathways linked to GIN, a shared characteristic between them is their association with replication stress (Gorgoulis et al., 2005). Indeed, replication stress has been suggested to be a prevalent source of DNA damage generally caused by oncogene activation or tumour suppressor inactivation, and contributes to GIN in most human cancers (Macheret and Halazonetis, 2015).

1.4.1 DNA Replication and Associated Inhibitors

DNA replication is a process by which the genome is duplicated prior to cell division. The replication machinery, known as the replisome, is a massive complex that consists of a network of specialised proteins that ensure precise and efficient replication of DNA during each cell cycle (Leman and Noguchi, 2013). In summary, the double-stranded DNA (dsDNA) molecule is unwound by DNA helicases, producing a replication fork with two single-stranded DNA (ssDNA) templates. Subsequently, DNA polymerases synthesise new DNA strands complementary to each parental template. This replication process generates two daughter DNA copies in a semiconservative fashion whereby one strand is formed from the original DNA helix, while the second is the nascent antiparallel strand (Meselson and Stahl, 1958). Due to the antiparallel nature of the DNA double helix, replication takes place in opposing orientations between the two daughter strands. Despite this, however, all DNA polymerases synthesise DNA

with 5' to 3' directionality (Hübscher, Nasheuer and Syväoja, 2000). DNA polymerase ϵ (epsilon) synthesises the leading strand in a continuous fashion (Pursell et al., 2007), whereas the opposite template (lagging) strand is synthesised in fragmented stretches of 100 to 200 bases in length, known as Okazaki fragments, by DNA polymerase δ (delta) (Okazaki et al., 1968; Nick McElhinny et al., 2008). On the other hand, DNA polymerase α (alpha) synthesises RNA-DNA hybrid primers at replication origins and is responsible for the initiation of replication on both, the leading and lagging strands (Hübscher, Nasheuer and Syväoja, 2000).

Eukaryotic DNA replication is a tightly controlled process essentially composed of two distinct stages: origin licensing and initiation. In the licensing stage, the multiprotein pre-replication complex (pre-RC) site is recognised, and during origin initiation, DNA synthesis is instigated (Fragkos et al., 2015). To ensure that DNA replication takes place only once per cell cycle, cells rely on a series of tightly regulated steps that begin with the assembly of the origin recognition complex (ORC) at the replication origin (Shen et al., 2012). In the G1-phase of the cell cycle, DNA replication factor 1 (CDT1) and cell division cycle protein 6 (CDC6) then assemble at the replication origin and recruit the replicative helicase minichromosome maintenance complex 2–7 (MCM2–7) (Cook, Chasse and Nevins, 2004). This leads to the formation of the pre-RC that licenses replication initiation in the subsequent S-phase ([Figure 1.9](#)) (reviewed in, Gaillard, García-Muse and Aguilera, 2015). Upon initiation of replication, CDT1 and CDC6 unbind from the pre-RC, thus preventing re-replication (Blow and Dutta, 2005; Fujita, 2006; Arias and Walter, 2007; Hook, Lin and Dutta, 2007). Although eukaryotic chromosomes contain thousands of licensed origins, only a small number of them are

fired (activated) in the S-phase, with the remaining origins preserved as a backup in case of replication failure (Blow, Ge and Jackson, 2011).

Replication initiation is activated at the onset of the S-phase through the concerted action of cyclin-dependent kinases (CDKs) and DBF4-dependent kinase (DDK/CDC7) (Sheu and Stillman, 2006, 2010). The assembly of CDK and DDK results in the phosphorylation of the pre-RC, which then allows the recruitment of the CDC45 and the GINS protein complex (Fragkos et al., 2015). In turn, this instigates the formation of the pre-initiation complex (pre-IC) and activates the replication helicase (CMG) complex (Moyer, Lewis and Botchan, 2006; Aparicio et al., 2009). Subsequently, the CMG complex unwinds the DNA duplex, forming a replication bubble, and generates two divergent replication forks (Figure 1.9) (Ilves et al., 2010; Costa et al., 2011). Finally, CDKs prevent re-replication by inhibiting MCM-7 recruitment until the following cycle, and the S-phase checkpoints safeguard cell cycle progression to maintain the genomic integrity of the replication fork (Pacek and Walter, 2004).

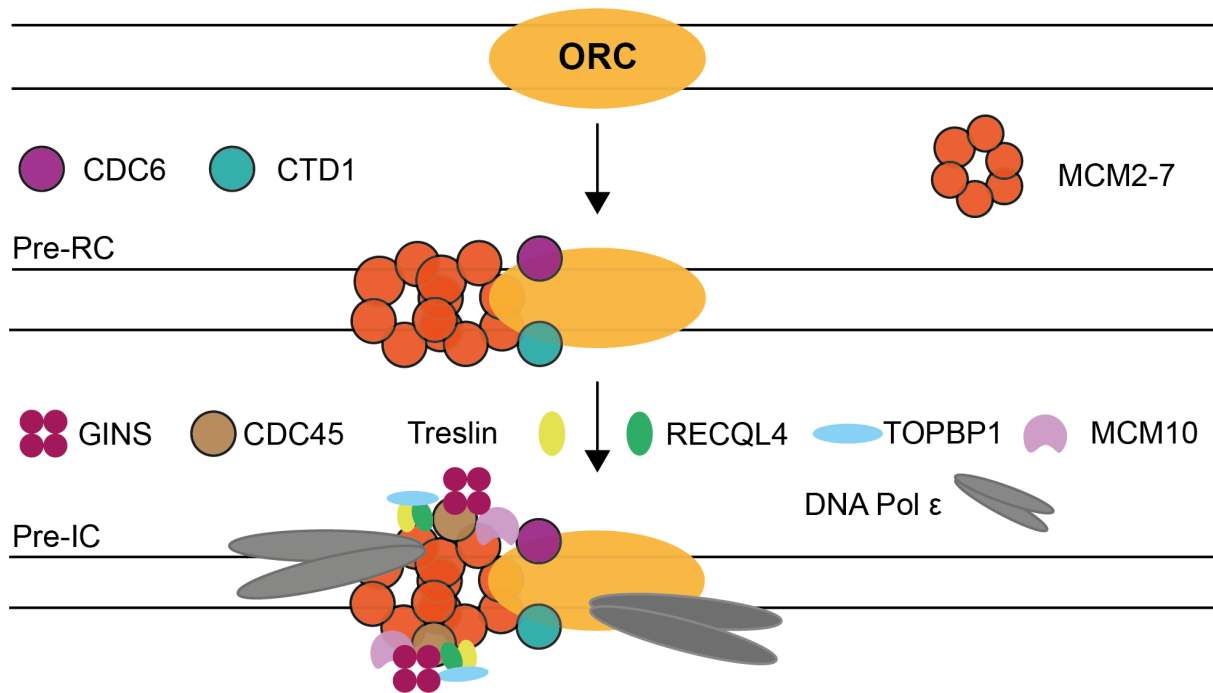


Figure 1.9. Schematic overview of the first steps of DNA replication initiation.

Upon binding to the Origin Recognition Complex (ORC), DNA replication factor 1 (CDT1) and cell division cycle protein 6 (CDC6) are assembled. CDT1 and CDC6 in turn recruit the replicative helicase minichromosome maintenance complex 2–7 (MCM2–7), forming the pre-replication complex (Pre-RC) which prevents re-replication. This triggers the recruitment of other various replication-related proteins including GINS complex, CDC45, Treslin, RECQL4, TOPBP1 and MCM10, that form the pre-initiation complex (Pre-IC) that unwind the duplex DNA to initiate replication.

Due to the complexity and several necessities of replication, many extrinsic and intrinsic factors constantly challenge the integrity of the replicating DNA and in turn, sensitise cells to replication stress. Some of these intrinsic factors include secondary DNA structures, limitation of essential replication components and the occurrence of transcription-replication collisions (reviewed in, Zeman and Cimprich, 2014). As for extrinsic sources of replication stress, examples include; all wavelengths of UV, IR and chemical compounds that are commonly used in laboratory-based research to induce replication stress (Vesela et al., 2017). Some of these chemical replication stress-inducers interfere with DNA replication by inhibiting replicative polymerases

(aphidicolin), directly interacting with DNA (cisplatin), resulting in DNA crosslinks and chemically inhibiting deoxyribonucleotide triphosphate metabolism (hydroxyurea) (Vesela et al., 2017). Importantly, since replication stress is a potent inducer of genomic instability, *in vitro* cell-based research involving models of induced replication stress provides a rich source of knowledge about the underlying mechanisms and interactions that occur during these processes.

1.4.2 The Replication Stress Response

The faithful transmission of genetic information requires an accurate and efficient replication of the genetic material in every cell division, and is a critical determinant of genomic stability. Although cells have adopted specialised pathways to maintain this accuracy, DNA replication is incessantly challenged by both, endogenous and exogenous agents that induce DNA damage, which impede the accurate replication of the DNA. This phenomenon, known as replication stress, is characterised by the stalling or slowing of replication fork progression and/or DNA synthesis, and is the main cause or source of genomic instability (reviewed in, Zeman and Cimprich, 2014). Replication stress can arise from several different sources including but not limited to; ionizing radiation, DNA lesions, nucleotide pool shortage, difficult-to-replicate genomic loci, transcription-replication conflicts, oncogene-induced stress, unscheduled DNA structures (cruciforms, R-loops, DNA repeats, hairpins, G-quadruplexes) and the expression of genomic regions that are particularly vulnerable to replication stress, known as common fragile sites (CFSs) (reviewed in, Zeman and Cimprich, 2014).

Replication stress is typically associated with the formation of long stretches of single-stranded DNA (ssDNA) bound by replicative protein A (RPA). The accumulation of

ssDNA frequently occurs as a result of the uncoupling of replicative helicase from DNA polymerases during replication fork stalling (Pacek and Walter, 2004). This orientation of RPA-coated ssDNA next to the newly synthesised dsDNA typically represents a primer-template junction (Byun et al., 2005). This structure serves as a signalling platform for the activation of the replication stress response, initiated by the recruitment of the conserved protein kinase, Ataxia telangiectasia and Rad3-related (ATR) through its cofactor, ATRIP (ATR-interacting protein) (Zou and Elledge, 2003; MacDougall et al., 2007; Nam and Cortez, 2011). Upon activation, ATR phosphorylates its primary kinase substrate downstream target, CHK1, at Serine-317 and Serine-345 (reviewed in, López-Contreras and Fernandez-Capetillo, 2010). Additionally, ATR phosphorylates the histone variant, H2AX, at Serine-319 (γ H2AX) at its C-terminal early on in the response (reviewed in, Kotsantis, Petermann and Boulton, 2018).

Activation of the ATR-CHK1 pathway essentially results in two key outcomes: inhibition of cell cycle progression and suppression of origin firing at new replication sites (late origins) (reviewed in, Labib and De Piccoli, 2011; Nam and Cortez, 2011). In addition, ATR-CHK1 activity promotes the stabilisation and restart of stalled replication forks (Trenz et al., 2006). This is mainly achieved by ATR-licensed firing of the preserved dormant origins which eventually rescue DNA synthesis at the stalled forks. These events collectively limit the pre-mature entry of un-replicated DNA into mitosis and provide additional time for the faithful completion of DNA replication within replication sites experiencing stress (Woodward et al., 2006; Ge, Jackson and Blow, 2007). If left unresolved, however, sustained replication stress can induce replication fork collapse or breakage, resulting in replication stress-associated DNA double-

stranded breaks (DSBs) at the stalled fork (reviewed in, Cortez, 2019). In this case, the ensuing DSBs lead to the activation of two other DNA damage response kinases, ATM and DNA-PK (section 1.4.3).

1.4.3 The DNA Damage Response

The conversion of ssDNA to replication stress-associated DSBs at stalled forks poses a serious threat to genomic stability (reviewed in, Ciccia and Elledge, 2010). In fact, DSBs are believed to be one of the most detrimental and mutagenic forms of DNA lesions as they lack a template strand that can be used for DNA repair (reviewed in, Helleday et al., 2007). If left unrepaired, DSBs can consequentially drive chromosomal aberrations, which may trigger cell death or carcinogenesis (Varga and Aplan, 2005; Scott and Pandita, 2006; Liu et al., 2017). To counteract these deleterious threats of DSBs, eukaryotic cells have evolved an intricate series of sophisticated mechanisms that sense and respond to DSBs to safeguard the genomic integrity of the cell (reviewed in, Trenz et al., 2006).

The DNA damage response (DDR) is a series of signal transduction events that orchestrates the cellular response to DNA damage and mediates its repair through several downstream effectors (reviewed in, Giglia-Mari, Zotter and Vermeulen, 2011). The DDR is primarily mediated by three kinases, ATR, ATM (ataxia telangiectasia-mutated) and DNA PKs (protein kinases). The replication stress response is mainly controlled by ATR, while ATM and DNA-PK mostly respond to DSBs and contribute to ATR kinase activation under specific conditions (Jazayeri et al., 2006; Buisson et al., 2015; Saldivar, Cortez and Cimprich, 2017). Much of the current understanding of the DDR, however, is based on studies on ATM and ATR activity. These DNA damage checkpoint kinases (ATR and ATM) are crucial components as they act as transducers

that signal for checkpoint activation and activate DNA repair pathways. This activity is essential as it triggers cell cycle arrest in the S-phase, allowing additional time for repair, which prevents the transmission of faulty DNA to the daughter cells (reviewed in, Ciccia and Elledge, 2010) (Figure 1.10).

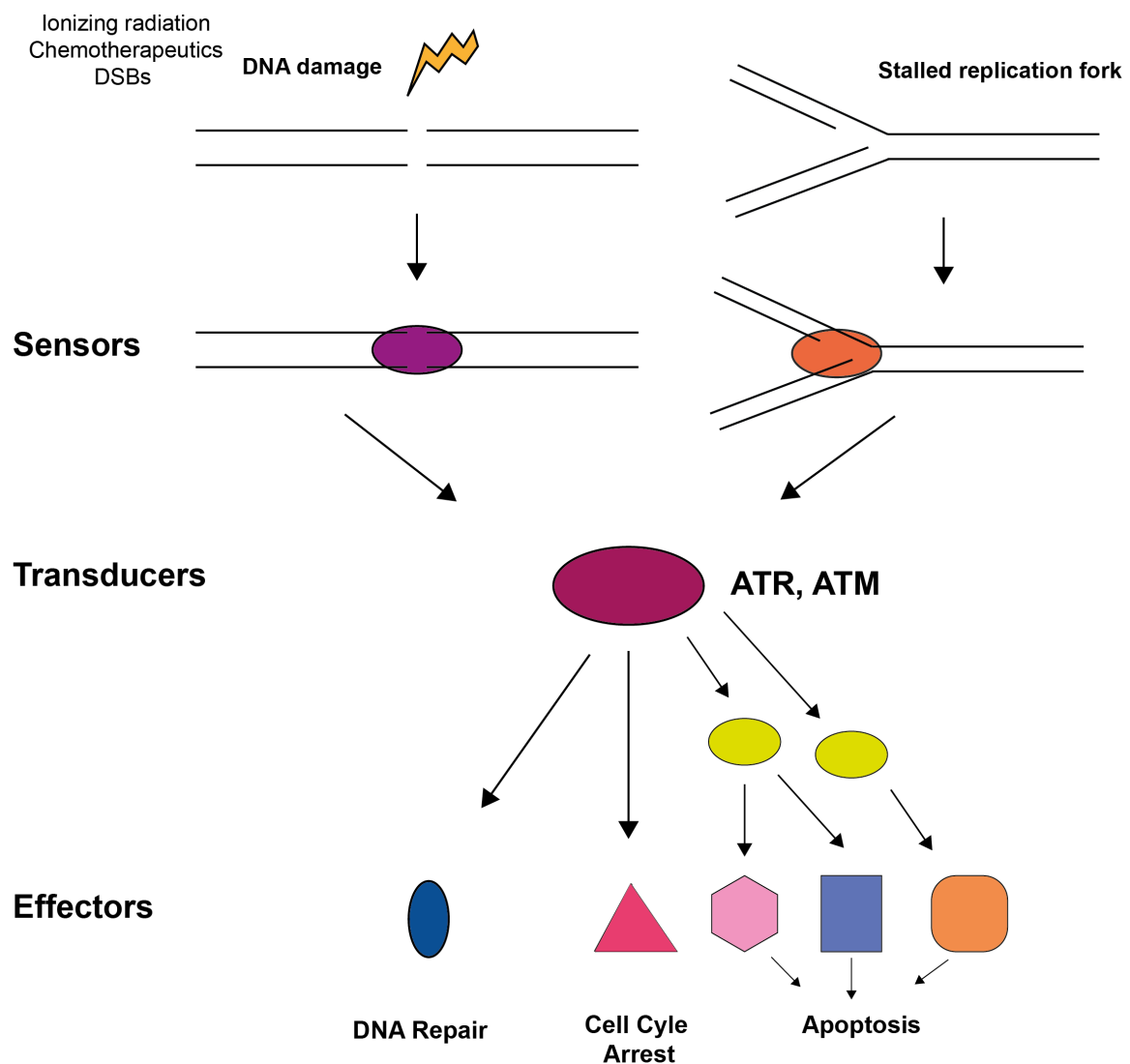


Figure 1.10. Schematic of the basic framework of the DDR signalling pathway.

The DDR signalling pathway is composed of signal sensors, transducers and effectors. Proteins that serve as sensors, recognise DNA regions that are inflicted with DNA damage or replication stress. This leads to the activation of signal transducers, ATR and ATM kinases, and their downstream kinases. In turn, ATR/ATM activation triggers the activation of their downstream substrates (effectors). These effectors mediate a diverse range of cellular processes involved in the preservation of genomic integrity. Adapted from Maréchal and Zhou (2013).

In response to DSBs, ATM is directly recruited by the DSB-sensor protein complex MRE11–RAD50–NBS1 (MRN) at the site of DNA damage (Lee and Paull, 2005). MRN is one of the first factors recruited to DSB sites and is essential for the rapid localisation of ATM to DSBs (Uziel et al., 2003; Lee and Paull, 2005). ATM kinase activity initially induces cell cycle arrest through the activation of the tumour suppressor, p53, and phosphorylation of checkpoint kinase 2 (CHK2) at threonine 68 (Kastan et al., 1992; Matsuoka et al., 2000; Melchionna et al., 2000). CHK2 in turn, phosphorylates the CDK activator CDC25, which suppresses CDK2 activity, thus inhibiting G1/S transition (Falck et al., 2002).

On the other hand, ATR activation is driven by the presence of stalled replication forks and resected DSBs (reviewed in, Cimprich and Cortez, 2008). The persistence of ssDNA-bound by RPA stimulates the recruitment of ATR kinase via co-localisation of ATRIP, along with RAD17–RFC and RAD9–RAD1–HUS1 (9-1-1) (Zou and Elledge, 2003). TOPBP1 also interacts with the 9-1-1 complex and triggers the activity of the ATR-ATRIP complex (Kumagai et al., 2006). Recently, Ewings tumour-related antigen 1 (ETAA1) was also identified as a novel RPA-binding protein that stimulates ATR kinase activity in response to replication stress and DNA damage (Bass et al., 2016; Feng et al., 2016; Haahr et al., 2016). The TIMELESS/TIPIN complex then triggers Claspin binding to RPA, which activates the ATR-downstream substrate, CHK1 (Chini and Chen, 2003; Liu et al., 2006). In turn, CHK1 phosphorylates CDC25A/C CDK activators that inhibit cell cycle progression at S, G2 or G2-M phase (Boutros, Lobjois and Ducommun, 2007). Additionally, CHK1 phosphorylates CDK antagonist WEE1, which causes G2-phase delay (Beck et al., 2012). A schematic overview of the replication stress response driven by ATR is depicted in [\(Figure 1.11\)](#).

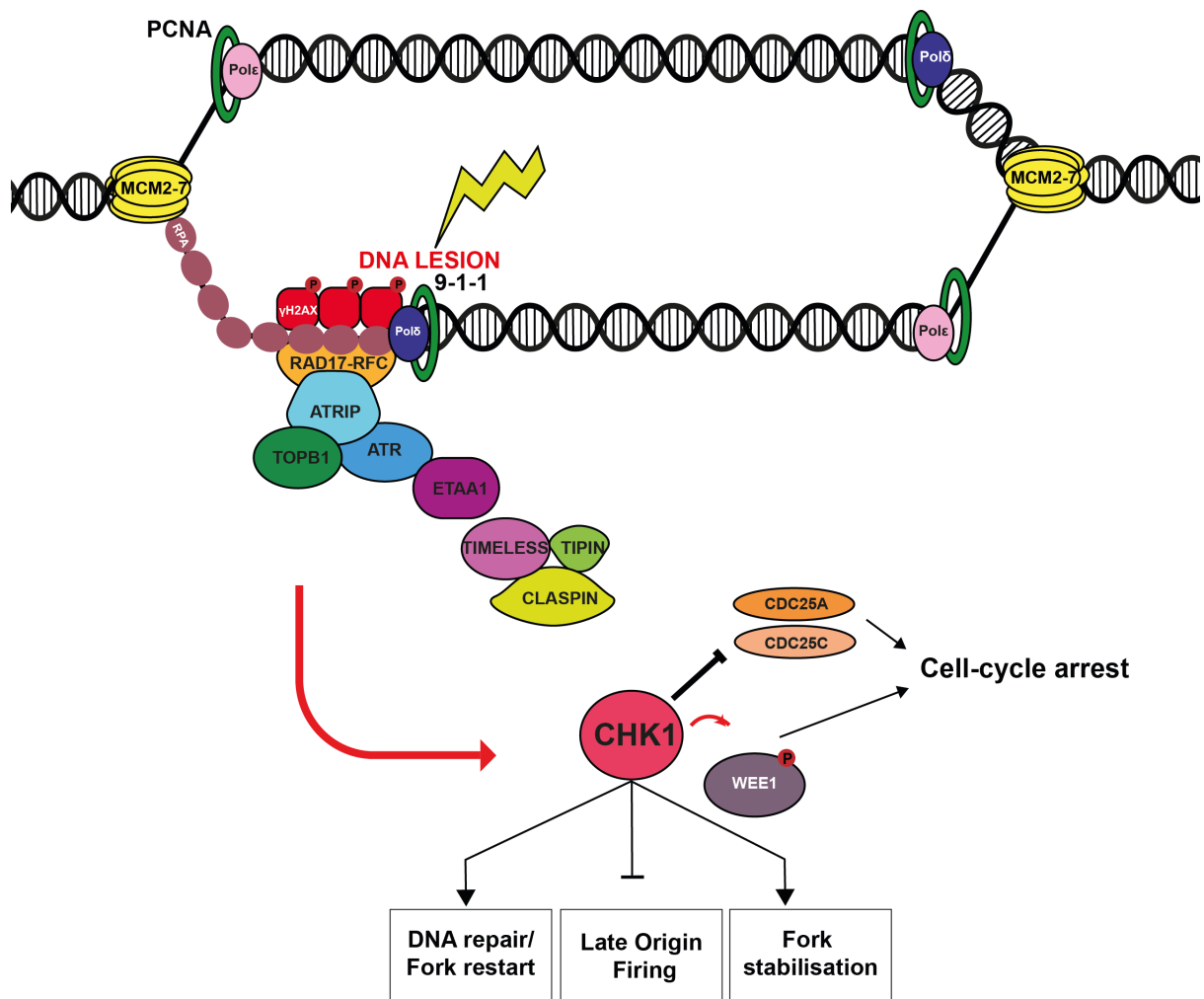


Figure 1.11. The replication stress-induced DNA damage response (DDR).

The persistence of ssDNA-bound by RPA stimulates the recruitment of the ATR kinase through the co-localisation of ATRIP, RAD17–RFC and the 9-1-1 (RAD9–RAD1– HUS1) complex. TOPBP1 and ETAA1 can also contribute to ATR activation. Subsequently, the TIMELESS complex triggers Claspin binding to RPA, which activates the ATR-downstream substrate, CHK1. CHK1 activation leads to the phosphorylation of CDC25A/C CDK activators and CDK antagonist, WEE1, that induce cell cycle arrest. ATR-induced CHK1 activation functions to limit the pre-mature entry of un-replicated DNA into mitosis and provide additional time for the cell to complete DNA replication prior to the next cell cycle.

While ATM and ATR encompass distinct DNA-damage specificities, a crosstalk between these kinases has also been described to occur (reviewed in, Maréchal and Zou, 2013). For instance, ATM was evidenced to phosphorylate CHK1 in response to ionising radiation (IR) (Gatei et al., 2003). On the other hand, CHK2 activation

stimulated by a replication stress-inducing DNA-crosslinking agent (cisplatin), was shown to be triggered in an ATR-dependent manner (Pabla et al., 2008). Following checkpoint activation, ATM, ATR, and DNA-PK stimulate a cascade of DDR events on the DNA damaged chromatin. The most prominent event in this process is the rapid phosphorylation of the histone variant H2AX (γ H2AX) by ATM kinase activity on the chromatin flanking DSBs (Falck, Coates and Jackson, 2005). Although γ H2AX is not required for ATM-dependent phosphorylation of p53 and CHK2, it is essential for the recruitment of numerous DNA repair proteins and chromatin-remodelling complexes to DSBs (Rogakou et al., 1998; Burma et al., 2001). Indeed, γ H2AX foci co-localise with DDR-associated proteins and serve as docking stations for the recruitment of downstream DDR effectors such as MDC1 (mediator of DNA damage checkpoint protein 1) and the E3 ubiquitin ligase RNF8 (Stucki et al., 2005; Kolas et al., 2007; Mailand et al., 2007). Finally, RNF8 and RNF168 signal the recruitment of further ATM-associated mediators including p53-binding protein 1 (53BP1) and breast cancer gene 1 (BRCA1), which promote DSB repair via NHEJ and HR, respectively (Doil et al., 2009; Stewart et al., 2009).

1.4.4 The Pathways of DSB repair

The repair of DSBs is mainly mediated by two distinct pathways; the error-prone non-homologous end joining (NHEJ) and the high-fidelity homologous recombination (HR) (Cahill, Connor and Carney, 2006; Wyman and Kanaar, 2006). Mechanistically, the HR pathway uses a homologous sister chromatid to synthesise and repair the damaged strands on the DNA, while the NHEJ repair pathway directly ligates the DSB site with minimal sequence homology between the broken ends (Helleday et al., 2007). The choice of DSB repair pathway is primarily determined by the nature of the DNA

break and by the phase of the cell cycle (Chapman, Taylor and Boulton, 2012). Since HR requires a sister chromatid, it is restricted to the S and G2-phase, while NHEJ repairs DSBs throughout all phases of the cell cycle (Helleday et al., 2007). Moreover, DSB repair fate by NHEJ and HR is antagonistically regulated by the tumour suppressors 53BP1 and BRCA1, respectively, in a DSB-repair independent manner (Chapman, Taylor and Boulton, 2012). In the G1-phase, 53BP1 caps 5' overhangs of the DSB ends and directs for NHEJ repair (Bunting et al., 2010). During the S/G2-phase, BRCA1 promotes the removal of 53BP1 to allow DSB end resection (Daley and Sung, 2014).

Classical NHEJ (C-NHEJ) is an error-prone DSB repair mechanism that directly rejoins broken DNA ends in a template-independent fashion ([Figure 1.12](#)) (Rodgers and McVey, 2016). In this repair pathway, the DSB ends are initially bound by the Ku70/Ku80 heterodimer, which subsequently signals the recruitment and activation of DNA-dependent protein kinase catalytic subunits (DNA-PKcs) (Uematsu et al., 2007). DNA-PKcs maintain close proximity of DSB ends and if necessary, recruit end-processing factors such as Artemis endonuclease to create compatible ends (Povirk et al., 2007). Following end modification, the DNA ends are finally ligated by a complex consisting of DNA ligase IV, X-ray cross-complementation group 4 (XRCC4) and XRCC4 like factor (XLF) (Ahnesorg, Smith and Jackson, 2006; Gu et al., 2007). Moreover, due to its error-prone trait, NHEJ can often result in frame-shift mutations and a potential premature stop codon, which can consequently cause gene inactivation. Due to this nature, however, NHEJ has been widely harnessed for the mediation of gene knockouts by a number of genome-editing technologies such as the CRISPR/Cas9 gene-editing system (reviewed in, Daley and Sung, 2014). Indeed,

NHEJ constitutes the principle means by which CRISPR/Cas9-introduced DSBs are repaired in the absence of a repair template (Ran et al., 2013) (discussed further in Chapter 3).

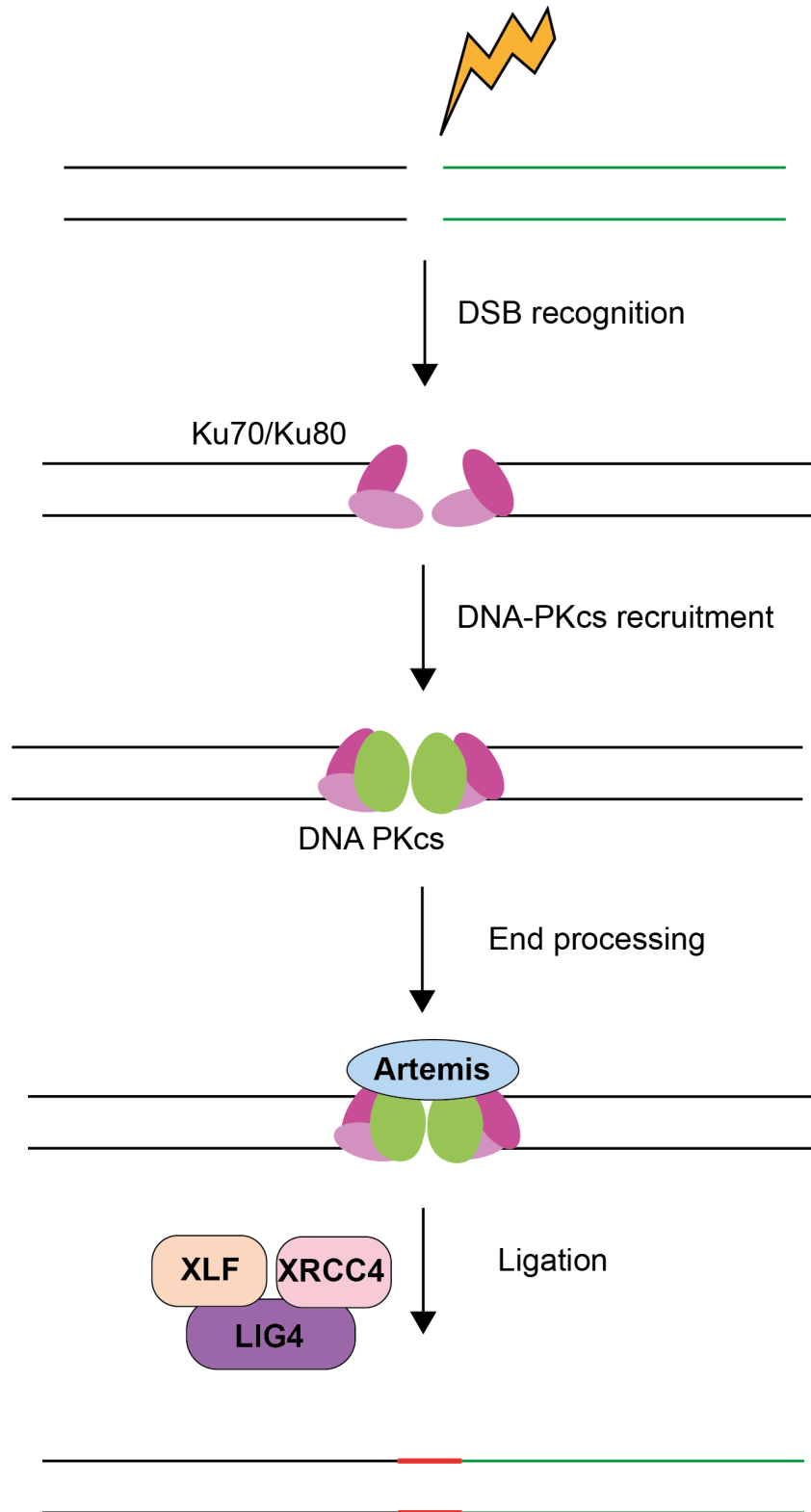


Figure 1.12. Classical Non-homologous end join binding (C-NHEJ) of DSB repair.

During C-NHEJ, the DSB is sensed by the Ku70/Ku80 heterodimer. DSB recognition then signals for the recruitment and activation of DNA PKcs to maintain close proximity of the DSB ends. The DSB ends are then processed by multiple factors including Artemis endonuclease to create compatible ends. Finally, the DNA ends are ligated by DNA Ligase 4 (LIG4), XRCC4 and XLF.

In contrast to NHEJ, homology-directed repair uses a sister chromatid template to accurately re-synthesise damaged DNA in an error-free manner ([Figure 1.13](#)). The HR-mediated repair pathway begins with 5'-3' resection of the DSB ends to generate 3' ssDNA (Heyer, Ehmsen and Liu, 2010). This initial resection process is facilitated by the Mre11–RAD50–NBS1/XRS2 (MRN) complex in conjunction with CtBP-interacting protein (CtIP) nuclease (Limbo et al., 2007; Sartori et al., 2007). Extensive end resection is then further catalysed by EXO1 and DNA2 nucleases along with BLM helicase (Mimitou and Symington, 2009). The produced ssDNA is rapidly bound by RPA to eliminate secondary structure formation and protect against further degradation (Chen, Lisby and Symington, 2013). Subsequently, BRCA2 and Rad51 recombinase paralogues mediate the loading of Rad51 recombinase in the place of RPA, to form a nucleoprotein filament with the 3' ssDNA (Moynahan, Pierce and Jasin, 2001; Tarsounas, Davies and West, 2004; Yang et al., 2005). Nucleoprotein filament formation triggers the search and invasion for a complementary sequence on the dsDNA sister chromatid to restore the damaged DNA end on the ssDNA strand (Sung and Robberson, 1995; Baumann, Benson and West, 1996). This results in the displacement of one of the strands, leading to the formation of a displacement loop (D-loop) structure, which encompasses the 3' end of the invading ssDNA newly annealed to the homologous template (Maher, Branagan and Morrical, 2011). The invading 3' end is then extended by DNA polymerase using the homologous template for DNA synthesis. This HR mechanism is known as recombination-dependent replication (RDR) and is a fundamental pathway of all HR-mediated repair of DSBs (Haber, 1999).

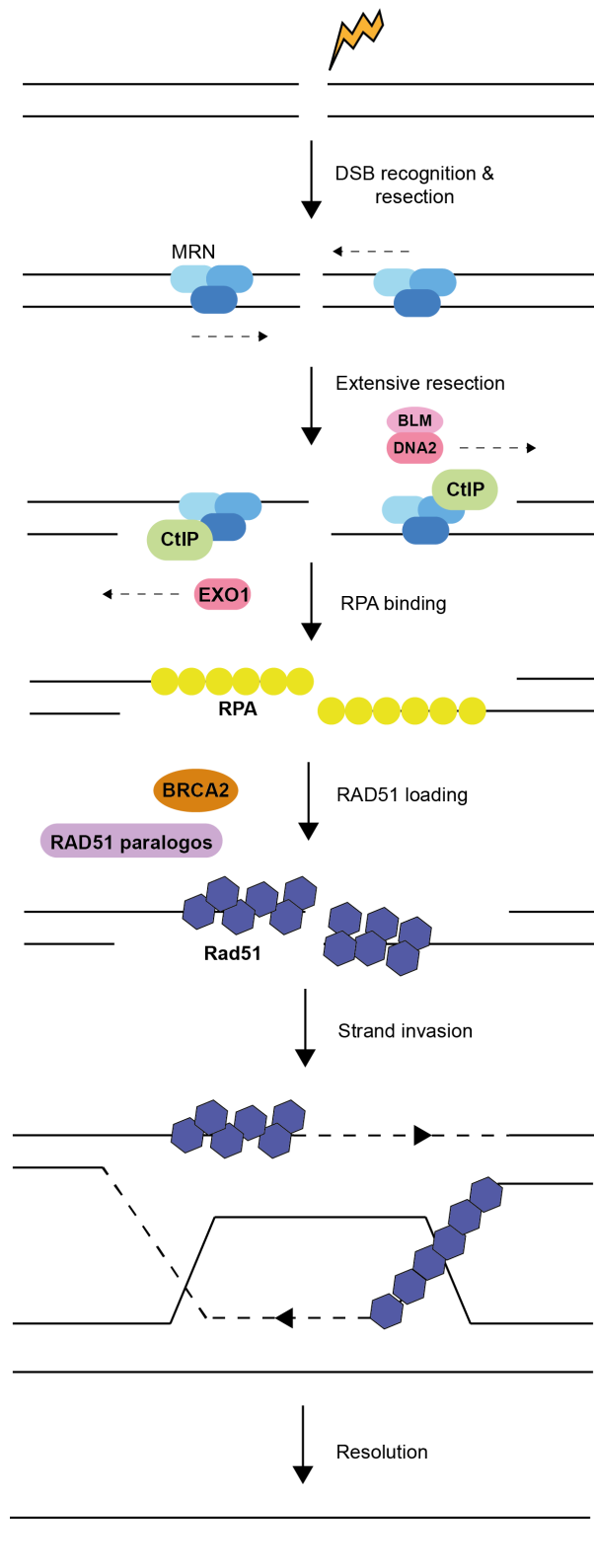


Figure 1.13. DSB repair by Homologous Recombination (HR).

HR is initiated by a resection process mediated by the MRN complex. Extensive resection is then further carried out by EXO1 and DNA2 nucleases along with BLM helicase. The resulting ssDNA is then rapidly bound by RPA to protect against degradation. Subsequently, BRCA2 and RAD51 paralogs mediate loading of RAD51 within the 3' ssDNA in the place of RPA. Lastly, the produced D-loop structure is resolved by RAD51 and the DSBs are re-joined.

1.5 RBPs in the Maintenance of Genomic Stability

Accumulating evidence has revealed novel functions for RBPs, with newly identified key roles in the coordination and maintenance of genome integrity (reviewed in, Dutertre et al., 2014). In addition to allowing selective expression of DDR and DNA repair encoding mRNAs in response to DNA damage using their mRNA regulatory role, certain RBPs have been found to directly bind to DNA damaged sites and interact with various DNA repair proteins (reviewed in, Nishida et al., 2017). Interestingly, several studies have also described RBPs to be post-translationally modified by DDR proteins, altering their DDR-related mRNA target expression and subcellular localisation, in response to DNA damage (reviewed in, Paulsen et al., 2009; Montecucco and Biamonti, 2013; Dutertre and Vagner, 2017). Moreover, pivotal roles for RBPs in the prevention of R-loop (DNA: RNA hybrid) formation, a primary source of replication stress, have also been reported (reviewed in, Santos-Pereira and Aguilera, 2015). Accordingly, RBPs are emerging as crucial factors that protect cells against genomic instability with unexpected biological roles in the DDR and in DNA repair.

1.5.1 RBP Regulation of DDR-related mRNA Targets

In response to DNA damage, certain RBPs have been evidenced to be crucial for the expression of DDR genes via their post-transcriptional regulatory function on targeted mRNAs. Human-Antigen R (HuR), an RBP that binds to AU-rich elements on 3' UTRs on mRNAs and increases mRNA stability, was found to directly bind on 3' UTR regions on p53 mRNAs and enhance p53 expression (Mazan-Mamczarz et al., 2003). In this study, HuR and the tumour suppressor p53 levels were shown to be specifically increased in response to ultraviolet (UV) irradiation, which indicated a protective role

of HuR against DNA damage (Mazan-Mamczarz et al., 2003). Regulation of p53 expression was consistently found to be controlled by other RBPs including PTB and RNPC1 (Grover, Sarothi Ray and Das, 2008; Zhang et al., 2011). Additionally, HuR was reported to be associated with the expression of various critical cell cycle modulators such as, Cyclin D1 and Cyclin E1, as well as with the tumour suppressor and HR-related mediator, BRCA1 (Saunus et al., 2008; Caldon and Musgrove, 2010). Moreover, HuR modulates levels of mRNAs that encode for key DDR-related proteins, proliferation-associated proteins and apoptosis such as 53BP1, MDM2, and p21 and K-Ras in response to IR-induced damage (Wang et al., 2000; Masuda et al., 2011; Mazan-Mamczarz et al., 2011). Importantly, ATM-dependent CHK2 activation was shown to influence HuR phosphorylation and activity in response to DNA damage (Masuda et al., 2011). In particular, CHK2 activation triggered the disassociation of HuR from virtually all of its mRNA targets after IR-induced DNA damage for cell survival in colorectal carcinoma cells (Masuda et al., 2011). More recently, HuR was described to post-transcriptionally regulate the mRNA expression of ARID1A, a tumour suppressor that interacts with TP53 and prevents genomic instability, in breast cancer cells (Andrade et al., 2019). Furthermore, the Ewing Sarcoma (EWS) protein is another multifunctional RBP with established roles in transcription and RNA processing, that has been implicated in the DDR. EWS's alternative splicing function was shown to be associated with mRNA-encoding DNA repair and genotoxic stress signals genes including ABL1, CHK2, MDM2 and MAP4K2 in response to IR-induced DNA damage (Paronetto, Miñana and Valcárcel, 2011). Consistent with its functional role in the DDR, EWS depletion was found to sensitise cells to DNA damage and reduce cell viability and proliferation (Paronetto, Miñana and Valcárcel, 2011).

1.5.2 Direct Roles of RBPs in the DDR

In addition to their regulatory roles in the selective expression of DDR-related mRNAs in response to DNA damage, RBPs have been reported to be directly involved in the DDR (reviewed in, Kai, 2016). A study that conducted genome-wide siRNA-based screens has identified the RBP RBMX (also known as hnRNP G), a heterogeneous nuclear ribonucleoprotein that associates with the spliceosome, as a DDR-associated protein that is functionally essential for resistance against DNA damage (Adamson et al., 2012). RBMX accumulated at DNA lesion sites in a poly(ADP-ribose) polymerase 1 (PARP1)-dependent manner and enhanced HR-mediated repair by ensuring proper expression of BRCA2 (Adamson et al., 2012). In a separate study, RBMX was also demonstrated to contribute to DSB repair by increasing the fidelity of DNA end joining, by binding and protecting DNA ends from nuclease-induced degradation (Shin et al., 2007).

Other members of the hnRNP family of RBPs have also been shown to be directly involved in DNA repair. For example, hnRNP C was identified as a crucial regulator of BRCA1 and BRCA2 expression and a contributor to HR-related DNA repair (Anantha et al., 2013). Indeed, hnRNP C deficiency was found to be associated with reduced HR activity, defective S-phase cell cycle progression, and downregulation of BRCA1, BRCA2 and Rad51 HR-related proteins (Anantha et al., 2013). Further, hnRNP U-like proteins 1 and 2 (hnRNPUL 1 and hnRNPUL 2) were identified as binding partners for the HR-related MRN DSB-sensor complex, in which they triggered DNA-end resection in response to DSB formation (Polo et al., 2012). Intriguingly, this activity was shown to stimulate BLM helicase recruitment to DSBs, which is mediated by MRN and CtIP (Polo et al., 2012). In another study, HnRNPUL 1 activity was additionally shown to

localise to DSB sites in a PARP-1-dependent manner, and has been implicated in the regulation of PARP-1 mRNA as part of the DDR and DNA repair (Hong et al., 2013). Further, the fused in sarcoma/translocated in liposarcoma (FUS) RBP, is another multifunctional member of the hnRNP family whose activity is associated with PARP-1 polymerase, that has been identified as a component of the DDR (Mastrocola et al., 2013; Rulten et al., 2014). In response to laser-induced DSBs, FUS RBP was evidenced to be immediately recruited to DNA damaged sites in a PAR-1 dependent-manner, contributing to HR and NHEJ-mediated repair to preserve genomic integrity (Mastrocola et al., 2013). Consistent with this finding, FUS was further shown to directly bind to PARP-1 *in vitro*, which allows its re-localisation to oxidative damaged sites as part of its response to UVA laser-induced DNA damage (Rulten et al., 2014).

Concomitant with its RNA processing function, the Y-box binding protein (YB-1) is an RNA and DNA-binding protein that interacts with several factors in the DNA duplex and repair system, and is directly involved with specific types of DNA damage (Ise et al., 1999; Gaudreault, Guay and Lebel, 2004). For instance, YB-1 has been shown to contribute to the separation of DNA strands containing stress-induced structures, an activity that is specifically increased towards cisplatin-induced stressed and mismatched DNA (Gaudreault, Guay and Lebel, 2004). In addition to its strand separation function, YB-1 can additionally regulate several DNA repair proteins including Ku80, DNA polymerase δ and MSH2 (Mut S Homolog 2) *in vitro* (Gaudreault, Guay and Lebel, 2004). More recently, the functional role of YB-1 was demonstrated to be directly associated with the DNA mismatch repair (MMR) process (Chang et al., 2014). DNA MMR is a conserved system that detects and repairs erroneous DNA mutations such as base substitutions, deletions and insertions to ensure genomic

integrity (Li, 2008). YB-1 was shown to exert a regulatory role on MutS α binding activity through MMR-related factors which directly impacted mismatch repair activity (Chang et al., 2014).

Finally, the functional role of the RBP with ubiquitin ligase activity, PRP19, has also been implicated in the DDR. Using a proteomic screen for ssDNA-RPA binding proteins, PRP19 was identified as a sensor of DNA damage that directly binds to and ubiquitinates RPA, assisting in the recruitment of downstream DDR proteins (Maréchal et al., 2014). Accordingly, PRP19 was found to localise to DNA damaged sites and promotes the recruitment of ATRIP in response to DNA damage (Maréchal et al., 2014). Importantly, PRP19 deficiency was shown to compromise the activation of ATRIP and replication fork integrity, which emphasised its intricate role in the maintenance of genomic stability (Maréchal et al., 2014). PRP19 activity in supporting the ATR response is specifically attributed to CDC5L, a member of the PRP19 complex, which is essential for ATR downstream signalling (Zhang et al., 2009).

1.5.3 Post-translational Modification of RBPs in Response to DNA Damage

A critical aspect of DDR signalling is the post-translational regulation of DDR-associated proteins by the major upstream signalling kinases (Matsuoka et al., 2007). Importantly, phosphoproteomic screens have identified some RBPs to be directly phosphorylated by DDR sensors such as ATM, ATR and DNA-PK as well as by other downstream kinases (CHK1, CHK2) upon DNA damage ([Figure 1.14](#)) (Bennetzen et al., 2010; Bensimon et al., 2010; Blasius et al., 2011). These DNA damage-dependent post-translational modifications regulate RBP activity and ensure genomic integrity. For example, IR-induced DNA damage triggers ATM-dependent phosphorylation of

hnRNP K and stabilises the RBP's function as a p53 transcriptional cofactor (Moumen et al., 2013). Moreover, DNA damage-dependent RBP phosphorylation can also impact their mRNA binding activity. For instance, the ATM kinase was found to alter the dynamic association of the HuR RBP with its mRNA targets in response to IR-induced DNA damage (Mazan-Mamczarz et al., 2011). Similarly, HuR-mRNA binding was shown to be additionally modulated in a CHK2-dependent manner (Masuda et al., 2011).

In addition to phosphorylation, RBP activity can also be modulated by other post-translational modifications in a DNA damage-dependent manner. PAR polymerase is a nuclear enzyme that signals for the recruitment of DDR-related proteins by catalysing the addition of ADP-ribose elements to DNA, and is a key factor in DSB repair (Caron et al., 2019). Importantly, the recruitment of certain RBPs to DSB sites relies on PAR and PARP activity as previously described (Adamson et al., 2012; Hong et al., 2013; Mastrocola et al., 2013; Rulten et al., 2014). Lastly, large-scale proteomic analysis has revealed that various RBPs are increasingly acetylated upon DNA damage (Beli et al., 2012). However, acetylation of the RBP, SRSF2, was found to decrease its activity in response to cisplatin-induced DNA damage (Edmond et al., 2011). These findings collectively suggested that RBPs may occupy a branch in the DDR signalling network and can be modulated by the DDR transducers in response to DNA damage.

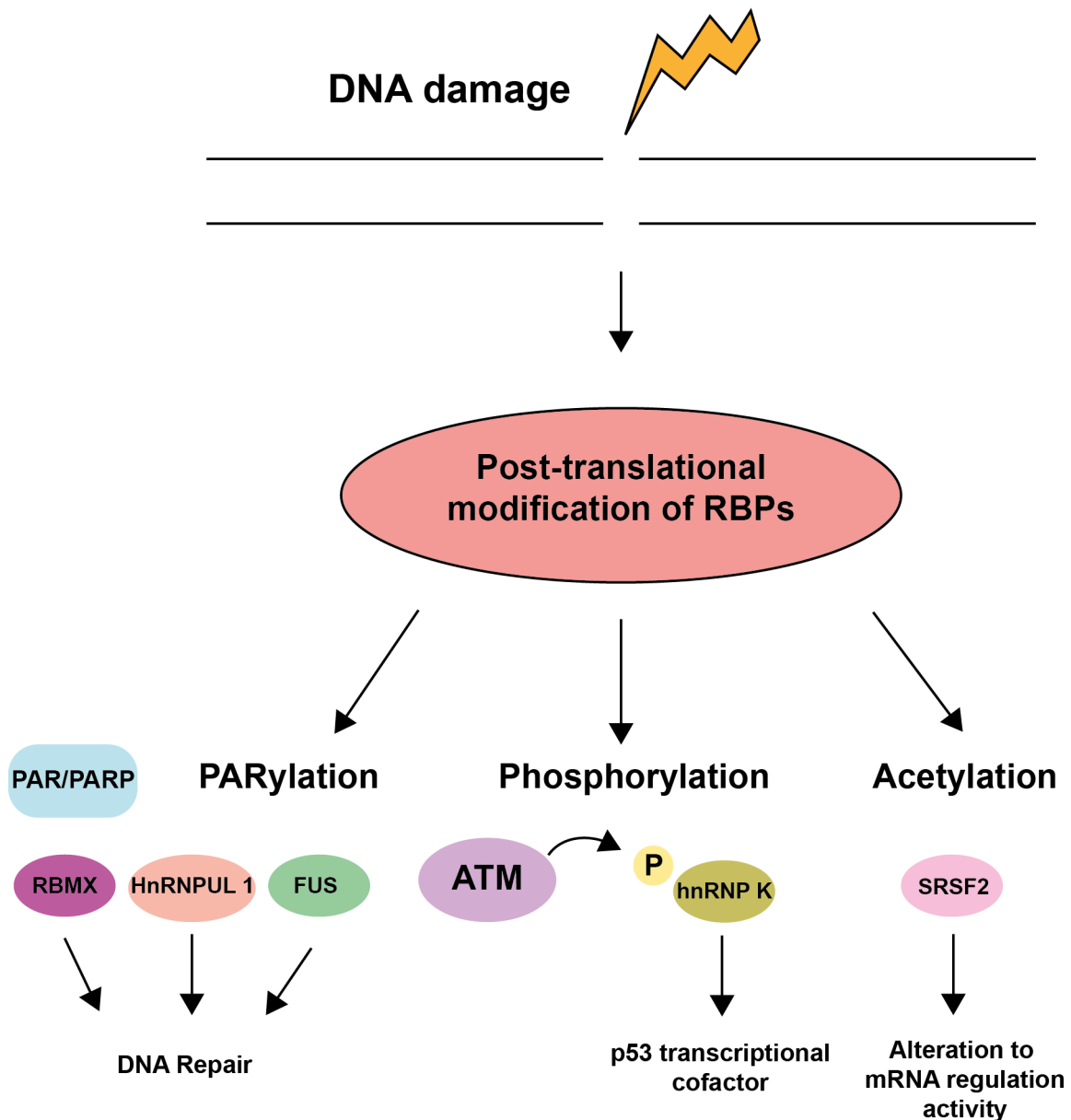


Figure 1.14. Post-translational modification of RBPs in response to DNA Damage.

Upon DNA damage, various RBPs undergo post-translational modifications including parylation, phosphorylation and acetylation. RBPs such as RBMX, hnRNPUL 1 and FUS function in a PAR/PARP-dependent manner and contribute to DNA repair. hnRNP K is phosphorylated by ATM, which in turn modulates its p53 co-factor function. Acetylation of RBPs including SRSF2 alter its mRNA processing activity. These DNA damage-dependent post-translational modifications regulate RBP activity and ensure genomic integrity.

Along with post-translational modifications, DNA damage can also induce subcellular re-localisation of some RBPs which may potentially alter their functional activities. As previously mentioned, DDR activation induces the re-localisation of hnRNP C and

RBMX to DNA damaged sites to promote DNA repair and facilitate the expression of DDR-related mRNAs (Adamson et al., 2012; Hong et al., 2013). Moreover, DNA damage-dependent intranuclear re-localisation has also been reported in some RBPs such as members of the Serine-Arginine (SR) family and EWS (Dutertre et al., 2010; Sakashita and Endo, 2010; Paronetto, Miñana and Valcárcel, 2011). Additionally, the splicing factor RBP, Sam68, was demonstrated to re-localise from the nucleoplasm to nuclear stress granules upon DNA damage, which altered its splicing activities on certain targeted mRNAs (Busà, Geremia and Sette, 2010). Furthermore, several RBPs have been reported to shuttle from the nucleus to the cytoplasm in response to cellular stress including, DNA damage, to further promote their RNA processing activities (Cammass et al., 2008). For example, the PTB RBP translocates from the nucleus to the cytoplasm to facilitate p53 mRNA translation in a DNA damage-dependent manner (Grover, Sarothi Ray and Das, 2008). Similarly, DNA damage-induced nuclear export of HuR was shown to modulate its mRNA processing function (Kim, Abdelmohsen and Gorospe, 2010).

1.5.4 The Functional Roles of RBPs in R-loop Stability

R-loops are three-stranded nucleic acid structures that form during transcription, when the newly transcribed RNA hybridises with one of the DNA templates, leaving the second non-template/hybridised DNA template displaced as ssDNA (Thomas, White and Davis, 1976). This arrangement of the DNA:RNA hybrid in conjunction with the associated non-hybridised exposed ssDNA forms the R-loop structure. While short (8-bp) DNA:RNA hybrids normally form during transcription and replication, R-loops are distinct to these short structures and span a length of 100-500 base-pairs (reviewed in, Santos-Pereira and Aguilera, 2015). The transient formation of R-loops is

functionally relevant to several physiological processes including transcriptional termination, mitochondrial DNA replication, chromatin modifications, regulation of gene expression and telomere dynamics (Lee and Clayton, 1998; Skourti-Stathaki, Proudfoot and Gromak, 2011; Santos-Pereira and Aguilera, 2015). However, stable (unscheduled) R-loops can also represent a major source of endogenous DNA damage, posing a threat to genomic stability. Therefore, it is essential that cells resolve or prevent stable R-loop formation to mitigate their deleterious effects and maintain genomic stability. Remarkably, eukaryotic cells have developed multiple pathways to resolve and prevent R-loop formation, some of which are partially attributed to the activity of certain RBPs (Bhatia et al., 2014, 2017; Santos-Pereira and Aguilera, 2015; Crossley, Bocek and Cimprich, 2019).

Certain RBPs have been proposed to suppress the formation of R-loop structures and subsequent DNA damage by coating the newly transcribed RNA, that in turn, would inhibit its hybridisation with the transcribed DNA template ([Figure 1.15](#)) (reviewed in, Santos-Pereira and Aguilera, 2015). For example, the prototype of the SR family of RBPs, SRSF1, was shown to be recruited to nascent RNA transcripts by RNA polymerase II, which in turn prevented the formation of R-loops (Li and Manley, 2005). Notably, depletion of SRSF1 was associated with a hyper-mutagenic cellular phenotype induced by an R-loop accumulation, which was subsequently converted to DSBs by transcription-coupled nucleotide excision repair factors (Li and Manley, 2005; Sollier et al., 2014). This R-loop suppression activity was consistently shown in two other SR-related proteins, SRSF2 and SRSF3, further supporting the role of SR proteins in the maintenance of genomic stability via R-loop suppression activity (Li and Manley, 2005). Additionally, Topoisomerase 1 (TOP1) has been suggested to

functionally cooperate with SR-related proteins for the proper resolution of R-loop formation through the interaction of TOP1-associated proteins with SR proteins (Pilch et al., 2001; Andersen et al., 2002; Tuduri et al., 2009). Moreover, the TREX/TREX-2 (TRanscription-Export) complex has also been implicated in the suppression of R-loop formation (Strässer et al., 2002; Bhatia et al., 2014) This activity was shown to be achieved through the complexes' functional role in packaging nascent RNAs with several RBPs (Strässer et al., 2002). Indeed, mutations in THO-encoding components (HRP1 and THO2) were shown to elicit a transcription-related hyper-mutagenic phenotype in yeast (Aguilera and Klein, 1990; Piruat and Aguilera, 1998). This THO/TREX transcription-associated genomic instability was later found to be attributed to the accumulation of R-loops (Huertas and Aguilera, 2003). Furthermore, the hnRNP RBP was also shown to inhibit the stabilisation of R-loop structures (Santos-Pereira et al., 2013), corroborating that transcription-associated mRNA processing significantly contributes to preserving genomic integrity.

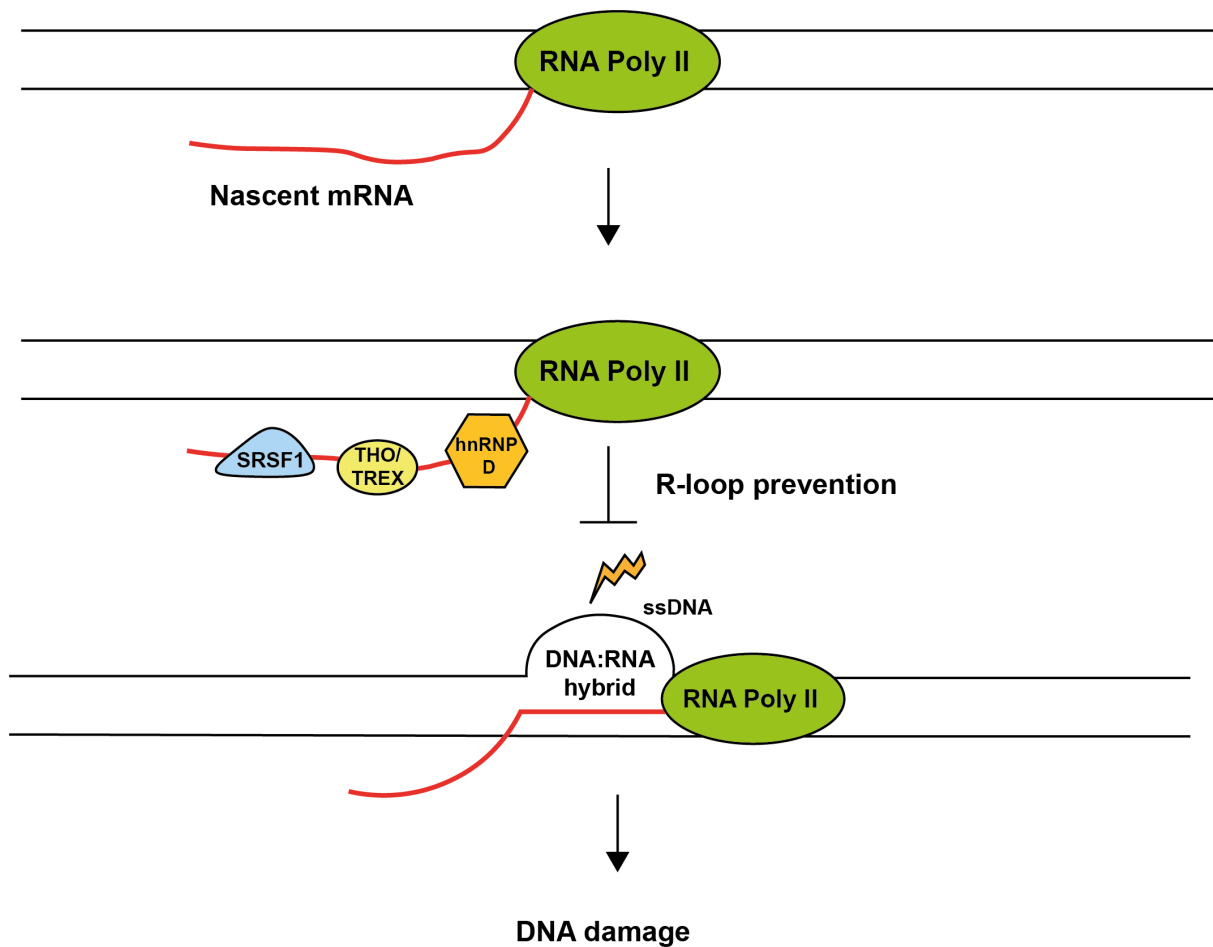


Figure 1.15. RBPs contribute to the prevention of R-loop structure formation. Certain RBPs including SRSF1, THO/TREX and hnRNP D, suppress the formation of R-loop structures by coating the newly transcribed RNA. This in turn inhibits its hybridisation with the transcribed DNA template and prevents the formation of R-loops and subsequent DNA damage.

Undoubtedly, all these studies have indicated that RBPs are emerging as crucial safeguards and coordinators of genomic integrity. Importantly, these studies imply that the multifaceted nature of RBPs may be linked with further unexpected physiological processes in DNA damage sensing, the DDR and DNA repair. Therefore, in an emerging RNA world, investigating the links between RBPs and DDR-related pathways may elucidate their potential role in the maintenance of genomic stability, opening windows for the development of future cancer-targeted therapies.

1.6 The Emerging Role of the ZFP36 Family of RBPs in the Maintenance of Genomic Stability

Similar to other discussed RBPs, members of the ZFP36 family have also been suggested to be potentially critical for the preservation of genomic integrity. For instance, the functional role of ZFP36L1 and ZFP36L2 was demonstrated to be directly associated with limiting cell cycle and DNA damage response signalling, by controlling mRNA transcripts encoding for proteins involved in DDR signalling pathways (Vogel et al., 2016). Intriguingly, DCKO mice lacking ZFP36L1 and ZFP36L2 resulted in elevated levels of the DSB marker, γ H2AX, as well as increased levels of ATM/ATR DDR-related signalling substrates in thymocytes (Vogel et al., 2016). Notably, gene-set enrichment analysis of mRNA transcripts that were significantly increased in ZFP36L1 and ZFP36L2-depleted murine cells included key DDR-encoding mRNAs such as the ATR kinase (Galloway et al., 2016). In fact, expression of ZFP36L1 and ZFP36L2 was found to be essential to ensure the genomic integrity during the development of B lymphocytes (Galloway et al., 2016). Moreover, ZFP36L2 was identified as a cell cycle-regulated protein that contributes to the maintenance of genomic stability, by inhibiting cell cycle progression at the S-phase in response to cisplatin-induced replication stress (Noguchi et al., 2018). Indeed, ZFP36L2-depleted cells were further sensitised to replication stress effects and resulted in defective cell viability due to cisplatin-induced DNA damage (Noguchi et al., 2018). More recently, ZFP36 was interestingly shown to regulate the replication stress response through the post-transcriptional control of mRNA levels of Claspin, an adaptor of ATR-mediated CHK1 activation (Lee et al., 2020). In this study, ZFP36-deficient cells compromised the phosphorylation and activation of CHK1 and exhibited increased CHK1-defective replication cellular phenotypes including DNA DSBs, structural chromosomal

aberrations and stalled replication forks in response to cisplatin and hydroxyurea-induced replication stress (Lee et al., 2020). Additionally, ZFP36 was interestingly found to be essential for replication fork and chromosomal stability even in the absence of exogenous DNA damage, by mechanistically regulating Claspin mRNA stability (Lee et al., 2020).

Together with the recent identification of *ZFP36L1* as a novel cancer driver gene, this compendium of landmark studies has now definitely indicated that ZFP36L1 expression and function may significantly impact the development and progression of human cancers, and that it may potentially encompass protective properties against genomic instability. Consistent with the emerging role of certain RBPs in the preservation of genomic integrity, ZFP36L1's multifaceted functional nature indicates the potential of this protein to be intricately connected to the maintenance of genomic stability, a vital pre-requisite for the suppression of carcinogenesis. However, the molecular mechanisms underlying this link between ZFP36L1 and cancer, particularly from the angle of genomic stability, remains unclear. Thus, the functional characterisation of ZFP36L1 in the preservation of genomic integrity may elucidate some of these underlying mechanisms and open new avenues that may enhance our understanding of cancer aetiology.

1.7 Study Aims

In line with the emerging roles in its preservation of genomic integrity along with its novel tumour-suppressive properties, we intended to explore whether ZFP36L1 may potentially be involved in the maintenance of genomic stability. Therefore, the objective of this work was to investigate the unexplored link between the multifaceted RBP, ZFP36L1, and the suppression of replication stress-induced genomic instability. Given the human osteosarcoma (U2OS) cell line is a well-characterised cellular model with intact (no mutations) in DNA repair pathway-related genes, and has been widely-accepted as a suitable system used for replication stress-based studies (Lukas et al., 2011; Minocherhomji et al., 2015; Chan et al., 2018), we sought study the role of ZFP36L1 in relevance to genomic stability in U2OS cells. Firstly, we aimed to generate cellular models by which ZFP36L1 expression was ablated using the CRISPR/Cas9 gene-editing technology (addressed in Chapter 3). Secondly, we sought to investigate the molecular consequences associated with loss of ZFP36L1 on chromosomal stability, using the generated CRISPR/Cas9-mediated cellular models of ZFP36L1 (addressed in Chapter 4). Thirdly, by using the CRISPR/Cas9-mediated cellular models, we aimed to determine whether the loss of ZFP36L1 was affiliated with increased replication stress induced-DNA damage markers (addressed in Chapter 5). Finally, we intended to explore a possible link between ZFP36L1 and the suppression of CFS expression. Along this line, we sought to characterise the effect of ZFP36L1 deficiency on CFS stability using the generated CRISPR/Cas9-directed cellular models (addressed in Chapter 6).

2 Materials and Methods

2.1 CRISPR gRNA Cloning into pSpCas9(BB)-2A-Puro (PX459) Plasmid

2.1.1 Target Selection for gRNA Design

The *ZFP36L1* gene is located on the antisense strand of chromosome 14. The first 300 base-pairs of exon 2 was selected as the target region for gRNA design (Ensembl transcript ID: ENST00000439696.2; Ensembl Genome Browser). Using an online CRISPR gRNA design tool, (<https://zlab.bio/guide-design-resources>), established by Dr Feng Zhang's laboratory, 3 suitable 20 bp gRNA sequences with the highest on-target binding score were selected. Selected gRNA sequences are listed in [Table 3](#).

Table 3. Selected gRNA sequences.

gRNA	On-target score	Sequence	On-target locus	PAM
1	93	CAGCTCCGTCTTGTAGCGGC	Ch14: -68790409	TGG
2	90	TGTCTCGCGAGCTCAGAGCG	Ch14: -68790302	GGG
3	89	GTCTCGCGAGCTCAGAGCGG	Ch14: -68790301	GGG

2.1.2 gRNA design and oligo annealing

To prepare the selected gRNA constructs for cloning into pSpCas9(BB)-2A-Puro (PX459) plasmid (Addgene, #62988; Appendix B), BbsI overhangs (CACC) that correspond to pSpCas9(BB) BbsI restriction enzyme sites were appended to the 5'-3' top strand followed by an extra Guanine (G) nucleotide as the first preference base of the U6 promoter on each of the selected gRNA oligos. Reverse complementary sequences to the gRNA sequences were added and the gRNA oligos were

synthesised by Eurofins ([Table 4](#)). Oligo phosphorylation and annealing was conducted as previously described in methods by Ran et al. (2013). In brief, 1 μ l of each of the gRNA forward and reverse oligos (100 μ M) were added to 1 μ l of 10x T4 DNA ligase buffer (NEB, #B0202S), 1 μ l of T4 Polynucleotide Kinase Enzyme (NEB, #M0201S) and 6 μ l RNase-free water (ThermoFisher Scientific, #AM9906). The samples were gently mixed and incubated at 95 °C for 5 min and the temperature was then allowed to ramp down to 25°C at room temperature (RT). Phosphorylated and annealed oligos were then diluted at a 1:100 ratio (oligo: RNase-free H₂O) for ligation.

Table 4. Modified gRNA oligos.

gRNA	gRNA oligo sequence	PAM	Supplier
1	5' CACCG CAGCTCCGTCTTGTAGCGGC 3' 3' C GTCGAGGCAGAACATCGCCG CAAA 5'	TGG	Eurofins
2	5' CACCG TGTCTCGCGAGCTCAGAGCG 3' 3' C ACAGAGCGCTCGAGTCTCGC CAAA 5'	GGG	Eurofins
3	5' CACCG GTCTCGCGAGCTCAGAGCGG 3' 3' C CAGAGCGCTCGAGTCTCGCC CAAA 5'	GGG	Eurofins

2.1.3 Restriction digestion of pSpCas9(BB)-2A-Puro (PX459) plasmid

pSpCas9(BB)-2A-Puro (PX459) plasmid was digested as previously described in CRISPR protocol (gRNA cloning) by Addgene, with modifications. In summary, 80 μ l (10 μ g) of pSpCas9(BB) was mixed with 10 μ l of 10x CutSmart Buffer (NEB, #B7204S), 5 μ l of BbsI enzyme (NEB, #R0539S) and 5 μ l of RNase-free water. The sample was then incubated at 37 °C for 2 hrs and BbsI enzyme was heat inactivated

at 65 °C for 10 min. Afterwards, BbsI digested pSpCas9(BB) samples were run on a 0.7% agarose gel at 100V for 30 minutes and DNA fragments from the gel were purified using the Qiagen Gel Extraction kit (cat# 28706) according to the manufacturer's instructions. To dephosphorylate the 5' and 3' ends of BbsI digested pSpCas9(BB), 56 µl (4 µg) of BbsI digested vector DNA was mixed with 8 µl of 10x CutSmart Buffer (NEB), 4 µl Shrimp Alkaline Phosphatase Enzyme (SAP) (NEB, #M0371S) and 12 µl RNase-free water (ThermoFisher Scientific). Samples were then incubated at 37 °C for 30 min, and SAP was then heat inactivated at 65 °C for 5 min. Afterwards, samples were purified using Qiaquick PCR purification Kit (Cat# 28104) as per the manufacturer's instructions.

2.1.4 Cloning gRNAs into pSpCas9(BB)-2A-Puro (PX459) plasmid vector

For gRNA oligo delivery into pSpCas9(BB) plasmid (ampicillin resistant), a ligation reaction mixture was first set up for each of the annealed paired gRNA oligos and BbsI digested pSpCas9(BB) samples using the following: 4 µl of BbsI digested pSpCas9(BB) and 4 µl of 1:100 diluted gRNA oligos were mixed with 2 µl T4 DNA ligase buffer (NEB, #B0202S), 2 µl T4 DNA ligase enzyme (NEB, #M0202S) and 8 µl of RNase-free water. The samples were then incubated in a water bath set at 16 °C in a cold room overnight (O/N). The following day, T4 DNA ligase enzyme was heat inactivated at 65 °C for 5 min. Subsequently, the ligated mixtures were transformed into Subcloning Efficiency DH5α Competent cells (ThermoFisher Scientific, Cat# 18265017) according to the manufacturer's instructions. In brief, 5 µl of the overnight ligation reaction mixture was gently mixed with 50 µl of DH5α competent cells and incubated on ice for 30 min. Cells were then subjected to heat-shock for 20 secs in a 42 °C water bath, placed on ice for 2 min and briefly spun down. 950 µl of pre-warmed

S.O.C medium (ThermoFisher Scientific, #15544034) was then added to each tube and the samples were incubated at 37 °C in a shaker for 1 hr. Subsequently, 300 µl of the transformation mix was then spread on pre-warmed agar plates containing 100µg/ml of ampicillin (Sigma-Aldrich, Cat# 108352001) and incubated at 37 °C O/N.

2.1.5 PCR screen for bacterial colonies harbouring sgRNA-pSpCas9(BB)

To verify for the accurate gRNA oligo construct insertion in pSpCas9(BB) plasmid, several transformed discrete bacterial colonies grown on the agar plates containing ampicillin were initially screened through colony PCR for analysis. Forward primer corresponding to the U6 promoter in pSpCas9(BB) plasmid and reverse complementary primers for corresponding gRNAs were designed and synthesised by Eurofins as summarised in [Table 5](#). Using a sterile pipette tip, half of each of the selected bacterial colonies were picked and prepared for colony PCR. PCR was performed using *Taq* DNA Polymerase PCR Buffer (10x) (ThermoFisher Scientific, #18067017) in accordance with the manufacturer's instructions, with modifications. A 20 µl reaction was prepared on ice for each picked bacterial colony containing the following components: 2 µl of *Taq* DNA Polymerase PCR Buffer (10x), 0.5 µl of dNTP (10mM) (ThermoFisher Scientific, #R0192), 0.5 µl of U6 forward primer (10µM), 0.5 µl gRNA reverse primer (10µM), 0.125 µl of *Taq* DNA Polymerase (ThermoFisher Scientific, #10342020) and 16.375 µl of RNase-free water. PCR was then carried out in a Biorad Mini thermocycler using the following conditions:

- i. 95 °C for 5 min (Initial denaturation)
- ii. 25 cycles of:
 - a. 95 °C for 1 min (Denaturation)
 - b. 50 °C for 30 secs (Annealing)

- c. 72 °C for 20 secs (Extension)
- iii. 72 °C for 5 min (Final extension)

Following PCR, amplified DNA samples were run on a 2% agarose gel at 100V for 1 hr (1 kb DNA Ladder, NEB #3232) and an image was captured using a UVIdoc gel documentation system.

Table 5. Primer sequences used for colony PCR screens.

Name	Target	Sequence	Supplier
U6 Promoter Fw	U6 Promoter	GAGGGCCTATTTCCCATGATTCC	Eurofins
Guide1 Rev	gRNA 1	GCCGCTACAAGACGG	Eurofins
Guide2 Rev	gRNA 2	CGCTCTGAGCTCGCG	Eurofins
Guide3 Rev	gRNA 3	CCGCTCTGAGCTCGC	Eurofins

2.1.6 Sequence validation of pSpCas9(BB)-sgRNA constructs

Following colony PCR, colonies that showed DNA amplicons running at the expected amplicon length of approximately 260 bps were selected for plasmid-miniprep. Using a sterile pipette tip, bacterial colonies were inoculated from each plate into a 5 mL of LB medium (ThermoFisher Scientific, #12780052) with 100µg/ml ampicillin and the cultured cells were incubated in a shaker at 37 °C O/N. The following day, cultured cells were harvested by centrifugation at 5000 rpm for 30 min and the DNA was purified using the Qiagen PCR Purification Kit (#28104) according to the manufacturer's instructions. Potential gRNA containing-pSpCas9(BB) plasmids were then Sanger sequenced from the U6 promoter using the U6 forward primer by Genewiz, UK. DNA Sequencing results were aligned with the pSpCas9(BB) plasmid

backbone (Addgene) to check for the 20 bp insertion of the gRNAs between the U6 promoter and sgRNA scaffold.

2.1.7 gRNA-containing pSpCas9(BB) plasmid amplification by Midiprep

Sequence verified gRNA-cloned into pSpCas9(BB) plasmid DNA was transformed in Subcloning Efficiency DH5 α Competent cells (ThermoFisher Scientific, Cat# 18265017) according to the manufacturer's instructions and method described in section [2.1.4](#) with modifications. In summary, 2 μ l of gRNA-expressed pSpCas9(BB) DNA was transformed in 50 μ l of Subcloning Efficiency Competent cells and 30 μ l of the transformation mixture was spread on agar plates containing ampicillin. Using a sterile pipette tip, a single isolated colony from each plate was inoculated into 5 mL of LB medium with 100 μ g/ml of ampicillin and cultured cells were incubated in a shaker at 37 °C O/N. The next day, 1 mL of each culture was added to 150 mL of LB medium with ampicillin and again incubated at 37 °C O/N. gRNA-expressed pSpCas9(BB) plasmid DNA was then isolated using a Qiagen Midi Kit (#12243) according to the manufacturer's instructions.

2.2 Cell line Manipulation and Generation

2.2.1 Cell lines and culture conditions

Cell lines used in this study were adherent and grown as monolayers at 37°C with 5% CO₂ at saturated humidity in T25 and T75 flasks (Nunc). Human Osteosarcoma U-2 OS (American Type Culture Collection, HTB-96™) and U-2OS H2B-GFP (kindly shared by Dr Kanagaraj Radhakrishnan, The Francis Crick Institute) were grown in Dulbecco's Modified Eagle's Medium (DMEM; ThermoFisher Scientific, #11995065) supplemented with 10% Fetal Bovine Serum (FBS; Sigma-Aldrich, #F-9665) and 1% Penicillin-Streptomycin (P/S) antibiotic (ThermoFisher Scientific, #11548876). U2OS

was initially derived and characterised by Ponten and Saksela (1964) and does not contain mutations in genes related to DNA repair (<https://www.atcc.org/products/htb-96>). U-2OS H2B-GFP cell line was generated from the WT U2OS cell line used in the study (ATCC HTB-96™) and was only modified to constitutively express H2B-GFP, by Dr Kanagaraj Radhakrishnan at The Francis Crick Institute. Cells were sub-cultured at 70-80% confluence. For cell disassociation, cells were washed with phosphate buffered saline (PBS; ThermoFisher Scientific, #10010023) and incubated with 0.05% Trypsin-EDTA (ThermoFisher Scientific, #25300054) at 37°C for 5 min. To neutralise trypsinisation, fresh DMEM media containing FBS serum was added to the detached cells. Cell viability was assessed with 0.4% Trypan Blue Solution (ThermoFisher Scientific, #15250061) and the cell concentration was determined using a standard haemocytometer. Images of U-2 OS were captured using a Leitz Wilovert inverted microscope and Zeiss Axiovert S100 for U-2 OS H2B-GFP cells.

2.2.2 Delivery of gRNA-expressed pSpCas9(BB) plasmid into U2OS cell lines

U2-OS and U-2 OS H2B-GFP cells (0.3×10^5) were grown on 6-well plates in an P/S-free DMEM medium to reach a confluency of 40-50% at the day of transfection. Cells were individually transfected with the three-designed gRNA-expressed pSpCas9(BB) plasmids, using Lipofectamine™ 3000 (ThermoFisher Scientific, #L3000-001) according to the manufacturer's instructions. Succinctly, 5 µl of Lipofectamine reagent was added to 125 µl of Opti-MEM reduced serum media (ThermoFisher Scientific, #A4124801). This solution was mixed with 250 µl of Opti-MEM reduced serum media, 10 µl of P3000 transfection reagent and 5 µg of gRNA-expressed pSpCas9(BB) plasmid, incubated for 10 min at RT and then added to the cells. Both U2OS cell lines were also individually transfected with pSpCas9(BB)-only plasmid (empty vector) and one

without pSpCas9(BB) (-DNA) conditions as negative controls using the same methods described above. 24 hrs post-transfection, the media was replaced with DMEM media containing P/S and incubated at 37°C for 4 hrs prior to puromycin selection. For the generation of U2OS ZFP36L1 K/O, cells were transfected using the same conditions described but with a 48 hrs incubation with the transfection reagents (U2OS ZFP36L1 K/O cell line was generated in collaboration with doctoral researcher, Ahmed Sidali, Genome Engineering Laboratory, University of Westminster).

2.2.3 Puromycin selection of transfected cell lines

Antibiotic selection for cells transfected with gRNA-expressed pSpCas9(BB) plasmid (puromycin resistant) was started off with 1 µg/ml of puromycin (Fisher Scientific, #A11138-03) and the cells were incubated at 37°C for 24 hrs. The following day, puromycin-treated cells were harvested and seeded in 10-cm dishes. Puromycin concentration was increased to 2 µg/ml and incubated at 37°C for 24 hrs. For the generation of U2OS ZFP36L1 K/O, cells were straightaway selected with 2 µg/ml of puromycin and were allowed to be grown till they reached 70% confluency.

2.2.4 Clonal isolation and expansion

Upon the observation of discrete single-cell colonies on the 10-cm dishes, (of which survived puromycin selection), dishes were replenished with fresh DMEM media and the cells were allowed to be grown into individual colonies until the colony size reached a minimum of 200 cells/colony. Discrete cell colonies were isolated from the dishes using cloning cylinders (Sigma-Aldrich, #C1059-1EA). Using sterile forceps, cloning cylinders were placed around the allocated colony and cells were disassociated with 15 µl of 0.05% Trypsin-EDTA then incubated at RT for 3 min. Trypsinised cells were

then neutralised with 50 μ l of DMEM media containing FBS, gently mixed and cells were then transferred to a 96-well plate. At 70% confluency (\sim 1 week), monoclones from the 96-well plates were harvested, seeded in a 24-well plate and were allowed to be grown until the cells reached 70% confluency (\sim 1 week). At the desired confluency in the 24-well plate, monoclonal cells were harvested and expanded in a 6-well plate. For the generation of U2OS ZFP36L1 K/O, cells were harvested from 6-well plates and cultured at a seeding density of 0.9 cells/100 μ l in a 96-well plate for clonal isolation using limiting dilution methods described by ThermoFisher Scientific. A summary of the main experimental design described in sections [2.2.2](#), [2.2.3](#) and [2.2.4](#) is demonstrated as a schematic in [Figure 2.1](#).

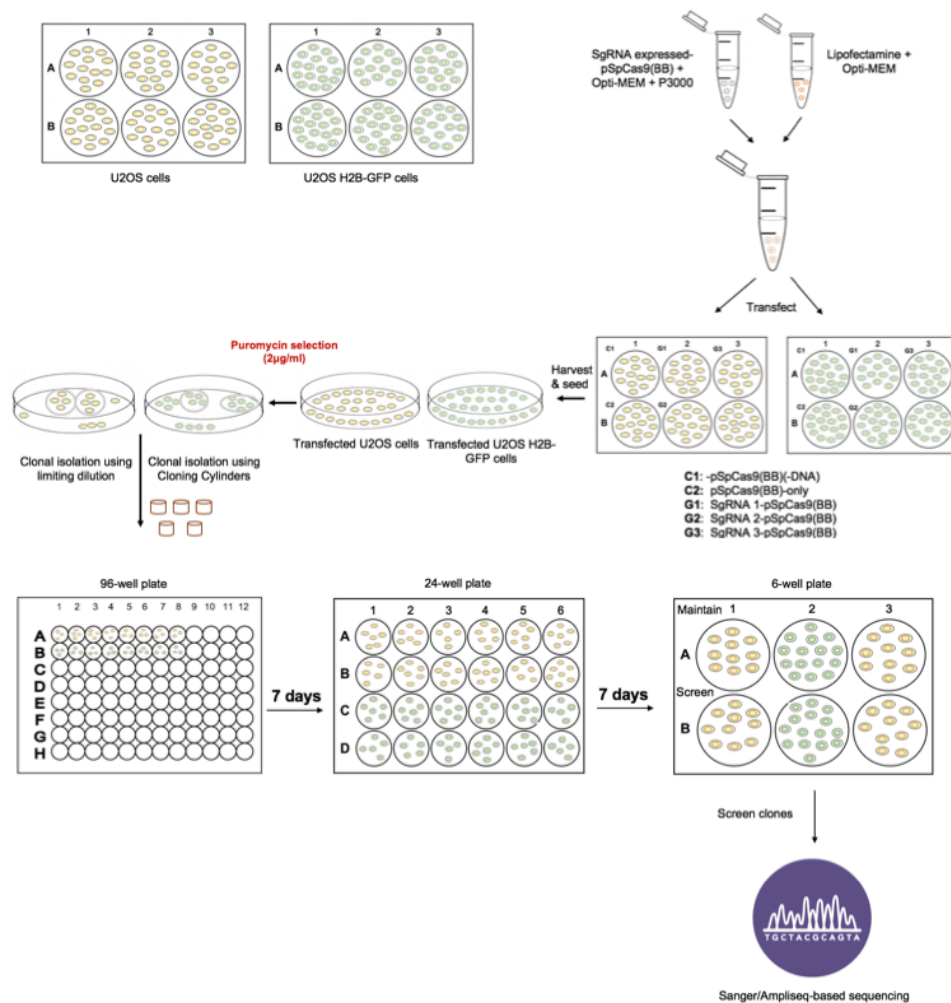


Figure 2.1. Experimental workflow of CRISPR-mediated genome-editing in U2OS cells.

U2OS and U2OS H2B-GFP cells were grown and transfected with sgRNA-expressed pSpCas9(BB). Transfected cells were harvested, plated on 10-cm dishes and selected with 2 µg/ml of puromycin. Discrete single cell colonies were isolated using cloning cylinders or by limiting dilution to obtain single-cell colonies. Single-cell colonies were then expanded and screened for ZFP36L1-targeted genomic mutations/indels using Sanger or Ampliseq-based NGS DNA sequencing.

2.3 Screening and Validation of ZFP36L1-targeted Monoclones

2.3.1 Genomic DNA isolation

To screen for DNA mutations/indels within the targeted region (exon 2) in *ZFP36L1* in U2OS cells, genomic DNA was first isolated using the Qiagen QiaAmp DNA mini kit (#51304) according to the manufacturer's instructions, with modifications. In summary, cells were harvested, washed with PBS and re-suspended in 200 µl of PBS. Cells were then gently mixed with 20 µl of proteinase K and 4 µl of RNase A (Qiagen, #19101) and incubated at RT for 5 min. Next, 200 µl of Buffer AL was added to the cells, mixed by vortexing for 15 secs and incubated at 56°C for 10 min. After a brief spin of the samples, 200 µl of molecular-grade ethanol (Sigma-Aldrich, #E7023) was added, mixed again and vortexed for 15 secs, and briefly spun. Samples were then transferred to QIAmp Mini spin columns and centrifuged at 14,000 rpm for 1 min. Afterwards, spin columns were placed in fresh collection tubes (this was done in every step after centrifugation until DNA elution), 500 µl of AW1 Buffer was added and the samples were centrifuged at 8000 rpm for 1 min. Samples were then mixed with 500 µl of AW2 Buffer and spun at 14,000 rpm for 3 min. Lastly, 80 µl of RNase-free water was added to the spin columns, incubated at RT for 5 min and the DNA was eluted in a fresh tube by centrifugation at 8000 rpm for 1 min. To assess the quality of genomic DNA, samples' purity was analysed using a Nanodrop (ND-1000, ThermoFisher, UK) and run on a 1% agarose gel for 45 min at 100 V, and an image was captured using a UVIdoc gel documentation system.

2.3.2 PCR genotyping screen of ZFP36L1-targeted monoclones

To check for variations within the targeted region in ZFP36L1, position 40-489 of the nucleotide sequence in exon 2 in *ZFP36L1* was PCR amplified from monoclonal genomic DNA for analysis. Forward and reverse complementary primers for the corresponding positions were designed and synthesised as described in [Table 6](#). A 50 µl reaction was prepared for PCR using the following composition: 5 µl of 10x *Taq* Polymerase Buffer, 1 µl of dNTPs (10mM), 1 µl of 10 µM forward primer, 1 µl of 10 µM reverse primer, 5 µl (200 ng) of genomic DNA, 0.25 µl of *Taq* DNA Polymerase and 36.75 µl of RNase-free water. PCR was then carried out in a Biorad Mini thermocycler using the following conditions:

- i. 95 °C for 5 min (Initial denaturation)
- ii. 30 cycles of:
 - a. 95 °C for 1 min (Denaturation)
 - b. 50 °C for 30 secs (Annealing)
 - c. 72 °C for 20 secs (Extension)
- iii. 72 °C for 5 min (Final extension)

After PCR, DNA amplicons were run on a 2% agarose gel at 100V for 45 min (100 bp DNA Ladder, NEB #3231) and PCR samples were DNA purified using the Qiaquick PCR purification kit (#28104) according to the manufacturer's instructions.

Table 6. Primer sequences used for screening ZFP36L1 clones.

Name	Target	Sequence	Supplier
40Fw	Exon 2; Bp #40	CTGCTGGACAGAAAGGCAGT	Eurofins
489Rev	Exon 2; Bp #489	ATCCACAACGCTGAAGAGCGC	Eurofins

2.3.3 Immunoblotting

Cells were harvested and re-suspended in RIPA buffer [50 mM Tris-HCl, (pH 8.0), 150 mM NaCl, 0.1% Triton X-100, 0.5% sodium deoxycholate, 0.1% sodium dodecyl sulphate (SDS), 1 mM sodium orthovanadate, 1 mM NaF and protease inhibitors cocktail tablet (EDTA-free; Roche, #1183617001)] and sonicated for 15 seconds to complete cell lysis. Cellular debris was isolated from soluble fraction by centrifugation at 16,000 g for 20 min at 4 °C. Relative protein concentrations were measured using a spectrophotometer. Equal amounts of protein were subjected to a 10% SDS-PAGE Nupage gel (Invitrogen, #NP0301) at 50V for 5 min then at 150V for 70 min, with MOPS running buffer (Invitrogen, #NP0001) using the XCell Sure Lock Mini-Cell System (ThermoFisher Scientific, #EI001). Separated proteins were transferred to a Hybond-P PVDF membrane (Merck, #IPVH00010) in a wet tank blotting system (BioRad) with Transfer Buffer [25 mM Tris, 190 mM Glycine and 20% Methanol] for 90 minutes at 100V at 4 °C (cold room). The membrane was then stained with Ponceau S (Sigma, #P3504) to check for protein transfer quality then washed twice with TBS-T [20 mM Tris-HCl (pH 7.5), 150 mM NaCl, 0.1% (v/v) Tween-20]. Subsequently, the membrane was blocked with 5% non-fat dry milk in TBS-T for 1 hr. The membrane was then incubated with appropriate primary antibody in 5% non-fat dry milk /TBS-T at 4 °C (cold room) O/N. The next day, the membrane was then washed four times with TBS-T and incubated with appropriate horseradish peroxidase-coupled (HRP) secondary antibody in 5% non-fat dry milk /TBS-T for 1 hr at RT. Following secondary antibody incubation, the membrane was washed four times with TBS-T and bands were detected by WesternSure chemiluminescence reagent (LI-COR) and imaged using a UVP BioSpectrum imaging system. Primary and Secondary antibodies used for immunoblots are summarised in [Table 7](#).

Table 7. Primary and secondary antibodies used for immunoblots.

Target Name	Host	Dilution	Supplier
BRF1/BRF2 (for the detection of ZFP36L1/ZFP36L2)	Rabbit	1:1000	Cell Signaling (2119)
MCM-7 (Minichromosome Maintenance Complex Component 7; loading control)	Mouse	1:1000	Santa Cruz (sc-9966)
Anti-Rabbit-HRP (secondary antibody)	Goat	1:5000	ThermoFisher Scientific (31460)
Anti-Mouse-HRP (secondary antibody)	Goat	1:2000	ThermoFisher Scientific (32430)

2.3.4 Sequence analysis of ZFP36L1 monoclonal lines

PCR products of wild-type ZFP36L1 and mutants/variants (ZFP36L1 K/O and ZFP36L1 N-terminal deletion 2) were prepared as described in [section 2.3.2](#) and Sanger sequenced using the 40-Forward primer. Wild-type ZFP36L1 and mutants, ZFP36L1 N-terminal deletion 1 (U2OS) and ZFP36L1 K/O (U2OS H2B-GFP), were prepared for Ampliseq-EZ-based Next-Generation sequencing according to the Amplicon-EZ service instructions provided by Genewiz (<https://www.genewiz.com/en-GB/>). Sequencing data for all cell lines was generated by Genewiz, U.K. Analysis of CRISPR/Cas9-mediated genome edited sequenced samples was conducted using Clustal Omega (<https://www.ebi.ac.uk/Tools/msa/clustalo/>) for Sanger sequenced data, and CRISPRressor (<https://crispresso.pinellolab.partners.org>) for samples subjected to Ampliseq-NGS. Sequencing data of ZFP36L1 wild-type and ZFP36L1-mutant clonal lines was submitted and successfully processed by NCBI (<https://www.ncbi.nlm.nih.gov/sra>). SRA reference: PRJNA663781.

2.4 Functional Characterisation of ZFP36L1-edited Cell lines

2.4.1 Growth curve analysis

U2OS and U2OS H2B-GFP cells were grown on 6-cm dishes at a seeding density of 50,000 cells/dish (day 0). Cell concentration was determined every 24 hr over a period of five days. Cell counts were made in triplicate on each day using a haemocytometer.

2.4.2 Immunofluorescence

Cells were grown on glass coverslips at a seeding density of 100,000 cells/well in a 6-well plate and individually treated with three concentrations [0.1 μ M, 0.2 μ M, 0.4 μ M] of aphidicolin (Sigma-Aldrich #A0781; IC₅₀: 5 μ M) for 24 hrs to induce mild replication stress. Cells were then washed once with PBS and fixed using PTEMF buffer [20 mM PIPES (pH 6.8), 10 mM EGTA, 0.2% Triton X-100, 1mM MgCl₂ and 4% Formaldehyde (ThermoFisher, #28906)] for 10 minutes at RT. After fixation, cells were washed once with PBS and permeabilised in 0.2% with Triton X-100 (Sigma-Aldrich #T8787) containing PBS for 5 mins at RT. Cells were then washed three times with PBS and incubated with 5mg/ml of BSA/PBS (Sigma-Aldrich, #A9647) with Glycine (20mM) for 15 mins at RT. Next, cells were washed with PBS three times and blocked with BSA/PBS (5mg/ml) for 15 mins. Afterwards, cells were incubated with appropriate primary antibody diluted in BSA/PBS (5mg/ml) overnight at 4 °C. The next day, cells were washed four times with PBS and incubated with the appropriate secondary antibody diluted in BSA/PBS (Sigma, 5mg/ml) in the dark for 1 hr at 37 °C. After incubation, cells were washed four times with PBS, dried and mounted on microscopic slides with Prolong Gold Antifade Mounting Medium containing DAPI (ThermoFisher Scientific, #P36935). Primary and secondary antibodies used for IF staining are summarised in [Table 8](#). Slides were analysed using an upright fluorescent microscope (Olympus BX41)

equipped with an Elite Micropix camera (Micropix Ltd). Images were acquired at 100x using Cytocam software Version 2.0 (Micropix).

Table 8. Primary and secondary antibodies used for immunofluorescence.

Name	Host	Dilution	Supplier
53BP1	Mouse	1:500	Merck (MAB3802)
Cyclin A	Rabbit	1:500	JG Laboratory
RPA32/RPA2	Mouse	1:200	Abcam (ab2175)
Phospo-yH2AX (Ser139)	Rabbit	1:500	Cell Signaling (2577)
PICH	Rabbit	1:200	Cell Signaling (D4G8)
FANCD2	Rabbit	1:500	Novus (NB-100-182)
Alexa Fluor 488 anti-Rabbit IgG	Goat	1:500	ThermoFisher Scientific (A11034)
Alexa Fluor 568 anti-Mouse IgG	Donkey	1:500	ThermoFisher Scientific (A-10037)
Alexa Fluor 555 anti-Rabbit IgG	Donkey	1:500	ThermoFisher Scientific (A32794)

2.4.3 Micronucleus formation assay

Cells were grown on Poly-D-Lysine-coated coverslips (Corning, #354086) in 12-well plates and individually treated with three concentrations [0.1 μ M, 0.2 μ M, 0.4 μ M] of aphidicolin for 24 hrs. Cell culture medium was supplemented 16 hrs before fixation with 2 mg/ml of Cytochalasin B (Sigma-Aldrich, #C6762) to block cells in cytokinesis. Cells were fixed with PTEMF buffer [20 mM PIPES (pH 6.8), 10 mM EGTA, 0.2% Triton X-100, 1mM MgCl₂ and 4% Formaldehyde] for 10 minutes at RT, stained with

appropriate antibodies using immunofluorescence (IF) methods as previously described, and mounted on microscopic slides with Prolong Gold Antifade mounting medium containing DAPI. Images were acquired and analysed as described in section [2.4.2](#). For quantification, only DAPI-stained binucleated cells were counted, and distinct micronuclei in the vicinity of these cells were considered as positive. 300 binucleated cells were scored for each condition per experiment.

2.4.4 Analysis of chromosome segregation

In the same experiment of micronucleus formation (section [2.4.3](#)), chromosome segregation in anaphase cells was examined. Mis-segregated chromosomes including DAPI-positive bulky bridges and lagging chromosomes were quantified. 50 anaphase cells were scored for each condition in each experiment.

2.4.5 Metaphase spreads preparation

Cells were grown in 10-cm dishes and individually treated with three concentrations [0.1 μ M, 0.2 μ M, 0.4 μ M] of aphidicolin for 24 hrs. Cells were then treated with 0.2 μ g/ml of Colcemid (ThermoFisher Scientific, #15212012) to enrich for mitotic cells for 90 mins and collected by mitotic shake-off. Mitotic cells were collected and placed in a 15 mL Falcon tube. The remaining adherent cells were trypsinised, added to the mitotic cells-containing medium and centrifuged at 1000 rpm for 10 min. The supernatant was removed and the cells were washed with PBS. Afterwards, 5 mL of pre-warmed 75 mM KCL hypotonic buffer (ThermoFisher Scientific, #10575-082) was added and the cells were incubated at 37 °C for 15 min. Five drops of freshly prepared fixative (3:1 methanol: acetic acid) (Sigma Aldrich, #179957, #A6283, respectively) was then added to the cell suspension, mixed by inversion followed by centrifugation at 1000

rpm for 10 min. After the removal of the supernatant, cells were fixed with 5 mL of fixative in a drop-wise manner over a vortex, incubated for 15 min and the cells were pelleted by centrifugation again. Fixing steps were then repeated three times with freshly prepared fixative each time in the same manner. After fixation, the pellet was re-suspended in 300 μ L of fresh fixative and the cells were dropped onto slides pre-soaked in cold dH₂O and left to dry O/N. For staining, metaphase spreads were incubated with freshly prepared Giemsa (ThermoFisher Scientific, 10092-013) [7% Giemsa, 500 mM PIPES and Milli-Q H₂O] for 15 min and washed three times with dH₂O prior to mounting. Dried slides were then mounted with DPX mounting medium (Fisher Scientific, #D/5319/05). Metaphase spreads were viewed with a Zeiss Axioskop 2 upright microscope equipped with an Elite Micropix camera (Micropix Ltd). Images were acquired at 100x using Cytocam software version 2.0 (Micropix).

2.4.6 5-ethynyl-2'-deoxyuridine (EdU) labelling in mitotic cells

Asynchronous U2OS cells growing on Poly-D-Lysine-coated coverslips in 6-well plates were synchronised to late G₂-phase of the cell cycle by incubation with 9 μ M of RO-3306 (Sigma-Aldrich, cat# SML-0569) in addition with 0.2 μ M of APH treatment for 16 hrs at 37°C. Cells were then washed three times with PBS and replenished with fresh DMEM medium containing 20 μ M EdU ((ThermoFisher Scientific, cat# C10638) and incubated at 37°C for 35 min. Following EdU incubation, cells were washed with PBS and fixed with PTEMF buffer [20 mM PIPES (pH 6.8), 10 mM EGTA, 0.2% Triton X-100, 1mM MgCl₂ and 4% Formaldehyde] for 10 min at RT. Cells were then processed using the Click-iT Alexa Fluor 555 Cell Proliferation Kit (ThermoFisher Scientific, cat# C10638) according to the manufacturer's instructions with modifications. In brief, a 500 μ L of Click-iT Plus reaction cocktail was prepared containing the following

components: 430 μL of 1x Click-iT reaction buffer, 20 μL of CuSO_4 , 1.2 μL of Alexa Fluor azide, and 50 μL of 10x of Click-iT EdU buffer additive. Cells fixed on coverslips were then incubated with the prepared Click-iT Plus reaction cocktail for 50 min at RT. Subsequently, cells were washed with 3% BSA/0.5% Triton in PBS three times for 5 min each. Afterwards, cells were processed for immunofluorescence for the labelling of anti-FANCD2 using methods described in section [2.4.2](#). Images were captured using an upright fluorescent microscope (Olympus BX41) equipped with an Elite Micropix camera (Micropix Ltd). Images were acquired at 100x using Cytocam software version 2.0 (Micropix).

2.5 Statistical Analysis

Statistical analysis was performed using Graphpad Prism 8 software (GraphPad). Student or Mann-whitney *t*-test were used to analyse significant difference between samples. Statistical details of experiments including number of events quantified, standard deviation, standard error of the mean, and statistical significance, are reported in the figures and figure legends. *P* values ≥ 0.05 was considered not significant. Levels of statistical significance are designated as follows: *, $p < 0.05$; **, $p < 0.01$; ***, $p < 0.001$; ****, $p < 0.0001$.

3 CRISPR/Cas9-mediated Generation of ZFP36L1-knockout and ZFP36L1-mutant Cell lines

3.1 Introduction

The development of efficient and reliable methods to genetically engineer biological systems has tremendously enhanced our ability to elucidate the impact of genetics on human disease. Historically, gene modification relied on chemical and UV-based approaches that were exploited to induce random DNA mutations (reviewed in, Bose, 2016). Although these techniques have contributed to crucial discoveries, they have been hampered by various factors, including their adverse mutagenic impact, time consumption and laborious nature. These limitations, however, were resolved by the advent of the current genome-editing technologies; zinc finger nucleases (ZFNs), transcription activator-like effector nucleases (TALENs) and the CRISPR-Cas nucleases, due to their ability to generate a DSB in the sequence of interest (Wood et al., 2011; Cho et al., 2013; Cong et al., 2013; Mali et al., 2013). ZFNs and TALENs-based technologies use a strategy of tethering engineered sequence-specific DNA-binding domains to a DNA cleavage endonuclease module to induce a DSB at targeted genomic sites (Carroll, 2011; Hockemeyer et al., 2011). By contrast, the endonuclease component of the CRISPR/Cas system, Cas, is guided by short RNAs (gRNAs) via Watson-Crick base pairing with the targeted sequence (Garneau et al., 2010; Jinek et al., 2012). Though the use of ZFNs and TALENs have profoundly contributed to the advancement of biological research, these technologies progress is often hampered by their limited applicability to complex genomes, editing efficiency and ease of customisation (reviewed in, Ran et al., 2013). These disadvantages, however, were circumvented with the recently discovered CRISPR/Cas nuclease

system that provides a simple and efficient alternative genetic tool to ZFNs and TALENs for the production of specific genetic modifications.

The CRISPR/Cas, clustered regularly interspaced short palindromic repeats/CRISPR associated proteins, is a naturally occurring system that has been adapted and engineered to function as a genome-editing tool and one that has revolutionised the field of synthetic biology. Originally discovered as an integral component of the adaptive immune system of numerous archaea and bacteria, the CRISPR/Cas system is an array consisting of short (20-40bp) repetitive DNA sequences (repeats) that are regularly interspaced by non-repetitive DNA sequences (spacers) (Grissa, Vergnaud and Pourcel, 2007). Further studies on bacterial genome sequences revealed that the CRISPR/Cas system plays a significant role in combatting foreign genetic materials including viruses by RNA interference (Barrangou et al., 2007; Jinek et al., 2012). Research conducted on CRISPR-Cas systems has provided researchers with insights into understanding the Cas protein endonuclease function and how through sgRNA modification, the Cas endonuclease can be exploited to facilitate cleavage at sites of interest (Jinek et al., 2012, 2013; Koike-Yusa et al., 2014; Shalem et al., 2014; Wang et al., 2014). The availability of synthesised Cas enzymes and the ability to design the sgRNA component enabled the use of CRISPR/Cas as a genome-editing tool. As a result, CRISPR-Cas systems have paved the way for an efficient, innovative, cost-effective technique to edit, modify and engineer DNA in various cell types and organisms including bacterial, mammalian, and human cells (reviewed in, Ratner, Sampson and Weiss, 2016).

Out of the three types of CRISPR/Cas systems (I, II, and III) that have been classified primarily based on *cas* gene phylogeny, the Type II CRISPR/Cas system, derived from the adaptive immune system of the bacterium *Streptococcus pyogenes* (Sp), is one of the best characterised systems to date (Deltcheva et al., 2011; Makarova et al., 2011; Jinek et al., 2012; Fonfara et al., 2014; Nishimasu et al., 2014). Due to its requirement of only a single and relatively stable Cas protein (Cas9), the Type II CRISPR/Cas9 system has been established as a useful and efficient tool for genome engineering applications (Cong et al., 2013; Wu et al., 2014).

Similar to ZFNs and TALENs, the Cas9 endonuclease facilitates gene-editing by generating a DSB at a specific targeted genomic site. The Type II CRISPR/Cas9 gene-editing system is essentially comprised of two components. The first is a short sgRNA guide sequence that is specifically designed to target a complementary 20 base-pair site upstream of a 5' NGG sequence (also known as the proto-spacer adjacent motif or PAM) within the genomic site (Sternberg and Doudna, 2015). The second is the Cas9 endonuclease that directs the generation of a DSB within the targeted site upon recognising the PAM sequence adjacent to the sgRNA ([Figure 3.1](#)) (Sternberg and Doudna, 2015). Upon cleavage of the genomic locus by the Cas9 protein, the DSB site is then resolved by the cell's endogenous repair machinery through NHEJ or HR, depending on the cell cycle stage and the presence of a repair DNA template (Wyman and Kanaar, 2006). In the absence of a repair DNA template, DSBs are typically resolved via the error-prone NHEJ repair pathway, which often results in mutations in the form of insertions or deletions (indels) (reviewed in, Daley and Sung, 2014). Accordingly, NHEJ can be harnessed to facilitate gene knockouts or disruptions, as mutations occurring within a targeted coding-exon often leads to the disruption of the

open reading frame (ORF), resulting in the inactivation of the targeted gene (Ran et al., 2013).

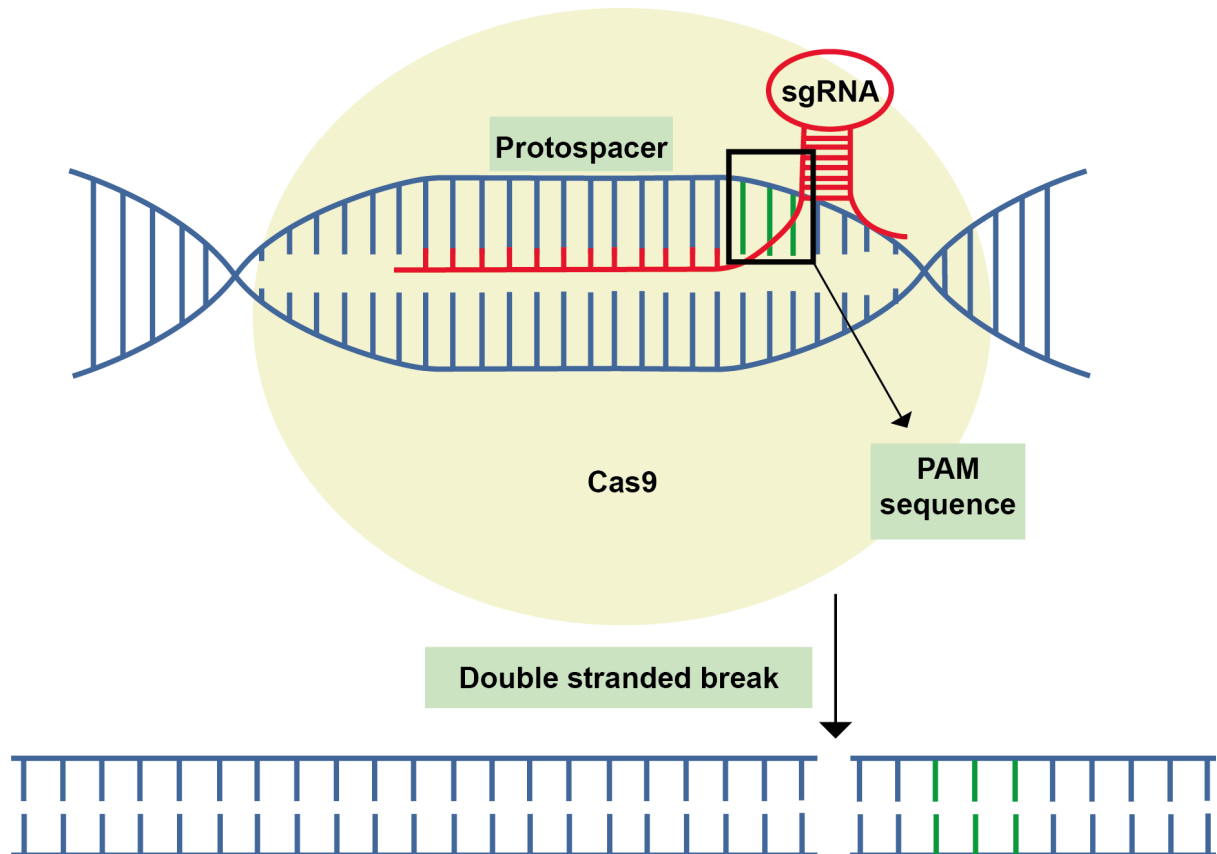


Figure 3.1. Schematic of the mechanism underlying the Type II *Streptococcus pyogenes*-derived CRISPR/Cas9 system.

The sgRNA oligo is designed to target a 20 base-pair site bearing sequence-complementarity that is adjacent to a 3-bp 5' 'NGG' PAM sequence. Upon recognition, the Cas9 endonuclease creates a DSB at the targeted genomic locus near the PAM (NGG) sequence. The resulting DSB can be repaired by the error-prone NHEJ or HDR (in the presence of a DNA repair template) repair pathways (not shown). Adapted from Ceasar et al. (2016).

3.2 Cloning of gRNA oligos into pSpCas9(BB)-2A-Puro Plasmid

To investigate the unexplored role of ZFP36L1 in the suppression of replication stress-induced genomic instability, we first aimed to utilise the CRISPR/Cas9-mediated gene-editing system to functionally disable ZFP36L1 in human cancer cells. In this report, we provide methodological details adapted from Ran et al. (2013), which were used to generate ZFP36L1-mutant and ZFP36L1-knockout cellular models in U2OS and U2OS H2B-GFP human osteosarcoma cell lines as tools of study. Firstly, to determine a suitable target site for gene-editing using the Type II *S. pyogenes*-derived CRISPR/Cas9 system, we analysed the genomic architecture of the human gene *ZFP36L1*, and chose exon 2 as the target region, as it corresponds to more than 90% of the coding region of the gene (www.ensembl.org; CCDS9791). With a base-pair length of 960, exon 2 comprises the coding region for the ZFDs and the highly-conserved lead-in sequences (R/KYKTEL) to the two ZFDs that constitute the *ZFP36L1* gene, both of which play a crucial role in the mRNA binding function of ZFP36L1 (Figure 3.2A). In particular, we selected the first 300 base-pairs of exon 2 on *ZFP36L1* for gRNA oligo design. We anticipated that targeting the early region within exon 2 will increase the likelihood of generating indels early in the coding sequence, which will potentially disrupt the ORF and ultimately result in a knockout of a functional full-length protein. Using Dr Feng Zhang's CRISPR design software (<https://zlab.bio/guide-design-resources>), we selected three generated gRNA oligo sequences with the highest score of on-target binding (details described in section 2.1.1) to maximise the likelihood of knocking-out our chosen target gene with minimal off-target activity (Figure 3.2B).

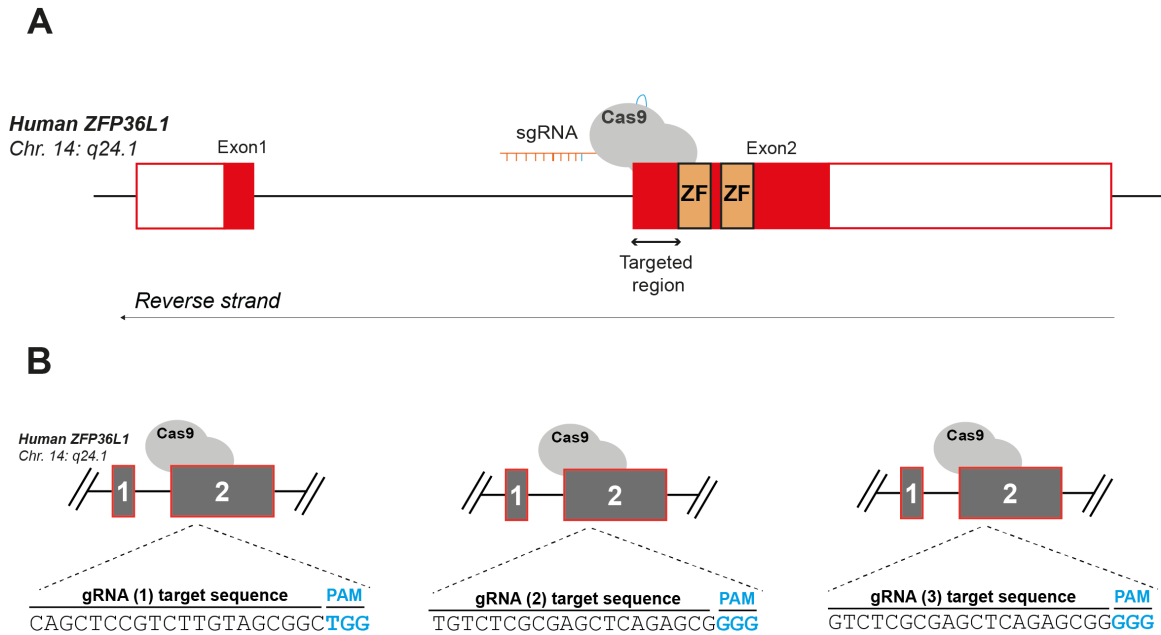


Figure 3.2. Architecture of *ZFP36L1* gene and gRNA targeted genomic sequences.

(A) Schematic illustration of the human *ZFP36L1* gene locus on Chromosome 14: q24.1. The human *ZFP36L1* gene consists of two exons (red boxes). The protein-coding region (mainly encoded by exon 2), encompassing the two putative zing finger motifs (orange) that are essential for *ZFP36L1* RBP function, was selected for CRISPR/Cas9-mediated gene-editing. (B) 20 base-pair sequences preceded by an NGG PAM sequence (blue) targeted by the selected gRNA oligos (1, 2 and 3) on exon 2 of *ZFP36L1*.

To generate sgRNA expressed-pSpCas9(BB) plasmids, we set out to clone the selected gRNA constructs into the sgRNA scaffold of pSpCas9(BB) plasmid vector. It is important to note that we designed the gRNA oligos to include BbsI overhangs and an extra Guanine nucleotide in compatibility with pSpCas9 (BB) BbsI sites and U6 promoter respectively, to achieve ‘scarless’ cloning. To this extent, digestion of pSpCas9 (BB) with BbsI restriction enzyme would allow the replacement of the corresponding restriction sites with the annealed oligos. Following gRNA annealing and pSpCas9 (BB) digestion, we successfully ligated the paired gRNA oligos into the pSpCas9 (BB) vector and transformed the ligation mixture in DH5 α competent cells. A schematic illustration of the methodological steps taken is depicted in [Figure 3.3](#).

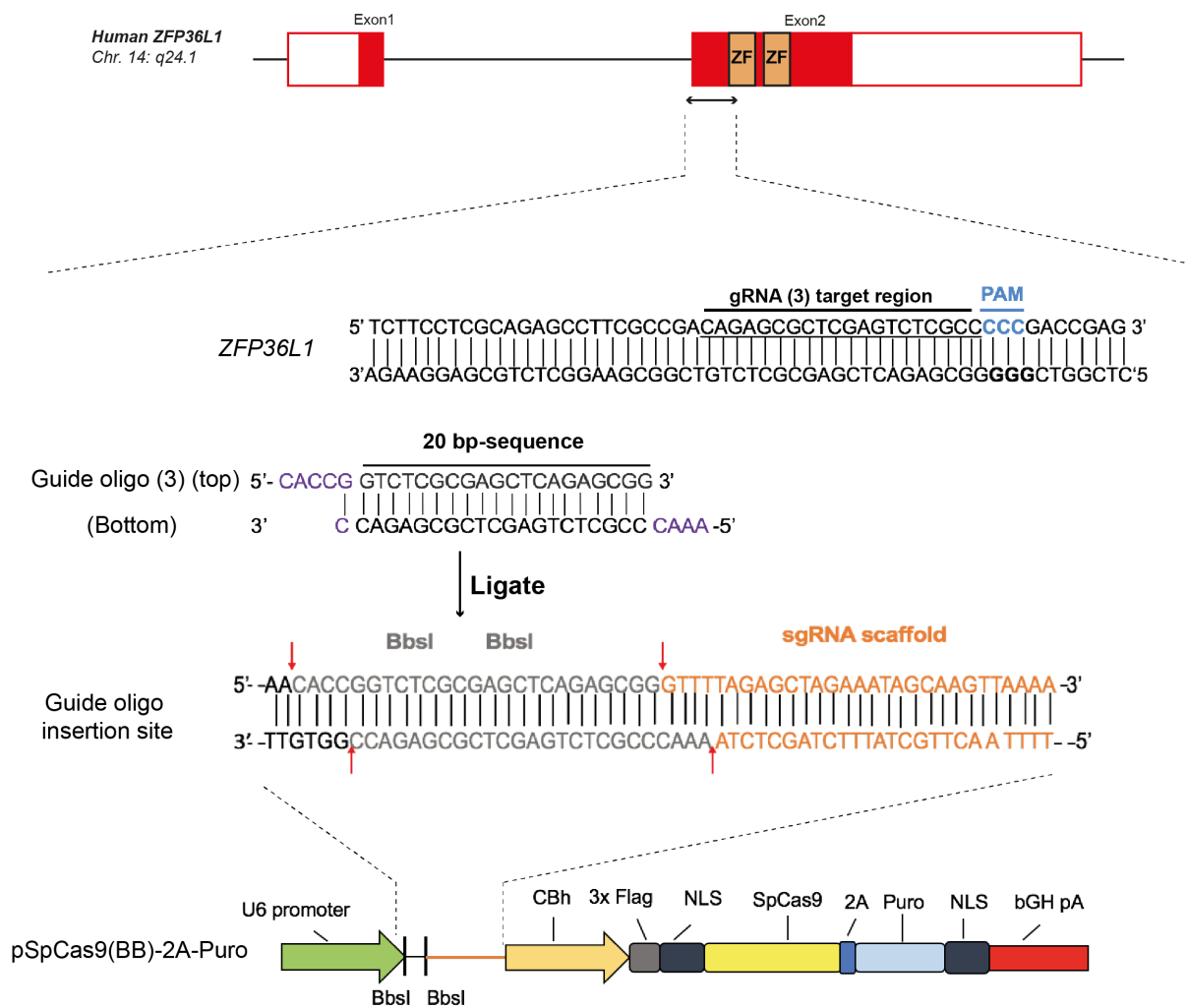


Figure 3.3. Schematic for gRNA design and scarless cloning into pSpCas9(BB).

BbsI overhangs, -CACC-, and an extra Guanine nucleotide (in purple) as a preference for the BbsI sites and U6 promoter on pSpCas9(BB), respectively, were added to the 20-nucleotide selected gRNA sequences (e.g. gRNA 3) for ligation into the pair of BbsI restriction sites in pSpCas9(BB)-2A-Puro plasmid. Digestion of pSpCas9(BB)-2A-Puro with BbsI restriction enzyme allows the replacement (red arrows) of BbsI sites with the annealed guide oligos.

3.3 Validation of gRNA oligo expression in pSpCas9(BB) Plasmid

We then sought to determine the presence of accurate gRNA oligo insertion in the pSpCas9(BB) plasmid by performing colony PCR on over thirty discrete transformed bacterial colonies for analysis. Using forward and reverse primers in correspondence to the U6 promoter and gRNAs respectively, we expected to detect a DNA amplicon length of 260 bps (vector backbone of pSpCas9 (BB) and gRNA constructs). PCR analysis revealed that all of the selected transformed bacterial colonies had potentially harboured the pSpCas9 (BB)-2A-Puro vector with their respective gRNA oligos. DNA amplicons produced a DNA fragment size of approximately 260 bps, in alignment with the DNA marker and positive control, as shown in [Figure 3.4](#).

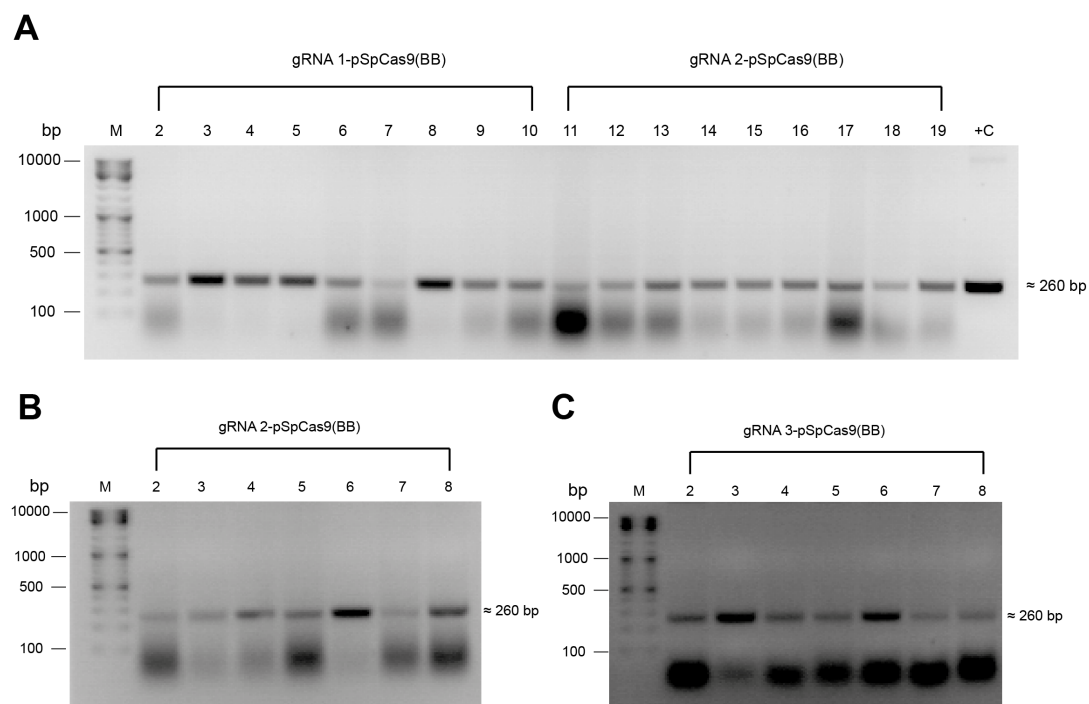


Figure 3.4. Gel electrophoresis of colony PCR screen of gRNA oligos ligated in pSpCas9(BB)-2A-Puro plasmid.

2% agarose gel of colony PCR products amplified from the U6 promoter to oligo constructs. PCR amplicons of (A) pSpCas9(BB)-gRNA 1 (Lane 2-10) and pSpCas9(BB)-gRNA 2 (Lane 11-19), (B) pSpCas9(BB)-gRNA 2 (Lane 2-8) and (C) pSpCas9(BB)-gRNA 3 (Lane 2-8), are shown. PCR amplicons produced an expected DNA fragment of approximately 260 bps. Lane M, 1 kb DNA Ladder. Lane +C; Positive control; a previously cloned and sequence verified sgRNA-expressed pSpCas9(BB)-2A-Puro plasmid.

According to the colony PCR analysis, we noted that all pSpCas9(BB) plasmids appeared to harbour the gRNA constructs. To corroborate our results, 15 suspected positive clones (5 for each designed gRNA) were Sanger sequenced to confirm gRNA oligo insertion in pSpCas9(BB) plasmid and positioned in the accurate orientation. As predicted, Sanger sequencing revealed that the majority (14/15) of the clones screened, carried the gRNA construct and that it was correctly oriented between the U6 Promoter and the remainder of the sgRNA scaffold in the pSpCas9(BB) plasmid (Figure 3.5).

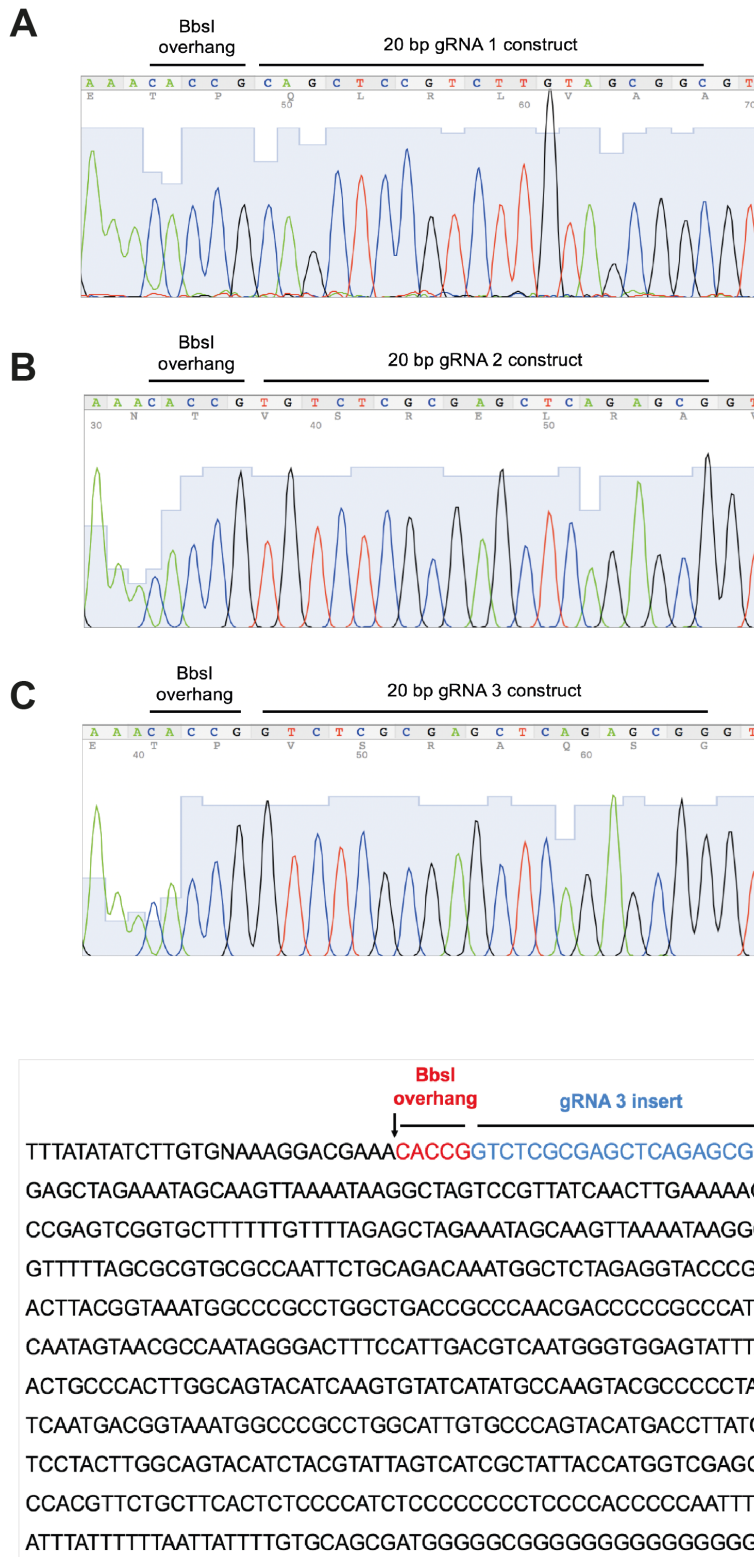


Figure 3.5. Sequence validation of sgRNA-expressed pSpCas9(BB)-2A-Puro plasmid. (A-C) Representative Sanger sequencing chromatograms of (A) gRNA 1, (B) gRNA 2 and (C) gRNA 3 oligos successfully ligated in pSpCas9(BB) vector. (D) Representative DNA sequence of gRNA-expressed pSpCas9(BB)-2A-Puro vector (e.g. gRNA 3) accurately inserted and positioned between the U6 Promoter and the remainder of the pSpCas9(BB)-2A-Puro sgRNA scaffold.

3.4 Cell Line Manipulation and Generation

In attempts to ablate the protein function of *ZFP36L1*, we employed CRISPR/Cas9-directed gene-editing in U2OS and U2OS H2B-GFP osteosarcoma cells using the verified sgRNA-expressed pSpCas9(BB) plasmids. U2OS cells were transfected with pSpCas9 (BB) plasmid expressing SpCas9 and the CRISPR gRNA insert targeting *ZFP36L1*. To increase our success rate in generating a *ZFP36L1* knockout and/or variants, we individually transfected each U2OS cell line with the three sgRNA-expressed pspCas9 (BB) plasmids for target cleavage. Transfection conditions also comprised of transfection controls including untreated/untransfected cells (no DNA/pSpCas9(BB)-2A-Puro) and an empty vector (pSpCas9(BB)-only-2A-Puro) as negative controls, to check for cell health and for any effect of the vector on the targeted-gene expression of the cells, respectively. Importantly, pSpCas9(BB)-2A-Puro plasmid contains a puromycin resistant gene, which allows for the isolation of individual cells that have been transfected with the plasmid by puromycin treatment. Accordingly, post-transfection, U2OS cells were subsequently treated with 2 µg/ml of puromycin to aid in the selection of transfected cells. The next day, we observed discrete single-cell growth with 2-4 cells/colony post-puromycin treatment. Single-cell derived colonies were then allowed to grow to sufficient quantity (minimum number of 200 cells/colony) to aid for their isolation. Potential monoclonal colonies were then isolated from the dishes and expanded for analysis. The experimental workflow in the generation of CRISPR/Cas9-mediated targeting of *ZFP36L1* described above, and examples of puromycin-selected U2OS and U2OS H2B-GFP cells are shown in [Figure 3.6A](#) and [Figure 3.6B](#), respectively.

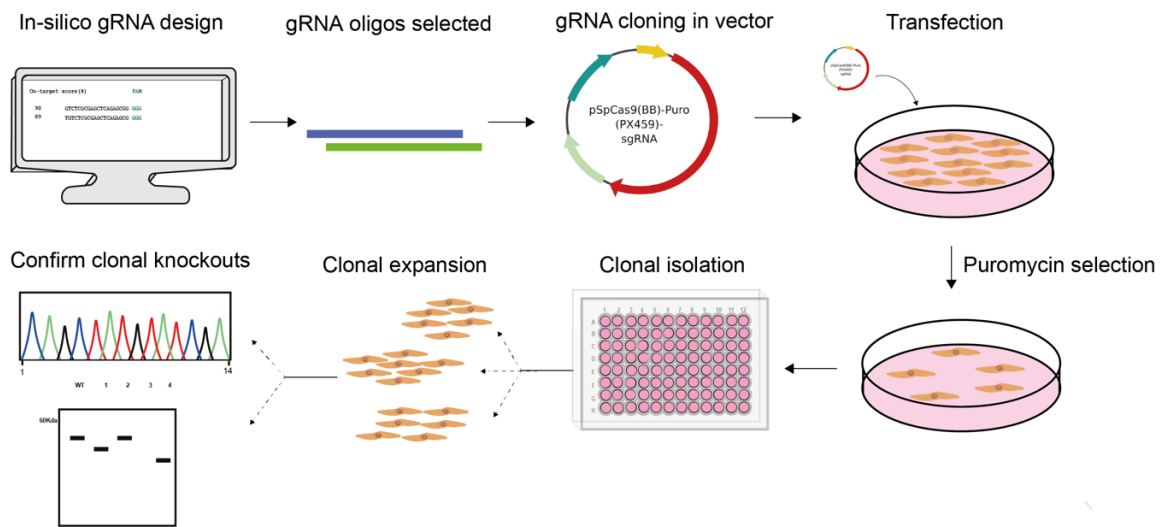
A

Figure 3.6. Experimental workflow of CRISPR/Cas9-mediated gene-editing of *ZFP36L1* in U2OS and U2OS H2B-GFP cells.

(A) Experimental design for the generation of CRISPR/Cas9-directed *ZFP36L1*-mutant clones in U2OS and U2OS H2B-GFP cells. Following *in-silico* gRNA design and synthesis, gRNAs were cloned in pSpCas9 (BB)-2A-Puro plasmid and transfected into U2OS cells. Transfected cells were then selected with 2 $\mu\text{g}/\text{ml}$ of puromycin and single-cell colonies were isolated and expanded for verification via DNA sequencing and western blot analysis.

3.5 Screening for On-target Mutations/Indels

Following single-cell clonal expansion, we sought to examine whether the generated U2OS monoclonal cell lines contained indels or mutations within the targeted region (exon 2) of *ZFP36L1*. To this extent, we initially assessed the targeted DNA region for (micro)deletions by PCR amplification for analysis. The genomic DNA was first extracted from the monoclonal cell lines and primers, both of which were designed to anneal outside of the targeted region, for base-pair positions 40 (Fw) to 489 (Rev) on exon 2 of the *ZFP36L1* gene, were used for PCR amplification. With an expected amplicon length of approximately 450 bps, we assessed the size (bp) of a total of 30 screened monoclonal cell lines and observed an amplicon size smaller than 450 bps in three of U2OS monoclonal cell lines in comparison to U2OS wild-type (WT) (Figure 3.7). In particular, one of the monoclonal cell lines appeared to encompass an amplicon size of approximately 430 bps (Figure 3.7, Lane 3. Generated in collaboration with Ahmed Sidali, Genome Engineering Laboratory) and two of the monoclonal cell lines produced an amplicon size of approximately 350 bps (Figure 3.7, Lane 4 and 5).

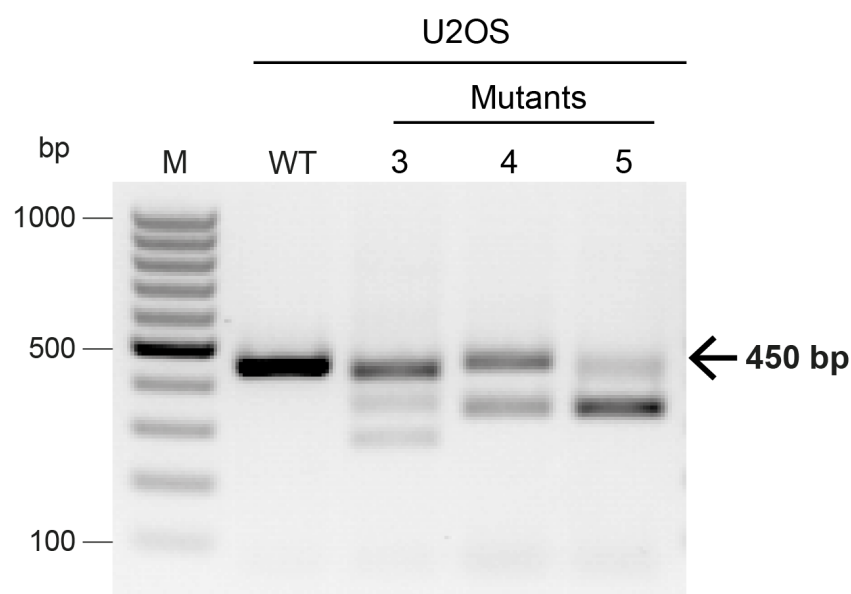


Figure 3.7. Genomic PCR products of *ZFP36L1*-targeted region in U2OS cells.

2% agarose gel of PCR amplified region from position 40-489 on exon 2 of the *ZFP36L1* gene in U2OS monoclonal cell lines. Genomic PCR resulted in DNA amplicons with a size of approximately 450 bps in the WT (Lane 2) with shorter (approximately 430, 350, 350 bps) fragments produced in the mutants (Lane 3-5, respectively) in U2OS cells. Lane M, 100 bp DNA Ladder.

Subsequently, the suspected PCR amplicons/clones were examined for targeted-homozygous or heterozygous mutations via Sanger or Ampliseq EZ-based Next Generation sequencing (NGS) analysis, respectively. As shown in [Figure 3.8B](#), DNA sequence of U2OS clone $\Delta ZFP36L1$, derived from gRNA 3-transfected cells, contained a 17-bp deletion within the targeted region (exon 2) of the *ZFP36L1* gene. Likewise, transfection of U2OS cells with gRNA 3, resulted in two additional clones in U2OS, $\Delta ZFP36L1$ -ND1 and $\Delta ZFP36L1$ -ND2 (ND; N-terminal deletion). Ampliseq EZ-based NGS analysis showed that mutations in the heterozygous $\Delta ZFP36L1$ -ND1 clone, consisted of a combination of deletions, insertions and substitutions near the N-terminal region of *ZFP36L1*. In this particular clone, 59.56% of the reads consisted of 108-bp deletion and 34.74% contained an insertion (Guanine), while only 2.45% and 0.57% of the reads consisted of a 117-bp deletion and substitutions, respectively ([Figure 3.8C](#), Appendix C, C-1). As for the homozygous $\Delta ZFP36L1$ -ND2 clone, a 108-bp deletion was detected, precisely 3 bps upstream of the PAM sequence, as shown by Sanger sequence analysis ([Figure 3.8D](#)).

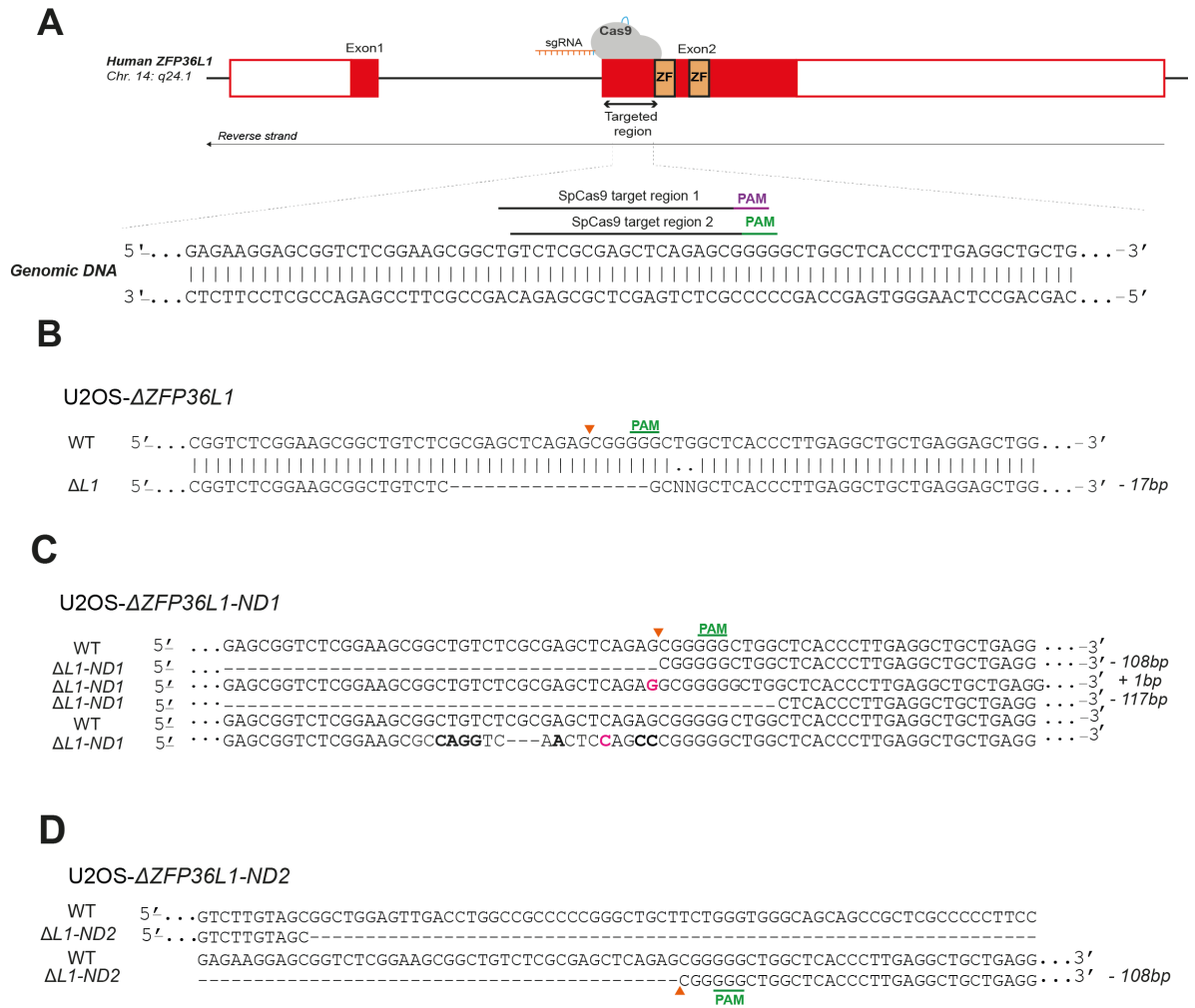


Figure 3.8. DNA sequence analysis of CRISPR/Cas9-mediated ZFP36L1 mutants in U2OS cells.

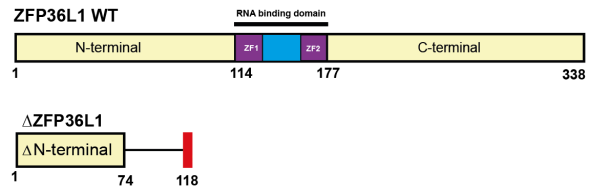
(A) Schematic illustration of the human *ZFP36L1* gene locus located on Chromosome 14 q24.1. 20 base-pair gRNAs genomic target regions on exon 2 and the protospacer-adjacent motif (PAM) sequences coloured in purple (gRNA 2) and green (gRNA 3) are indicated. (B-D) Genomic DNA analysis of the PCR amplified region (450 bps) encompassing the targeted region within exon 2 of *ZFP36L1* in U2OS cells. (B) Sequence alignment of *ZFP36L1* wild-type (WT) and Δ ZFP36L1 with a 17 bp deletion detected (dashed lines). SgRNA PAM sequence (green) and the Cas9 expected cleavage site (orange arrow) are indicated. (C) Next-Generation Sequencing (NGS) analysis of targeted region in *ZFP36L1*, derived from U2OS cells. Sequence alignment of wild-type *ZFP36L1* (WT) and *ZFP36L1*-N-terminal Deletion 1 (Δ ZFP36L1-ND1). Detected nucleotide deletions (dashed lines), insertions (emboldened in pink) and substitutions (emboldened in black) are indicated. (D) Sequence alignment of *ZFP36L1* wild-type (WT) and *ZFP36L1*-N-terminal Deletion 2 (Δ ZFP36L1-ND2) with a 108 bp deletion detected (dashed lines).

Interestingly, analysis of the predicted amino acid translation of the DNA sequences of the ZFP36L1-mutants in U2OS cell lines suggested that the carried mutations in the three ZFP36L1-targeted clones gave rise to a disruption in the ORF of *ZFP36L1* (Figure 3.9). Specifically, the 17-bp deletion detected in the Δ ZFP36L1 clone appeared to introduce an out-of-frame mutation that significantly disrupted the ORF of *ZFP36L1*, causing a premature stop codon downstream of the deletion, indicating a possible no-protein product (Figure 3.9A). Moreover, in addition to the in-frame 108 and 117-bp deletion that occurred in Δ ZFP36L1-ND1 which led to a predicted 35 and 39-amino acid deletion, respectively, the resulting 1-bp (Guanine) insertion in Δ ZFP36L1-ND1 also appeared to cause an out-of-frame mutation, causing a total disruption in the ORF and a premature stop codon downstream of the insertion (Figure 3.9B). Thus, we expected the Δ ZFP36L1-ND1 cell line to produce either a truncated or a non-functional protein product of ZFP36L1. As for the predicted amino acid translation of the Δ ZFP36L1-ND2 cell line, the detected 108-bp deletion appeared to produce an in-frame mutation with a resulting 35-amino acid deletion, which suggested a truncated protein product of ZFP36L1 (Figure 3.9C). Importantly, the 36-amino acid deletion that occurred in both Δ ZFP36L1-ND1 and Δ ZFP36L1-ND2 cell lines, as a result of the 108-bp deletion, included the deletion of the first amino acid (Arginine (R)) of the highly-conserved lead-in sequence (RYKTEL) to the first zinc finger binding domain of ZFP36L1.

A

>ZFP36L1 WT (338 aa)
 MTTTLVSATIFDLSEVLCKGNKMLNYSAPSAGGCLLDRKAVGTPA
 GGGFPRRHVSVTLPSKFFHQQLLSSSLKGEAPALSSRDSRFRDR
 SFSEGERLLPTQKQPGGGQVNSRYKTELCRPFEEENGACKYGD
 KCQFAHGIHELRLSLTRHPKYKTELCRTFHTIGFCPYGPRCHF
 AEERRALAGARDLSADRPRLQHSFSFAGFPSSAAATAATGLLDSP
 TSITPPILSADDLLGSPPTLPDGTNNPFAFSSQELASLAFAPSMGLP
 GGGSPPTTFLFRPMSESPHMFDSPPSPQDLSLSDQEGYLSSSSSSH
 SGGSDSPTLDNSRRLPIFISRLSISDD*

> ΔZFP36L1 17bp del (118 aa)
 MTTTLVSATIFDLSEVLCKGNKMLNYSAPSAGGCLLDRKAVGTPA
 GGGFPRRHVSVTLPSKFFHQQLLSSSLKGE**LARQPLRPLLLGRGR**
AAAAHPEAARGRPGQLQLQDGAVPPPL*



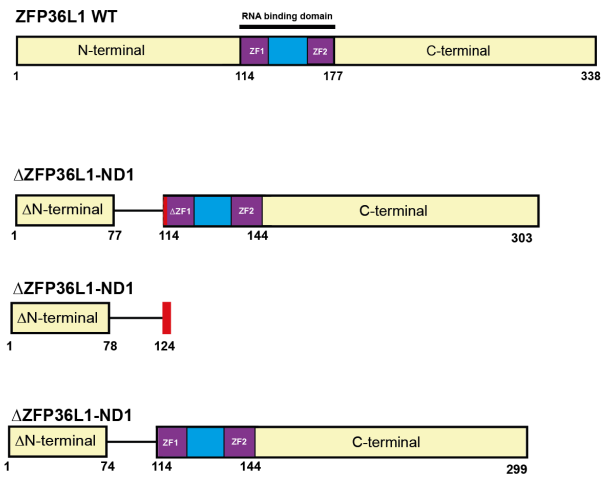
B

>ZFP36L1 WT (338 aa)
 MTTTLVSATIFDLSEVLCKGNKMLNYSAPSAGGCLLDRKAVGT
 PGGGFPRRHVSVTLPSKFFHQQLLSSSLKGEAPALSSRDSR
 FRDRSFSEGERLLPTQKQPGGGQVNSRYKTELCRPFEEENG
ACKYGDKCCQFAHGIHELRLSLTRHPKYKTELCRTFHTIGFCPYG
PRCHFIIHNAEERRALAGARDLSADRPRLQHSFSFAGFPSSAAAT
AAATGLLDSPTSITPPILSADDLLGSPPTLPDGTNNPFAFSSQE
 LASLFAPSMGLPGGGSPPTTFLFRPMSESPHMFDSPPSPQDLS
 SDQEGYLSSSSSSHSGSDSPTLDNSRRLPIFISRLSISDD*

>ΔZFP36L1-ND1 108bp del (303 aa)
 MTTTLVSATIFDLSEVLCKGNKMLNYSAPSAGGCLLDRKAVGT
 PGGGFPRRHVSVTLPSKFFHQQLLSSSLKGEAPALSSRDSR
FEENGACKYGDKCCQFAHGIHELRLSLTRHPKYKTELCRPFEE
NGACKYGDKCCQFAHGIHELRLSLTRHPKYKTELCRTFHTIGFCPY
GPRCHFIIHNAEERRALAGARDLSADRPRLQHSFSFAGFPSSAA
TAAATGLLDSPTSITPPILSADDLLGSPPTLPDGTNNPFAFSSQE
 LASLFAPSMGLPGGGSPPTTFLFRPMSESPHMFDSPPSPQDLS
 SDQEGYLSSSSSSHSGSDSPTLDNSRRLPIFISRLSISDD*

>ΔZFP36L1-ND1 1bp insertion (124 aa)
 MTTTLVSATIFDLSEVLCKGNKMLNYSAPSAGGCLLDRKAVGT
 PGGGFPRRHVSVTLPSKFFHQQLLSSSLKGEAPALSSRDSR
PRPLLLGRGRAAAAHPEAARGRPGQLQLQDGAVPPPL*

>ΔZFP36L1-ND1 117bp deletion (299 aa)
 MTTTLVSATIFDLSEVLCKGNKMLNYSAPSAGGCLLDRKAVGT
 PGGGFPRRHVSVTLPSKFFHQQLLSSSLKGERYKTELCRPFEE
NGACKYGDKCCQFAHGIHELRLSLTRHPKYKTELCRTFHTIGFCPY
GPRCHFIIHNAEERRALAGARDLSADRPRLQHSFSFAGFPSSAA
TAAATGLLDSPTSITPPILSADDLLGSPPTLPDGTNNPFAFSSQE
 LASLFAPSMGLPGGGSPPTTFLFRPMSESPHMFDSPPSPQDLS
 SDQEGYLSSSSSSHSGSDSPTLDNSRRLPIFISRLSISDD*



C

>ZFP36L1 WT (338 aa)
 MTTTLVSATIFDLSEVLCKGNKMLNYSAPSAGGCLLDRKAVGT
 PGGGFPRRHVSVTLPSKFFHQQLLSSSLKGEAPALSSRDSR
 FRDRSFSEGERLLPTQKQPGGGQVNSRYKTELCRPFEEENG
ACKYGDKCCQFAHGIHELRLSLTRHPKYKTELCRTFHTIGFCPYG
PRCHFIIHNAEERRALAGARDLSADRPRLQHSFSFAGFPSSAAAT
AAATGLLDSPTSITPPILSADDLLGSPPTLPDGTNNPFAFSSQE
 LASLFAPSMGLPGGGSPPTTFLFRPMSESPHMFDSPPSPQDLS
 SDQEGYLSSSSSSHSGSDSPTLDNSRRLPIFISRLSISDD*

>ΔZFP36L1-ND2 108bp del (303 aa)
 MTTTLVSATIFDLSEVLCKGNKMLNYSAPSAGGCLLDRKAVGT
 PGGGFPRRHVSVTLPSKFFHQQLLSSSLKGEAPALSSRDSR
FEENGACKYGDKCCQFAHGIHELRLSLTRHPKYKTELCRPFEE
NGACKYGDKCCQFAHGIHELRLSLTRHPKYKTELCRTFHTIGFCPY
GPRCHFIIHNAEERRALAGARDLSADRPRLQHSFSFAGFPSSAA
TAAATGLLDSPTSITPPILSADDLLGSPPTLPDGTNNPFAFSSQE
 LASLFAPSMGLPGGGSPPTTFLFRPMSESPHMFDSPPSPQDLS
 SDQEGYLSSSSSSHSGSDSPTLDNSRRLPIFISRLSISDD*

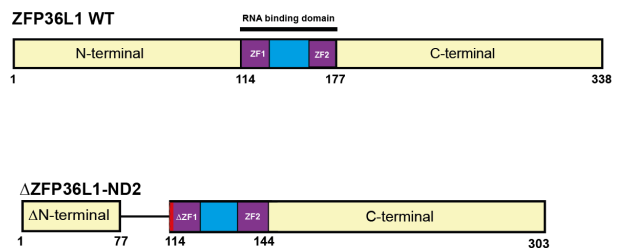


Figure 3.9. Predicted amino acid translation of open reading frames identified in ZFP36L1-mutants in U2OS cells.

(A-C) Translation of detected mutations within the ORF of ZFP36L1 (left) along with corresponding schematic of amino-acid architecture (right) of (A) ΔZFP36L1, (B) ΔZFP36L1-ND1 and (C) ΔZFP36L1-ND2 compared to the WT are shown. Amino acids emboldened in black in ΔZFP36L1 denote amino-acid sequence matching with WT ZFP36L1. Red asterisk represents a premature stop codon.

To investigate whether the detected mutations in *ZFP36L1* translated into an ablation in protein expression, an immunoblot on *ZFP36L1* mutants was conducted. Whole-cell protein extracts were prepared, and a primary antibody that detects both, ZFP36L1 and ZFP36L2 was used, along with an antibody that detects MCM7 protein which was used as a loading control. Western blot analysis of the homozygous mutant, Δ ZFP36L1, showed a full-length knockout of *ZFP36L1* (Δ L1) from the parental U2OS WT cell line with a complete absence/knockout of ZFP36L1 protein expression observed in comparison to WT and empty vector (pSpCas9(BB)-only) (Figure 3.10A, Appendix C, C-2). On the other hand, mutations in Δ ZFP36L1-ND1 (Δ L1-ND1) and Δ ZFP36L1-ND2 (Δ L1-ND2) derived from U2OS cells translated into truncated variants of ZFP36L1 protein. In particular, Δ L1-ND1 appeared to have a lower ZFP36L1 expression than the WT, while Δ ZFP36L1-ND2 produced a higher level of truncated ZFP36L1 protein expression (Figure 3.10A and B). Importantly, ZFP36L2 expression in all cell lines remained unchanged, supporting the specificity of CRISPR/Cas9-mediated gene-editing given DNA sequence similarity between *ZFP36L1* and *ZFP36L2*. Taken together, these results validate the optimised methodological approach that we used to generate truncated and knockout variants of ZFP36L1, and indicate that disruption of ZFP36L1 using the CRISPR/Cas9 system in U2OS cell lines is possible.

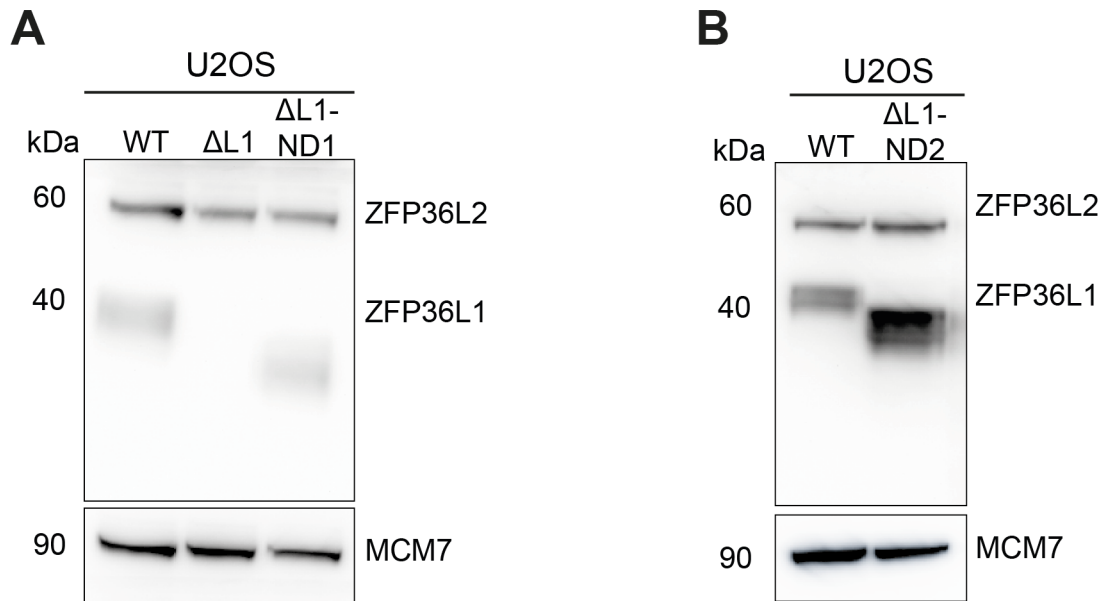
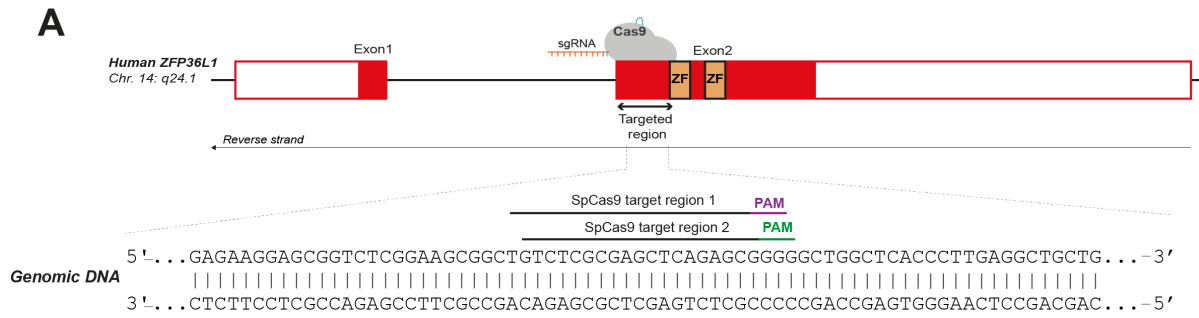


Figure 3.10. Western blot analysis of ZFP36L1 from whole-cell extracts of U2OS cells. (A) Protein expression of wild-type (WT), ZFP36L1 knockout ($\Delta L1$) and truncated ZFP36L1 ($\Delta L1$ -ND1) derived from U2OS cells, using the indicated antibodies. (B) Protein expression of wild-type (WT) and truncated ZFP36L1 2 ($\Delta L1$ -ND2) extracted from U2OS cells, using the indicated antibodies. $\Delta L1$ -ND cells expressed a shorter (truncated) protein of ZFP36L1 compared to ZFP36L1 WT. ZFP36L2 and MCM7 were used as loading controls.

Using the same approach, we were also successful in generating a ZFP36L1-knockout ($\Delta L1$) in U2OS H2B-GFP cells, a cellular model that can be used for the visualisation of chromosome dynamics and the study of various types of nuclear-related processes (Kanda, Sullivan and Wahl, 1998; Yamamoto et al., 2004). Ampliseq EZ-based NGS analysis revealed that the heterozygous gRNA 2-derived $\Delta ZFP36L1$ clone consisted of multiple mutations, including deletions and insertions (Figure 3.11A and B). Specifically, an out-of-frame insertion (Adenine) was detected in 44.78% of the reads, a 41-bp deletion in 27.94% and 25.06% of the reads consisted of a 17-bp deletion, all within the SpCas9 cleavage site, causing premature stop codons in the corresponding ORFs within ZFP36L1 as shown in the predicted amino-acid analysis (Figure 3.11D). Thus, we expected a full-length knockout of ZFP36L1. This was confirmed by immunoblot analysis, which consistently showed ZFP36L1 expression to be completely knocked out compared to the WT (Figure 3.11E).



B

U2OS H2B-GFP- Δ ZFP36L1

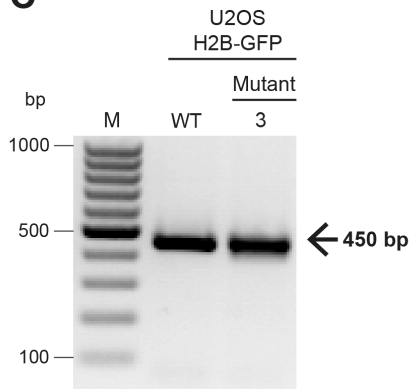
WT 5' . . . AAGCGGCTGTCTCGCGAGCTCAGAGCGGGGGCTGGCTCACCCCTTGAGGCTGCTGAGGAGCTGGTTCTGG . . . 3' -17bp

Δ L1-Del1 5' . . . AAGCGGCTGTCTCGCGAGCTCA-----CCCTTGAGGCTGCTGAGGAGCTGGTTCTGG . . . 3' -17bp

Δ L1-Del2 5' . . . AAGCGGCTGTCT-----GAGGAGCTGGTTCTGG . . . 3' -41bp

Δ L1-Insert 5' . . . AAGCGGCTGTCTCGCGAGCTCAGAAGCGGGGGCTGGCTCACCCCTTGAGGCTGCTGAGGAGCTGGTTCTGG . . . 3' +1bp

C



D

>U2OS H2B-GFP Δ ZFP36L1 1bp insertion (124 aa)

MTTTLVSAIFDLSEVLCKGNKMLNYSAPSAGGCLDRKAVGTPA
GGGFPRRHSVTLPPSSKFHQNLQLSSLKGE~~ELARQPLRPL~~
LLGRGAAAAHPEAARGRPGQLQLQDGA~~V~~PPL*

>U2OS H2B-GFP Δ ZFP36L1 17bp del (118 aa)

MTTTLVSAIFDLSEVLCKGNKMLNYSAPSAGGCLDRKAVGTPA
GGGFPRRHSVTLPPSSKFHQNLQLSSLKGE~~ELARQPLRPL~~LLGRG
RAAAAHPEAARGRPGQLQLQDGA~~V~~PPL*

>U2OS H2B-GFP Δ ZFP36L1 41bp del (132 aa)

MTTTLVSAIFDLSEVLCKGNKMLNYSAPSAGGCLDRKAVGTPA
GGGFPRRHSVTLPPSSKFHQNLQLLA~~ASETAPSRK~~GASGCCPPRSS
PGAARSTPAATRRS~~CAAPLRK~~TVPVSTGTSASSHTASTSSAA*

ZFP36L1 WT

RNA binding domain

N-terminal ZF1 ZF2 C-terminal

1 114 177 338

Δ ZFP36L1

Δ N-terminal 1 78 124

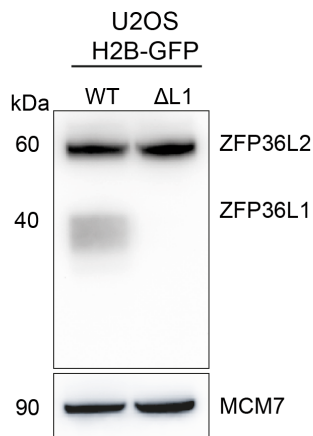
Δ ZFP36L1

Δ N-terminal 1 74 118

Δ ZFP36L1

Δ N-terminal 1 68 132

E



F

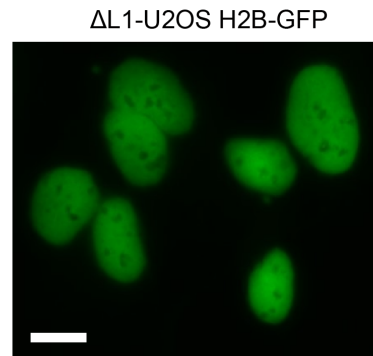


Figure 3.11. Characterisation of CRISPR/Cas9-mediated ZFP36L1 knockout in U2OS H2B-GFP cells.

(A) Schematic illustration of the human *ZFP36L1* gene locus located on Chromosome 14 q24.1. 20 base-pair gRNAs genomic target regions in exon 2 and the protospacer-adjacent motif (PAM) sequences coloured in purple (gRNA 2) and green (gRNA 3) are indicated. **(B)** Sequence analysis of targeted region in exon 2 of *ZFP36L1* derived from U2OS H2B-GFP cells. Nucleotide deletions (dashed lines) and insertions (emboldened in pink) are indicated. **(C)** 2% agarose gel of PCR amplicons derived from U2OS H2B-GFP cells showed a DNA fragment of approximately 450 bps in the WT (Lane 2) and a similar band size observed in the mutant (Lane 3). Lane M, 100 bp DNA Ladder. **(D)** Predicted amino acid translation of three reading frames identified in *ZFP36L1* knockout ($\Delta ZFP36L1$) in U2OS H2B-GFP cells. Translation of detected genomic 1 bp insertion (top), 17 bp deletion (middle) and 41 bp deletion (bottom) are shown. Amino acids emboldened in black in $\Delta ZFP36L1$ denote sequence matching with WT *ZFP36L1*. Red asterisk represents a premature stop codon. **(E)** Western blot analysis of *ZFP36L1* from whole-cell extracts derived from U2OS H2B-GFP wild-type (WT) and *ZFP36L1* knockout ($\Delta L1$). *ZFP36L2* and *MCM7* were used as loading controls. **(F)** Representative image of $\Delta ZFP36L1$ U2OS H2B-GFP cells. Scale bar, 10 μm .

3.6 CRISPR/Cas9-mediated deletion of *ZFP36L1* in U2OS Cells Compromises Cell Growth

A fundamental trait of cancer cells involves their aberrant cell growth (Hanahan and Weinberg, 2011). One of the cellular phenotypes that has been shown to be compromised by the absence of *ZFP36L1* is the rate at which cells proliferate (Suk et al., 2018). In particular, transient shRNA-mediated knockdown of *ZFP36L1* was previously shown to increase cell number in human colorectal cancer cell lines (HCT116) and was also associated with increased cell viability (Suk et al., 2018). To investigate the impact of *ZFP36L1* deficiency on the growth rate of U2OS cells, we performed a growth curve analysis on $\Delta L1$ and $\Delta L1$ -ND cell lines along with their respective wild-type (WT) control cells over a period of five days. WT U2OS cells typically grow at an average doubling time of approximately 29 hours. Interestingly, we observed U2OS cells to exhibit a slower growth rate in the absence of *ZFP36L1* compared to the WT cells. As shown in [Figure 3.12A](#) and [B](#), a distinct and significant growth difference among the $\Delta L1$ knockout clones compared to the WT was apparent. Similarly, U2OS cells with a truncated/mutant variant of *ZFP36L1* ($\Delta L1$ -ND1 and $\Delta L1$ -

ND2) were also observed to grow significantly slower relative to the WT (Figure 3.12C and D). Thus, this suggested that ZFP36L1 may potentially play a critical role in the normal cell growth of human bone cancer cells.

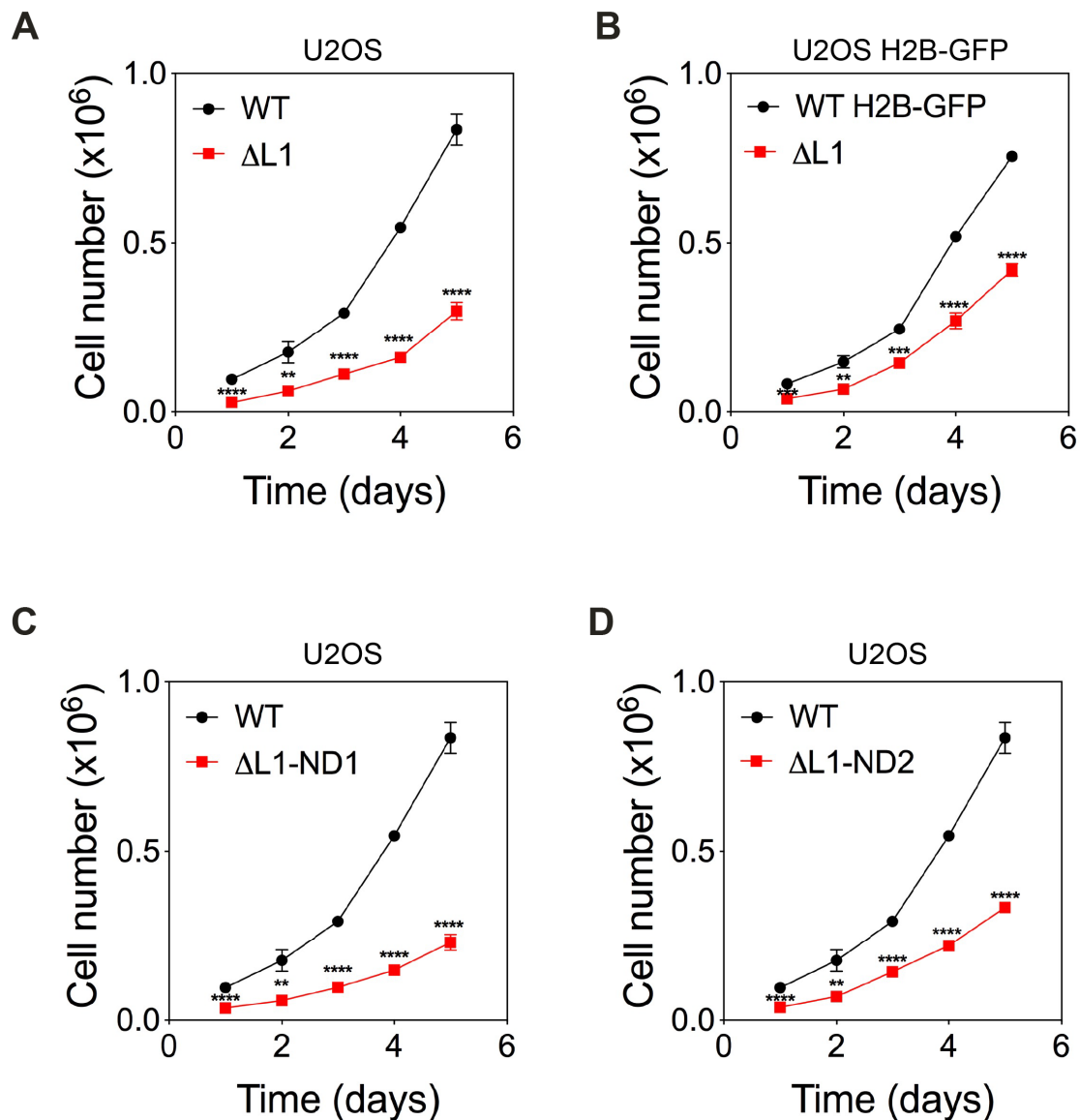


Figure 3.12. Loss of ZFP36L1 results in a slower growth rate in U2OS cells.

(A and B) Growth curve analysis of WT and ZFP36L1 knockout (Δ L1) derived from (A) U2OS and (B) U2OS H2B-GFP cells. (C and D) Growth curve analysis of WT and ZFP36L1-mutants; (C) Δ L1-ND1 and (D) Δ L1-ND2, made in U2OS cells. Growth curve analysis was performed over a period of 5 days. Data are means of triplicate values obtained from three independent experiments. Error bars represent standard deviation (SD). *p* values were calculated using an unpaired two-tailed *t*-test, *, *p* < 0.05; **, *p* < 0.01; ***, *p* < 0.001; ****, *p* < 0.0001.

3.7 Discussion

It has become increasingly evident that CRISPR/Cas9-directed gene-editing has revolutionised research on the human genome, and facilitated our ability to elucidate the phenotypic consequences associated with the loss of function of a single-gene product on pathological diseases. The CRISPR/Cas9 system is essentially composed of a gRNA that directs the Cas9 endonuclease to generate a DSB at a target-specific sequence. Due to its simplicity, improved precision and high editing-efficiency, this gene-editing tool has gained wide recognition amongst other gene-editing approaches (reviewed in, Rodríguez-Rodríguez et al., 2019). In this report, we present an optimised CRISPR/Cas9-directed method for generating a U2OS cellular model by which ZFP36L1 is functionally disabled and compromised/truncated. We used a plasmid-based Sp-derived-CRISPR/Cas9 methodological approach adapted from Ran et al. (2013) CRISPR-based methods. In particular, the all-in-one pSpCas9(BB)-2A-Puro plasmid vector that we used for gRNA expression and delivery contained a Cas9 endonuclease expression cassette and a sgRNA scaffold tailored for gRNA cloning using BbsI restriction enzyme. Importantly, pSpCas9(BB)-2A-Puro also consists of an ampicillin and puromycin resistant gene that aided in the selection of transformed bacterial and transfected mammalian cells, respectively.

The first step of a CRISPR-based method involves the design of a gRNA, which bears sequence-complementarity to the targeted genomic site. Given exon 2 encodes for the main protein-coding region of ZFP36L1, we selected an early region within the coding sequence that contains the ORF for gRNA design, to maximise the probability of generating frame-shift mutations that disrupt gene function (Figure 3.2). Moreover, It has been recommended that at least two separate gRNAs are designed to ensure

editing of the target site (Ran et al., 2013). Therefore, we designed and synthesised three gRNAs with the highest computationally predicted on-target binding scores, to target distinct genomic sites within the protein-coding region of *ZFP36L1* (Figure 3.2). Indeed, while transfection with gRNA 2 and gRNA3-expressing pSpCas9(BB) plasmids resulted in the disruption of *ZFP36L1* (U2OS; Δ L1, Δ L1-ND1 and Δ L1-ND2 and U2OS H2B-GFP; Δ L1), gRNA 1-expressing plasmids failed to eliminate *ZFP36L1* expression (data not shown) (Figure 3.10). Altogether, these observations validate our optimised method used in the construction, selection and delivery of the sgRNA-expressing pSpCas9(BB) plasmids in U2OS and U2OS H2B-GFP cells.

Our genomic analysis of the targeted region within *ZFP36L1* in U2OS and U2OS H2B-GFP cells confirmed successful editing of *ZFP36L1*, as evidenced by the random CRISPR-induced mutations within exon 2 of *ZFP36L1* (Figure 3.8). It is important to note that in the event where the CRISPR-induced lesion was found to be heterozygous when subjected to Sanger sequencing (the presence of overlapping bases visualised on a chromatogram or non-specific/uninterpretable data), the DNA fragments were analysed via Ampliseq-based NGS (reviewed in, Giuliano et al., 2019). Among the four *ZFP36L1*-mutant clones, Δ L1 and Δ L1-ND2 (U2OS) were identified as homozygous clones, and Δ L1-ND1 (U2OS) and Δ L1 (U2OS H2B-GFP) showed a heterozygous genotype. This merely reflected the diverse and random nature of mutations that can take place via NHEJ-mediated repair upon Cas9 cleavage. Interestingly, however, some of the deletions generated by gRNA 3 were identical between different clones. For example, Δ L1-ND1 and Δ L1-ND2 clones both harboured a 108-bp deletion within the same region of the targeted site (Figure 3.8C and D), supporting the emerging view that CRISPR-induced mutations, in some

circumstances, can result in a non-random repair outcome and produce similar indel patterns (Chakrabarti et al., 2019).

Our western blot analysis confirmed that our gene-editing approach was successful in the generation of a knockout as well as a truncated variant of ZFP36L1 in U2OS cells. The complete absence of ZFP36L1 protein expression in both Δ L1 (knockout) clones can be explained by the resulting frame-shift mutations and premature stop codons, which completely disrupted the ORF, as shown in the predicted amino acid analysis of the clones (Figure 3.9A, Figure 3.11D). On the other hand, the generated mutations within Δ L1-ND1 and Δ L1-ND2 produced a truncated form of ZFP36L1. Truncated ZFP36L1 expression between these two clones differed from one another in that Δ L1-ND1 expression was lower compared to full-length WT ZFP36L1, while Δ L1-ND2 showed a higher level of truncated ZFP36L1 expression. This difference can be partially explained by the distinct mutations that occurred within the clones, whereby multiple types of mutations including an out-of-frame mutation had occurred within Δ L1-ND1's ORF, compared to the single 108-bp deletion detected in Δ L1-ND2, which may have resulted in differential protein conformational and expression changes. Nonetheless, the increased level of ZFP36L1 protein expression in Δ L1-ND2 remains to be investigated in further studies.

In line with previous findings on ZFP36L1 modulation of cellular proliferation, we observed a significant reduction in the growth rate of U2OS cells in the context of ZFP36L1 deficiency. This finding was in contrast to ZFP36L1's effect in human colorectal cancer cell lines (HCT116), whereby shRNA-mediated knockdown of ZFP36L1 was associated with increased cellular viability and cell number (Suk et al.,

2018). This may reflect that ZFP36L1 encompasses a cell type-specific function in relation to cell proliferation.

4 Loss of ZFP36L1 Leads to Replication Stress-induced Chromosomal Instability

4.1 Introduction

Chromosomal instability (CIN) is a hallmark of cancer that is denoted by an increased rate of numerical and structural chromosomal changes, and is the most prominent form of genomic instability in most human cancers (reviewed in, Negrini, Gorgoulis and Halazonetis, 2010; Sansregret, Vanhaesebroeck and Swanton, 2018). A common cause of CIN is the occurrence of mitotic dysfunctions that consequently lead to whole chromosome mis-segregation during cell division (reviewed in, Bakhoun et al., 2014). In addition to dysregulation of the mitotic apparatus, unequal chromosome segregation has also been shown to be caused by unresolved DNA structures that form as a repercussion of replication stress, which have escaped checkpoint activation and persisted into mitosis (Chan et al., 2009; Naim and Rosselli, 2009; Burrell et al., 2013). If not resolved in a safe and timely manner, these replication stress-induced DNA defects can impede faithful chromosome segregation, and are commonly manifested into segregation errors such as anaphase bridges, chromosome laggards and micronuclei (Chan et al., 2009; Naim and Rosselli, 2009; Burrell et al., 2013).

Anaphase bridges are a type of chromosome segregation defect characterised by DNA strings connecting two segregating chromosomes during anaphase (Chan et al., 2009). Anaphase bridges can arise as chromatin bridges (also known as bulky anaphase bridges) and can be detected with conventional DNA ligands such as 4,6-diamidino-2-phenylindole (DAPI) dye (Nielsen et al., 2015). In contrast, Ultra-fine bridges (UFBs) are a form of fine DNA linkage structures that are histone-free, and are undetectable with DAPI (DAPI-negative) (Fernández-Casañas and Chan, 2018).

Instead, UFBs have been shown to be coated by several nuclear factors including Bloom's syndrome helicase (BLM) and the DNA translocase, Plk1-interacting checkpoint helicase (PICH), both of which can be visualised by immunofluorescence-based methods (Baumann et al., 2007; Chan, North and Hickson, 2007). Although the exact function of PICH on UFBs is not completely understood, it is thought that PICH localises to UFBs to suppress DNA bridge formation and additionally contributes to BLM recruitment that, together with other nuclear factors, promote the resolution and processing of UFBs (Hengeveld et al., 2015). Importantly, UFBs are considered to constitute the last resort employed by cells to ensure proper chromosome segregation (reviewed in, Fernandez-Vidal, Vignard and Mirey, 2017).

Another frequent consequence of replicative stressed DNA that persists into mitosis is the formation of extra-nuclear bodies known as Howell-Jolly bodies or micronuclei (Xu et al., 2011). These small nuclear fragments are considered as hallmarks of genomic instability that mainly originate from mis-attached chromosomes or chromatid fragments that failed to incorporate into the nuclei of the daughter cells (Fenech et al., 2011). These mis-attached chromosome fragments often manifest as lagging chromosomes (also known as chromosome laggards) during anaphase, and represent a chromosome segregation error (reviewed in, Wilhelm et al., 2019).

In line with the emerging roles of ZFP36L1 in the maintenance of genome stability, we sought to investigate whether the loss of ZFP36L1 was associated with increased replication stress-induced chromosomal instability, given CIN is the predominant form of genomic instability in most human cancers and is majorly driven by replication stress. Accordingly, we utilised the CRISPR/Cas9-generated ZFP36L1 knockout and ZFP36L1 truncated cellular models derived from U2OS and U2OS H2B-GFP cell lines,

as genetic tools, to examine the link between ZFP36L1 and chromosomal stability. More specifically, we assessed whether the loss of ZFP36L1 was affiliated with an increased number of chromosome segregation defects including chromosome laggards, anaphase bridges and micronuclei. To induce replication stress, we applied low doses (0.1 μ M, 0.2 μ M and 0.4 μ M) of the replicative DNA polymerase inhibitor, aphidicolin (APH), a chemical compound commonly used for replication stress-related studies (Vesela et al., 2017). Mechanistically, APH interferes with DNA replication by inhibiting DNA polymerases, alpha (α), epsilon (ϵ) and delta (δ), and mimics replication stress conditions that naturally occur in cells (Vesela et al., 2017).

4.2 ZFP36L1 Facilitates Faithful Chromosome Segregation

Unresolved DNA structures that form as a consequence of replication stress are often associated with mitotic defects leading to incomplete chromosome segregation, and are commonly manifested as lagging chromosomes or DNA bulky bridges (Chan et al., 2009; Naim and Rosselli, 2009; Burrell et al., 2013). To assess the impact of ZFP36L1 deficiency with regard to chromosome segregation, we first measured the frequency of chromosome mis-segregation markers in U2OS wild-type (WT) and Δ ZFP36L1 cells under mild replication stress conditions induced by low doses of APH. Accordingly, we examined the proportion of cells that segregated their chromosomes without visible segregation defects, with lagging chromosome fragments or DNA bulky bridges. Interestingly, deletion of ZFP36L1 was found to significantly increase the frequency of lagging chromosomes in anaphase cells compared to the WT in an APH dose-dependent manner (Figure 4.1). Untreated cells deficient in ZFP36L1 displayed approximately a 14% increase ($p < 0.05$) in chromosome laggards, and even a significantly higher frequency of chromosome laggard formation across all three doses of APH-induced mild replication stress (Figure 4.1A and B). Our quantification specifically suggested ZFP36L1 deficiency to result in the highest chromosome laggard formation in Δ L1-U2OS cells when treated with 0.4 μ M ($>24\%$, $p < 0.01$), with almost 50% of the scored cells displaying chromosome laggards compared to the WT (Figure 4.1B). This finding was consistently observed in Δ L1-U2OS H2B-GFP cells with the highest significant increase in chromosome laggards detected at 0.1 μ M of APH ($p < 0.001$) (Figure 4.1E and F). Intriguingly, an increase in chromosome laggards was also observed in the context of a ZFP36L1 truncation, even in the absence of APH treatment (untreated Δ L1-ND1, $p < 0.01$; untreated Δ L1-ND2, $p < 0.05$) (Figure 4.1C and D, Appendix D; D.1).

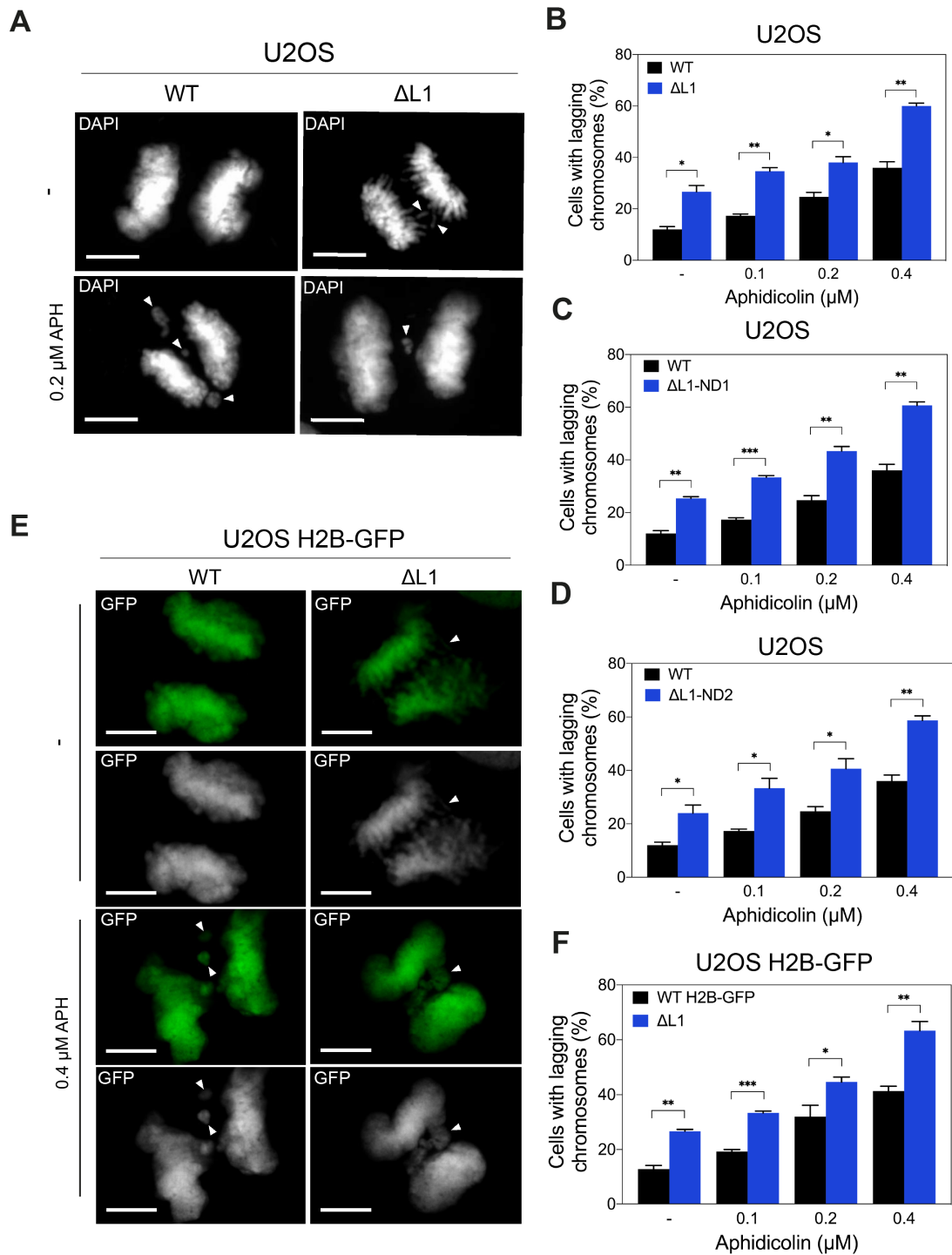


Figure 4.1. Loss of ZFP36L1 results in increased chromosome laggard formation.

(A) Representative images of lagging chromosomes scored in wild-type (WT) and ZFP36L1 knockout (Δ L1) U2OS cells. (B-D) Quantifications of the frequency of anaphase cells with lagging chromosomes in untreated and APH-treated (B) Δ L1, (C) Δ L1-ND1 and (D) Δ L1-ND2 U2OS cells. (E) Representative images of lagging chromosomes scored in wild-type (WT) and ZFP36L1 knockout (Δ L1) U2OS H2B-GFP cells. (F) Quantification of the frequency of anaphase cells with lagging chromosomes in untreated and APH-treated Δ L1 U2OS H2B-GFP cells. White arrows indicate chromosome laggards. Scale bar, 10 μ m. Data are means of three independent experiments with a total of 50 anaphase cells analysed per condition for each experiment. Error bars represent S.E.M. *p* values were calculated using unpaired *t*-test; ns, not significant, *, *p* < 0.05; **, *p* < 0.01; ***, *p* < 0.001; ****, *p* < 0.0001.

Similarly, we also found an elevated frequency of DAPI-positive anaphase bridges in ZFP36L1-deficient and ZFP36L1-truncated U2OS cells compared to the WT ([Figure 4.2](#)). This significant increase was consistently detected across all four of Δ ZFP36L1 clones and was strikingly high in untreated ZFP36L1-truncated cell lines (Δ L1-ND1 and Δ L1-ND2), given ZFP36L1 protein in these clones is only partially compromised ([Figure 4.2C and D](#), [Appendix D; D.2](#)). Indeed, Δ L1-ND1 and Δ L1-ND2 cells displayed a relatively distinct phenotype where a highly significant increase ($>12\%$; $p < 0.001$, $>16\%$; $p < 0.001$, respectively) in anaphase bridge formation compared to the WT was observed in the absence of mild replication stress. Taken together, these results indicate that a partial or complete knockout of ZFP36L1 in U2OS results in increased susceptibility of anaphase cells to the formation of chromosome laggards and DNA bulky bridges, both of which are morphological hallmarks of chromosome mis-segregation.

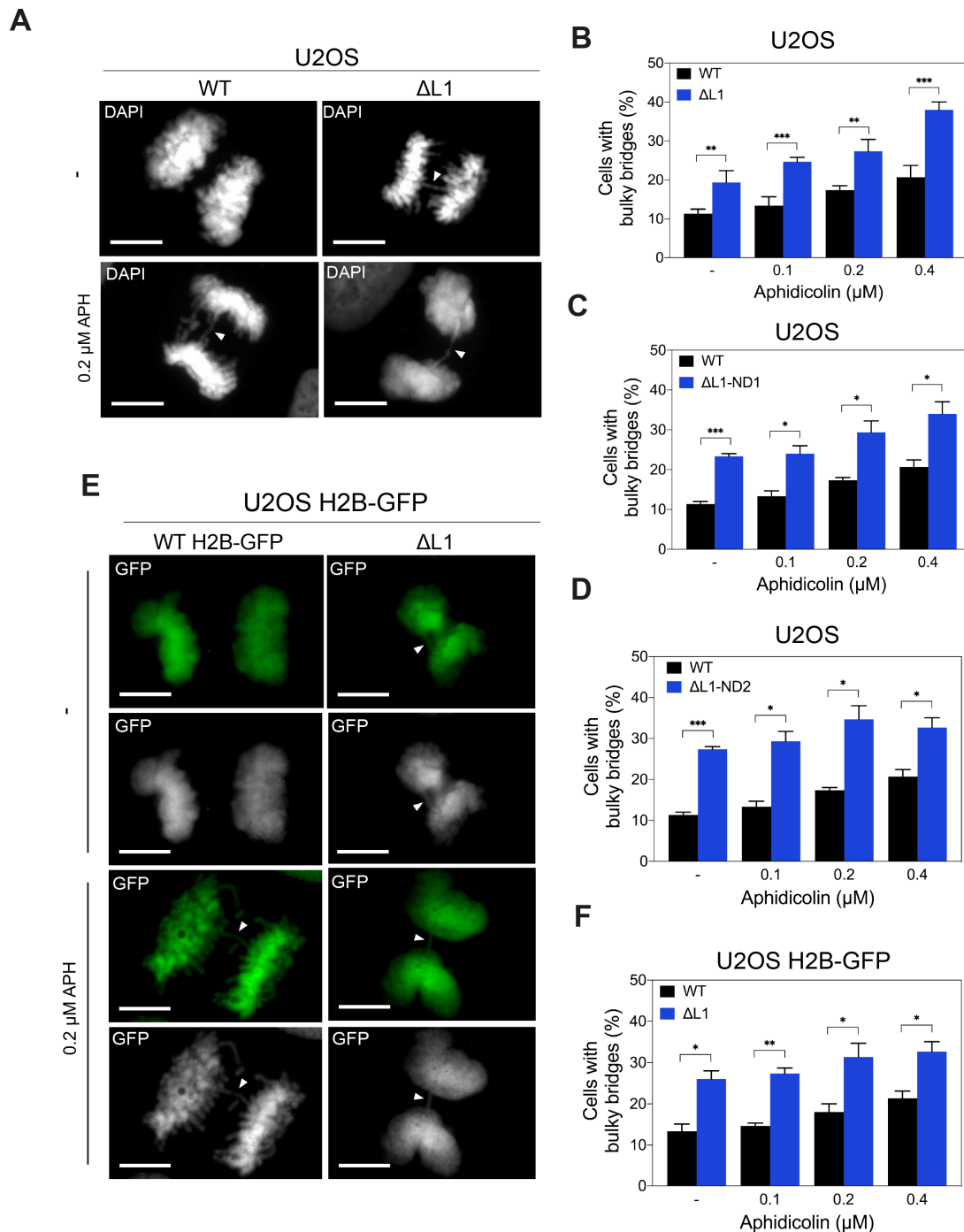


Figure 4.2. Loss of ZFP36L1 induces the formation of DNA bulky bridges.

(A) Representative images of DAPI-positive anaphase bridges scored in wild-type (WT) and ZFP36L1 knockout ($\Delta 1$) U2OS cells. (B-D) Quantifications of the frequency of anaphase cells with DAPI-positive bulky bridges in untreated and APH-treated (B) $\Delta 1$, (C) $\Delta 1$ -ND1 and (D) $\Delta 1$ -ND2 U2OS cells. (E) Representative images of H2B-GFP and DAPI-positive anaphase bridges scored in wild-type (WT) and ZFP36L1 knockout ($\Delta 1$) U2OS H2B-GFP cells. White arrowheads indicate bulky bridges. Scale bar, 10 μ m. (F) Quantification of the frequency of DAPI-positive anaphase bridges in untreated and APH-treated $\Delta 1$ U2OS H2B-GFP cells. Data are means of three independent experiments with a total of 50 anaphase cells analysed per condition in each experiment. Error bars represent S.E.M. *p* values were calculated using an unpaired *t*-test, ns, not significant, *, *p* < 0.05; **, *p* < 0.01; ***, *p* < 0.001; ****, *p* < 0.0001.

4.3 Mitotic Defects in ZFP36L1-deficient Cells are Mediated by the Formation of UFBs

A more recent form of a DNA-bridging structure that arises as a result of unresolved replication stress-induced DNA entanglements carried into mitosis, are the so-called ultra-fine bridges (UFBs) (reviewed in, Tiwari, Jones and Chan, 2018). In contrast to DNA bulky bridges, UFBs cannot be stained by conventional DNA dyes (e.g. DAPI), but instead can be detected using immunofluorescence-based methods. Given our findings suggested ZFP36L1 to limit chromosome instability, we hypothesised that its deficiency may exacerbate replication stress in U2OS cells and impact UFB formation, a common outcome of replication stress. Therefore, we evaluated the effect of ZFP36L1 deficiency on the frequency of UFB formation through immunofluorescence staining of a UFB-binding protein; PICH. Consistent with previous results, immunofluorescence analysis revealed that the proportion of cells with PICH-positive UFBs was significantly increased in Δ ZFP36L1 knockout clone compared to the WT, in both, the absence and presence of APH-induced replication stress (Figure 4.3A and B). In particular, a 10-14% increase of PICH-positive UFBs was detected in Δ L1 cells when treated with 0.2 μ M of APH and a 12-16% increase at 0.4 μ M APH treatment compared to the WT ($p < 0.01$, $p < 0.001$), respectively (Figure 4.3B). This observation was also consistent in cells expressing a truncated variant of ZFP36L1 (Δ L1-ND 1 and Δ L1-ND 2) in that they displayed a significantly greater level of UFB formation relative to the WT in an APH dose-dependent manner (Figure 4.3C and D, respectively; Appendix, D.3). Together, these observations support our findings that the elevated segregation errors resulting from ZFP36L1-deficiency and ZFP36L1-truncation are highly likely caused by aggravated replication stress which resulted in an exacerbation in chromosome-disjunction, posing a threat to the cells' genomic stability.

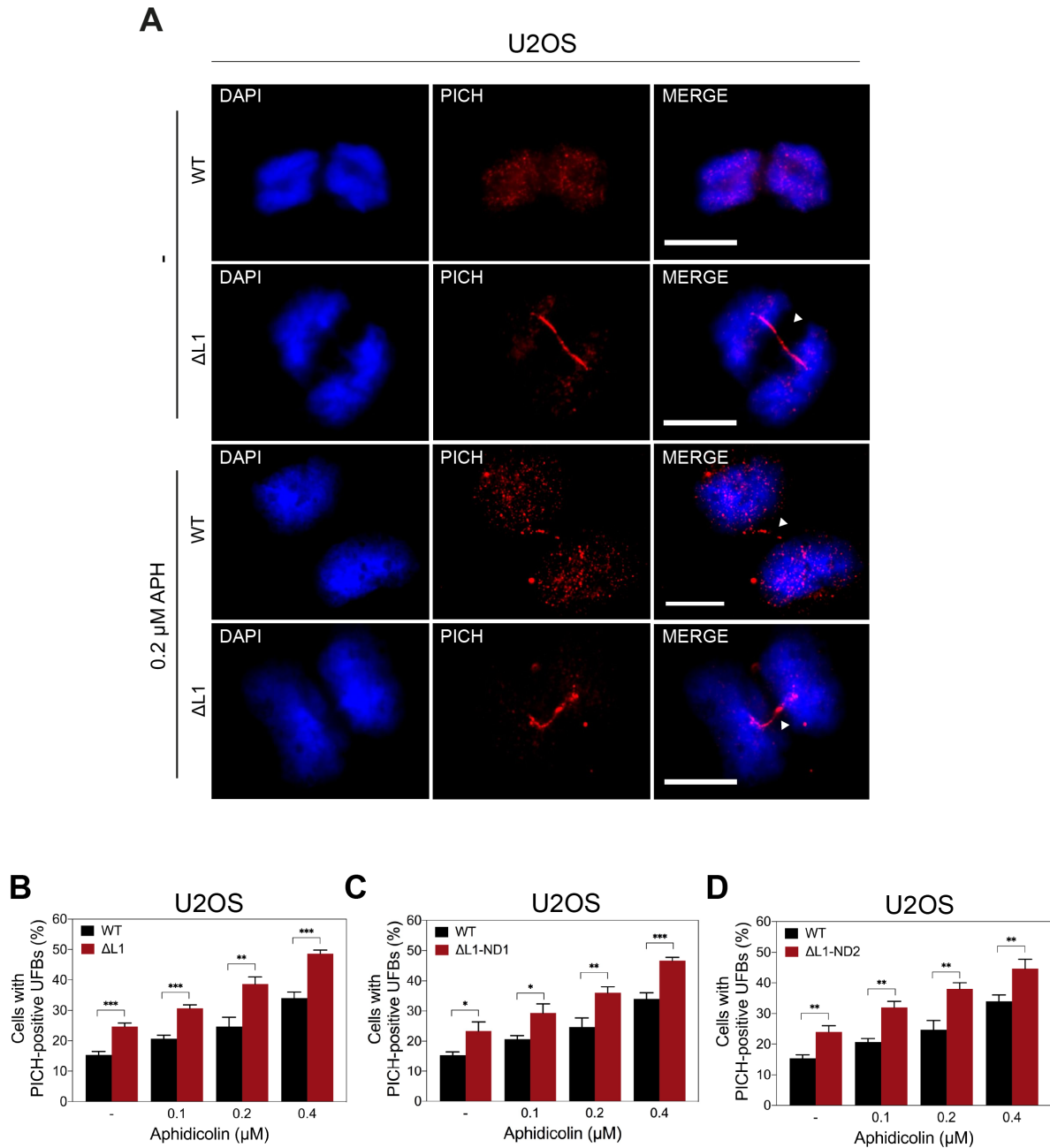


Figure 4.3. Loss of ZFP36L1 induces PICH-positive UFB formation.

(A) Representative images of PICH-UFBs (red) scored in wild-type (WT) and ZFP36L1 knockout (Δ L1) U2OS cells. White arrowheads indicate PICH-UFBs. Scale bar, 10 μ m. (B-D) Quantifications of the frequency of anaphase cells positive for PICH decorated-UFBs in (B) Δ L1, (C) Δ L1-ND1 and (D) Δ L1-ND2 U2OS cells. Data are means of three independent experiments with a total of 50 anaphase cells analysed per condition in each experiment. Error bars represent S.E.M. *p* values were calculated using an unpaired *t*-test, ns, not significant, *, *p* < 0.05; **, *p* < 0.01; ***, *p* < 0.001; ****, *p* < 0.0001.

4.4 Loss of ZFP36L1 Increases Micronuclei Formation

Replication stress can drive intrinsic genomic instability and is affiliated with abnormal chromosome segregation in cancerous and pre-cancerous lesions (Burrell et al., 2013). Based on our earlier chromosome mis-segregation analysis, we sought to characterise further impacts of ZFP36L1 deficiency on chromosome segregation. Since micronuclei are frequently formed as a consequence of the presence of mis-attached chromosomes, we speculated that a deletion of ZFP36L1 might be associated with increased micronuclei formation. To block cells in cytokinesis, we used cytochalasin-B for the appropriate analysis of micronuclei formation in binucleated cells ([Figure 4.4A](#)) (Fenech et al., 2011). Strikingly, the frequency of cells with micronuclei was significantly increased across all four ZFP36L1-mutant U2OS cell lines, in both, non-treated and APH-treated conditions compared to the WT and empty vector (pSpCas9(BB)-2A-Puro-only) cells ([Figure 4.4B, C and E, Appendix E](#)). Treatment with 0.2 μ M of APH in Δ L1-U2OS and Δ L1-U2OS H2B-GFP cells was found to result in a significant increase in micronuclei formation ($>12.22\%$, $p < 0.01$; $>9.22\%$, $p < 0.01$), respectively, while for Δ L1-ND1 cells a highly significant increase was observed at 0.4 μ M of APH ($>8.89\%$, $p < 0.05$) compared to WT. Interestingly, we observed Δ L1-ND2 cells to exhibit a greater significant increase in micronuclei when treated with 0.1 and 0.2 μ M of APH ($>10.89\%$, $p < 0.01$; $>14.11\%$, $p < 0.001$, respectively) compared to Δ L1-ND1 cells ($>6.88\%$, $p < 0.05$; $>6.89\%$, $p < 0.05$, respectively), relative to the WT, a phenotype more similar to ZFP36L1 knockout (Δ L1) than ZFP36L1-truncated (Δ L1-ND1) cells. Collectively, these data build a strong case supporting the proposed role for ZFP36L1 in limiting replication stress-induced CIN.

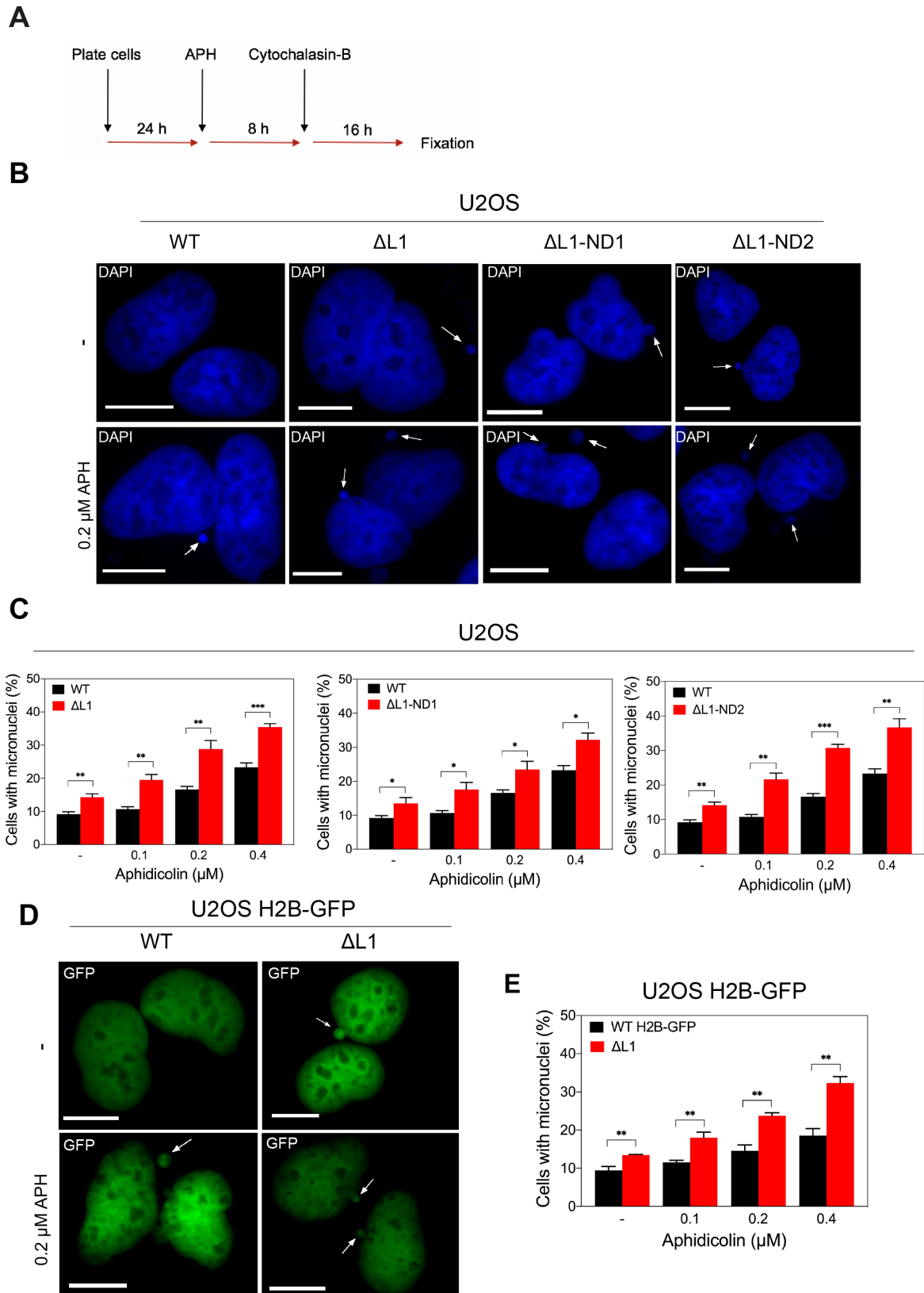


Figure 4.4. Loss of ZFP36L1 induces micronuclei formation in U2OS cells.

(A) Experimental workflow for the analysis of micronuclei. Cells were treated with APH for 24 h and supplemented with 2 mg/ml of cytochalasin-B 16 h before fixation. (B) Representative images of cytochalasin-B induced binucleated cells with micronuclei scored in wild-type (WT) and ZFP36L1 knockout (Δ L1) U2OS cells. (C) Quantification of the frequency of micronuclei

scored in untreated and APH-treated WT and Δ L1 (left), Δ L1-ND1 (middle) and Δ L1-ND2 (right) U2OS cells. **(D)** Representative images of cytochalasin-B induced binucleated cells with micronuclei scored in wild-type (WT) and ZFP36L1 knockout (Δ L1) U2OS H2B-GFP cells with H2B-GFP staining the nuclei. **(E)** Quantification of the frequency of micronuclei in untreated and APH-treated wild-type (WT) and Δ L1 U2OS H2B-GFP cells. White arrows indicate micronuclei. Scale bar, 10 μ m. Data are means of three independent experiments with a total of 300 binucleated cells analysed per condition in each experiment. Error bars represent SD. *p* values were calculated using an unpaired *t*-test, *, *p* < 0.05; **, *p* < 0.01; ***, *p* < 0.001; ****, *p* < 0.0001.

4.5 Discussion

Chromosome stability is a hallmark of genomic stability that critically relies on faithful chromosome segregation between the sister chromatids during anaphase (Sansregret, Vanhaesebroeck and Swanton, 2018). While defects in the mitotic machinery can cause chromosome mis-segregation, recent studies have indicated that replication stress also acts as a driving force of chromosomal instability and lead to segregation errors (Ichijima et al., 2010; Burrell et al., 2013). Although growing evidence has shed light on the emerging role of ZFP36L1 in curbing genomic instability, the molecular base of this association remains unclear. In this report, we have identified a novel role for ZFP36L1, characterised in human U2OS and U2OS H2B-GFP cancer cells, in that it suppresses replication stress-induced chromosome mis-segregation.

Unresolved DNA structures that form as a consequence of replication stress often lead to the formation of chromosome laggards and micronuclei (Wilhelm et al., 2019). To date, there is little evidence that has functionally linked RBPs with chromosome segregation. Conversely, the cold-inducible RBP (CIRBP) was recently shown to promote DSB repair and genomic stability, whereby CIRBP depletion was associated with HR and NHEJ impairment as well as increased micronuclei formation (Chen et al., 2018). Here, we demonstrate, for the first time, that these segregation error

phenotypes occur in cells deficient for the RBP, ZFP36L1. Indeed, ZFP36L1-knockout cells exhibited elevated levels of micronucleus formation, a morphological hallmark of genomic instability, even in the absence of APH-induced replication stress (Figure 4.4). This effect was further exacerbated under conditions of mild replication stress in an APH dose-dependent manner, which indicated ZFP36L1 to potentially play a critical role in preserving chromosomal stability. Consistent with the notion that micronuclei typically form as an outcome of chromosome laggards that failed to be incorporated within the daughter nuclei, ZFP36L1-deficient cells were significantly sensitised to the formation of chromosome laggards during anaphase, especially under mild replication stress (Figure 4.1). This explains the resulting micronuclei formation phenotype and suggests that ZFP36L1 is important for faithful chromosome segregation.

To corroborate these phenotypes, we characterised further impacts of ZFP36L1 deficiency on chromosome segregation in the context of DNA anaphase bridges, a well-established marker of a segregation error (reviewed in, Fernández-Casañas and Chan, 2018). Importantly, we found that loss of ZFP36L1 is associated with increased levels of anaphase DNA bulky bridges, a phenotype that was consistently observed to be significantly increased under conditions of mild replication stress (Figure 4.2). This observation further validated the link between ZFP36L1 and the preservation of chromosomal stability. Another striking finding in the current study was that ZFP36L1 deficiency resulted in an elevated level of anaphase cells with PICH-positive UFBs, a signature of replication stress and/or DNA damage (Figure 4.3) (Chan et al., 2009). UFBs are typically decorated with the DNA translocase, PICH, and other nuclear factors that continue to attempt to resolve stressed DNA that persisted into mitosis,

and play key roles in UFB resolution before the end of anaphase (Nielsen et al., 2015). This result signified that loss of ZFP36L1 is strongly related to replication stress-induced genomic instability, and suggested that the resulting exacerbated replication stress imposed by ZFP36L1-deficiency had potentially activated DNA repair mechanisms.

Remarkably, all of the key phenotypic changes observed in ZFP36L1-knockout cells were also detected in cells expressing a truncated variant of ZFP36L1 (Δ L1-ND1 and Δ L1-ND 2 cells). This indicated that even a partial loss of function associated with a compromised ZF-domain of ZFP36L1 was sufficient to elicit a significant increase in chromosome mis-segregation events and lead to increased chromosomal instability. It is also noteworthy that Δ L1-ND1 and Δ L1-ND2 cell lines harbour a 35-aa deletion that includes the first amino acid (Arginine (R)) of the RYKTEL motif, which is critical for the ZF domain of ZFP36L1 (Lai et al., 2000). Although the protein-level conformational changes linked with these phenotypes remain to be investigated, we speculate that one of the possible reasons underlying these phenotypes, is due to the 108-bp deletion in Δ L1-ND cells, that resulted in partial disruption of the first ZF-domain of ZFP36L1. However, further studies will need to re-visit the reason(s) for these distinct phenotypes.

5 ZFP36L1 Suppresses Replication Stress-induced DNA Damage

5.1 Introduction

In response to replication stress, eukaryotic cells are devised to activate a specialised branch of the DDR, that orchestrates a series of events that detect, signal and repair DNA lesions (reviewed in, Jossen and Bermejo, 2013). The activation of the replication stress response is initially triggered by the generation of stretches of ssDNA that are typically bound with the ssDNA-binding protein, RPA, at damaged or stalled replication forks (Pacek and Walter, 2004). The persistence of ssDNA coated with RPA activates the ATR kinase pathway, which in turn signals for the phosphorylation of numerous downstream substrates (reviewed in, Zeman and Cimprich, 2014). This series of DDR events is central to delaying cell cycle progression and provides additional time for the cell to deploy lesion repair and faithfully complete DNA replication within replication-stressed sites (Branzei and Foiani, 2009).

Many of the methodological markers used as readouts of replication stress represent the activation of these replication stress-induced pathways such as the recruitment of RPA and γ H2AX (Zeman and Cimprich, 2014). Concomitant with its ssDNA-binding function, RPA is an indispensable player in almost all aspects of DNA metabolism including DNA replication, DNA repair and DNA damage checkpoints (Zou et al., 2006). In fact, the generated replication stress-induced ssDNA-RPA filaments serve as the primary platform required for the activation of the DDR (Zou and Elledge, 2003). RPA can additionally be phosphorylated in an ATR kinase-dependent manner at Serine 33, which in turn modulates its function specifically for DNA repair (Liu et al.,

2012; Soniat et al., 2019). Owing to its numerous key roles in DNA metabolism, the detection of RPA foci via immunofluorescence is therefore considered a specific readout or sensor of replication stress (reviewed in, Maréchal and Zou, 2013; Zeman and Cimprich, 2014).

Failure to restart replication fork progression can lead to fork collapse and result in the formation of DNA DSBs, which are considered to be among the most deleterious forms of DNA lesions (Karagiannis and El-Osta, 2004). One of the earliest cellular responses to DSB formation involves the rapid phosphorylation of the histone H2A variant, H2AX, at Serine-139 (γ H2AX) at the C-terminus, and this is responsible for the initiation of DSB repair (Redon et al., 2002; Rothkamm and Löbrich, 2003). Phosphorylation of H2AX is a crucial step in the DDR as γ H2AX serves as a docking station for the recruitment of numerous DDR-associated proteins and downstream DDR effectors (Falck, Coates and Jackson, 2005). Accordingly, the visualisation and quantification of γ H2AX in the form of discrete nuclear foci via immunofluorescence-based assays has been established as a highly reliable and sensitive method for the measure of DNA damage/DSBs (Mah, El-Osta and Karagiannis, 2010).

Another well-established indicator of replication stress-induced DNA DSBs is the formation of 53BP1 nuclear bodies (NBs) in the G1-phase of the nascent daughter cells, that typically form in the vicinity of DSBs or DNA lesions (reviewed in, Fernandez-Vidal, Vignard and Mirey, 2017). Originally described as a binding protein of the tumour suppressor, p53, 53BP1 is a key component of the DDR that plays numerous roles in DNA damage signalling and DNA repair (reviewed in, Mirza-Aghazadeh-Attari et al., 2019). Interestingly, replication stress-induced DNA lesions

that have failed to be repaired at UFBs, which constitute the final chance to repair stressed genomic loci, have been shown to be frequently transmitted into the following G1-phase daughter cells, and manifest into nuclear bodies enriched with 53BP1 (Harrigan et al., 2011; Lukas et al., 2011). These 53BP1-containing sites essentially represent replication stressed sites from the previous S-phase and are thought to promote DNA repair via NHEJ in the G1-phase or shield the inherited DNA lesions from further DNA erosion until the following S-phase, where they can be resolved by HR-mediated repair pathways (Harrigan et al., 2011; Lukas et al., 2011). Importantly, the formation of 53BP1 NBs in G1-phase cells has been demonstrated to be intrinsically associated with replication stress, supported by the observation of an increase of 53BP1 NBs in response to APH treatment (Harrigan et al., 2011; Lukas et al., 2011). Thus, the detection and quantification of G1-phase 53BP1 NBs, which are visible by immunofluorescence-based assays as large ($> 1\mu\text{m}$) nuclear foci, serve as a reliable marker of replication stress.

Here, we investigated whether the exacerbated replication stress conditions exhibited by ZFP36L1-deficient cells were translated into DNA damage and thus, in the accumulation of DDR-related proteins. Accordingly, we further characterised the molecular consequences associated with loss of ZFP36L1, by specifically quantifying the changes in the level of DSB markers, γH2AX and 53BP1 NBs, as well as endogenous RPA levels. Consistent with our speculations, we provide novel evidence showing that loss of ZFP36L1 is additionally associated with replication stress-induced DNA damage, reflected by the observed increased levels of G1-phase 53BP1 NBs, γH2AX and RPA, which strongly suggested that ZFP36L1 serves as a genomic stability guardian against replication stress-induced DNA damage.

5.2 ZFP36L1 Limits Replication Stress-induced DSB Formation

Unrestrained replication stress can cause the formation of DNA DSBs and drive genomic instability (Ciccio and Elledge, 2010). Based on our earlier observations, that ZFP36L1 contributes to the suppression of replication stress-induced chromosomal instability, we hypothesised that loss of ZFP36L1 might also be associated with replication fork collapse and hence, DNA damage in the form of DNA DSBs. To assess this possibility, we first analysed the levels of phosphorylated H2AX (γ H2AX), a morphological marker of DNA DSBs, in the context of ZFP36L1 deficiency under mild replication stress. As shown in [Figure 5.1A](#) and [B](#), immunofluorescence staining of γ H2AX indicated that deletion of ZFP36L1 significantly increased the number of γ H2AX foci compared to the WT control cells, consistent with the assumption that ZFP36L1 and ZFP36L2 limit DNA damage signalling (Vogel et al., 2016). Importantly, loss of full-length ZFP36L1 protein significantly elevated γ H2AX foci levels in non-treated and APH-treated cells ($p < 0.0001$; $p < 0.0001$, respectively) ([Figure 5.1B](#)). This increase in γ H2AX foci formation was also observed in cells expressing a truncated variant of ZFP36L1 ([Figure 5.1C](#), Appendix F, F.1). Indeed, Δ L1-ND1 cells displayed a significant elevation in the number of γ H2AX foci in both, non-treated and APH-treated conditions ($p < 0.0001$; $p < 0.0001$, respectively) ([Figure 5.1C](#)). Together, these findings implied that ZFP36L1 limits replication stress-induced DNA damage in U2OS cells.

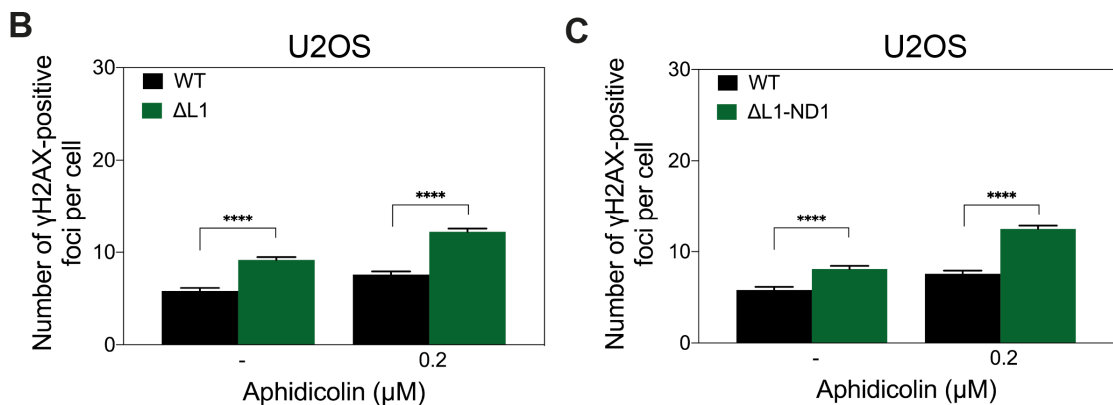
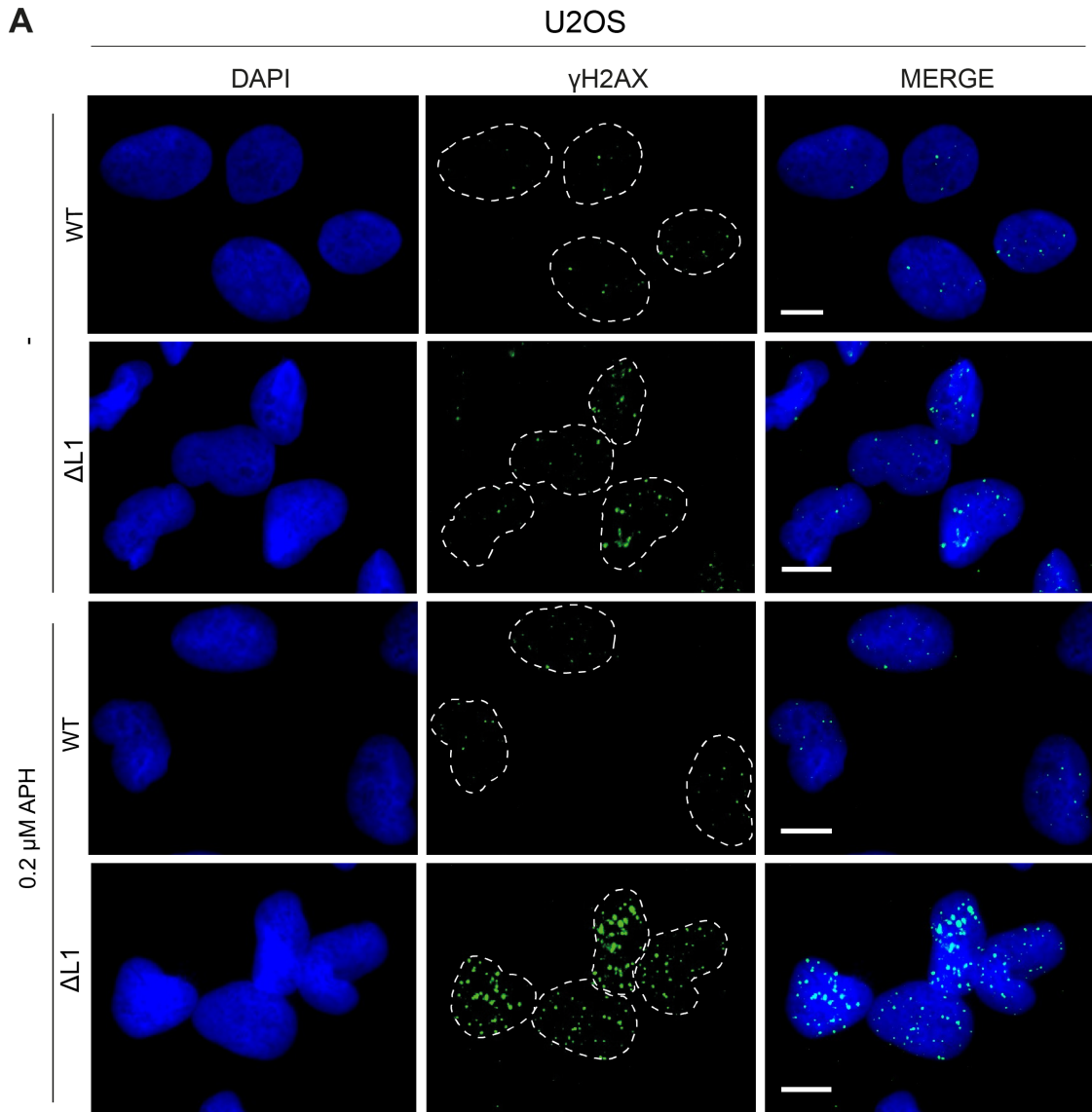


Figure 5.1. Deletion of ZFP36L1 induces DSBs in the form of γH2AX.

(A) Representative images of untreated and APH-treated cells containing γH2AX foci scored in wild-type (WT) and ZFP36L1-knockout (ΔL1) U2OS cells. (B and C) Quantification of the frequency of γH2AX foci in WT and (B) ΔL1 and (C) ΔL1-ND1 U2OS cells. Scale bar, 10 μm. Data are means of three independent experiments with a total of 100 interphase cells analysed per condition in each experiment. Error bars represent S.E.M. *p* values were calculated using Mann-Whitney *t*-test, *, *p* < 0.05; **, *p* < 0.01; ***, *p* < 0.001; ****, *p* < 0.0001.

5.3 Loss of ZFP36L1 Increases Micronuclei Positive for γ H2AX

It has been previously shown that characterisation of the DNA damage content in micronuclei can further demonstrate the association between these extra-nuclear bodies and intrinsic genomic instability in the form of replication stress (Terradas et al., 2009). Indeed, the formation of micronuclei labelled with DDR factors including the DNA DSB marker, γ H2AX, was shown to display an additional consequence associated with nuclei afflicted with replication stress, specifically when induced with APH (Xu et al., 2011). To explore whether the resulting micronuclei associated with the loss of ZFP36L1 harboured DDR-related factors, we monitored foci formation of γ H2AX using immunofluorescence-based methods (Figure 5.2A). Interestingly, across all ZFP36L1-knockout and ZFP36L1-truncated clones, we found that the frequency of micronuclei that stained positive for γ H2AX was higher compared to the WT in non-treated and as well as APH-treated conditions (Figure 5.2; Appendix F, F.2). This difference was found to be particularly significant in Δ L1, Δ L1-ND1 and Δ L1-ND2 cells when treated respectively with 0.1 μ M of APH (>9.33%, $p < 0.001$; >6.77%, $p < 0.01$; >10.78%, $p < 0.01$, respectively) and at 0.4 μ M of APH for Δ L1-U2OS H2B-GFP cells (>11.33%, $p < 0.01$) compared to the WT (Figure 5.2B-G). It is important to note, however, that the increase in the frequency of cells with γ H2AX (+) micronuclei is also relative to the number of micronuclei formed in each cell line. Since the loss of ZFP36L1 was shown in our earlier findings to significantly increase the frequency of micronuclei formation compared to the WT, we expected to observe a greater rise in γ H2AX (+) micronuclei in ZFP36L1-deficient cells. Nevertheless, this observation presented further evidence supporting an association between ZFP36L1 and the preservation of genomic stability against replication stress-induced DNA damage.

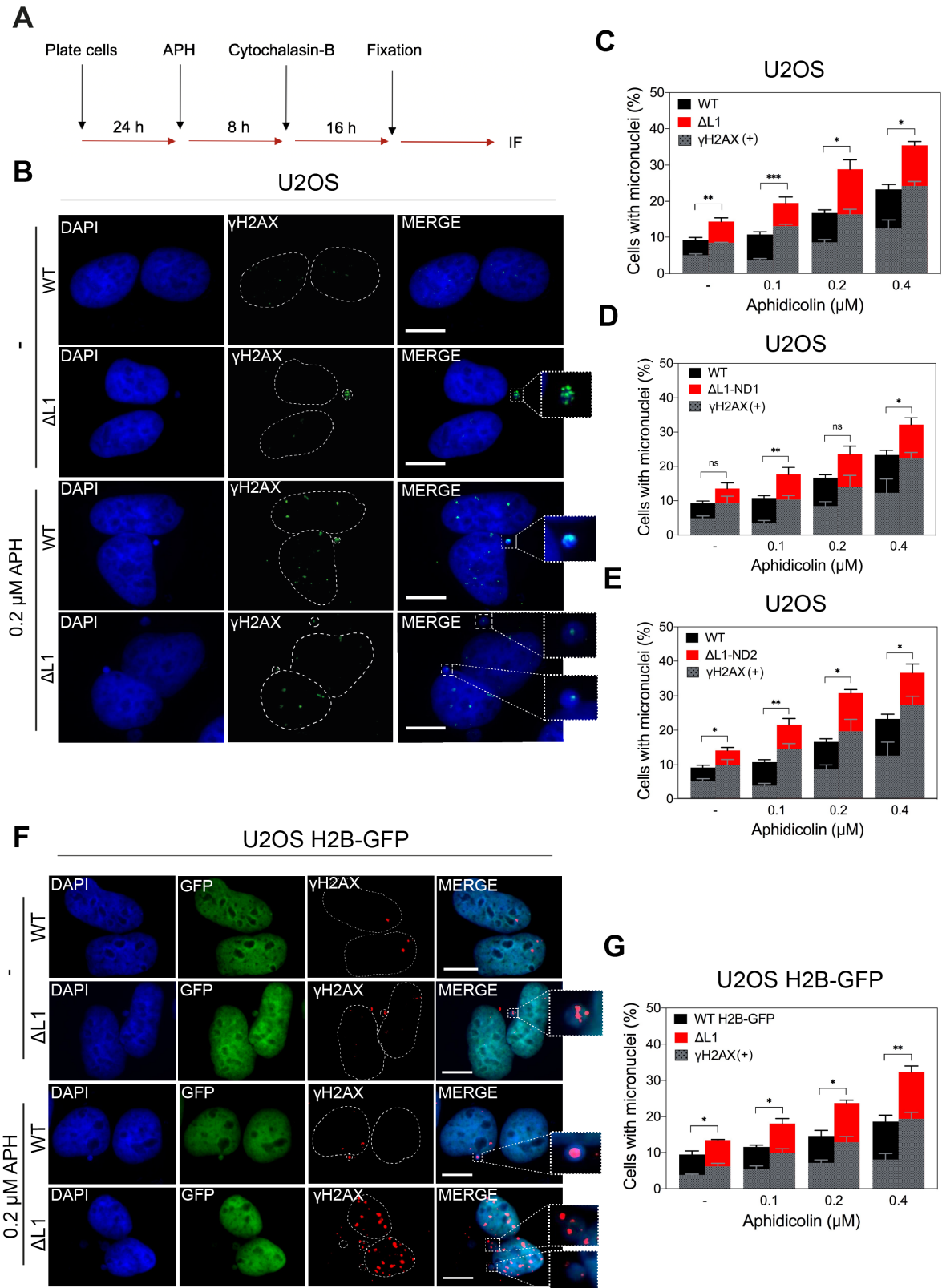


Figure 5.2. ZFP36L1 deficiency induces micronuclei positive for γ H2AX.

(A) Experimental workflow for the analysis of γ H2AX(+)-micronuclei. U2OS cells were treated with APH for 24 h before addition of 2 mg/ml of cytochalasin-B for 16 h followed by fixation and immunofluorescence staining. (B) Representative images of cytochalasin-B induced binucleated cells with γ H2AX (+) micronuclei scored in wild-type (WT) and ZFP36L1-knockout (Δ L1) U2OS cells. (C-E) Quantifications of the proportion of the total micronuclei (previously

quantified) positive for γ H2AX (grey bars) in untreated and APH-treated in WT and **(C)** Δ L1, **(D)** Δ L1-ND1 and **(E)** Δ L1-ND2 U2OS cells. **(F)** Representative images of cytochalasin-B induced binucleated cells with γ H2AX (+) micronuclei scored in WT and Δ L1 U2OS H2B-GFP cells. **(G)** Quantifications of the frequency of micronuclei positive for γ H2AX in untreated and APH-treated WT and Δ L1 U2OS H2B-GFP cells. Dashed squares indicate γ H2AX (+) micronuclei. Scale bar, 10 μ m. Data are means of three independent experiments with a total of 300 binucleated cells analysed per condition in each experiment. Error bars represent SD. *p* values, shown for micronuclei positive γ H2AX data, were calculated using an unpaired *t*-test, *, *p* < 0.05; **, *p* < 0.01; ***, *p* < 0.001; ****, *p* < 0.0001.

5.4 Deletion of ZFP36L1 Induces DSBs Sequestered into 53BP1 NBs

It is well-established that 53BP1 localises to microscopically visible discrete bodies/foci at sites of DNA lesions and DSBs that are largely confined to G1-phase cells, as a surrogate of replication stress (Harrigan et al., 2011; Lukas et al., 2011). Because a large proportion of mitotic cells deficient in ZFP36L1 displayed chromosomal segregation defects (UFBs), we next analysed the levels of 53BP1-positive nuclear bodies (NBs) in G1-phase cells to determine whether this chromosomal stress was transmitted to the daughter cells, as a marker of DNA DSBs. Therefore, we conducted immunofluorescence-based experiments on U2OS WT and Δ ZFP36L1 cell lines using antibodies against 53BP1 and cyclin A as a marker of S/G2-phase. Remarkably, we found that ZFP36L1-deficient cells exhibited a significantly increased number of 53BP1-positive NBs relative to WT and empty vector (pSpCas9(BB)-2A-Puro-only) cells, even in the absence of exogenous DNA replication stress ([Figure 5.3A](#); Appendix G, G.1, G.2, G.4). This effect was further aggravated under conditions of APH-induced mild replication stress, which particularly resulted in a 40% increase in Δ ZFP36L1 cells showing more than three 53BP1-positive NBs in G1-phase cells compared to WT control cells, when treated with 0.2 μ M of APH ([Figure 5.3B](#)). Furthermore, a similar pattern in the increase of 53BP1-positive NBs in the context of an N-terminus deletion of ZFP36L1 was also detected. Indeed, we observed a 24% and 34% increase in Δ ZFP36L1-ND1 and Δ ZFP36L1-

ND2 cells, respectively, that exhibited 53BP1-positive NBs relative to WT cells when treated with 0.2 μM of APH (Figure 5.3C and D; Appendix G, G.3, G.4). Overall, these data suggested that the replication stress-induced DSBs that resulted in response to ZFP36L1 deficiency persisted through mitosis, remained unrepaired, and were consequently transmitted into the G1-phase nuclei of daughter cells, shielded by 53BP1 NBs that are known to prevent further DNA erosion and promote DNA repair.

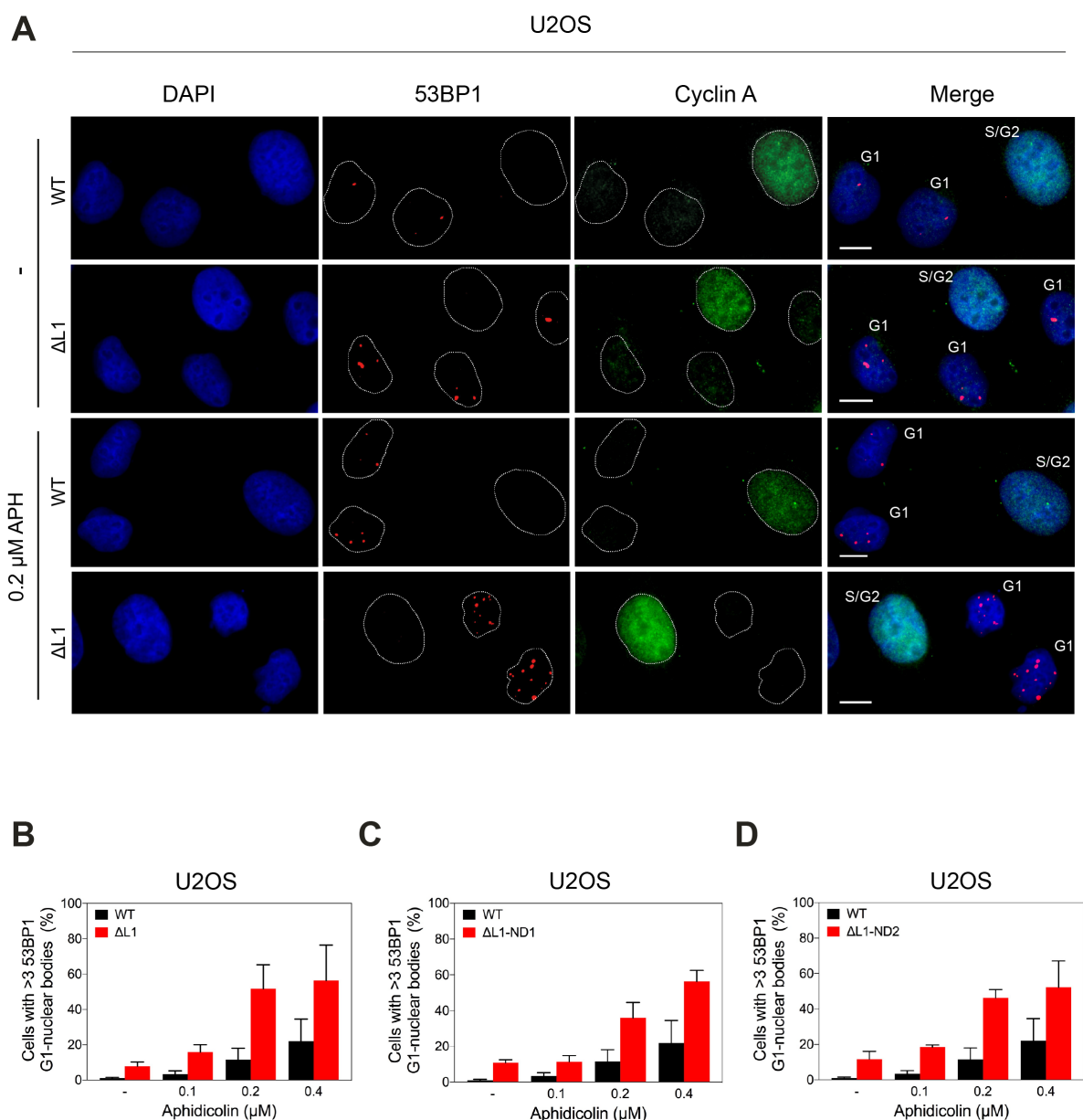


Figure 5.3. Loss of ZFP36L1 induces the accumulation of 53BP1 nuclear bodies (NBs).

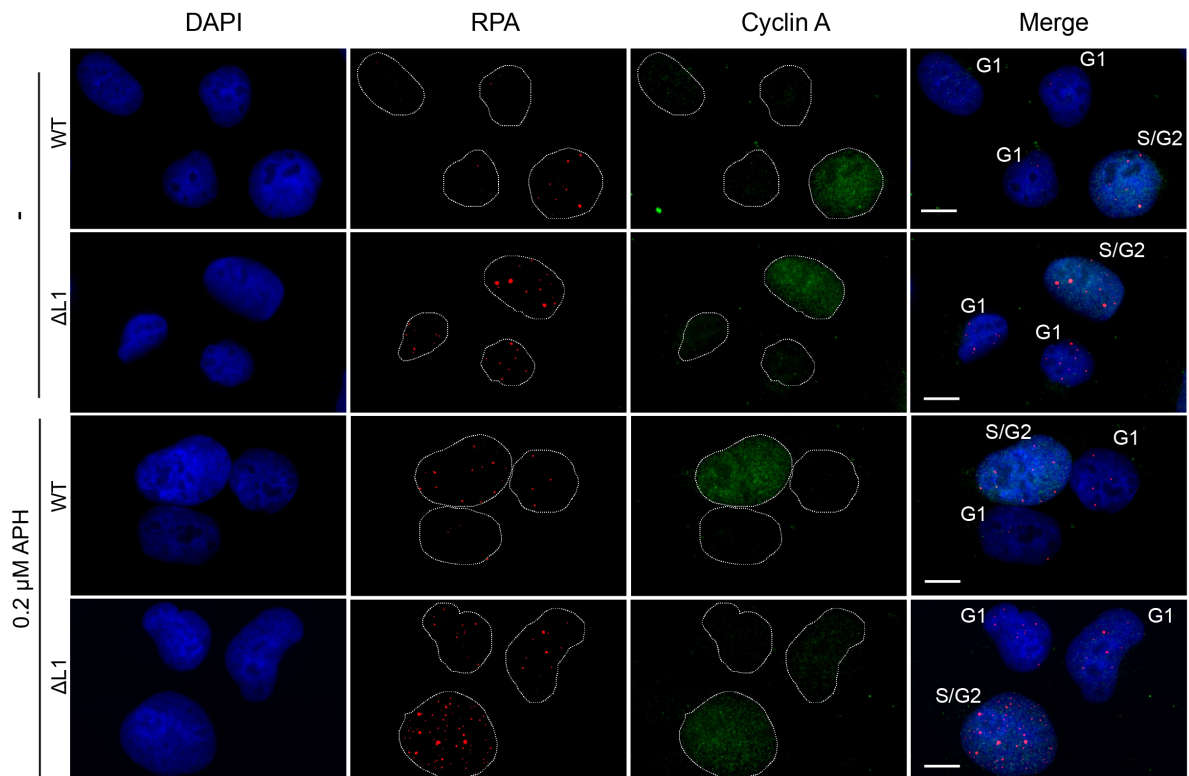
(A) Representative images of untreated and APH-treated G1-phase cells (cyclin A-negative, green) containing 53BP1 nuclear bodies (NBs) (red) scored in wild-type (WT) and ZFP36L1-knockout (Δ L1) U2OS cells. Scale bar, 10 μ m. (B-D) Quantification of G1-phase-specific 53BP1 NBs in untreated and APH-treated WT and (B) Δ L1, (C) Δ L1-ND1 and (D) Δ L1-ND 2 U2OS cells. Percentage of G1 cells with >3 nuclear bodies is plotted. Data are means of three independent experiments with 200 cyclin A-negative cells analysed for each condition per experiment. Error bars show S.E.M. Statistical analysis of 53BP1 NB data is presented in Appendix G.

5.5 ZFP36L1 Deficiency Triggers the Recruitment of RPA During G1-phase and S/G2-phase

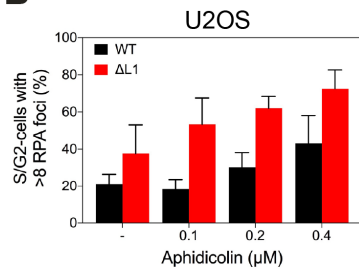
Consistent with its importance in ssDNA binding, RPA is essential for a wide range of DNA transactions, including chromosomal DNA replication and almost all major types of DNA repair (Vassin et al., 2009). Due to its extensive involvement in the DNA damage response, we were prompted to monitor the assembly of nuclear RPA foci as a read-out of ssDNA and DNA repair in the context of ZFP36L1 deficiency. To this end, we quantified levels of endogenous RPA in S/G2-phase as well as in G1-phase of ZFP36L1-deficient and WT U2OS cells using an immunofluorescence-based approach. Strikingly, we found that a truncated variant (Δ L1-ND) as well as a full knockout (Δ L1) of ZFP36L1 not only elicited a significantly increased number of RPA foci in S/G2 but also in the G1-phase of cells, in both, the absence and presence of APH-induced mild replication stress (Figure 5.4A, Appendix H). Indeed, 61% of Δ L1 S/G2-phase cells were found to display more than 8 RPA foci compared to the 30% observed in WT when treated with 0.2 μ M of APH (Figure 5.4B). This phenotype was similarly observed in Δ L1-ND S/G2-phase cells with approximately a 26% increase in RPA detected at 0.2 μ M of APH compared to WT (Figure 5.4C, D). These observations further indicated that ZFP36L1 deficiency is associated with DNA damage, given RPA is a characteristic marker of ssDNA and a crucial hallmark of DNA repair.

A

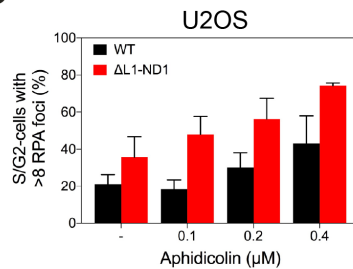
U2OS



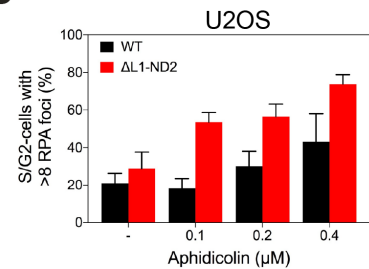
B



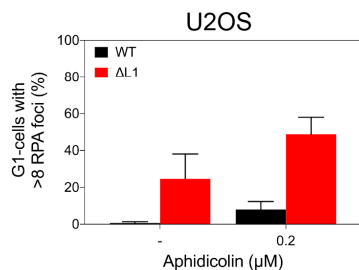
C



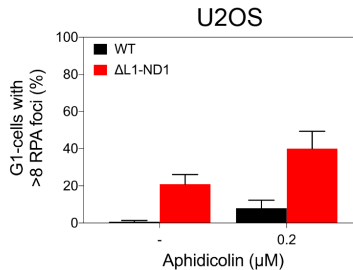
D



E



F



G

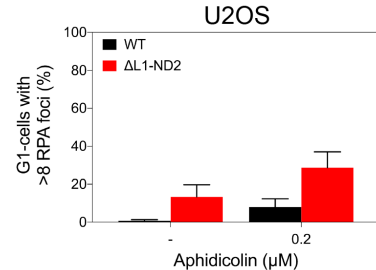


Figure 5.4. RPA is recruited to G1 and S/G2 in response to loss of ZFP36L1.

(A) Representative images of S/G2 (cyclin A-positive, green) and G1 (cyclin A-negative, green) phase cells containing RPA foci (red) scored in untreated and APH-treated wild-type (WT) and ZFP36L1-knockout (ΔL1) U2OS cells. Scale bar, 10 μm. (B-D) Quantification of RPA foci in WT and (B) ΔL1, (C) ΔL1-ND1 and (D) ΔL1-ND2 in S/G2-phase U2OS cells.

Percentage of S/G2-phase cells with >8 RPA foci is plotted. **(E-G)** Quantification of WT and **(E)** Δ L1, **(F)** Δ L1-ND1 and **(G)** Δ L1-ND2 in G1-phase U2OS cells. Percentage of G1-phase cells with >8 RPA foci is plotted. Data are means of three independent experiments with 150 phase-specific cells analysed for each condition per experiment. Error bars show S.E.M. Statistical analysis of RPA data is presented in Appendix H.

Furthermore, we were surprised to find RPA foci in abundance in G1-phase cells in response to a loss of ZFP36L1 ([Figure 5.4A](#)), since there is only modest evidence on RPA's involvement in G1-phase DNA resection (Barlow, Lisby and Rothstein, 2008; Averbeck et al., 2014; Biehs et al., 2017). Interestingly, however, our quantification revealed that even in the absence of exogenous replication stress, 24% of Δ L1 G1-cells displayed more than 8 RPA-positive foci relative to the 1% shown in WT ([Figure 5.4E](#)). Δ L1 cells were even further sensitised to RPA accumulation under conditions of replication stress where almost 50% of the G1-cells gave rise to more than 8 RPA-positive foci compared to the 8% displayed by the WT. Consistently, an N-terminus truncated variant of ZFP36L1 (Δ L1-ND1 and ND2) was shown to elicit a similar phenotype in increased RPA accumulation in the G1-phase compared to WT ([Figure 5.4F, G](#)). Thus, these observations indicate that replication stress-induced DNA damage caused by a disruption or a deletion of ZFP36L1 induces the recruitment of RPA for DNA repair, in both, S/G2 and G1-phase of the cell cycle, further reflecting ZFP36L1's multifunctional role in limiting DNA damage across various stages of the cell cycle in U2OS cells.

5.6 Discussion

Aberrant DNA replication and sustained replication stress can consequently induce replication fork breakage and DNA damage, and result in the formation of DNA DSBs, that require repair activity by the downstream effectors of DDR-associated transducers, ATM and ATR kinases (Ciccia and Elledge, 2010). In light of increasing studies indicating that certain RBPs are functionally linked to the DDR (reviewed in, Dutertre et al., 2014; Dutertre and Vagner, 2017; Nishida et al., 2017), we provide several lines of evidence supporting a novel role for the RBP, ZFP36L1, in protecting genomic stability against replication stress-induced DNA damage. Specifically, we delineate a novel association between ZFP36L1 and suppression of DNA DSB formation, especially under replication stress conditions, across various stages of the cell cycle in U2OS cells.

Besides their role in post-transcriptional regulation of immune-related mRNA targets, members of the ZFP36 family of RBPs have previously been linked to conferring protection of genomic integrity against DNA damage ([section 1.6](#)). Here, we show that even in the absence of mild replication stress, ZFP36L1-deficient cells exhibit a dramatic increase in γ H2AX foci formation as well as G1-phase 53BP1 NBs, which are both morphological hallmarks of DNA DSBs. These results provide new insight into corroborating the relationship between ZFP36L1 and the preservation of genomic integrity and suggest that the multifaceted nature of ZFP36L1 is also functionally linked to the suppression of replication stress-induced DNA DSBs. In agreement with our findings, double conditional knockout (DKCO) of ZFP36L1 and ZFP36L2 in murine thymocytes has been shown to be associated with increased levels of γ H2AX signalling (Vogel et al., 2016). Similarly, a recent study by Lee et al. (2020) indicated

that ZFP36 limits the formation of 53BP1 NBs and γ H2AX foci in response to HU and cisplatin-induced replication stress. Our findings agree with both of these observations and provide evidence demonstrating a critical role for ZFP36L1, specifically in protecting cells' genomic stability against APH-induced replication stress.

In addition to the elevated levels of 53BP1 NBs and γ H2AX foci formation, we also show that in non-treated and APH-treated cells, loss of ZFP36L1 results in increased levels in RPA foci, in both, G1 and S/G2-phase of the cell cycle. Consistent with its ssDNA-binding function, RPA contributes to numerous DNA repair processes and is considered a specific DNA repair marker and a readout of replication stress (reviewed in, Maréchal and Zou, 2013; Zeman and Cimprich, 2014). Thus, collectively, these data further support the proposed role for ZFP36L1 in curbing DSB formation and suppressing replication stress-induced DNA damage. Importantly, all the presented phenotypes exhibited by ZFP36L1-deficient cells were also similarly demonstrated in cells expressing a truncated variant of ZFP36L1. Indeed, Δ L1-ND cells displayed elevated levels for γ H2AX foci, 53BP1 NB formation and RPA foci, corroborating the notion that even a partial disruption of function linked to the ZF binding domain of ZFP36L1 is sufficient to elicit similar replication stress-associated phenotypes. Although the molecular mechanism underlying ZFP36L1's functional role in preserving genomic integrity against replication stress-induced DNA damage is limited by the presented data, our findings provide important potential clues that contribute to the understanding of ZFP36L1's role in maintaining genomic stability. Nevertheless, further research is required to establish the functional molecular base of this association.

6 Loss of ZFP36L1 Potentially Associated with CFS fragility

6.1 Introduction

Chromosomal fragile sites (FSs) are specific genomic loci or regions that are particularly vulnerable to replication stress-induced DSBs (Durkin and Glover, 2007). FSs are generally classified as rare or common based on their frequency in the population and pattern of inheritance (Durkin and Glover, 2007). Rare fragile sites are found in less than 5% of human individuals, segregate in a Mendelian manner and their instability is commonly caused by the expansion of nucleotide repeats (Kremer et al., 1991; Sutherland, Baker and Richards, 1998). On the other hand, common fragile sites (CFSs) are found in all human individuals, represent part of the normal chromosome structure and their instability is not associated with expansion of nucleotide repeats (Durkin and Glover, 2007). Instead, CFS instability or 'expression' is caused by replication stress conditions, and is strongly correlated with cancer (Yunis, 1984; Durkin and Glover, 2007). CFSs can be specifically induced by exposing cells to low doses of APH (Glover et al., 1984) and are often cytologically manifested as gaps, breaks or constrictions on metaphase chromosomes (Durkin and Glover, 2007). Moreover, most CFSs are located within long genes, ranging from a length of several hundred kb to 4 Mb, and also within late-replication domains, which may consequently delay DNA replication (Becker et al., 2002; Smith et al., 2006; Durkin and Glover, 2007). Due to these characteristics, CFSs were characterised as part of difficult-to-replicate regions and therefore, completion of DNA replication at CFSs is often compromised before entry into mitosis (Letessier et al., 2011; Ozeri-Galai et al., 2011). Further, the Fanconi anemia complementation group D2 (FANCD2), a protein

involved in the repair of DNA DSBs, plays a critical role in the protection of CFS stability (Howlett et al., 2005; Madireddy et al., 2016) and was interestingly found to localise to several CFSs under replication stress conditions during mitosis (Chan et al., 2009; Naim and Rosselli, 2009). Accordingly, FANCD2 serves as a reliable marker of certain CFSs undergoing replication stress (Chan et al., 2009).

Until recently, the conventional understanding of DNA replication was that it fully takes place during the S-phase of the cell cycle. However, this view has been recently challenged by the observation that some intrinsically difficult-to-replicate genomic regions, such as CFSs, are only completely replicated during the early stages of mitosis (Minocherhomji et al., 2015). This mitotic DNA synthesis occurring at CFSs loci, termed as 'MiDAS', was found to be particularly apparent in the presence of APH-induced replication stress and is considered as a DNA-repair based pathway that assists cells to faithfully complete DNA replication at genomic regions such as CFSs (Minocherhomji et al., 2015; Bhowmick, Minocherhomji and Hickson, 2016). Thus, since increased MiDAS is strongly associated with CFS instability, CFS expression can be readily detected through the combinatorial use of DNA synthesis-labels with IF-based detection of FANCD2 (Minocherhomji et al., 2015).

In this study, we report another unexpected role for ZFP36L1 in preserving CFS stability. We find that, in addition to replication stress-induced chromosomal instability and DSBs, ZFP36L1 deficiency also induces CFS expression in response to APH-induced replication stress. We provide novel evidence showing that ZFP36L1 deficiency is associated with increased characteristic chromosomal aberrations in the form of gaps, breaks and constrictions on metaphase chromosomes and increased

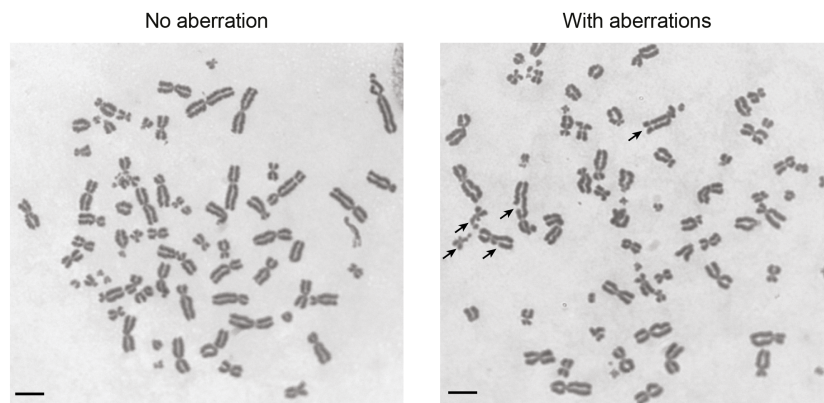
MiDAS events at CFSs in prometaphase cells, which suggested ZFP36L1 to play an active role in the suppression of CFS instability in response to replication stress.

6.2 Loss of ZFP36L1 Results in Increased Chromosomal Fragility

Impaired replication fork progression at CFSs is typically associated with DNA breakage/DSBs, which are commonly manifested into CFS-characteristic chromosome aberrations on metaphase chromosomes (Durkin and Glover, 2007). To explore the relationship between ZFP36L1 and CFS stability, we first investigated the effect of ZFP36L1 deficiency on the appearance of characteristic chromosomal aberrations on Giemsa-stained metaphase chromosome spreads from Δ L1 cells exposed to low doses of APH for 24 hrs ([Figure 6.1A](#)). In particular, we examined whether chromosomes appeared without visible structural changes or with chromatid breaks/gaps, constrictions or with chromosome breaks ([Figure 6.1B-D](#)). Notably, in response to treatment with a low dose of APH (0.2 μ M), ZFP36L1-deficient cells appeared to trigger the expression of chromosome fragility, with about five or six chromosome aberrations detected compared to the two to three shown by the WT-control U2OS cells ($p < 0.0001$) ([Figure 6.1E](#)). This effect was also shown to be consistent in U2OS H2B-GFP cells deficient in ZFP36L1, particularly when exposed to 0.2 μ M of APH ($p < 0.05$) ([Figure 6.1F](#)). Intriguingly, this phenotype was also found in cells expressing a truncated variant of ZFP36L1 (Δ L1-ND1 and ND2), with a significant increase in characteristic chromosome aberrations observed compared to the WT control cells, in response to APH-induced replication stress ([Figure 6.1G and H](#)). Thus, given these characteristic chromosome aberrations are typically associated with CFS instability, these data suggested that ZFP36L1 plays a role in the suppression of CFS expression in response to mild replication stress.

A

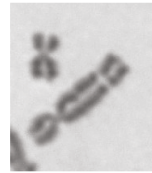
U2OS

**B**

Chromatid break (Gap)

**C**

Chromosome break (Break)

**D**

Constrictions

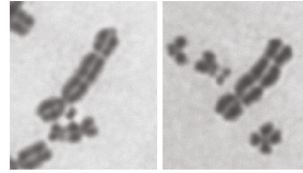
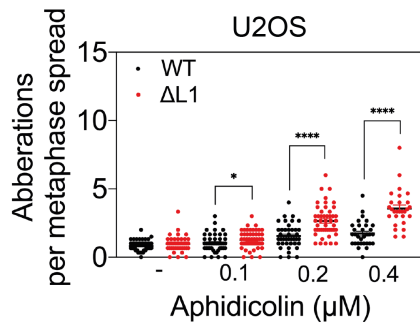
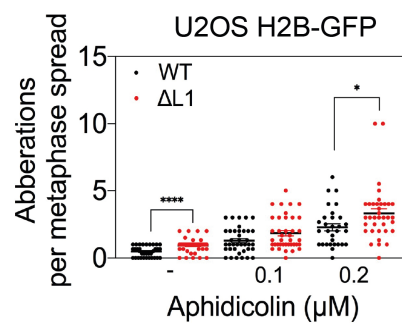
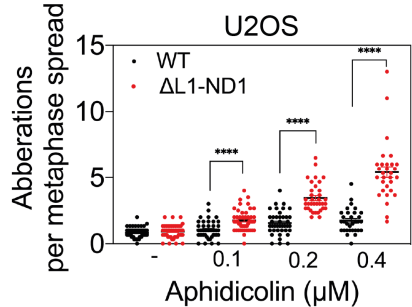
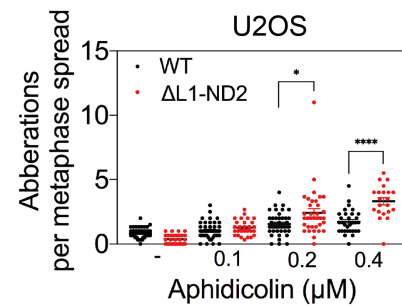
**E****F****G****H**

Figure 6.1. Deletion of ZFP36L1 triggers chromosome fragility.

(A) Examples of Giemsa-stained metaphase spreads with (right) and without (left) chromosomal aberrations in U2OS cells. Colcemid (0.2 $\mu\text{g/ml}$) was added 1.5 hr before collection of cells. Black arrows indicate chromosomal abnormalities. Images were captured at 60x objective. Scale bar, 10 μm (B-D) Examples of chromosomal aberrations scored including (B) Chromatid Breaks (Gaps), (C) Chromosome Breaks and (D) Constrictions. (E-H) Quantification of the number of observed chromosomal aberrations in untreated and APH-treated wild-type (WT) and ZFP36L1-mutants in (E, G and H) U2OS and (F) U2OS H2B-GFP cells. Data are means of three independent experiments. Error bars represent S.E.M. p values were calculated using the Mann-Whitney t -test, *, $p < 0.05$; **, $p < 0.01$; ***, $p < 0.001$; ****, $p < 0.0001$.

6.3 ZFP36L1 Deficiency Linked with increased MiDAS at CFSs during Early Mitosis

By measuring the incorporation of 5-ethynyl-2'-deoxyuridine (EdU) on pro-metaphase nuclei, we next investigated whether ZFP36L1 plays an active role in suppressing CFS instability, through analysis of MiDAS events in ZFP36L1-deficient and ZFP36L1-truncated cells arrested at G2/M transition by CDK1 inhibition with RO-3306, in response to APH-induced replication stress ([Figure 6.2A](#)) (Minocherhomji et al., 2015). Notably, loss of ZFP36L1 appeared to result in a significant increase in the frequency of EdU foci in pro-metaphase nuclei in both non-treated and APH-treated cells ($p < 0.0001$; $p < 0.0001$, respectively) ([Figure 6.2B](#) and C, Appendix I). Indeed, 13% of $\Delta L1$ pro-metaphase nuclei were observed to display more than three EdU foci compared to the 3% observed in WT in non-treated cells, while a 25% increase in EdU foci in $\Delta L1$ was observed compared to the 6.5% detected in WT under APH-induced replication stress ([Figure 6.2C](#)). Moreover, we also assessed the impact of ZFP36L1 deficiency on the number of FANCD2 foci (marker of stalled forks at CFSs) co-localising with EdU foci in $\Delta L1$ pro-metaphase cells (Minocherhomji et al., 2015). Strikingly, in response to APH-induced replication stress, $\Delta L1$ cells appeared to exhibit a significant increase in the number of EdU-positive FANCD2 foci compared to the WT control cells ($p < 0.001$) ([Figure 6.2D](#)). Taken together, these results corroborated the proposed role for ZFP36L1 in suppressing CFS expression during conditions of replication stress.

(A) Experimental workflow for the analysis of EdU incorporation events in combination with IF staining for FANCD2 in pro-metaphase nuclei. Asynchronised U2OS cells were treated with RO-3306 and APH for 16 h and then released into mitosis prior to the detection of EdU and IF-staining for FANCD2. **(B)** Representative images for pro-metaphase nuclei containing EdU-incorporation events and FANCD2 foci, scored in untreated and APH-treated wild-type (WT) and ZFP36L1 knockout (Δ L1) U2OS cells. Scale bar, 5 μ m. **(C)** Quantification of EdU-incorporation events in WT and Δ L1 U2OS cells. Percentage of pro-metaphase nuclei with >3 Edu-incorporation events is plotted. Statistical analysis is presented in Appendix I **(D)** Quantification of EdU co-localised with FANCD2 foci in WT and Δ L1 U2OS cells. Data are means of two independent experiments with a total of 100 pro-metaphase nuclei quantified for each condition per experiment. Error bars represent S.E.M. *p* values were calculated using Mann-Whitney *t*-test, *, *p* < 0.05; **, *p* < 0.01; ***, *p* < 0.001; ****, *p* < 0.0001.

6.4 Discussion

CFSs are recognised as hotspots for genomic instability that are particularly susceptible to breakage upon replication stress conditions during mitosis, and whose expression/instability is commonly observed during the early stages of cancer development (Durkin and Glover, 2007; Glover, Wilson and Arlt, 2017). Growing evidence has accentuated the complexity associated with CFS expression, and multiple mechanisms are believed to be involved in the preservation of CFS stability (reviewed in, Glover et al., 2005). However, one definite trigger for CFS expression is the exposure of cells to mild replication stress, especially when induced by APH treatment (Glover et al., 1984). Here, we report novel evidence showing that, in addition to the suppression of replication stress-induced chromosomal instability and DSBs, ZFP36L1 may play a role in limiting CFS expression in response to replication stress.

A characteristic trait of CFSs is that they preferentially form chromatid breaks/gaps, chromosome breaks and constrictions on metaphase chromosomes under conditions of APH-induced replication stress (Durkin and Glover, 2007). Although increasing evidence has highlighted the emerging role of the ZFP36 family of RBPs in the maintenance of genomic stability, the functional role of members of this RBP family

has not been previously linked to the preservation of CFS stability. Here, we demonstrate data showing distinctive phenotypes for CFS expression occurring in cells where ZFP36L1 expression is permanently abolished, for the first time in literature. Indeed, ZFP36L1-deficient cells displayed a significant increase in characteristic chromosome aberrations compared to the WT control cells in response to APH-induced replication stress (Figure 6.1). While previous research has shown ZFP36 to limit replication stress-induced chromosome aberrations (chromosome breaks and fusions) in response to cisplatin and HU treatment in A549 cells (Lee et al., 2020), our results demonstrate ZFP36L1 to potentially suppress chromosome aberrations that are particularly associated with CFS expression in response to APH treatment. Thus, the induction of CFS expression on metaphase chromosomes suggested that loss of ZFP36L1 may contribute to the protection of U2OS cells against CFS fragility.

To substantiate these findings, we evaluated the frequency of MiDAS events at CFS loci, by measuring the levels of FANCD2 foci co-localising with EdU foci, in intact pro-metaphase nuclei. The significant increase in EdU-positive foci as well as EdU-positive foci co-localising with FANCD2 in ZFP36L1-deficient cells in response to APH treatment (Figure 6.2), indicated that loss of ZFP36L1 appears to compromise the completion of DNA replication at CFSs in response to replication stress. This corroborated our proposed role for ZFP36L1 in limiting CFS expression under conditions of replication stress and also implied that loss of ZFP36L1 might be linked with impaired replication dynamics at CFS loci (Maccaroni et al., 2020). Importantly, these findings provide a possible mechanism by which ZFP36L1 suppresses replication stress-induced genomic instability, given CFS expression is strongly

associated with chromosomal instability and is a common source of replication stress (reviewed in, Ma et al., 2012). Interestingly, however, since the fragility of certain CFSs has also been shown to be driven by the accumulation of R-loops under conditions of replication stress (Helmrich, Ballarino and Tora, 2011), it is therefore also possible that ZFP36L1 suppresses replication stress by limiting unscheduled R-loop formation (potential underlying mechanisms are discussed further in Chapter 7). Altogether, these data strongly suggest ZFP36L1 to be functionally linked to the protection of CFS stability.

7 General Discussion

The faithful transmission of genetic information is a critical determinant of genomic stability and relies on the accurate and efficient replication of the genetic material during each cell division. Cells require the coordination of numerous factors to maintain this accuracy, of which their dysfunction can consequently cause stalling or slowing of replication fork progression, resulting in replication stress (reviewed in, Gaillard, García-Muse and Aguilera, 2015). Accumulating knowledge indicates a multifaceted nature of RBPs with newly identified roles linking them to the coordination and preservation of genomic integrity (Dutertre et al., 2014; Dutertre and Vagner, 2017; Nishida et al., 2017). Recent studies have reported plausible evidence highlighting an emerging tumour-suppressive role for the RBP, ZFP36L1, supported by observations on its downregulated or mutated expression in various cancer cell types (Nik-Zainal et al., 2016; Martincorena et al., 2017; Baxter et al., 2018; Behan et al., 2019; Priestley et al., 2019) and post-transcriptional regulatory role of key cell cycle mRNA targets (Galloway et al., 2016; Suk et al., 2018; Martínez-Calle et al., 2019). Concurrently, increasing reports suggest that ZF-containing proteins, which constitute the most abundant proteins encoded by the human genome, are crucial for maintaining genomic stability (reviewed in, Vilas et al., 2018). Hereof, exploring the precise molecular association between ZFP36L1 and cancer progression in the context of genomic stability may elucidate this underlying link, opening a window for the potential development of novel cancer-targeted therapies. Therefore, in this study, we aimed to investigate the under-recognised role of ZFP36L1 in the preservation of genomic integrity.

ZFP36L1 was first identified as an immediate early-response gene stimulated by the activation of TPA-treated B lymphocytes (Murphy and Norton, 1990; Bustin et al., 1994; Ning et al., 1996). Members of the ZFP36 family are multifunctional proteins that were described to tightly regulate ARE-rich-mRNA stability at the post-transcriptional level (Blackshear, 2002; Murphy, Baou and Jewell, 2009). In addition to their post-transcriptional regulatory role in the development and function of the immune system, the ZFP36 family of proteins have also emerged as crucial regulators of various cancer-related hallmarks (section 1.3.8). Further, recent studies have also suggested that members of the ZFP36 family could also contribute to the maintenance of genomic stability. ZFP36L1 and ZFP36L2 concertedly ensure genomic integrity during B lymphocyte development (Galloway et al., 2016), and limit cell cycle DNA damage signalling in thymocytes (Vogel et al., 2016). ZFP36L2 inhibits cell cycle progression at the S-phase in response to cisplatin-induced replication stress, thus, contributing to the maintenance of genomic stability (Noguchi et al., 2018). Moreover, ZFP36 limits genomic instability by post-transcriptionally regulating mRNA levels of Claspin in response to cisplatin and HU-induced replication stress (Lee et al., 2020). In the present study, we demonstrate a novel role for the RBP ZFP36L1 in the suppression of replication stress-induced genomic instability in human osteosarcoma cells. We describe, for the first time, the generation of CRISPR/Cas9-mediated ZFP36L1-knockout and ZFP36L1-truncated cancer cellular models, that can be used as valuable genetic tools to investigate the multifunctional role of ZFP36L1, and show that ZFP36L1 safeguards genomic integrity against chromosomal instability, DNA damage and CFS expression. Taken together, our data demonstrated here allowed us to present a schematic model that integrates the various replication stress-related

genomic instability phenotypes triggered by the loss of ZFP36L1 across various stages of the cell cycle (Figure 7.1).

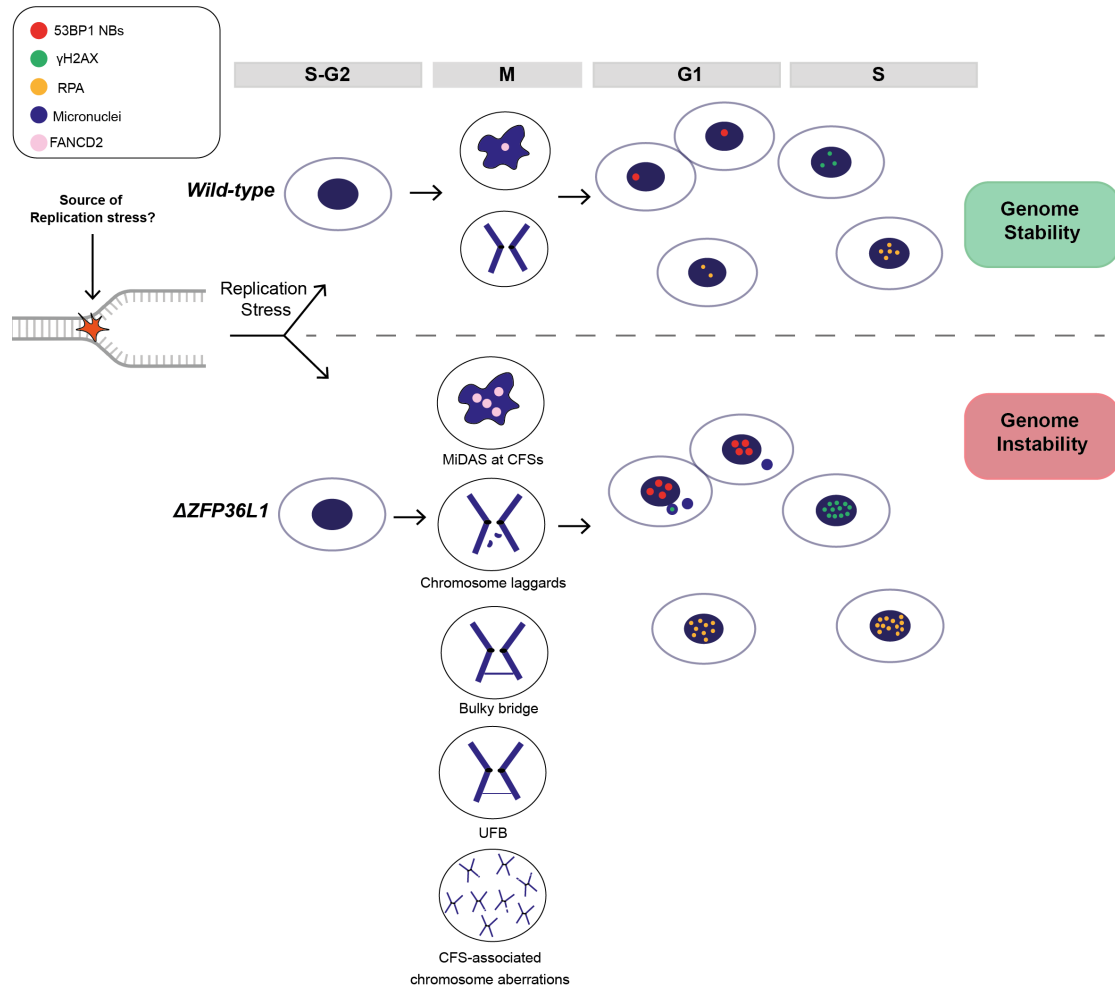


Figure 7.1. Comprehensive model depicting replication stress-related phenotypic consequences associated with ZFP36L1 deficiency in human osteosarcoma cells.

Firstly, we employed the *S. pyogenes*-derived CRISPR/Cas9 gene-editing system and genetically engineered human cancer cellular models by which ZFP36L1 was functionally abolished in U2OS and U2OS H2B-GFP cells as well as a ZFP36L1-truncation that was compromised in the lead-in sequence of its ZF-domain (Chapter 3) (Ran et al., 2013). It is well-established that the CRISPR/Cas9 system is an efficient gene-editing tool which can be used to examine the phenotypic consequences

associated with the loss of function of a gene product in human disease (reviewed in, Adli, 2018). Our strategy involved the use of an all-in-one sgRNA-expressed-plasmid-based delivery of the CRISPR/Cas9 system due to its simplified workflow in mammalian cell lines (reviewed in, Liu et al., 2017). In this case, we targeted exon 2 of the *ZFP36L1* gene which corresponds to more than 90% of the protein-coding region and includes the two highly-conserved zinc finger domains that are critical for *ZFP36L1* function (Lai et al., 2000). Our genetic analysis of the targeted cells indicated successful CRISPR/Cas9-mediated editing within the targeted locus, Ch.14q24.1, of *ZFP36L1*. CRISPResso and Sanger sequencing analysis indicated that the four distinct clonal lines contained specific indels/mutations within the targeted Cas9-cleavage site (Figure 3.8, Figure 3.11B). Immunoblot analysis confirmed the successful knockout of *ZFP36L1* ($\Delta L1$) in both, U2OS and U2OS H2B-GFP cell lines, which were characterised as a homozygous knockout and heterozygous knockout, respectively (Figure 3.10A, Figure 3.11E). The full-length knockout of *ZFP36L1* in both U2OS clonal lines indicated that the specific edited region led to a disruption of the ORF, resulting in a frameshift mutation and a premature stop codon downstream of the targeted region, as evidenced by the analysis of the predicted amino acid sequence of the clones (Figure 3.9A, Figure 3.11D).

In addition to the *ZFP36L1*-knockout cell lines, our methodological approach also successfully resulted in two additional clones; a heterozygous ($\Delta L1$ -ND1) and a homozygous ($\Delta L1$ -ND2) variant, both of which harboured a prominent mutation near the N-terminus domain of *ZFP36L1* (Figure 3.8C and D). Although immunoblot analysis indicated that *ZFP36L1* protein was still produced in these clones, protein expression was significantly truncated (Figure 3.10). We believe that this truncated

expression was mainly due to a 108-bp deletion (35-aa deletion) that was identically carried by both Δ L1-ND1 and Δ L1-ND2 clonal lines. It remains uncertain why there are differences in the expression level of truncated ZFP36L1 between these two clonal lines. Interestingly, the genotypic and phenotypic protein expression exhibited by Δ L1-ND2 was observed to be identical to a third CRISPR/Cas-mediated truncated variant of ZFP36L1 (Δ L1-ND3, data not shown). We speculate, however, that since ZFP36L1 expression is primarily controlled by post-translational modifications (reviewed in, Mackintosh, 2004), a possible cause for this differential phenotype could be due to the nature of the harboured CRISPR/Cas9-resulting amino acid deletions between the two clonal lines, which included differential deletions of identified phosphorylation sites in ZFP36L1, that in turn, may have consequently resulted in differential ZFP36L1 expression. Nonetheless, further examinations are required to explain the phenotypic expression differences between these two clonal lines. Importantly, however, the resulting 35-aa deletion that had occurred within Δ L1-ND1 and Δ L1-ND2 included the first amino acid (Arginine (R)) of the RYKTEL aa motif, a lead-in sequence to the first ZF binding motif that is critical for the optimal activity of ZFP36L1 (Lai et al., 2013). Thus, the ZFP36L1-truncated cellular models provided our study with valuable tools to not only examine the cellular impact of having a partial expression of ZFP36L1 but also the effect of having a compromised RYKTEL motif on the functional activity of ZFP36L1 in relation to genomic stability.

In line with mounting evidence on ZFP36L1's regulatory role in cellular proliferation and cell cycle progression across various cancer cell types (section 1.3.8), we found CRISPR/Cas9-mediated knockout of ZFP36L1 to significantly reduce the growth rate consistently in both U2OS cell lines (Figure 3.12), suggesting that ZFP36L1 is possibly

associated with proliferative-related processes in human osteosarcoma cells and is required for the maintenance of cell growth. This finding challenges previous observations, whereby transient shRNA-mediated knockdown of ZFP36L1 was observed to increase cell number and cell viability in human colorectal cancer cells (Suk et al., 2018), and siRNA-mediated silencing of ZFP36L1 enhanced the proliferation of bladder cancer cells (Loh et al., 2020). Although this may reflect a cell type-specific function for ZFP36L1, our work distinctively shows a reduced-growth phenotype in cells permanently abolished in ZFP36L1 protein. However, further studies will be required to extend the analysis of the proliferative and cellular viability properties of osteosarcoma cancer cells in the context of ZFP36L1 deficiency. Given that we subsequently observed ZFP36L1 to suppress replication stress-induced genomic instability (Chapter 4, 5 and 6), which is typically associated with impaired replication fork progression (Zeman and Cimprich, 2014), we speculate that ZFP36L1-knockout may have consequently impeded replication fork progression in response to elevated replication stress, slowing down cell cycle progression. One way to determine this in future work would be to measure DNA replication progression via DNA fiber analysis on ZFP36L1-knockout/variant clonal lines. Moreover, it is also possible that loss of ZFP36L1 may have altered the levels of its cell cycle-related mRNA targets. However, ZFP36L1's association with progression of the cell cycle in the context of its mRNA targets is beyond the scope of this study. Nonetheless, it will be interesting to explore the cell cycle dynamics in response to the loss of ZFP36L1, especially under replication stress conditions, in future studies.

Secondly, the potential role of ZFP36L1 in the preservation of genomic integrity (section 1.6), which is known to be predominantly jeopardised by chromosomal

instability (Negrini, Gorgoulis and Halazonetis, 2010; Sansregret, Vanhaesebroeck and Swanton, 2018), was investigated by assessing the phenotypic impact of ZFP36L1-deficiency on chromosome segregation (Chapter 4). Here, we show that even in the absence of exogenous DNA replication stress, loss of ZFP36L1 appears to compromise the faithful segregation of chromosomes during cell division. In particular, ZFP36L1-deficiency was associated with increased morphological chromosome mis-segregation hallmarks including, anaphase bridges (DNA bulky bridges and UFBs), lagging chromosomes and micronuclei (Figure 4.1, Figure 4.2, Figure 4.3, Figure 4.4). Notably, these segregation error phenotypes appeared to be further exacerbated under conditions of APH-induced mild replication stress. Thus, these observations implied that ZFP36L1 is required for the complete and efficient segregation of chromosomes during anaphase, especially under conditions of replication stress, which is ultimately required to preserve chromosomal stability.

It has become increasingly evident that in addition to dysregulation of the mitotic machinery, unresolved DNA structures that form as a consequence of replication stress, may persist into mitosis, and cause the mis-segregation of chromosomes (Chan et al., 2009; Naim and Rosselli, 2009; Burrell et al., 2013). Although certain RBPs including ZFP36L1 have been reported to contribute to the regulation of the mitotic apparatus assembly (Kondo et al., 2018; Ito, Watanabe and Kitagawa, 2020), there are only a limited number of studies that have characterised their potential role in curbing replication stress or DNA damage-induced chromosome mis-segregation. In one recent study, however, CIRBP was identified as a critical contributor to the regulation of DNA DSB repair and genomic stability, whereby it was shown to accumulate to DNA damage sites in a PARP1-dependent manner (Chen et al., 2018).

In response to IR-induced DNA damage, CIRBP-depleted cells were associated with HR and NHEJ impairment as well as with increased micronuclei formation (Chen et al., 2018). Although we have not yet determined the exact pathways connected to ZFP36L1's functional activity in preserving chromosomal stability, our work provides the first evidence that chromosome mis-segregation is directly associated with ZFP36L1-deficiency. Nevertheless, further work is required to unravel the precise pathways that ZFP36L1 relies on for this activity.

Thirdly, considering that sustained replication stress can induce replication fork breakage and result in DSB formation (Ciccia and Elledge, 2010), we explored the potential of ZFP36L1 in suppressing replication stress-induced DNA damage (Chapter 5). Consistent with recent studies highlighting the emerging roles of RBPs in limiting DNA damage, we report that ZFP36L1 appears to function not only to preserve chromosomal stability at mitosis but may also protect cells against replication stress-induced DNA damage across various stages of the cell cycle of U2OS cells. Importantly, we demonstrate that ZFP36L1 may be linked with limiting DSB formation in the G1 and S-phase of the cell cycle, as evidenced by the increased accumulation of endogenous RPA, γ H2AX and G1-phase 53BP1 NBs in the context of ZFP36L1 deficiency, even in the absence of exogenous replication stress (Figure 5.1, Figure 5.2, Figure 5.3, Figure 5.4).

It is well-established that the ssDNA-binding protein, RPA, plays a vital role in various aspects of DNA metabolism, including the repair of DSBs during HR-related mechanisms, and is frequently used as a cytological marker for DNA damage/repair (reviewed in, Ruff et al., 2016). In this study, we show that ZFP36L1-deficient cells

exhibit a high frequency of endogenous RPA in both, the G1 and S-phase of the cell cycle (Figure 5.4), which indicated the presence of ssDNA or complex damaged DNA that required DNA resection in both cell cycle phases. Although previous research has shown that certain RBPs such as PRP19 accumulate at DNA damaged sites by directly interacting with RPA as part of the DDR (Maréchal et al., 2014), we understand that the mechanism underlying the accumulation of RPA in response to ZFP36L1 deficiency is limited by the presented data and requires further investigation. Interestingly, however, unpublished observations from our laboratory have identified ZFP36L1 on chromatin fractions, inviting the possibility that ZFP36L1 may potentially directly interact with nuclear-associated factors under conditions of replication stress. The functional significance of this interaction, however, is yet to be determined, and studies are currently underway for the investigation of the specific molecular repair mechanisms associated with ZFP36L1 deficiency.

Further, our studies reveal that even in the absence of exogenous replication stress, ZFP36L1-deficient cells lead to an increased accumulation of γ H2AX (Figure 5.1), a hallmark of DSBs typically triggered as an initial response to DNA damage (Redon et al., 2002; Rothkamm and Löbrich, 2003). This finding supports our proposed role for ZFP36L1 in contributing to curbing sustained replication stress, that would have otherwise led to replication fork breakage and resulted in DNA damage. Moreover, these results agree with previous studies that demonstrated DCKO of ZFP36L1 and ZFP36L2 to conjointly result in increased DNA damage in the form of DSBs, evidenced by increased γ H2AX formation, in mouse thymocytes (Vogel et al., 2016). Our work distinctly shows, however, that this genome destabilisation phenotype can occur

exclusively by ZFP36L1 deficiency, indicating that ZFP36L1 and ZFP36L2 do not always act in a redundant manner.

As a result of impaired resolution of DNA replication defects during mitosis (i.e. at UFB structures in anaphase), unresolved DNA structures are often transmitted into DNA lesions sequestered in 53BP1 NBs in the G1-phase of the daughter cells (reviewed in, Fernandez-Vidal, Vignard and Mirey, 2017). 53BP1 NBs form as microscopically visible foci at DSB sites and have been shown to primarily originate as an outcome of APH-induced replication stress (Harrigan et al., 2011; Lukas et al., 2011). A striking consequence of ZFP36L1 deficiency was the elevated levels of 53BP1 NBs in the G1-phase of the cells, observed even in the absence of APH (Figure 5.3). Thus, these findings collectively support our speculation that ZFP36L1 is intrinsically linked with suppressing replication stress-induced DSB formation and suggests DNA damage inflicted by ZFP36L1-deficiency persists through mitosis, which can have detrimental effects on genomic stability. In line with these findings, siRNA-mediated transient knockdown of ZFP36 was recently shown to be associated with increased DNA damage markers including, 53BP1 and γ H2AX, in response to cisplatin and HU-induced replication stress in A549 (lung carcinoma cells) (Lee et al., 2020). Although the experimental approach and underlying mechanism governing ZFP36 activity investigated (Lee et al., 2020) differs from our study, Lee et al. (2020) observations together with ours, support the emerging role of the ZFP36 family in the preservation of genomic integrity and suggests that ZFP36 protein members may govern distinct pathways in suppressing GIN.

Fourthly, since late replicating regions, such as CFSs, are particularly susceptible to APH-induced replication stress, we investigated whether the genomic instability-associated phenotypes observed in ZFP36L1-deficient cells may also be linked to increased levels of CFS fragility (Chapter 6). Here, we describe an unanticipated role for ZFP36L1, in potentially contributing to the suppression of CFS fragility under conditions of replication stress. Our results demonstrate, for the first time, ZFP36L1 to limit the formation of characteristic chromosomal aberrations as well as the number of MiDAS events occurring at CFSs during mitosis (Figure 6.1, Figure 6.2).

CFSs, which are characteristically prone to DNA breakage, are preferentially affected by genomic instability upon replication stress and are particularly unstable during the early stages of cancer development (Durkin and Glover, 2007; Glover, Wilson and Arlt, 2017). Hereof, elucidating some of the mechanisms underlying CFS instability will further advance our understanding of cancer aetiology and contribute to the development of cancer targeted-therapies. Our study has identified ZFP36L1 as a factor that may contribute to the suppression of CFS expression, supported by our observations of increased CFS-associated chromosomal aberrations, elevated MiDAS events and EdU-positive foci co-localising with FANCD2 at CFS loci during mitosis in cells deficient in ZFP36L1, in response to APH-induced replication stress in U2OS cells (Figure 6.1, Figure 6.2). These findings implied that ZFP36L1 may potentially protect against CFS instability and suppression of impediments that lead to impaired replication fork progression at CFS loci. In agreement with these data, we also observed an enrichment of DNA damage markers in genomic regions that lie within identified CFS loci in U2OS cells in the context of ZFP36L1 deficiency (in collaboration with Dr Kanagaraj Radhakrishnan, The Francis Crick Institute). Indeed,

chromatin immunoprecipitation (ChIP) combined with quantitative real-time PCR revealed that ZFP36L1-deficient cells exposed to APH-induced replication stress were associated with an enrichment of RPA, γ H2AX and 53BP1 NBs within CFSs; *FRA3B*, *FRA16D*, *FRA7H-1*, *FRA7H-2* loci (unpublished data). Taken together, these data strongly supported the notion that ZFP36L1 contributes to the protection of CFS stability against DNA breakage.

Several CFSs such as *FRA3B* and *FRA16D* contain one or more tumour suppressor genes whose structure and function are commonly associated with chromosomal fragility. CFS-associated tumour suppressors such as *FHIT* and *WWOX* mapped on *FRA3B* and *FRA16D*, respectively, were shown to be frequently altered or deleted in many cancers types (reviewed in, Glover, Wilson and Arlt, 2017). Interestingly, the gene locus of *ZFP36L1* has been mapped at CFS; *FRA14C* (commonly induced by APH) (Jang, Shen and McBride, 2014). Thus, since instability of CFSs and their associated genes are closely linked with the early stages of tumourigenesis, uncovering the roles that surround ZFP36L1 with such sites would be particularly interesting to unravel in future work, as it may reveal further links between this protein and human health and disease.

Certain CFSs such as *FRA3B* and *FRA16D* positioned within genes larger than 800 kb require more than one cell cycle to complete transcription (Helmrich, Ballarino and Tora, 2011). Increasing evidence has suggested that the instability of these CFSs is caused by inevitable collisions between the transcription machinery and the replication fork complex, likely caused by the formation of DNA:RNA hybrids (R-loops) (Helmrich, Ballarino and Tora, 2011). Since we observed ZFP36L1 deficiency to be associated

with increased CFS fragility at these sites, we speculate that the genome destabilisation phenotypes exhibited by ZFP36L1-deficient cells may be primarily caused by the formation of unscheduled R-loops. In agreement with this hypothesis, we observed loss of ZFP36L1 to increase the formation of DNA:RNA hybrids in response to APH-induced replication stress, suggesting ZFP36L1 limits R-loop accumulation (in collaboration with Dr Kanagaraj Radhakrishnan, The Francis Crick Institute; unpublished data). Importantly, the protective role of ZFP36L1 against R-loop formation could provide a potential mechanism by which ZFP36L1 suppresses replication stress-induced genomic instability, given unscheduled R-loops represent a major source of replication stress and DNA damage, and are especially driven by the fragility of these CFSs. Thus, we propose that the genome destabilisation phenotypes exhibited by ZFP36L1-deficient cells, at least in part, are consequences of the accumulation of unstable R-loops. These data are in line with recent studies showing several RBPs to suppress R-loop structures' formation and subsequent DNA damage effects (Bhatia et al., 2014, 2017; Santos-Pereira and Aguilera, 2015; Crossley, Bocek and Cimprich, 2019). However, future studies will be required to elucidate the precise mechanism by which ZFP36L1 preserves genomic integrity against R-loop instability.

Finally, we further demonstrate that a mutant/truncated variant of ZFP36L1 carrying a compromised structure of the ZF-related RYKTEL motif, shown in CRISPR/Cas9-generated Δ L1-ND1 and Δ L1-ND2 cellular models, increases replication stress phenotypes similar to that of complete ablation of ZFP36L1 (ZFP36L1-deficient/knockout cells). Indeed, cells expressing a truncated variant of ZFP36L1 were observed to result in elevated levels of chromosome mis-segregation, replication stress-induced DNA damage and CFS-associated chromosome aberrations

compared to the WT. Although ZFP36L1 protein was partially expressed in these cellular models, these data suggested that the truncated expression was sufficient to reduce ZFP36L1 function in preserving genomic stability against replication stress. Further, these results may also imply that deletion of Arginine (R) at the RYKTEL aa-motif, a conserved lead-in sequence to the first ZF domain of ZFP36L1 (Lai et al., 2000), potentially jeopardised the structural integrity of the encoded CCCH zinc finger domain (Lai, Kennington and Blackshear, 2002; Lai et al., 2003; Brewer et al., 2004). This is in line with previous research that has shown the RYKTEL aa lead-in sequence to be of importance for the ZFD and therefore, for the optimal function of the ZFP36 family members (Lai et al., 2013). These data, therefore, may suggest that the intactness of RYKTEL structure is essential for ZFP36L1 functions in maintaining genomic stability. Consistent with our interpretation, previous research has highlighted the significance of the ZF-binding domains for the function of the ZFP36 family members. For example, a mutation in the ZF-binding domain of ZFP36 was shown to completely attenuate its post-transcriptional mRNA destabilisation function on its targeted TNF- α transcripts (Lai et al., 1999). Mutations within the ZF-domains of ZFP36 also resulted in increased proliferation of breast cancer cells (Al-Souhibani et al., 2010). In another study, defects in the ZF-domain of ZFP36L1 were shown to consequently ablate its mRNA binding function on Notch1 transcripts in T lymphocytic leukaemia cells (Hodson et al., 2010). More recently, ZF-mutated ZFP36L1 and ZFP36L2 were similarly described to jeopardise the proteins' function in inhibiting cyclin D expression and proliferation in human colorectal cancer cells (Suk et al., 2018). Although the precise cause for the replication stress phenotypes exhibited by ZFP36L1-truncated cells remains to be investigated, it is possible that the disruption of the RYKTEL aa-sequence compromised the stability of the ZFD, suggesting that

that the ZFDs are critical for the suppression of replication stress-induced genomic instability. Nonetheless, further studies will be required to elucidate the origin of the distinctive phenotypes displayed by Δ L1-ND1 and Δ L1-ND2 cells.

8 Conclusions

Collectively, our findings strongly suggest a novel role for ZFP36L1 in serving as a guardian of genomic stability with a crucial role in combatting endogenous replication stress. The increase in CIN hallmarks, accumulation of DSBs-indicative markers and elevation in CFS-associated characteristics in ZFP36L1-deficient and ZFP36L1-truncated cells, in both, the absence and presence of APH-induced replication stress, provide compelling evidence that supports the direct involvement of ZFP36L1 in the preservation of genomic integrity against consequences related to replication stress. In line with recent observations underscoring the emerging role of the ZFP36 family of RBPs in curbing genomic instability, our work provides an extensive inventory of genome destabilisation phenotypes, which were previously unrecognised, associated with ZFP36L1-deficiency in U2OS cells. These data are consistent with recent observations suggesting a crosstalk between RBPs and genome stability, and further highlight a multifaceted nature for the RBP, ZFP36L1. Importantly, given the growing number of different cancers in which ZFP36L1 has been reported to be dysregulated, these findings illuminate the underlying molecular links with ZFP36L1 that may govern some of these processes, and suggests that ZFP36L1 may be an important genome stability-related regulator in many other cancer cell types. Although the exact means by which ZFP36L1 protects genomic integrity against replication stress remains to be determined, our results provide important clues to the mechanisms potentially involved in ZFP36L1's inherent capacity to preserve genomic integrity. An important agenda for future research, currently focused on in our laboratory, involves a more in-depth

analysis of ZFP36L1's role in limiting R-loop instability and other possible replication stress-causing factors, proteomic analysis and characterisation of the interactome of ZFP36L1 and characterisation of the protein in other cancer cell types. Thus, an array of follow up studies will be required to dissect the exact molecular mechanisms by which ZFP36L1 suppresses replication stress-induced genomic instability.

Appendices

Appendix A- related to section 1.3.4.



Figure A-1. Phosphorylation sites identified in Human ZFP36L1.

Full-length amino acid sequence of human ZFP36L1 (UniProtKB/Swiss-Prot: Q07352.1). Identified phosphorylation sites in human ZFP36L1 are emboldened in red and include S⁵⁴, S⁹², T¹¹⁷, T¹⁵⁵, Y¹⁶⁹, S²⁰¹, S²⁰³, S²²⁵, S²²⁷, S²⁴⁰, S²⁹¹, S²⁹⁴, S²⁹⁸, Y³⁰⁵, S³¹⁶, S³¹⁸ and S³³⁴. CCCH residues in the tandem zinc finger motifs are emboldened in black and R/K(EKTEL) lead-in sequences to the ZFDs in ZFP36L1 are highlighted in pink. Adapted from Cao, Deterding and Blackshear (2007).

Appendix B- pSpCas9(BB)-2A-Puro (PX459) plasmid-related to Chapter 3.

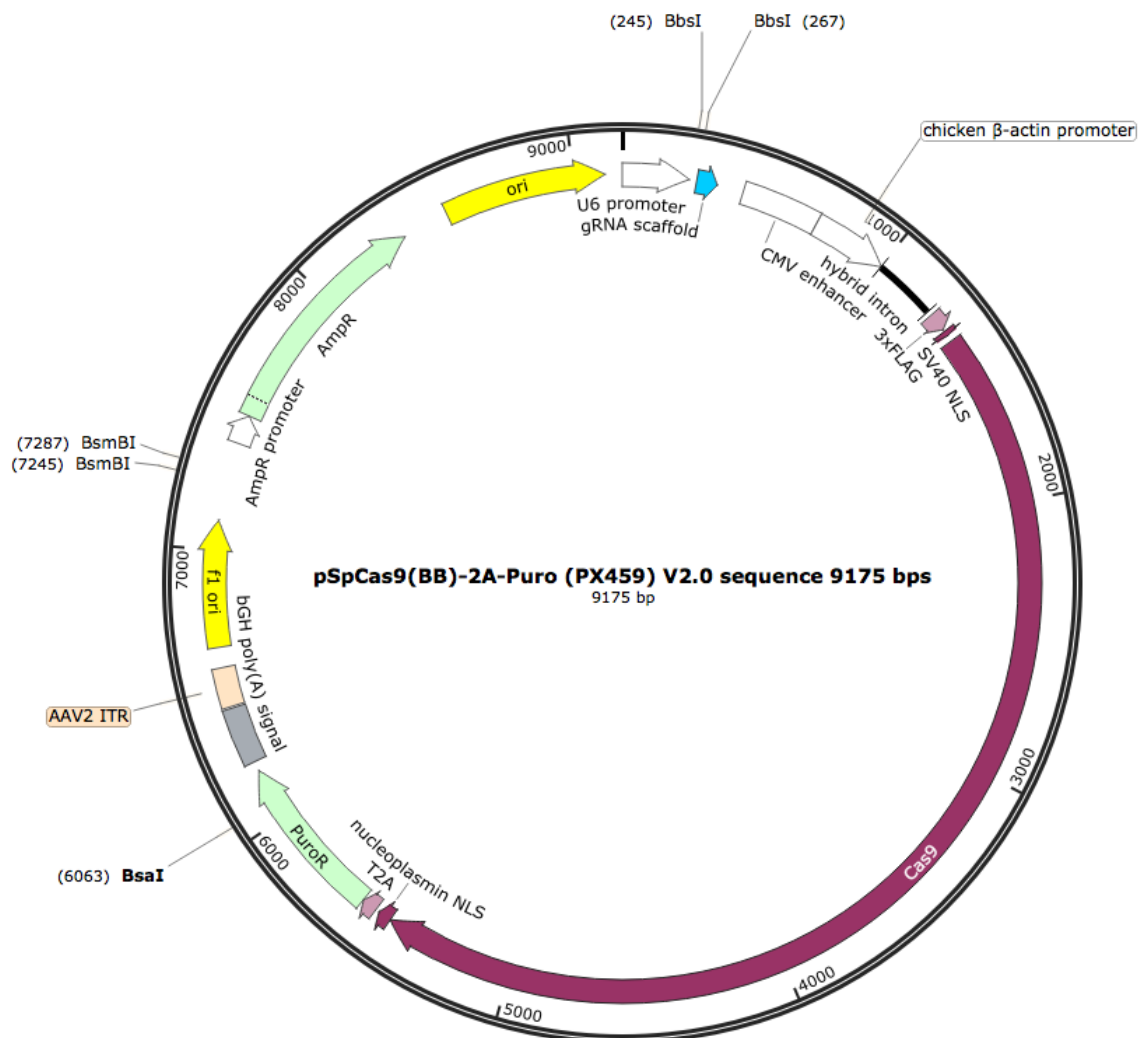


Figure B-1. Schematic representation of pSpCas9(BB)-2A-Puro (PX459) plasmid features. pSpCas9(BB)-2A-Puro (PX459) plasmid contains a Cas9-expression cassette and sgRNA scaffold. BbsI restriction sites near the sgRNA scaffold represent the region used for cloning the designed gRNA oligos. Selectable markers, ampicillin and puromycin, aided in the selection of transformed bacterial and transfected mammalian cells, respectively, due to the presence of an ampicillin and puromycin resistant gene in pSpCas9(BB)-2A-Puro (PX459) plasmid (AmpR, PuroR; light green). Image adapted from Addgene. pSpCas9(BB)-2A-Puro (PX459) plasmid was designed and engineered by Ran et al. (2013).

Appendix C-related to Figure 3.8 and Figure 3.10

Appendix C-1

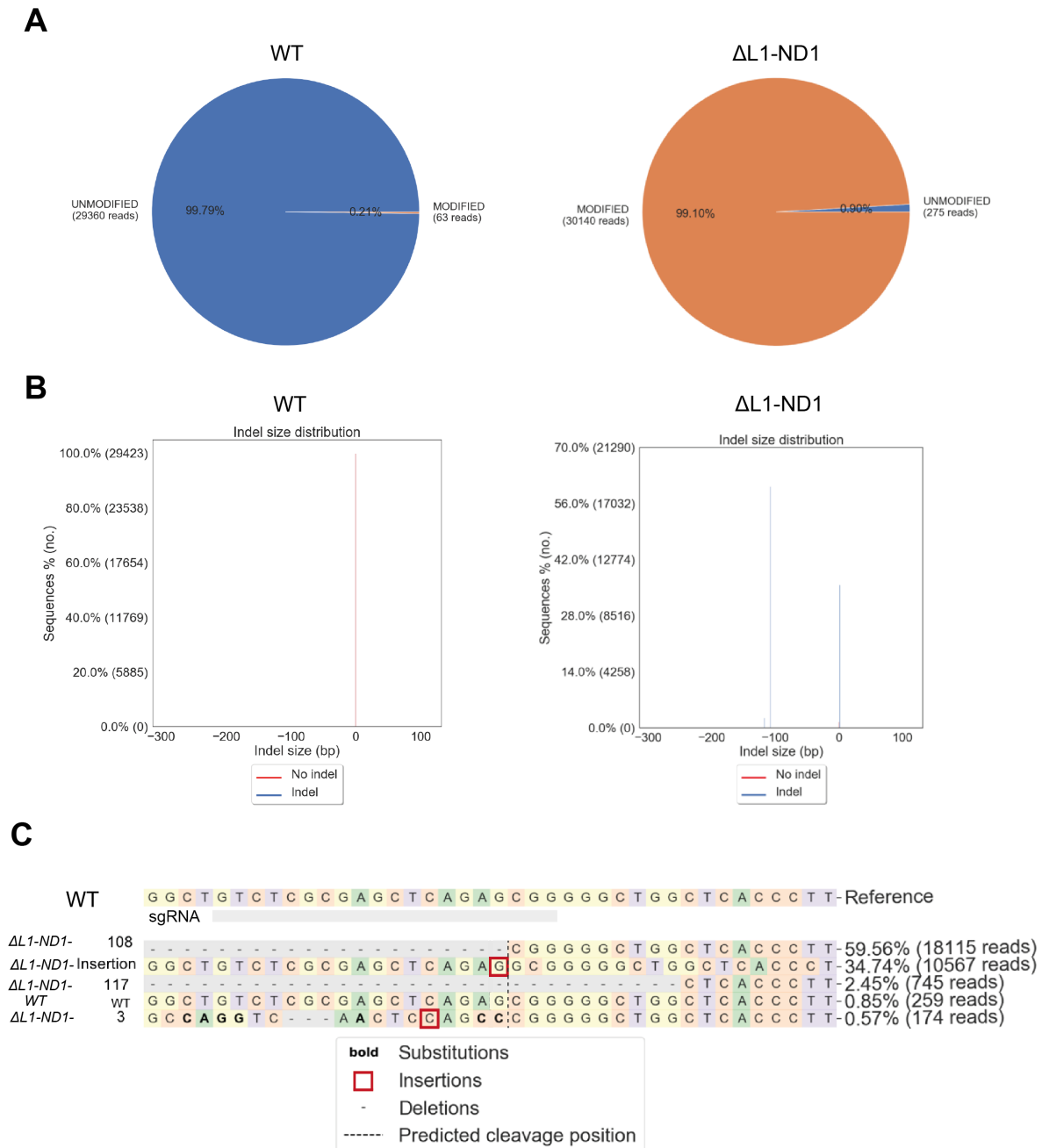


Figure C-1. CRISPResso analysis of CRISPR/Cas9-generated ΔL1-ND1 clonal genotype. (A) Quantification and visualisation of the percentage of editing frequency, determined by the number of sequenced reads showing modified and unmodified alleles, in wild-type (WT; left) and ZFP36L1-N-Terminal Deletion 1 (ΔL1-ND1; right). (B) The percentage of sequenced reads with and without indels/mutations in WT (left) and ΔL1-ND1 (right). (C) Ampliseq-EZ-NGS sequence alignment of the targeted region within *ZFP36L1* in WT and ΔL1-ND1. Detected substitutions (emboldened in black), insertions (red box) deletions (dashed lines) are indicated.

Appendix C-2- related to Figure 3.10.

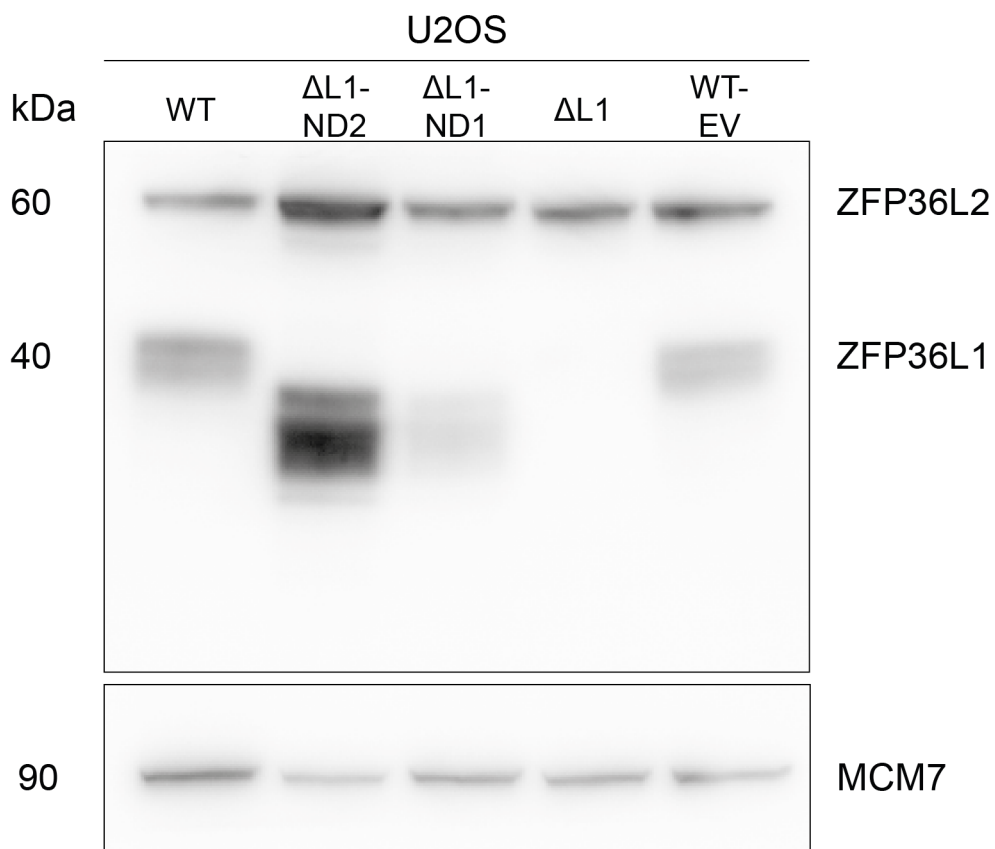


Figure C-2. Western blot analysis of ZFP36L1 from whole-cell extracts of U2OS cells. Protein expression of wild-type (WT), WT-empty vector (pSpCas9(BB)-2A-Puro-only) (WT-EV), truncated ZFP36L1 (Δ L1-ND1 and Δ L1-ND2) and ZFP36L1 knockout (Δ L1), derived from U2OS cells, using the indicated antibodies. ZFP36L2 and MCM7 were used as loading controls.

Appendix D- related to Figure 4.1 (D.1), 4.2 (D.2) and 4.3 (D.3).

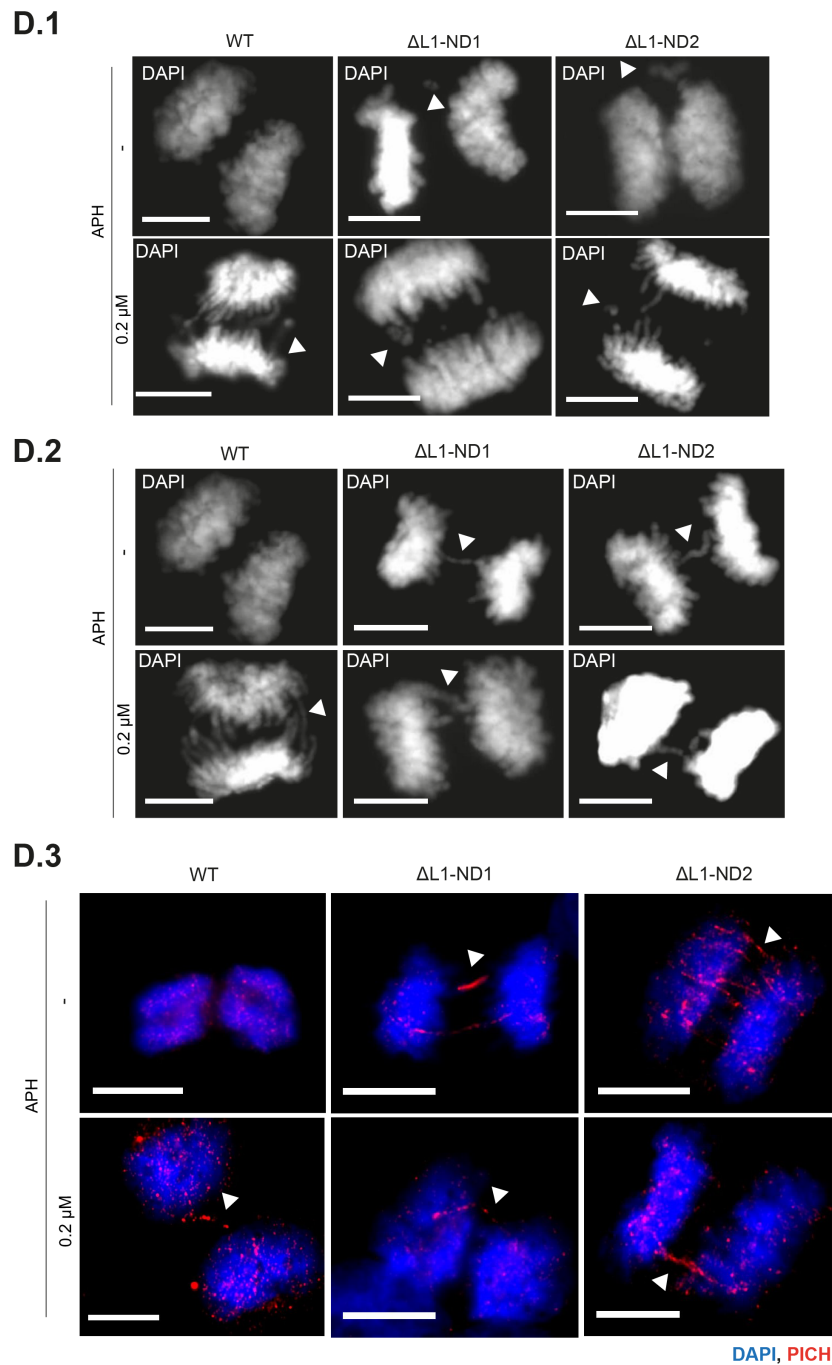


Figure D-1. Examples of lagging chromosomes, bulky bridges and UFBs in WT and Δ L1-ND U2OS Cells.

Representative images of (D.1) lagging chromosomes, (D.2) bulky anaphase bridges and (D.3) UFBs in wild-type (WT), Δ L1-ND1 and Δ L1-ND2 U2OS cells. White arrows indicate chromosome segregation error. Scale bar, 10 μ m.

Appendix E- related to Figure 4.4.

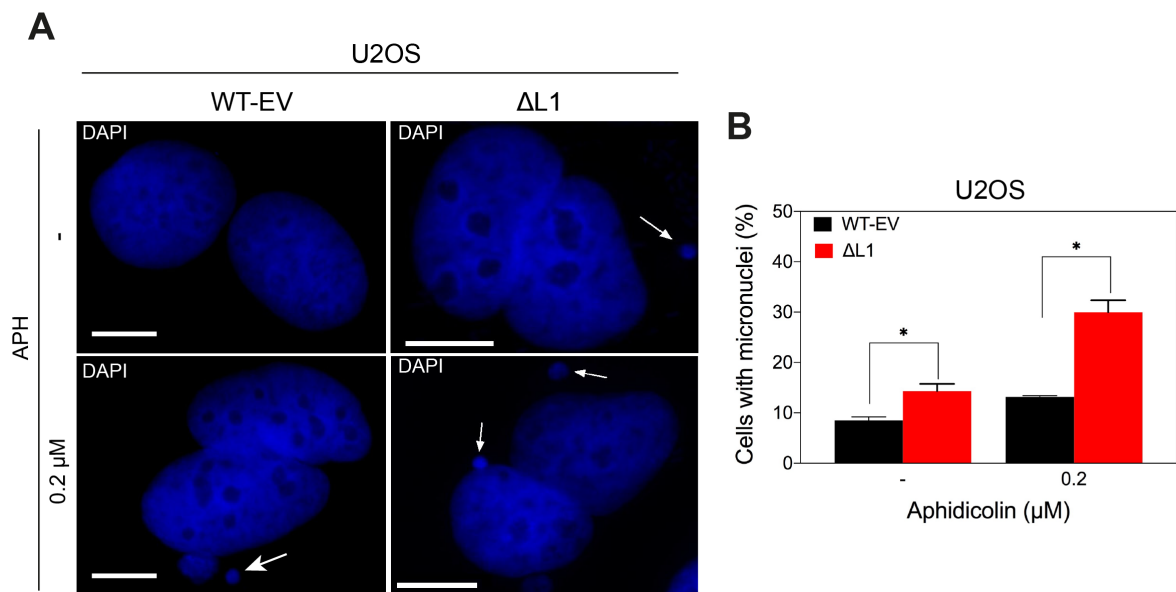


Figure E-1. Micronuclei formation analysis of WT- empty vector (pSpCas9(BB)-2A-Puro-only) (EV) and ZFP36L1 knockout ($\Delta L1$) derived from U2OS cells.

(A) Representative images of cytochalasin-B induced binucleated cells with micronuclei scored in WT-empty vector (pSpCas9(BB)-2A-Puro-only) (WT-EV) and ZFP36L1 knockout ($\Delta L1$) in U2OS cells **(B)** Quantification of the frequency of micronuclei scored in untreated and APH-treated WT-empty vector (pSpCas9(BB)-only) (WT-EV) and $\Delta L1$ U2OS cells. White arrows indicate micronuclei. Scale bar, 10 μm . Data are means of two independent experiments with a total of 300 binucleated cells analysed per condition in each experiment. Error bars represent SD. *p* values were calculated using an unpaired *t*-test, *, *p* < 0.05; **, *p* < 0.01; ***, *p* < 0.001; ****, *p* < 0.0001.

Appendix F – related to Figure 5.1 (F.1) and 5.2 (F.2).

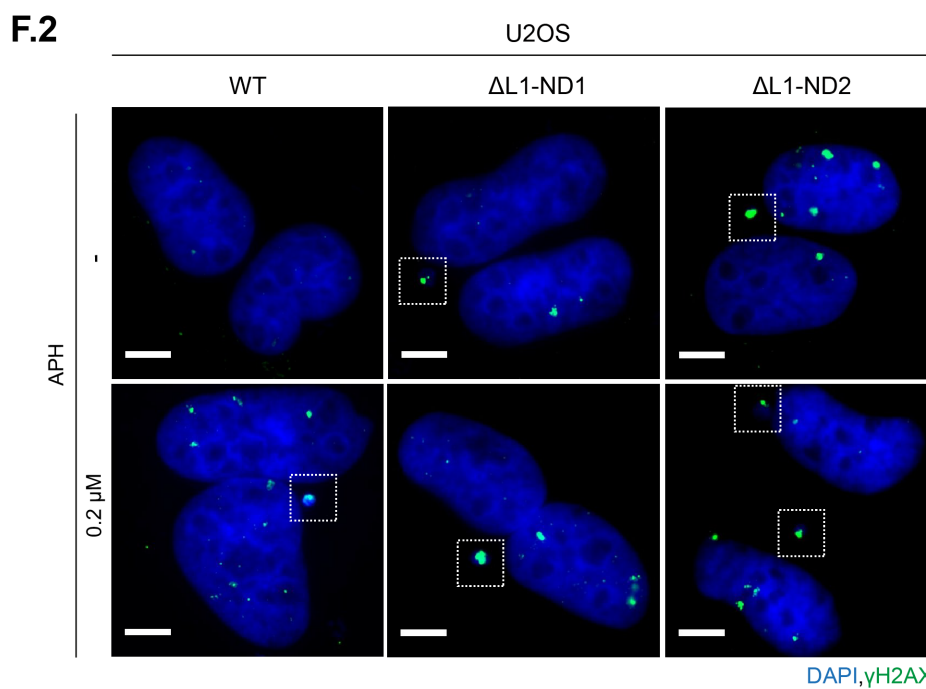
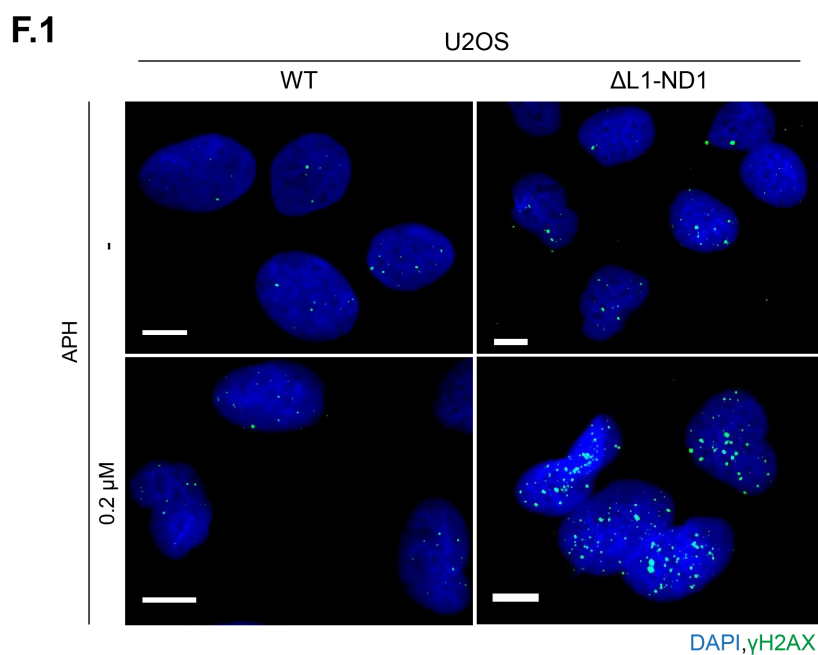
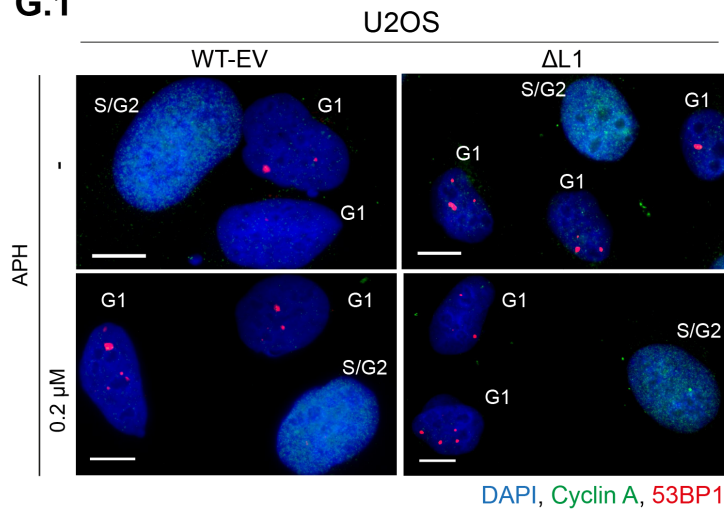


Figure F-1. Examples of interphase cells with γ H2AX-positive foci and γ H2AX-positive micronuclei in WT and Δ L1-ND U2OS cells.

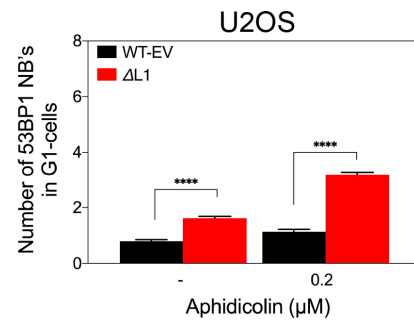
(F.1) Examples of interphase cells with γ H2AX-positive foci in untreated and APH-treated wild-type (WT) and Δ L1-ND1 U2OS cells. (F.2) Representative images of cytochalasin-B induced binucleated cells with micronuclei positive for γ H2AX scored in untreated and APH-treated WT and Δ L1-ND Cells. Dashed squares indicate γ H2AX (+) micronuclei. Scale bar, 5 μ m.

Appendix G – related to Figure 5.3.

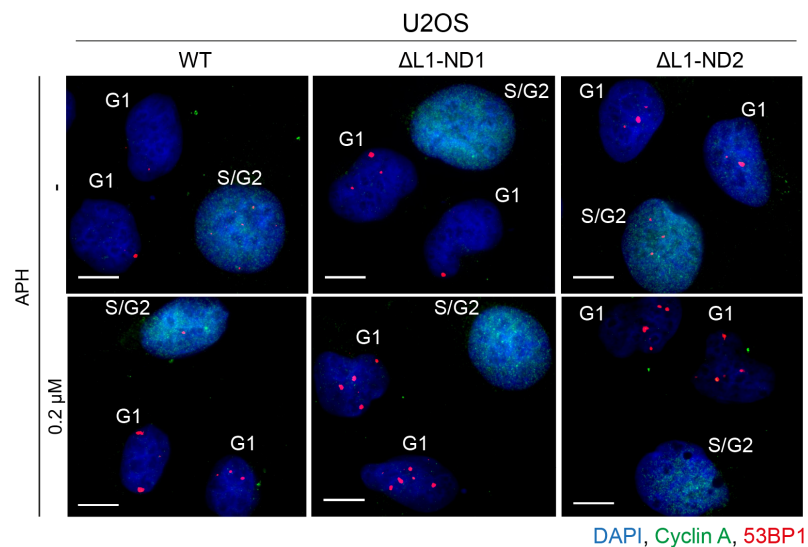
G.1



G.2



G.3



G.4

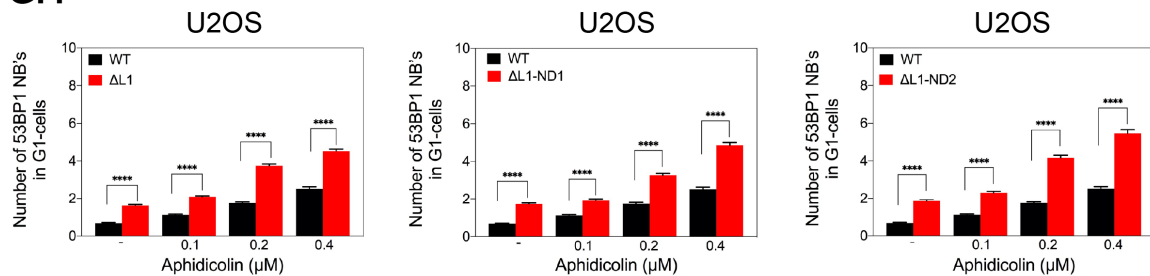


Figure G-1. 53BP1 NB analysis in WT-empty vector (pSpCas9(BB)-2A-Puro-only), examples of 53BP1 NB formation in Δ L1-ND cells and statistical analysis of 53BP1 NB formation in Δ L1 and Δ L1-ND U2OS cells.

(G.1) Representative images of untreated and APH-treated G1-phase cells (cyclin A-negative, green) containing 53BP1 nuclear bodies (NBs) (red) scored in WT-empty vector (pSpCas9(BB)-2A-Puro-only) (WT-EV) and ZFP36L1-knockout (Δ L1) U2OS cells. (G.2)

Quantification of G1-phase 53BP1 NBs in untreated and APH-treated WT-empty vector (pSpCas9(BB)-2A-Puro-only) (WT-EV) and Δ L1 U2OS cells. **(G.3)** Representative images of untreated and APH-treated G1-phase cells (cyclin A-negative, green) containing 53BP1 nuclear bodies (red) scored in WT and Δ L1-ND U2OS cells. **(G.4)** Quantification of G1-phase 53BP1 NBs in untreated and APH-treated in WT and **(left)** Δ L1, **(middle)** Δ L1-ND1 and **(right)** Δ L1-ND2 U2OS cells with statistical analysis. Scale bar, 10 μ m. Data are means of three independent experiments with 200 cyclin A-negative cells analysed for each condition per experiment. Error bars show S.E.M. *p* values were calculated using Mann-Whitney *t*-test, *, *p* < 0.05; **, *p* < 0.01; ***, *p* < 0.001; ****, *p* < 0.0001.

Appendix H – related to Figure 5.4.

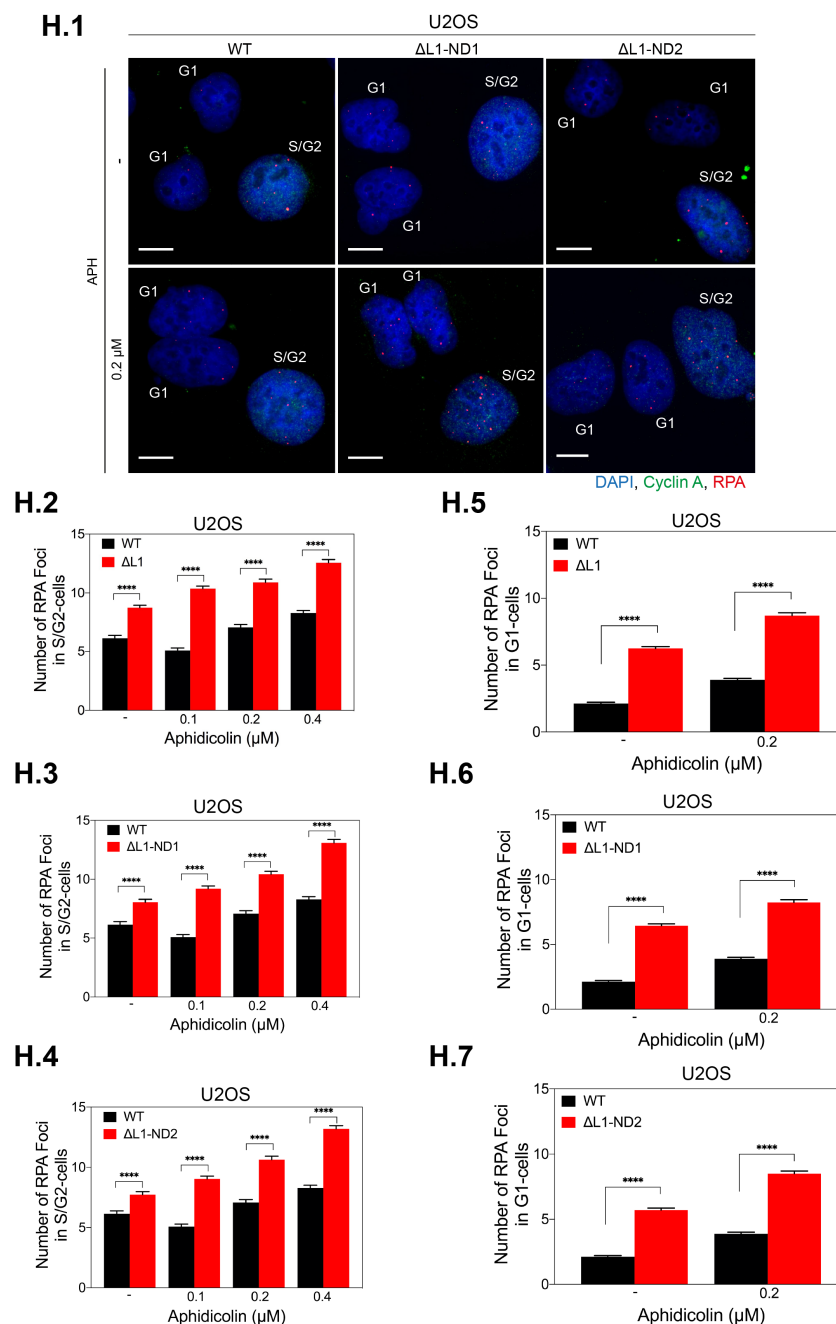


Figure H-1. Examples of S/G2 and G1-phase nuclei containing RPA in Wild-type (WT) and ZFP36L1-truncated (Δ L1-ND) U2OS cells and statistical analysis of RPA accumulation in Δ L1 and Δ L1-ND U2OS cells.

(H.1) Representative images of S/G2 (cyclin A-positive, green) and G1-phase (cyclin A-negative, green) cells containing RPA foci (red) scored in untreated and APH-treated wild-type (WT) and ZFP36L1-truncated (Δ L1-ND) U2OS cells. Scale bar, 10 μ m. (H.2-H.4) Quantification of RPA foci in WT and (H.2) Δ L1, (H.3) Δ L1-ND1 and (H.4) Δ L1-ND2 in S/G2-phase U2OS cells. (H.5-H.7) Quantification of WT and (H.5) Δ L1, (H.6) Δ L1-ND1 and (H.7) Δ L1-ND2 in G1-phase U2OS cells. Data are means of three independent experiments with

150 phase-specific cells analysed for each condition per experiment. Error bars show S.E.M. p values were calculated using Mann-Whitney t -test, *, $p < 0.05$; **, $p < 0.01$; ***, $p < 0.001$; ****, $p < 0.0001$.

Appendix I – related to Figure 6.2.

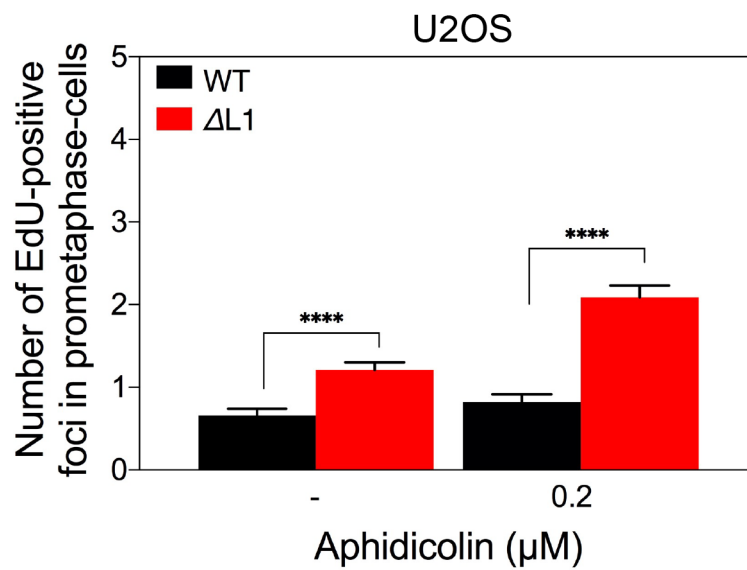


Figure I-1. Statistical analysis of EdU-positive foci in WT and Δ L1 U2OS cells.

Quantification of EdU-positive foci in WT and Δ L1 pro-metaphase U2OS cells. Data are means of two independent experiments with a total of 100 pro-metaphase nuclei quantified for each condition. Error bars represent S.E.M. *p* values were calculated using Mann-Whitney *t*-test, *, $p < 0.05$; **, $p < 0.01$; ***, $p < 0.001$; ****, $p < 0.0001$.

Glossary

53BP1 – p53 binding protein 1

aa – amino acid

ALS – Amyotrophic lateral sclerosis

AML – Acute myeloid leukaemia

APH – Aphidicolin

ARE – Adenine-uridine rich elements

ARIDA1-A – AT-Rich Interaction Domain 1A

ATM – Ataxia telangiectasia-mutated

ATR – Ataxia telangiectasia and Rad3-related

ATRIP – ATR-interacting protein

BCL2 – B-cell lymphoma 2

BER – Base excision repair

BLM – Bloom Syndrome RecQ Like Helicase

bp – Base pair

BRCA – Breast cancer gene

Cas – CRISPR associated protein

Cas9 – CRISPR associated protein 9

CCR4-NOT – Ccr4/Caf1/Not deadenylase

CDC – Cell division cycle

CDKs – Cyclin-dependent kinases

CFS – Common fragile site

CHK – Checkpoint kinase

CIN – Chromosomal instability

CIRBP – Cold-inducible RBP

COX – Cyclooxygenase

CRISPR – Clustered regularly interspaced short palindromic repeats

CTD1 – DNA replication factor 1

DAPI – 4,6-diamidino-2-phenylindole

DCKO – Double conditional knockout

DDR – DNA damage response

DMEM – Dulbecco's modified Eagle medium

DNA-PKcs – DNA-dependent protein kinase catalytic subunits

DSBs – Double-stranded breaks
dsDNA – Double-stranded DNA
EdU – 5-ethynyl-2'-deoxyuridine
EMT – Epithelial-mesenchymal transition
ETAA1 – Ewing's tumour-related antigen 1
EWS – Ewing Sarcoma
EXO – Exonuclease
FANCD2 – Fanconi anemia complementation group D2
FSs –Fragile sites
FUS – Fused in sarcoma/translocated in liposarcoma
GIN – Genomic instability
GM-CSF – Granulocyte macrophage colony-stimulating factor
GFP – Green fluorescent protein
gRNA – Guide RNA
HIF1A – Hypoxia inducible factor 1 subunit alpha
HnRNP – Heterogeneous nuclear RNPs
HR – Homologous recombination
HRP – Horseradish peroxidase
HU – Hydroxyurea
HuR – Human antigen R
IAV – Influenza A virus
IF – Immunofluorescence
IFN – Interferon
Ig – Immunoglobulin g
IL – Interleukin
IR – Ionizing radiation
kDa – kilo Dalton(s)
LATS2 – Large tumour suppressor kinase 2
LDLR – Low-density lipoprotein receptor
MCM2-7 – Minichromosome maintenance complex 2–7
MDM2 – Mouse double minute 2 homolog
mg – milligram
MiDAS – Mitotic DNA synthesis
MIN – Micro-satellite instability

MK2 – MAPK2-activated protein kinase 2
MMP – Matrix metalloproteinase
MMR – Mismatch repair
MRN – MRE11–RAD50–NBS1
MSH2 – Mut S Homolog 2
MZ – Marginal zone
NES – Nuclear export signal
NF-κB – Nuclear Kappa B
NHEJ – Non-homologous end joining
NME1 – Nucleoside diphosphate kinase A
NOTCH1 – Notch homologue 1
NS1 – Non-structural protein 1
OA – Osteoarthritis
ORC – Origin recognition complex
ORF – Open reading frame
P-bodies – Processing bodies
PARN – PolyA specific ribonuclease
PARP – Poly(ADP-ribose) polymerase
PBS – Phosphate buffered saline
PCR – Polymerase chain reaction
PICH – Plk1-interacting checkpoint helicase
PIM-1 – Proto-oncogene serine/threonine-protein kinase
PK – Protein Kinase
PKB – Protein kinase B
Pre-IC – Pre-initiation complex
Pre-RC – Pre-replication complex
PRP19 – Pre-mRNA-processing factor 19
RA – Rheumatoid arthritis
RBD – RNA-binding domains
RBP – RNA-binding protein
RNP – Ribonucleoprotein
RPA – Replication protein A
SGs – Stress granules
shRNA – Short-hairpin RNA

siRNA – Short interfering RNA
SLE – Systemic lupus erythematosus
SMN1 – Survival motor neuron 1
SNP – Single nucleotide polymorphism
SR – Serine-arginine
ssDNA – Single-stranded DNA
TALENs – Transcription activator-like effector nucleases
TIS11 – Tetradecanoylphorbol-13-acetate inducible sequence 11
TNF – Tumour necrosis factor
TOP1 – Topoisomerase 1
TOPBP1 – DNA Topoisomerase II Binding Protein 1
UFB – Ultra-fine bridge
uPA – Urokinase plasminogen activator
UTR – Untranslated region
UV – Ultraviolet radiation
VEGF – Vascular endothelial growth factor
WT – Wild-type
XLF – XRCC4 like factor
XRCC4 – X-ray cross-complementation group 4
YB-1 – Y-box binding protein
ZF – Zinc Finger
ZFNs – Zinc finger nucleases
ZFP36 – Zinc finger protein 36
ZFP36L1 – Zinc finger protein 36-like 1
ZFP36L2 – Zinc finger protein 36-like 2
 α – Alpha
 γ H2AX – phosphorylated histone H2AX
 δ – Delta
 Δ L1 – ZFP36L1 knockout
 Δ L1-ND – N-terminal deletion of ZFP36L1
 ϵ – Epsilon
 μ L – microliter
 μ M – micromolar
 μ m –micrometre

Bibliography

Adachi, S., Homoto, M., Tanaka, R., Hioki, Y., Murakami, H., Suga, H., Matsumoto, M., Nakayama, K.I., Hatta, T., Iemura, S.I. and Natsume, T. (2014). ZFP36L1 and ZFP36L2 control LDLR mRNA stability via the ERK-RSK pathway. *Nucleic Acids Research*, 42 (15), 10037–10049. Available from <https://doi.org/10.1093/nar/gku652> [Accessed 2 August 2020].

Adamson, B., Smogorzewska, A., Sigoillot, F.D., King, R.W. and Elledge, S.J. (2012). A genome-wide homologous recombination screen identifies the RNA-binding protein RBMX as a component of the DNA damage response. *Nature Cell Biology*, 14 (3), 318–28. Available from <https://doi.org/10.1038/NCB2426> [Accessed 23 August 2020].

Adli, M. (2018). The CRISPR tool kit for genome editing and beyond. *Nature Communications*, 9 (1), 1911. Available from <https://doi.org/10.1038/s41467-018-04252-2> [Accessed 6 October 2020].

Aguilera, A. and Gómez-González, B. (2008). Genome instability: A mechanistic view of its causes and consequences. *Nature Reviews Genetics*, 9 (3), 204–217. Available from <https://doi.org/10.1038/nrg2268> [Accessed 16 August 2020].

Aguilera, A. and Klein, H.L. (1990). HPRJ, a Novel Yeast Gene That Prevents Intrachromosomal Excision Recombination, Shows Carboxy-Terminal Homology to the *Saccharomyces cerevisiae* TOPJ Gene. *Molecular and Cellular Biology*, 10 (4), 1439–1451. Available from <https://www.ncbi.nlm.nih.gov/pmc/articles/PMC362246/pdf/molcellb00040-0149.pdf> [Accessed 27 August 2020].

Ahnesorg, P., Smith, P. and Jackson, S.P. (2006). XLF interacts with the XRCC4-DNA ligase IV complex to promote DNA nonhomologous end-joining. *Cell*, 124 (2), 301–13. Available from <https://doi.org/10.1016/j.cell.2005.12.031> [Accessed 21 August 2020].

Al-Ahmadi, W., Al-Ghamdi, M., Al-Souhibani, N. and Khabar, K.S.A. (2013). miR-29a inhibition normalizes HuR over-expression and aberrant AU-rich mRNA stability in invasive cancer. *The Journal of Pathology*, 230 (1), 28–38. Available from <https://doi.org/10.1002/path.4178> [Accessed 11 August 2020].

Al-Khalaf, H.H., Colak, D., Al-Saif, M., Al-Bakheet, A., Hendrayani, S.-F., Al-Yousef, N., Kaya, N., Khabar, K.S. and Aboussekhra, A. (2011). p16(INK4a) positively regulates cyclin D1 and E2F1 through negative control of AUF1. *PloS One*, 6 (7), e21111. Available from <https://doi.org/10.1371/journal.pone.0021111> [Accessed 4 September 2020].

Al-Souhibani, N., Al-Ahmadi, W., Hesketh, J.E., Blackshear, P.J. and Khabar, K.S.A. (2010). The RNA-binding zinc-finger protein tristetraprolin regulates AU-rich mRNAs involved in breast cancer-related processes. *Oncogene*, 29 (29), 4205–15. Available from <https://doi.org/10.1038/onc.2010.168> [Accessed 26 October 2020].

Al-Tassan, N., Chmiel, N.H., Maynard, J., Fleming, N., Livingston, A.L., Williams, G.T., Hodges, A.K., Davies, D.R., David, S.S., Sampson, J.R. and Cheadle, J.P. (2002). Inherited variants of MYH associated with somatic G:C-->T:A mutations in colorectal tumors. *Nature Genetics*, 30 (2), 227–32. Available from <https://doi.org/10.1038/ng828> [Accessed 13 August 2020].

Anantha, R.W., Alcivar, A.L., Ma, J., Cai, H., Simhadri, S., Ule, J., König, J. and Xia, B. (2013). Requirement of heterogeneous nuclear ribonucleoprotein C for BRCA gene expression and homologous recombination. *PloS One*, 8 (4), e61368. Available from <https://doi.org/10.1371/journal.pone.0061368> [Accessed 24 August 2020].

Andersen, F.F., Tange, T.Ø., Sinnathamby, T., Olesen, J.R., Andersen, K.E., Westergaard, O., Kjems, J. and Knudsen, B.R. (2002). The RNA splicing factor ASF/SF2 inhibits human topoisomerase I mediated DNA relaxation. *Journal of Molecular Biology*, 322 (4), 677–86. Available from [https://doi.org/10.1016/s0022-2836\(02\)00815-x](https://doi.org/10.1016/s0022-2836(02)00815-x) [Accessed 27 August 2020].

Anderson, P. (2010). Post-transcriptional regulons coordinate the initiation and resolution of inflammation. *Nature Reviews Immunology*, 10 (1), 24–35. Available from <https://doi.org/10.1038/nri2685> [Accessed 9 August 2020].

Anderson, P. and Kedersha, N. (2002). Stressful Initiations. *Journal of Cell Science*, 110 (23), 2925–2934. Available from <https://jcs.biologists.org/content/115/16/3227.long> [Accessed 20 December 2020].

Andrade, D., Mehta, M., Griffith, J., Oh, S., Corbin, J., Babu, A., De, S., Chen, A., Zhao, Y.D., Husain, S., Roy, S., Xu, L., Aube, J., Janknecht, R., Gorospe, M., Herman, T., Ramesh, R. and Munshi, A. (2019). HuR Reduces Radiation-Induced DNA Damage by Enhancing Expression of ARID1A. *Cancers*, 11 (12), 2014. Available from <https://doi.org/10.3390/cancers11122014> [Accessed 23 August 2020].

Änkö, M.L. and Neugebauer, K.M. (2012). RNA-protein interactions in vivo: Global gets specific. *Trends in Biochemical Sciences*, 37 (7), 255–262. Available from <https://doi.org/10.1016/j.tibs.2012.02.005> [Accessed 23 August 2020].

Aparicio, T., Guillou, E., Coloma, J., Montoya, G. and Méndez, J. (2009). The human GINS complex associates with Cdc45 and MCM and is essential for DNA replication. *Nucleic Acids Research*, 37 (7), 2087–2095. Available from <https://doi.org/10.1093/nar/gkp065> [Accessed 23 December 2020].

Arias, E.E. and Walter, J.C. (2007). Strength in numbers: preventing rereplication via multiple mechanisms in eukaryotic cells. *Genes & Development*, 21 (5), 497–518. Available from <https://doi.org/10.1101/GAD.1508907> [Accessed 23 December 2020].

Artandi, S.E., Chang, S., Lee, S.-L., Alson, S., Gottlieb, G.J., Chin, L. and DePinho, R.A. (2000). Telomere dysfunction promotes non-reciprocal translocations and epithelial cancers in mice. *Nature*, 406 (6796), 641–645. Available from <https://doi.org/10.1038/35020592> [Accessed 14 August 2020].

Ascano, M., Hafner, M., Cekan, P., Gerstberger, S. and Tuschl, T. (2012). Identification of RNA-protein interaction networks using PAR-CLIP. *Wiley Interdisciplinary Reviews. RNA*, 3 (2), 159–177. Available from <https://doi.org/10.1002/wrna.1103> [Accessed 13 July 2020].

Averbeck, N.B., Ringel, O., Herrlitz, M., Jakob, B., Durante, M. and Taucher-Scholz, G. (2014). DNA end resection is needed for the repair of complex lesions in G1-phase human cells. *Cell Cycle*, 13 (16), 2509–16. Available from <https://doi.org/10.4161/15384101.2015.941743> [Accessed 7 June 2020].

Bakheet, T., Williams, B.R.G. and Khabar, K.S.A. (2006). ARED 3.0: the large and diverse AU-rich transcriptome. *Nucleic Acids Research*, 34 (Database issue), D111.

Available from <https://doi.org/10.1093/NAR/GKJ052> [Accessed 19 December 2020].

Bakhoun, S.F., Silkworth, W.T., Nardi, I.K., Nicholson, J.M., Compton, D.A. and Cimini, D. (2014). The mitotic origin of chromosomal instability. *Current Biology : CB*, 24 (4), R148-9. Available from <https://doi.org/10.1016/j.cub.2014.01.019> [Accessed 19 September 2020].

Baou, M., Jewell, A., Muthurania, A., Wickremasinghe, R.G., Yong, K.L., Carr, R., Marsh, P. and Murphy, J.J. (2009). Involvement of Tis11b, an AU-rich binding protein, in induction of apoptosis by rituximab in B cell chronic lymphocytic leukemia cells. *Leukemia*, 23 (5), 986–989. Available from <https://doi.org/10.1038/leu.2008.340> [Accessed 28 July 2020].

Baou, M., Norton, J.D. and Murphy, J.J. (2011). AU-rich RNA binding proteins in hematopoiesis and leukemogenesis. *Blood*, 118 (22), 5732–5740. Available from <https://doi.org/10.1182/blood-2011-07-347237> [Accessed 30 July 2020].

Barlow, J.H., Lisby, M. and Rothstein, R. (2008). Differential Regulation of the Cellular Response to DNA Double-Strand Breaks in G1. *Molecular Cell*, 30 (1), 73–85. Available from <https://doi.org/10.1016/j.molcel.2008.01.016> [Accessed 13 August 2020].

Barrangou, R., Fremaux, C., Deveau, H., Richards, M., Boyaval, P., Moineau, S., Romero, D.A. and Horvath, P. (2007). CRISPR provides acquired resistance against viruses in prokaryotes. *Science*, 315 (5819), 1709–12. Available from <https://doi.org/10.1126/science.1138140> [Accessed 11 September 2020].

Bass, T.E., Luzwick, J.W., Kavanaugh, G., Carroll, C., Dungrawala, H., Glick, G.G., Feldkamp, M.D., Putney, R., Chazin, W.J. and Cortez, D. (2016). ETAA1 acts at stalled replication forks to maintain genome integrity. *Nature Cell Biology*, 18 (11), 1185. Available from <https://doi.org/10.1038/NCB3415> [Accessed 18 August 2020].

Baumann, C., Körner, R., Hofmann, K. and Nigg, E.A. (2007). PICH, a centromere-associated SNF2 family ATPase, is regulated by Plk1 and required for the spindle checkpoint. *Cell*, 128 (1), 101–14. Available from <https://doi.org/10.1016/j.cell.2006.11.041> [Accessed 19 September 2020].

Baumann, P., Benson, F.E. and West, S.C. (1996). Human Rad51 Protein Promotes ATP-Dependent Homologous Pairing and Strand Transfer Reactions In Vitro. *Cell*, 87 (4), 757–766. Available from [https://doi.org/10.1016/S0092-8674\(00\)81394-X](https://doi.org/10.1016/S0092-8674(00)81394-X) [Accessed 21 August 2020].

Baxter, J.S., Leavy, O.C., Dryden, N.H., Maguire, S., Johnson, N., Fedele, V., Simigdala, N., Martin, L.A., Andrews, S., Wingett, S.W., Assiotis, I., Fenwick, K., Chauhan, R., Rust, A.G., Orr, N., Dudbridge, F., Haider, S. and Fletcher, O. (2018). Capture Hi-C identifies putative target genes at 33 breast cancer risk loci. *Nature Communications*, 9 (1), 1028. Available from <https://doi.org/10.1038/s41467-018-03411-9> [Accessed 2 August 2020].

Beck, H., Nähse-Kumpf, V., Larsen, M.S.Y., O'Hanlon, K.A., Patzke, S., Holmberg, C., Mejlvang, J., Groth, A., Nielsen, O., Syljuåsen, R.G. and Sørensen, C.S. (2012). Cyclin-dependent kinase suppression by WEE1 kinase protects the genome through control of replication initiation and nucleotide consumption. *Molecular and Cellular Biology*, 32 (20), 4226–36. Available from <https://doi.org/10.1128/MCB.00412-12> [Accessed 18 August 2020].

Becker, N.A., Thorland, E.C., Denison, S.R., Phillips, L.A. and Smith, D.I. (2002). Evidence that instability within the FRA3B region extends four megabases. *Oncogene*, 21 (57), 8713–8722. Available from <https://doi.org/10.1038/sj.onc.1205950> [Accessed 23 December 2020].

Behan, F.M., Iorio, F., Picco, G., Gonçalves, E., Beaver, C.M., Migliardi, G., Santos, R., Rao, Y., Sassi, F., Pinnelli, M., Ansari, R., Harper, S., Jackson, D.A., McRae, R., Pooley, R., Wilkinson, P., van der Meer, D., Dow, D., Buser-Doepner, C., Bertotti, A., Trusolino, L., Stronach, E.A., Saez-Rodriguez, J., Yusa, K. and Garnett, M.J. (2019). Prioritization of cancer therapeutic targets using CRISPR–Cas9 screens. *Nature*, 568 (7753), 511–516. Available from <https://doi.org/10.1038/s41586-019-1103-9> [Accessed 21 August 2020].

Beli, P., Lukashchuk, N., Wagner, S.A., Weinert, B.T., Olsen, J.V., Baskcomb, L., Mann, M., Jackson, S.P. and Choudhary, C. (2012). Proteomic Investigations Reveal a Role for RNA Processing Factor THRAP3 in the DNA Damage Response. *Molecular Cell*, 46 (2), 212–225. Available from <https://doi.org/10.1016/J.MOLCEL.2012.01.026>

[Accessed 25 August 2020].

Bell, S.E., Sanchez, M.J., Spasic-Boskovic, O., Santalucia, T., Gambardella, L., Burton, G.J., Murphy, J.J., Norton, J.D., Clark, A.R. and Turner, M. (2006). The RNA binding protein *Zfp36/1* is required for normal vascularisation and post-transcriptionally regulates VEGF expression. *Developmental Dynamics*, 235 (11), 3144–3155. Available from <https://doi.org/10.1002/dvdy.20949> [Accessed 5 August 2020].

Benjamin, D., Schmidlin, M., Min, L., Gross, B. and Moroni, C. (2006). BRF1 protein turnover and mRNA decay activity are regulated by protein kinase B at the same phosphorylation sites. *Molecular and Cellular Biology*, 26 (24), 9497–507. Available from <https://doi.org/10.1128/MCB.01099-06> [Accessed 22 July 2020].

Bennetzen, M. V., Larsen, D.H., Bunkenborg, J., Bartek, J., Lukas, J. and Andersen, J.S. (2010). Site-specific Phosphorylation Dynamics of the Nuclear Proteome during the DNA Damage Response. *Molecular & Cellular Proteomics: MCP*, 9 (6), 1314. Available from <https://doi.org/10.1074/MCP.M900616-MCP200> [Accessed 25 August 2020].

Bensimon, A., Schmidt, A., Ziv, Y., Elkon, R., Wang, S.-Y., Chen, D.J., Aebersold, R. and Shiloh, Y. (2010). ATM-dependent and independent dynamics of the nuclear phosphoproteome after DNA damage. *Science Signaling*, 3 (151), rs3. Available from <https://doi.org/10.1126/scisignal.2001034> [Accessed 25 August 2020].

Bhatia, V., Barroso, S.I., García-Rubio, M.L., Tumini, E., Herrera-Moyano, E. and Aguilera, A. (2014). BRCA2 prevents R-loop accumulation and associates with TREX-2 mRNA export factor PCID2. *Nature*, 511 (7509), 362–5. Available from <https://doi.org/10.1038/nature13374> [Accessed 27 August 2020].

Bhatia, V., Herrera-Moyano, E., Aguilera, A. and Gómez-González, B. (2017). The Role of Replication-Associated Repair Factors on R-Loops. *Genes*, 8 (7), 171. Available from <https://doi.org/10.3390/genes8070171> [Accessed 27 August 2020].

Bhowmick, R., Minocherhomji, S. and Hickson, I.D. (2016). RAD52 Facilitates Mitotic DNA Synthesis Following Replication Stress. *Molecular Cell*, 64 (6), 1117–1126. Available from <https://doi.org/10.1016/j.molcel.2016.10.037> [Accessed 13 August 2020].

2020].

Biehls, R., Steinlage, M., Barton, O., Shibata, A., Jeggo, P.A. and Lö Brich Correspondence, M. (2017). DNA Double-Strand Break Resection Occurs during Non-homologous End Joining in G1 but Is Distinct from Resection during Homologous Recombination. *Molecular Cell*, 65 (4), 671-684.e5. Available from <https://doi.org/10.1016/j.molcel.2016.12.016> [Accessed 12 June 2020].

Blackshear, P.J. (2002). mRNA Degradation: an Important Process in Controlling Gene Expression. *Biochemical Society Transactions*, 30 (6), 945-952. Available from <https://portlandpress.com/biochemsoctrans/article-pdf/30/6/945/510131/bst0300945.pdf> [Accessed 19 July 2020].

Blackshear, P.J. and Perera, L. (2014). Phylogenetic Distribution and Evolution of the Linked RNA-Binding and NOT1-Binding Domains in the Tristetraprolin Family of Tandem CCCH Zinc Finger Proteins. *Journal of Interferon & Cytokine Research*, 34 (4), 297-306. Available from <https://doi.org/10.1089/JIR.2013.0150> [Accessed 20 July 2020].

Blackshear, Perry J., Lai, W.S., Kennington, E.A., Brewer, G., Wilson, G.M., Guan, X. and Zhou, P. (2003). Characteristics of the Interaction of a Synthetic Human Tristetraprolin Tandem Zinc Finger Peptide with AU-rich Element-containing RNA Substrates. *The Journal of Biochemistry*, 278 (22), 19947–19955. Available from <https://doi.org/10.1074/jbc.M301290200> [Accessed 21 July 2020].

Blackshear, Perry J., Phillips, R.S., Vazquez-Matias, J. and Mohrenweiser, H. (2003). Polymorphisms in the Genes Encoding Members of the Tristetraprolin Family of Human Tandem CCCH Zinc Finger Proteins. *Progress in Nucleic Acid Research and Molecular Biology*, 75, 43–68. Available from [https://doi.org/10.1016/S0079-6603\(03\)75002-8](https://doi.org/10.1016/S0079-6603(03)75002-8) [Accessed 18 July 2020].

Blackshear, P.J., Phillips, R.S., Ghosh, S., Ramos, S.V.B., Richfield, E.K. and Lai, W.S. (2005). Zfp36l3, a Rodent X Chromosome Gene Encoding a Placenta-Specific Member of the Tristetraprolin Family of CCCH Tandem Zinc Finger Proteins. *Biology of Reproduction* 73 (2), 297–307. Available from <https://doi.org/10.1095/biolreprod.105.040527> [Accessed 19 July 2020].

Blasco, M.A. (2005). Telomeres and human disease: ageing, cancer and beyond. *Nature Reviews. Genetics*, 6 (8), 611–22. Available from <https://doi.org/10.1038/nrg1656> [Accessed 14 August 2020].

Blasius, M., Forment, J. V, Thakkar, N., Wagner, S.A., Choudhary, C. and Jackson, S.P. (2011). A phospho-proteomic screen identifies substrates of the checkpoint kinase Chk1. *Genome Biology*, 12 (8), R78. Available from <https://doi.org/10.1186/gb-2011-12-8-r78> [Accessed 25 August 2020].

Blow, J.J. and Dutta, A. (2005). Preventing re-replication of chromosomal DNA. *Nature Reviews. Molecular Cell Biology*, 6 (6), 476-486. Available from <https://doi.org/10.1038/NRM1663> [Accessed 23 December 2020].

Blow, J.J., Ge, X.Q. and Jackson, D.A. (2011). How dormant origins promote complete genome replication. *Trends in Biochemical Sciences*, 36 (8), 405–414. Available from <https://doi.org/10.1016/J.TIBS.2011.05.002> [Accessed 15 August 2020].

Bose, J. (2016). Chemical and UV Mutagenesis. *Methods in Molecular Biology*, 1373, 111-115. Available from https://doi.org/10.1007/7651_2014_190 [Accessed 10 September 2020].

Bourcier, C., Griseri, P., Grépin, R., Bertolotto, C., Mazure, N. and Pagès, G. (2011). Constitutive ERK activity induces downregulation of tristetraprolin, a major protein controlling interleukin8/CXCL8 mRNA stability in melanoma cells. *American Journal of Physiology*, 301 (3), C609-18. Available from <https://doi.org/10.1152/ajpcell.00506.2010> [Accessed 4 September 2020].

Boutaud, O., Dixon, D.A., Oates, J.A. and Sawaoka, H. (2003). Tristetrapolin Binds to the COX-2 mRNA 3' Untranslated Region in Cancer Cells. *Advances in Experimental and Medical Biology*, 525, 157–160. Available from https://doi.org/10.1007/978-1-4419-9194-2_32 [Accessed 28 July 2020].

Boutros, R., Lobjois, V. and Ducommun, B. (2007). CDC25 phosphatases in cancer cells: key players? Good targets? *Nature Reviews. Cancer*, 7 (7), 495–507. Available from <https://doi.org/10.1038/nrc2169> [Accessed 18 August 2020].

Branzei, D. and Foiani, M. (2009). The checkpoint response to replication stress. *DNA*

Repair, 8 (9), 1038–1046. Available from <https://doi.org/10.1016/J.DNAREP.2009.04.014> [Accessed 25 September 2020].

Brewer, B.Y., Malicka, J., Blackshear, P.J. and Wilson, G.M. (2004). RNA Sequence Elements Required for High Affinity Binding by the Zinc Finger Domain of Tristetraprolin. *The Journal of Biological Chemistry*, 279 (27), 27870–27877. Available from <https://doi.org/10.1074/jbc.M402551200> [Accessed 21 July 2020].

Brook, M., Tchen, C.R., Santalucia, T., Mcilrath, J., Simon, J., Arthur, C., Saklatvala, J. and Clark, A.R. (2006). Posttranslational Regulation of Tristetraprolin Subcellular Localization and Protein Stability by p38 Mitogen-Activated Protein Kinase and Extracellular Signal-Regulated Kinase Pathways. *Molecular and Cellular Biology*, 26 (6), 2408–2418. Available from <https://doi.org/10.1128/MCB.26.6.2408-2418.2006> [Accessed 23 July 2020].

Brooks, S.A. and Blackshear, P.J. (2013). Tristetraprolin (TTP): Interactions with mRNA and proteins, and current thoughts on mechanisms of action. *Biochimica et biophysica acta*, 1829 (0), 666-679. Available from <https://doi.org/10.1016/J.BBAGRM.2013.02.003> [Accessed 19 July 2020].

Brooks, S.A., Connolly, J.E., Diegel, R.J., Fava, R.A. and Rigby, W.F.C. (2002). Analysis of the function, expression, and subcellular distribution of human tristetraprolin. *Arthritis & Rheumatism*, 46 (5), 1362–1370. Available from <https://doi.org/10.1002/art.10235> [Accessed 19 December 2020].

Brooks, S.A., Connolly, J.E. and Rigby, W.F.C. (2004). Element-Dependent, Autoregulatory Pathway Signal-Regulated Kinase-Specific, AU-Rich Evidence for an Extracellular Regulation of Tristetraprolin Expression: The Role of mRNA Turnover in the. *J Immunol*, 172, 7263–7271. Available from <https://doi.org/10.4049/jimmunol.172.12.7263> [Accessed 28 July 2020].

Buisson, R., Boisvert, J.L., Benes, C.H. and Zou, L. (2015). Distinct but Concerted Roles of ATR, DNA-PK, and Chk1 in Countering Replication Stress during S Phase. *Molecular Cell*, 59 (6), 1011–24. Available from <https://doi.org/10.1016/j.molcel.2015.07.029> [Accessed 17 August 2020].

Bunting, S.F., Callén, E., Wong, N., Chen, H.-T., Polato, F., Gunn, A., Bothmer, A., Feldhahn, N., Fernandez-Capetillo, O., Cao, L., Xu, X., Deng, C.-X., Finkel, T., Nussenzweig, M., Stark, J.M. and Nussenzweig, A. (2010). 53BP1 inhibits homologous recombination in Brca1-deficient cells by blocking resection of DNA breaks. *Cell*, 141 (2), 243–54. Available from <https://doi.org/10.1016/j.cell.2010.03.012> [Accessed 21 August 2020].

Burma, S., Chen, B.P., Murphy, M., Kurimasa, A. and Chen, D.J. (2001). ATM phosphorylates histone H2AX in response to DNA double-strand breaks. *The Journal of Biological Chemistry*, 276 (45), 42462–7. Available from <https://doi.org/10.1074/jbc.C100466200> [Accessed 18 August 2020].

Burrell, R.A., McClelland, S.E., Endesfelder, D., Groth, P., Weller, M.-C., Shaikh, N., Domingo, E., Kanu, N., Dewhurst, S.M., Gronroos, E., Chew, S.K., Rowan, A.J., Schenk, A., Sheffer, M., Howell, M., Kschischo, M., Behrens, A., Helleday, T., Bartek, J., Tomlinson, I.P. and Swanton, C. (2013). Replication stress links structural and numerical cancer chromosomal instability. *Nature*, 494 (7438), 492–496. Available from <https://doi.org/10.1038/nature11935> [Accessed 1 June 2020].

Busà, R., Geremia, R. and Sette, C. (2010). Genotoxic stress causes the accumulation of the splicing regulator Sam68 in nuclear foci of transcriptionally active chromatin. *Nucleic Acids Research*, 38 (9), 3005–3018. Available from <https://doi.org/10.1093/nar/gkq004> [Accessed 25 August 2020].

Bustin, S.A., Nie, X.F., Barnard, R.C., Kumar, V., Pascall, J.C., Brown, K.D., Leigh, I.M., Williams, N.S. and McKay, I.A. (1994). Cloning and Characterization of ERF-1, a Human Member of the Tis11 Family of Early-Response Genes. *DNA and Cell Biology*, 13 (5), 449–459. Available from <https://doi.org/10.1089/dna.1994.13.449> [Accessed 1 August 2020].

Byun, T.S., Pacek, M., Yee, M., Walter, J.C. and Cimprich, K.A. (2005). Functional uncoupling of MCM helicase and DNA polymerase activities activates the ATR-dependent checkpoint. *Genes & Development*, 19 (9), 1040–52. Available from <https://doi.org/10.1101/gad.1301205> [Accessed 16 August 2020].

Cahill, D., Connor, B. and Carney, J.P. (2006). Mechanisms of eukaryotic DNA double

strand break repair. *Frontiers in Bioscience : a journal and virtual library*, 11, 1958–76. Available from <https://doi.org/10.2741/1938> [Accessed 19 August 2020].

Caldon, C. and Musgrove, E.A. (2010). Distinct and redundant functions of cyclin E1 and cyclin E2 in development and cancer. *Cell Division*, 5 (1), 2. Available from <https://doi.org/10.1186/1747-1028-5-2> [Accessed 23 August 2020].

Cammas, A., Lewis, S.M., Vagner, S. and Holcik, M. (2008). Post-transcriptional control of gene expression through subcellular relocalization of mRNA binding proteins. *Biochemical Pharmacology*, 76 (11), 1395–1403. Available from <https://doi.org/10.1016/J.BCP.2008.05.022> [Accessed 25 August 2020].

Cao, H. (2004). Expression, purification, and biochemical characterization of the antiinflammatory tristetraprolin: a zinc-dependent mRNA binding protein affected by posttranslational modifications. *Biochemistry*, 43 (43), 13724–38. Available from <https://doi.org/10.1021/bi049014y> [Accessed 24 July 2020].

Cao, H., Dzineku, F. and Blackshear, P.J. (2003). Expression and purification of recombinant tristetraprolin that can bind to tumor necrosis factor- α mRNA and serve as a substrate for mitogen-activated protein kinases. *Archives of Biochemistry and Biophysics*, 412 (1), 106–20. Available from [https://doi.org/10.1016/s0003-9861\(03\)00012-2](https://doi.org/10.1016/s0003-9861(03)00012-2) [Accessed 24 July 2020].

Cao, H., Deterding, L.J. and Blackshear, P.J. (2007). Phosphorylation site analysis of the anti-inflammatory and mRNA-destabilizing protein tristetraprolin. *Expert Review of Proteomics*, 4 (6), 711–26. Available from <https://doi.org/10.1586/14789450.4.6.711> [Accessed 24 July 2020].

Carballo, E., Lai, W.S. and Blackshear, P.J. (1998). Feedback Inhibition of Macrophage Tumor Necrosis Factor- Production by Tristetraprolin. *Science*, 281 (5379), 1001–1005. Available from <https://doi.org/10.1126/science.281.5379.1001> [Accessed 7 July 2020].

Carballo, E., Lai, W.S. and Blackshear, P.J. (2000). Evidence that tristetraprolin is a physiological regulator of granulocyte-macrophage colony-stimulating factor messenger RNA deadenylation and stability. *Blood*, 95 (6), 1891–1899. Available from

<https://doi.org/10.1182/blood.V95.6.1891> [Accessed 28 July 2020].

Carballo, E., Cao, H., Lai, W.S., Kennington, E.A., Campbell, D. and Blackshear, P.J. (2001). Decreased sensitivity of tristetraprolin-deficient cells to p38 inhibitors suggests the involvement of tristetraprolin in the p38 signaling pathway. *The Journal of Biological Chemistry*, 276 (45), 42580–7. Available from <https://doi.org/10.1074/jbc.M104953200> [Accessed 24 July 2020].

Carballo, Ester, Gilkeson, Gary S, Blackshear, P.J., Taylor, G.A., Carballo, E, Lee, D.M., Lai, W.S., Thompson, M.J., Patel, D.D., Schenkman, D.I., Gilkeson, G S, Broxmeyer, H.E. and Haynes, B.F. (1997). Bone Marrow Transplantation Reproduces the Tristetraprolin-Deficiency Syndrome in Recombination Activating Gene-2 (/) Mice Evidence That Monocyte/Macrophage Progenitors May Be Responsible for TNF Overproduction. *J. Clin. Invest*, 100(5), 986-995. Available from <http://www.jci.org> [Accessed 20 July 2020].

Caron, M.-C., Sharma, A.K., O'Sullivan, J., Myler, L.R., Ferreira, M.T., Rodrigue, A., Coulombe, Y., Ethier, C., Gagné, J.-P., Langelier, M.-F., Pascal, J.M., Finkelstein, I.J., Hendzel, M.J., Poirier, G.G. and Masson, J.-Y. (2019). Poly(ADP-ribose) polymerase-1 antagonizes DNA resection at double-strand breaks. *Nature Communications*, 10 (1), 2954. Available from <https://doi.org/10.1038/s41467-019-10741-9> [Accessed 25 August 2020].

Carrick, D.M. and Blackshear, P.J. (2007). Comparative expression of tristetraprolin (TTP) family member transcripts in normal human tissues and cancer cell lines. *Archives of Biochemistry and Biophysics*, 462 (2), 278–285. Available from <https://doi.org/10.1016/j.abb.2007.04.011> [Accessed 5 July 2020].

Carrick, D.M., Chulada, P., Donn, R., Fabris, M., McNicholl, J., Whitworth, W. and Blackshear, P.J. (2006). Genetic variations in ZFP36 and their possible relationship to autoimmune diseases. *Journal of Autoimmunity*, 26 (3), 182–196. Available from <https://doi.org/10.1016/j.jaut.2006.01.004> [Accessed 19 August 2020].

Carroll, D. (2011). Genome engineering with zinc-finger nucleases. *Genetics*, 188 (4), 773–82. Available from <https://doi.org/10.1534/genetics.111.131433> [Accessed 10 September 2020].

Ceasar, S.A., Rajan, V., Prykhozhij, S. V, Berman, J.N. and Ignacimuthu, S. (2016). Insert, remove or replace: A highly advanced genome editing system using CRISPR/Cas9. *Biochemica et Biophysica Acta*, 1863(9), 2333-44. Available from <https://doi.org/10.1016/j.bbamcr.2016.06.009> [Accessed 24 July 2017].

Cha, H.J., Lee, H.H., Chae, S.W., Cho, W.J., Kim, Y.M., Choi, H.-J., Choi, D.H., Jung, S.W., Min, Y.J., Lee, B.J., Park, S.E. and Park, J.W. (2011). Tristetraprolin downregulates the expression of both VEGF and COX-2 in human colon cancer. *Hepato-gastroenterology*, 58 (107–108), 790–5. Available from <http://www.ncbi.nlm.nih.gov/pubmed/21830391> [Accessed 10 August 2020].

Chakrabarti, A.M., Henser-Brownhill, T., Monserrat, J., Poetsch, A.R., Luscombe, N.M. and Scaffidi, P. (2019). Target-Specific Precision of CRISPR-Mediated Genome Editing. *Molecular Cell*, 73 (4), 699-713.e6. Available from <https://doi.org/10.1016/j.molcel.2018.11.031> [Accessed 23 June 2020].

Chan, K.-L., North, P.S. and Hickson, I.D. (2007). BLM is required for faithful chromosome segregation and its localization defines a class of ultrafine anaphase bridges. *The EMBO Journal*, 26 (14), 3397–409. Available from <https://doi.org/10.1038/sj.emboj.7601777> [Accessed 19 September 2020].

Chan, K.L., Palmai-Pallag, T., Ying, S. and Hickson, I.D. (2009a). Replication stress induces sister-chromatid bridging at fragile site loci in mitosis. *Nature Cell Biology*, 11 (6), 753–760. Available from <https://doi.org/10.1038/ncb1882> [Accessed 12 May 2020].

Chan, K.L., Palmai-Pallag, T., Ying, S. and Hickson, I.D. (2009b). Replication stress induces sister-chromatid bridging at fragile site loci in mitosis. *Nature Cell Biology*, 11 (6), 753–760. Available from <https://doi.org/10.1038/ncb1882> [Accessed 19 September 2020].

Chang, S.-H. and Hla, T. (2011). Gene regulation by RNA binding proteins and microRNAs in angiogenesis. *Trends in Molecular Medicine*, 17 (11), 650–8. Available from <https://doi.org/10.1016/j.molmed.2011.06.008> [Accessed 10 August 2020].

Chang, Y.-W., Mai, R.-T., Fang, W.-H., Lin, C.-C., Chiu, C.-C. and Wu Lee, Y.-H.

(2014). YB-1 disrupts mismatch repair complex formation, interferes with MutS α recruitment on mismatch and inhibits mismatch repair through interacting with PCNA. *Oncogene*, 33 (43), 5065–5077. Available from <https://doi.org/10.1038/onc.2013.450> [Accessed 24 August 2020].

Chapman, J.R., Taylor, M.R.G. and Boulton, S.J. (2012). Playing the End Game: DNA Double-Strand Break Repair Pathway Choice. *Molecular Cell*, 47 (4), 497–510. Available from <https://doi.org/10.1016/j.molcel.2012.07.029> [Accessed 15 August 2020].

Chen, C.Y., Gherzi, R., Ong, S.E., Chan, E.L., Raijmakers, R., Pruijn, G.J.M., Stoecklin, G., Moroni, C., Mann, M. and Karin, M. (2001). AU binding proteins recruit the exosome to degrade ARE-containing mRNAs. *Cell*, 107 (4), 451–464. Available from [https://doi.org/10.1016/S0092-8674\(01\)00578-5](https://doi.org/10.1016/S0092-8674(01)00578-5) [Accessed 16 July 2020].

Chen, H., Lisby, M. and Symington, L.S. (2013). RPA coordinates DNA end resection and prevents formation of DNA hairpins. *Molecular Cell*, 50 (4), 589–600. Available from <https://doi.org/10.1016/j.molcel.2013.04.032> [Accessed 21 August 2020].

Chen, J.-K., Lin, W.-L., Chen, Z. and Liu, H.-W. (2018). PARP-1-dependent recruitment of cold-inducible RNA-binding protein promotes double-strand break repair and genome stability. *Proceedings of the National Academy of Sciences of the United States of America*, 115 (8), E1759–E1768. Available from <https://doi.org/10.1073/pnas.1713912115> [Accessed 23 September 2020].

Chen, M.-T., Dong, L., Zhang, X.-H., Yin, X.-L., Ning, H.-M., Shen, C., Su, R., Li, F., Song, L., Ma, Y.-N., Wang, F., Zhao, H.-L., Yu, J. and Zhang, J.-W. (2015). ZFP36L1 promotes monocyte/macrophage differentiation by repressing CDK6. *Scientific Reports*, 5 (1), 16229. Available from <https://doi.org/10.1038/srep16229> [Accessed 9 August 2020].

Chini, C.C.S. and Chen, J. (2003). Human claspin is required for replication checkpoint control. *The Journal of Biological Chemistry*, 278 (32), 30057–62. Available from <https://doi.org/10.1074/jbc.M301136200> [Accessed 18 August 2020].

Cho, S.W., Kim, S., Kim, J.M. and Kim, J.-S. (2013). Targeted genome engineering in

human cells with the Cas9 RNA-guided endonuclease. *Nature Biotechnology*, 31 (3), 230–232. Available from <https://doi.org/10.1038/nbt.2507> [Accessed 10 September 2020].

Chrestensen, C.A., Schroeder ¶ ‡, M.J., Shabanowitz, J., Hunt ¶ § §, D.F., Pelo, J.W., Worthington, M.T. and Sturgill, T.W. (2004). MAPKAP Kinase 2 Phosphorylates Tristetraprolin on in Vivo Sites Including Ser 178 , a Site Required for 14-3-3 Binding* Downloaded from. *The Journal of Biological Chemistry*, 279 (11), 10176–10184. Available from <https://doi.org/10.1074/jbc.M310486200> [Accessed 24 July 2020].

Ciais, D., Cherradi, N., Bailly, S., Grenier, E., Berra, E., Pouyssegur, J., LaMarre, J. and Feige, J.-J. (2004). Destabilization of vascular endothelial growth factor mRNA by the zinc-finger protein TIS11b. *Oncogene*, 23 (53), 8673–8680. Available from <https://doi.org/10.1038/sj.onc.1207939> [Accessed 10 August 2020].

Ciais, D., Cherradi, N. and Feige, J.J. (2013). Multiple functions of tristetraprolin/TIS11 RNA-binding proteins in the regulation of mRNA biogenesis and degradation. *Cellular and Molecular Life Sciences*, 70 (12), 2031–2044. Available from <https://doi.org/10.1007/s00018-012-1150-y> [Accessed 10 July 2020].

Ciccia, A. and Elledge, S.J. (2010a). The DNA damage response: making it safe to play with knives. *Molecular Cell*, 40 (2), 179–204. Available from <https://doi.org/10.1016/j.molcel.2010.09.019> [Accessed 16 August 2020].

Cimprich, K.A. and Cortez, D. (2008). ATR: an essential regulator of genome integrity. *Nature reviews. Molecular Cell Biology*, 9 (8), 616–27. Available from <https://doi.org/10.1038/nrm2450> [Accessed 18 August 2020].

Clark, A.R. and Dean, J.L.E. (2016). The control of inflammation via the phosphorylation and dephosphorylation of tristetraprolin: a tale of two phosphatases. *Biochemical Society Transactions*, 44 (5), 1321–1337. Available from <https://doi.org/10.1042/BST20160166> [Accessed 25 July 2020].

Clement, S.L., Scheckel, C., Stoecklin, G. and Lykke-Andersen, J. (2011). Phosphorylation of Tristetraprolin by MK2 Impairs AU-Rich Element mRNA Decay by Preventing Deadenylation Recruitment. *Molecular and Cellular Biology*, 31 (2), 256–

266. Available from <https://doi.org/10.1128/MCB.00717-10> [Accessed 24 July 2020].

Cong, L., Ran, F.A., Cox, D., Lin, S., Barretto, R., Habib, N., Hsu, P.D., Wu, X., Jiang, W., Marraffini, L.A. and Zhang, F. (2013). Multiplex genome engineering using CRISPR/Cas systems. *Science*, 339 (6121), 819–23. Available from <https://doi.org/10.1126/science.1231143> [Accessed 10 September 2020].

Cook, J.G., Chasse, D.A.D. and Nevins, J.R. (2004). The Regulated Association of Cdt1 with Minichromosome Maintenance Proteins and Cdc6 in Mammalian Cells. *Journal of Biological Chemistry*, 279 (10), 9625–9633. Available from <https://doi.org/10.1074/jbc.M311933200> [Accessed 15 August 2020].

Cooper, T.A., Wan, L. and Dreyfuss, G. (2009). RNA and disease. *Cell*, 136 (4), 777–93. Available from <https://doi.org/10.1016/j.cell.2009.02.011> [Accessed 15 July 2020].

Corcoran, D.L., Georgiev, S., Mukherjee, N., Gottwein, E., Skalsky, R.L., Keene, J.D. and Ohler, U. (2011). PARalyzer: definition of RNA binding sites from PAR-CLIP short-read sequence data. *Genome Biology*, 12(8), r79. Available from <https://doi.org/10.1186/gb-2011-12-8-r79> [Accessed 13 July 2020].

Corley, M., Burns, M.C. and Yeo, G.W. (2020). How RNA-Binding Proteins Interact with RNA: Molecules and Mechanisms. *Molecular Cell*, 78 (1), 9–29. Available from <https://doi.org/10.1016/j.molcel.2020.03.011> [Accessed 20 August 2020].

Cortez, D. (2019). Replication-Coupled DNA Repair. *Molecular Cell*, 74 (5), 866–876. Available from <https://doi.org/10.1016/j.molcel.2019.04.027> [Accessed 16 August 2020] [Accessed 8 August 2020].

Costa, A., Ilves, I., Tamberg, N., Petojevic, T., Nogales, E., Botchan, M.R. and Berger, J.M. (2011). The structural basis for MCM2-7 helicase activation by GINS and Cdc45. *Nature Structural & Molecular Biology*, 18 (4), 471–7. Available from <https://doi.org/10.1038/nsmb.2004> [Accessed 15 August 2020].

Crick, F. (1970). Central dogma of molecular biology. *Nature*, 227 (5258), 561–3. Available from <https://doi.org/10.1038/227561a0> [Accessed 30 August 2020].

Crossley, M.P., Bocek, M. and Cimprich, K.A. (2019). R-Loops as Cellular Regulators

and Genomic Threats. *Molecular Cell*, 73 (3), 398–411. Available from <https://doi.org/10.1016/j.molcel.2019.01.024> [Accessed 27 August 2020].

Crusz, S.M. and Balkwill, F.R. (2015). Inflammation and cancer: advances and new agents. *Nature Reviews Clinical Oncology*, 12 (10), 584–596. Available from <https://doi.org/10.1038/nrclinonc.2015.105> [Accessed 9 August 2020].

Daley, J.M. and Sung, P. (2014). 53BP1, BRCA1, and the choice between recombination and end joining at DNA double-strand breaks. *Molecular and Cellular Biology*, 34 (8), 1380–8. Available from <https://doi.org/10.1128/MCB.01639-13> [Accessed 21 August 2020].

Davoli, T., Denchi, E.L. and de Lange, T. (2010). Persistent telomere damage induces bypass of mitosis and tetraploidy. *Cell*, 141 (1), 81–93. Available from <https://doi.org/10.1016/j.cell.2010.01.031> [Accessed 14 August 2020].

De Bruin, R.G., Rabelink, T.J., Jan Van Zonneveld, A. and Van Der Veer, E.P. (2017). Emerging roles for RNA-binding proteins as effectors and regulators of cardiovascular disease. *Translational Medicine*, 38, 1380–1388. Available from <https://doi.org/10.1093/eurheartj/ehw567> [Accessed 9 July 2020].

Decker, C.J. and Parker, R. (2012). P-bodies and stress granules: possible roles in the control of translation and mRNA degradation. *Cold Spring Harbor Perspectives in Biology*, 4 (9), a012286. Available from <https://doi.org/10.1101/cshperspect.a012286> [Accessed 26 July 2020].

Deltcheva, E., Chylinski, K., Sharma, C.M., Gonzales, K., Chao, Y., Pirzada, Z.A., Eckert, M.R., Vogel, J. and Charpentier, E. (2011). CRISPR RNA maturation by trans-encoded small RNA and host factor RNase III. *Nature*, 471 (7340), 602–7. Available from <https://doi.org/10.1038/nature09886> [Accessed 11 September 2020].

Deng, K., Wang, H., Shan, T., Chen, Y., Zhou, H., Zhao, Q. and Xia, J. (2016). Tristetraprolin inhibits gastric cancer progression through suppression of IL-33. *Scientific reports*, 6, 24505. Available from <https://doi.org/10.1038/srep24505> [Accessed 4 September 2020].

Diaz-Muñoz, M.D., Bell, S.E., Fairfax, K., Monzon-Casanova, E., Cunningham, A.F.,

Gonzalez-Porta, M., Andrews, S.R., Bunik, V.I., Zarnack, K., Curk, T., Heggermont, W.A., Heymans, S., Gibson, G.E., Kontoyiannis, D.L., Ule, J. and Turner, M. (2015). The RNA-binding protein HuR is essential for the B cell antibody response. *Nature Immunology*, 16 (4), 415–425. Available from <https://doi.org/10.1038/ni.3115> [Accessed 1 August 2020].

Díaz-Muñoz, M.D. and Turner, M. (2018). Uncovering the Role of RNA-Binding Proteins in Gene Expression in the Immune System. *Frontiers in Immunology*, 9, 1094. Available from <https://doi.org/10.3389/fimmu.2018.01094> [Accessed 10 July 2020].

Diehl, J.A. (2002). Cycling to cancer with cyclin D1. *Cancer Biology & Therapy*, 1 (3), 226–31. Available from <https://doi.org/10.4161/cbt.72> [Accessed 30 July 2020].

Doil, C., Mailand, N., Bekker-Jensen, S., Menard, P., Larsen, D.H., Pepperkok, R., Ellenberg, J., Panier, S., Durocher, D., Bartek, J., Lukas, J. and Lukas, C. (2009). RNF168 binds and amplifies ubiquitin conjugates on damaged chromosomes to allow accumulation of repair proteins. *Cell*, 136 (3), 435–46. Available from <https://doi.org/10.1016/j.cell.2008.12.041> [Accessed 18 August 2020].

DuBois, R.N., McLane, M.W., Ryder, K., Lau, L.F. and Nathans, D. (1990). A growth factor-inducible nuclear protein with a novel cysteine/histidine repetitive sequence. *Journal of Biological Chemistry*, 265 (31), 19185–19191 [Accessed 21 July 2020].

Durkin, S.G. and Glover, T.W. (2007). Chromosome fragile sites. *Annual Review of Genetics*, 41, 169–192. Available from <https://doi.org/10.1146/annurev.genet.41.042007.165900> [Accessed 23 August 2020].

Dutertre, M. and Vagner, S. (2017b). DNA-Damage Response RNA-Binding Proteins (DDRBP): Perspectives from a New Class of Proteins and Their RNA Targets. *Journal of Molecular Biology*, 429 (21), 3139–3145. Available from <https://doi.org/10.1016/j.jmb.2016.09.019> [Accessed 26 August 2020].

Dutertre, M., Sanchez, G., De Cian, M.-C., Barbier, J., Dardenne, E., Gratadou, L., Dujardin, G., Le Jossic-Corcós, C., Corcos, L. and Auboeuf, D. (2010). Cotranscriptional exon skipping in the genotoxic stress response. *Nature Structural &*

Molecular Biology, 17 (11), 1358–1366. Available from <https://doi.org/10.1038/nsmb.1912> [Accessed 25 August 2020].

Dutertre, M., Lambert, S., Carreira, A., Amor-Gu ret, M. and Vagner, S. (2014). DNA damage: RNA-binding proteins protect from near and far. *Trends in Biochemical Sciences*, 39 (3), 141–149. Available from <https://doi.org/10.1016/j.tibs.2014.01.003> [Accessed 17 August 2020].

Edmond, V., Moysan, E., Khochbin, S., Matthias, P., Brambilla, C., Brambilla, E., Gazzeri, S. and Eymin, B. (2011). Acetylation and phosphorylation of SRSF2 control cell fate decision in response to cisplatin. *The EMBO Journal*, 30 (3), 510–523. Available from <https://doi.org/10.1038/emboj.2010.333> [Accessed 25 August 2020].

Essafi-Benkhadir, K., Onesto, C., Stebe, E., Moroni, C. and Pag s, G. (2007). Tristetraprolin inhibits Ras-dependent tumor vascularization by inducing vascular endothelial growth factor mRNA degradation. *Molecular Biology of the Cell*, 18 (11), 4648–58. Available from <https://doi.org/10.1091/mbc.e07-06-0570> [Accessed 10 August 2020].

Fairhurst, A.-M., Connolly, J.E., Hintz, K.A., Goulding, N.J., Rassias, A.J., Yeager, M.P., Rigby, W. and Wallace, P.K. (2003). Regulation and localization of endogenous human tristetraprolin. *Arthritis Research & Therapy*, 5 (4), R214. Available from <https://doi.org/10.1186/ar778> [Accessed 25 July 2020].

Falck, J., Petrini, J.H.J., Williams, B.R., Lukas, J. and Bartek, J. (2002). The DNA damage-dependent intra-S phase checkpoint is regulated by parallel pathways. *Nature Genetics*, 30 (3), 290–294. Available from <https://doi.org/10.1038/ng845> [Accessed 18 August 2020].

Falck, J., Coates, J. and Jackson, S.P. (2005). Conserved modes of recruitment of ATM, ATR and DNA-PKcs to sites of DNA damage. *Nature*, 434 (7033), 605–11. Available from <https://doi.org/10.1038/nature03442> [Accessed 18 August 2020].

Fang, J., Bolanos, L.C., Choi, K., Liu, X., Christie, S., Akunuru, S., Kumar, R., Wang, D., Chen, X., Greis, K.D., Stoilov, P., Filippi, M.D., Maciejewski, J.P., Garcia-Manero, G., Weirauch, M.T., Salomonis, N., Geiger, H., Zheng, Y. and Starczynowski, D.T.

(2017). Ubiquitination of hnRNPA1 by TRAF6 links chronic innate immune signaling with myelodysplasia. *Nature Immunology*, 18 (2), 236–245. Available from <https://doi.org/10.1038/ni.3654> [Accessed 28 August 2020].

Fenech, M., Kirsch-Volders, M., Natarajan, A.T., Surralles, J., Crott, J.W., Parry, J., Norppa, H., Eastmond, D.A., Tucker, J.D. and Thomas, P. (2011). Molecular mechanisms of micronucleus, nucleoplasmic bridge and nuclear bud formation in mammalian and human cells. *Mutagenesis*, 26 (1), 125–132. Available from <https://doi.org/10.1093/mutage/geq052> [Accessed 5 August 2020].

Feng, S., Zhao, Y., Xu, Y., Ning, S., Huo, W., Hou, M., Gao, G., Ji, J., Guo, R. and Xu, D. (2016). Ewing Tumor-associated Antigen 1 Interacts with Replication Protein A to Promote Restart of Stalled Replication Forks. *The Journal of Biological Chemistry*, 291 (42), 21956–21962. Available from <https://doi.org/10.1074/jbc.C116.747758> [Accessed 18 August 2020].

Fenger-Grøn, M., Fillman, C., Norrild, B. and Lykke-Andersen, J. (2005). Multiple Processing Body Factors and the ARE Binding Protein TTP Activate mRNA Decapping. *Molecular Cell*, 20, 905–915. Available from <https://doi.org/10.1016/j.molcel.2005.10.031> [Accessed 23 July 2020].

Fernández-Casañas, M. and Chan, K.L. (2018). The unresolved problem of DNA bridging. *Genes*, 9 (12). Available from <https://doi.org/10.3390/genes9120623> [Accessed 11 August 2020].

Fernandez-Vidal, A., Vignard, J. and Mirey, G. (2017). Around and beyond 53BP1 nuclear bodies. *International Journal of Molecular Sciences*. Available from <https://doi.org/10.3390/ijms18122611> [Accessed 23 August 2020].

Fishel, R., Lescoe, M.K., Rao, M.R., Copeland, N.G., Jenkins, N.A., Garber, J., Kane, M. and Kolodner, R. (1993). The human mutator gene homolog MSH2 and its association with hereditary nonpolyposis colon cancer. *Cell*, 75 (5), 1027–38. Available from [https://doi.org/10.1016/0092-8674\(93\)90546-3](https://doi.org/10.1016/0092-8674(93)90546-3) [Accessed 13 August 2020].

Fonfara, I., Le Rhun, A., Chylinski, K., Makarova, K.S., Lécrivain, A.-L., Bzdrenga, J.,

Koonin, E. V and Charpentier, E. (2014). Phylogeny of Cas9 determines functional exchangeability of dual-RNA and Cas9 among orthologous type II CRISPR-Cas systems. *Nucleic Acids Research*, 42 (4), 2577–90. Available from <https://doi.org/10.1093/nar/gkt1074> [Accessed 11 September 2020].

Fragkos, M., Ganier, O., Coulombe, P. and Méchali, M. (2015). DNA replication origin activation in space and time. *Nature Reviews Molecular Cell Biology*, 16 (6), 360–374. Available from <https://doi.org/10.1038/nrm4002> [Accessed 12 July 2020].

Franks, T.M. and Lykke-Andersen, J. (2007). TTP and BRF proteins nucleate processing body formation to silence mRNAs with AU-rich elements. *Genes and Development*, 21 (6), 719–735. Available from <https://doi.org/10.1101/gad.1494707> [Accessed 23 July 2020].

Fujita, M. (2006). Cdt1 revisited: complex and tight regulation during the cell cycle and consequences of deregulation in mammalian cells. *Cell Division*, 1, 22. Available from <https://doi.org/10.1186/1747-1028-1-22> [Accessed 23 December 2020].

Gaillard, H., García-Muse, T. and Aguilera, A. (2015). Replication stress and cancer. *Nature Reviews Cancer*, 15 (5), 276–280. Available from <https://doi.org/10.1038/nrc3916> [Accessed 25 July 2020].

Galloway, A. and Turner, M. (2017). Cell cycle RNA regulons coordinating early lymphocyte development. *Wiley Interdisciplinary Reviews: RNA*, 8 (5), e1419. Available from <https://doi.org/10.1002/wrna.1419> [Accessed 28 July 2020].

Galloway, A., Saveliev, A., Łukasiak, S., Hodson, Daniel J, Bolland, D., Balmanno, K., Ahlfors, H., Monzón-Casanova, E., Mannurita, S.C., Bell, L.S., Andrews, S., Díaz-Muñoz, M.D., Cook, S.J., Corcoran, A. and Turner, M. (2016). RNA-binding proteins ZFP36L1 and ZFP36L2 promote cell quiescence. *Science*, 352 (6284), 453–9. Available from <https://doi.org/10.1126/science.aad5978> [Accessed 29 August 2020].

Garneau, J.E., Dupuis, M.-È., Villion, M., Romero, D.A., Barrangou, R., Boyaval, P., Fremaux, C., Horvath, P., Magadán, A.H. and Moineau, S. (2010). The CRISPR/Cas bacterial immune system cleaves bacteriophage and plasmid DNA. *Nature*, 468 (7320), 67–71. Available from <https://doi.org/10.1038/nature09523> [Accessed 10

September 2020].

Gatei, M., Sloper, K., Sorensen, C., Syljuäsen, R., Falck, J., Hobson, K., Savage, K., Lukas, J., Zhou, B.-B., Bartek, J. and Khanna, K.K. (2003). Ataxia-telangiectasia-mutated (ATM) and NBS1-dependent phosphorylation of Chk1 on Ser-317 in response to ionizing radiation. *The Journal of Biological Chemistry*, 278 (17), 14806–11. Available from <https://doi.org/10.1074/jbc.M210862200> [Accessed 18 August 2020].

Gately, S. and Li, W.W. (2004). Multiple roles of COX-2 in tumor angiogenesis: a target for antiangiogenic therapy. *Seminars in Oncology*, 31 (2 Suppl 7), 2–11. Available from <https://doi.org/10.1053/j.seminoncol.2004.03.040> [Accessed 10 August 2020].

Gaudreault, I., Guay, D. and Lebel, M. (2004). YB-1 promotes strand separation in vitro of duplex DNA containing either mispaired bases or cisplatin modifications, exhibits endonucleolytic activities and binds several DNA repair proteins. *Nucleic Acids Research*, 32 (1), 316–27. Available from <https://doi.org/10.1093/nar/gkh170> [Accessed 24 August 2020].

Ge, X.Q., Jackson, D.A. and Blow, J.J. (2007). Dormant origins licensed by excess Mcm2-7 are required for human cells to survive replicative stress. *Genes & development*, 21 (24), 3331–41. Available from <https://doi.org/10.1101/gad.457807> [Accessed 16 August 2020].

Gerstberger, S., Hafner, M. and Tuschl, T. (2014). A census of human RNA-binding proteins. *Nature Reviews Genetics*, 15 (12), 829–845. Available from <https://doi.org/10.1038/nrg3813> [Accessed 14 July 2020].

Giglia-Mari, G., Zotter, A. and Vermeulen, W. (2011). DNA damage response. *Cold Spring Harbor Perspectives in Biology*, 3 (1), a000745. Available from <https://doi.org/10.1101/cshperspect.a000745> [Accessed 17 August 2020].

Giuliano, C.J., Lin, A., Girish, V. and Sheltzer, J.M. (2019). Generating Single Cell-Derived Knockout Clones in Mammalian Cells with CRISPR/Cas9. *Current Protocols in Molecular Biology*, 128 (1), e100. Available from [https://doi.org/10.1002/CPMB.100@10.1002/\(ISSN\)1934-3647.GENOMEEDITING](https://doi.org/10.1002/CPMB.100@10.1002/(ISSN)1934-3647.GENOMEEDITING)

[Accessed 22 June 2020].

Glisovic, T., Bachorik, J.L., Yong, J. and Dreyfuss, G. (2008). RNA-binding proteins and post-transcriptional gene regulation. *FEBS Letters*, 582 (14), 1977–86. Available from <https://doi.org/10.1016/j.febslet.2008.03.004> [Accessed 14 July 2020].

Glover, T.W., Berger, C., Coyle, J. and Echo, B. (1984). DNA polymerase α inhibition by aphidicolin induces gaps and breaks at common fragile sites in human chromosomes. *Human Genetics*, 67 (2), 136–142. Available from <https://doi.org/10.1007/BF00272988> [Accessed 15 October 2020].

Glover, T.W., Arlt, M.F., Casper, A.M. and Durkin, S.G. (2005). Mechanisms of common fragile site instability. *Human Molecular Genetics*, 14 (2), R197–R205. Available from <https://doi.org/10.1093/hmg/ddi265> [Accessed 5 July 2020].

Glover, T.W., Wilson, T.E. and Arlt, M.F. (2017a). Fragile sites in cancer: More than meets the eye. *Nature Reviews Cancer*, 17 (8), 489–501. Available from <https://doi.org/10.1038/nrc.2017.52> [Accessed 29 July 2020].

Gorgoulis, V.G., Vassiliou, L.V.F., Karakaidos, P., Zacharatos, P., Kotsinas, A., Liloglou, T., Venere, M., DiTullio, R.A., Kastrinakis, N.G., Levy, B., Kletsas, D., Yoneta, A., Herlyn, M., Kittas, C. and Halazonetis, T.D. (2005). Activation of the DNA damage checkpoint and genomic instability in human precancerous lesions. *Nature*, 434 (7035), 907–913. Available from <https://doi.org/10.1038/nature03485> [Accessed 5 July 2020].

Gourraud, P.-A., Harbo, H.F., Hauser, S.L. and Baranzini, S.E. (2012). The genetics of multiple sclerosis: An up-to-date review A brief history of MS genetics. *Immunology Reviews*, 248(1), 87–103. Available from <https://doi.org/10.1111/j.1600-065X.2012.01134.x> [Accessed 21 July 2020].

Griseri, P. and Pagès, G. (2014). Control of Pro-Angiogenic Cytokine mRNA Half-Life in Cancer: The Role of AU-Rich Elements and Associated Proteins. *Journal of Interferon & Cytokine Research*, 34 (4), 242–254. Available from <https://doi.org/10.1089/jir.2013.0140> [Accessed 10 August 2020].

Grissa, I., Vergnaud, G. and Pourcel, C. (2007). The CRISPRdb database and tools

to display CRISPRs and to generate dictionaries of spacers and repeats. *BMC Bioinformatics*. 8 (1), 172. Available from <https://doi.org/10.1186/1471-2105-8-172> [Accessed 26 July 2020].

Grivennikov, S.I., Greten, F.R. and Karin, M. (2010). Immunity, inflammation, and cancer. *Cell*, 140 (6), 883–99. Available from <https://doi.org/10.1016/j.cell.2010.01.025> [Accessed 9 August 2020].

Grover, R., Sarothi Ray, P. and Das, S. (2008). Polypyrimidine tract binding protein regulates IRES-mediated translation of p53 isoforms. *Cell Cycle*, 7, 2189–2198. Available from <https://doi.org/10.4161/cc.7.14.6271> [Accessed 23 August 2020].

Gu, J., Lu, H., Tippin, B., Shimazaki, N., Goodman, M.F. and Lieber, M.R. (2007). XRCC4:DNA ligase IV can ligate incompatible DNA ends and can ligate across gaps. *The EMBO Journal*, 26 (4), 1010–23. Available from <https://doi.org/10.1038/sj.emboj.7601559> [Accessed 21 August 2020].

Guo, J., Qu, H., Chen, Y. and Xia, J. (2017a). The role of RNA-binding protein tristetraprolin in cancer and immunity. *Medical Oncology*, 34 (12), 1–12. Available from <https://doi.org/10.1007/s12032-017-1055-6> [Accessed 17 July 2020].

Guo, J., Qu, H., Shan, T., Chen, Yigang, Chen, Ye and Xia, J. (2018). Tristetraprolin Overexpression in Gastric Cancer Cells Suppresses PD-L1 Expression and Inhibits Tumor Progression by Enhancing Antitumor Immunity. *Molecules and Cells*, 41 (7), 653–664. Available from <https://doi.org/10.14348/molcells.2018.0040> [Accessed 4 September 2020].

Haahr, P., Hoffmann, S., Tollenaere, M.A.X., Ho, T., Toledo, L.I., Mann, M., Bekker-Jensen, S., Räschle, M. and Mailand, N. (2016). Activation of the ATR kinase by the RPA-binding protein ETAA1. *Nature Cell Biology*, 18 (11), 1196–1207. Available from <https://doi.org/10.1038/ncb3422> [Accessed 18 August 2020].

Haber, J.E. (1999). DNA recombination: the replication connection. *Trends in Biochemical Sciences*, 24 (7), 271–5. Available from [https://doi.org/10.1016/s0968-0004\(99\)01413-9](https://doi.org/10.1016/s0968-0004(99)01413-9) [Accessed 21 August 2020].

Hanahan, D. and Weinberg, R.A. (2011). Hallmarks of Cancer: The Next Generation.

Cell, 144 (5), 646–674. Available from <https://doi.org/10.1016/J.CELL.2011.02.013> [Accessed 27 April 2020].

Harrigan, J.A., Belotserkovskaya, R., Coates, J., Dimitrova, D.S., Polo, S.E., Bradshaw, C.R., Fraser, P. and Jackson, S.P. (2011). Replication stress induces 53BP1-containing OPT domains in G1 cells. *The Journal of Cell Biology*, 193 (1), 97–108. Available from <https://doi.org/10.1083/jcb.201011083> [Accessed 5 June 2020].

Hau, H.H., Walsh, R.J., Ogilvie, R.L., Williams, D.A., Reilly, C.S. and Bohjanen, P.R. (2007). Tristetraprolin recruits functional mRNA decay complexes to ARE sequences. *Journal of Cellular Biochemistry*, 100 (6), 1477–1492. Available from <https://doi.org/10.1002/jcb.21130> [Accessed 29 July 2020].

Helleday, T., Lo, J., van Gent, D.C. and Engelward, B.P. (2007). DNA double-strand break repair: from mechanistic understanding to cancer treatment. *DNA repair*, 6 (7), 923–35. Available from <https://doi.org/10.1016/j.dnarep.2007.02.006> [Accessed 19 August 2020].

Helmrich, A., Ballarino, M. and Tora, L. (2011). Collisions between Replication and Transcription Complexes Cause Common Fragile Site Instability at the Longest Human Genes. *Molecular Cell*, 44 (6), 966–977. Available from <https://doi.org/10.1016/j.molcel.2011.10.013> [Accessed 15 November 2020].

Hengeveld, R.C.C., de Boer, H.R., Schoonen, P.M., de Vries, E.G.E., Lens, S.M.A. and van Vugt, M.A.T.M. (2015). Rif1 Is Required for Resolution of Ultrafine DNA Bridges in Anaphase to Ensure Genomic Stability. *Developmental Cell*, 34 (4), 466–474. Available from <https://doi.org/10.1016/j.devcel.2015.06.014> [Accessed 19 September 2020].

Heyer, W.-D., Ehmsen, K.T. and Liu, J. (2010). Regulation of homologous recombination in eukaryotes. *Annual Review of Genetics*, 44, 113–39. Available from <https://doi.org/10.1146/annurev-genet-051710-150955> [Accessed 21 August 2020].

Hitti, E., Bakheet, T., Al-Souhibani, N., Moghrabi, W., Al-Yahya, S., Al-Ghamdi, M., Al-Saif, M., Shoukri, M.M., Lanczky, A., Grepin, R., Gyorffy, B., Pages, G. and Khabar, K.S.A. (2016). Systematic analysis of AU-Rich element expression in cancer reveals

common functional clusters regulated by key RNA-Binding proteins. *Cancer Research*, 76(14), 4068-4080. Available from <https://doi.org/10.1158/0008-5472.CAN-15-3110> [Accessed 5 July 2020].

Hockemeyer, D., Wang, H., Kiani, S., Lai, C.S., Gao, Q., Cassady, J.P., Cost, G.J., Zhang, L., Santiago, Y., Miller, J.C., Zeitler, B., Cherone, J.M., Meng, X., Hinkley, S.J., Rebar, E.J., Gregory, P.D., Urnov, F.D. and Jaenisch, R. (2011). Genetic engineering of human pluripotent cells using TALE nucleases. *Nature Biotechnology*, 29 (8), 731–4. Available from <https://doi.org/10.1038/nbt.1927> [Accessed 10 September 2020].

Hodson, D.J., Janas, M.L., Galloway, A., Bell, S.E., Andrews, S., Li, C.M., Pannell, R., Siebel, C.W., MacDonald, H.R., De Keersmaecker, K., Ferrando, A.A., Grutz, G. and Turner, M. (2010). Deletion of the RNA-binding proteins ZFP36L1 and ZFP36L2 leads to perturbed thymic development and T lymphoblastic leukemia. *Nature Immunology*, 11 (8), 717–724. Available from <https://doi.org/10.1038/ni.1901> [Accessed 20 July 2020].

Hong, Z., Jiang, J., Ma, J., Dai, S., Xu, T., Li, H. and Yasui, A. (2013). The role of hnRPU1 involved in DNA damage response is related to PARP1. *PloS One*, 8 (4), e60208. Available from <https://doi.org/10.1371/journal.pone.0060208> [Accessed 24 August 2020].

Hook, S.S., Lin, J.J. and Dutta, A. (2007). Mechanisms to Control Rereplication and Implications for Cancer. *Current Opinion in Cell Biology*, 19 (6), 663-671. Available from <https://doi.org/10.1016/J.CEB.2007.10.007> [Accessed 23 December 2020].

Howlett, N.G., Taniguchi, T., Durkin, S.G., D'Andrea, A.D. and Glover, T.W. (2005). The Fanconi anemia pathway is required for the DNA replication stress response and for the regulation of common fragile site stability. *Human Molecular Genetics*, 14 (5), 693–701. Available from <https://doi.org/10.1093/hmg/ddi065>.

Hübscher, U., Nasheuer, H.P. and Syvöja, J.E. (2000). Eukaryotic DNA polymerases, a growing family. *Trends in Biochemical Sciences*, 25 (3), 143–147. Available from [https://doi.org/10.1016/S0968-0004\(99\)01523-6](https://doi.org/10.1016/S0968-0004(99)01523-6) [Accessed 23 September 2020].

Hubstenberger, A., Courel, M., Bénard, M., Souquere, S., Ernoult-Lange, M., Chouaib, R., Yi, Z., Morlot, J.-B., Munier, A., Fradet, M., Daunesse, M., Bertrand, E., Pierron, G., Mozziconacci, J., Kress, M. and Weil, D. (2017). P-Body Purification Reveals the Condensation of Repressed mRNA Regulons. *Molecular Cell*, 68 (1), 144-157.e5. Available from <https://doi.org/10.1016/j.molcel.2017.09.003> [Accessed 26 July 2020].

Huertas, P. and Aguilera, A. (2003). Cotranscriptionally formed DNA:RNA hybrids mediate transcription elongation impairment and transcription-associated recombination. *Molecular Cell*, 12 (3), 711–21. Available from <https://doi.org/10.1016/j.molcel.2003.08.010> [Accessed 27 August 2020].

Ichijima, Y., Yoshioka, K., Yoshioka, Y., Shinohe, K., Fujimori, H., Unno, J., Takagi, M., Goto, H., Inagaki, M., Mizutani, S. and Teraoka, H. (2010). DNA Lesions Induced by Replication Stress Trigger Mitotic Aberration and Tetraploidy Development. *PLoS One*, 5 (1), e8821. Available from <https://doi.org/10.1371/journal.pone.0008821> [Accessed 22 September 2020].

Ilves, I., Petojevic, T., Pesavento, J.J. and Botchan, M.R. (2010). Activation of the MCM2-7 helicase by association with Cdc45 and GINS proteins. *Molecular Cell*, 37 (2), 247–58. Available from <https://doi.org/10.1016/j.molcel.2009.12.030> [Accessed 15 August 2020].

Ise, T., Nagatani, G., Imamura, T., Kato, K., Takano, H., Nomoto, M., Izumi, H., Ohmori, H., Okamoto, T., Ohga, T., Uchiumi, T., Kuwano, M. and Kohno, K. (1999). Transcription Factor Y-Box Binding Protein 1 Binds Preferentially to Cisplatin-modified DNA and Interacts with Proliferating Cell Nuclear Antigen. *Cancer Res.*, 56 (18), 4224–4228. Available from <https://cancerres.aacrjournals.org/content/59/2/342.long> [Accessed 24 August 2020].

Ito, K.K., Watanabe, K. and Kitagawa, D. (2020). The emerging role of ncRNAs and RNA-binding proteins in mitotic apparatus formation. *Non-coding RNA*, 6 (1), 13. Available from <https://doi.org/10.3390/NCRNA6010013> [Accessed 13 July 2020].

Iwanaga, E., Nanri, T., Mitsuya, H. and Asou, N. (2011). Mutation in the RNA binding protein TIS11D/ZFP36L2 is associated with the pathogenesis of acute leukemia. *International Journal of Oncology*, 38 (1), 25–31. Available from

<http://www.ncbi.nlm.nih.gov/pubmed/21109922> [Accessed 22 July 2020].

Jalonen, U., Nieminen, R., Vuolteenaho, K., Kankaanranta, H. and Moilanen, E. (2006). Down-regulation of tristetraprolin expression results in enhanced IL-12 and MIP-2 production and reduced MIP-3 α synthesis in activated macrophages. *Mediators of Inflammation*, 2006 (6), 40691. Available from <https://doi.org/10.1155/MI/2006/40691> [Accessed 28 July 2020].

Jang, M.K., Shen, K. and McBride, A.A. (2014). Papillomavirus Genomes Associate with BRD4 to Replicate at Fragile Sites in the Host Genome. *PLoS Pathogens*, 10 (5), e1004117. Available from <https://doi.org/10.1371/journal.ppat.1004117> [Accessed 5 July 2020].

Jazayeri, A., Falck, J., Lukas, C., Bartek, J., Smith, G.C.M., Lukas, J. and Jackson, S.P. (2006). ATM- and cell cycle-dependent regulation of ATR in response to DNA double-strand breaks. *Nature Cell Biology*, 8 (1), 37–45. Available from <https://doi.org/10.1038/ncb1337> [Accessed 17 August 2020].

Jeganathan, K., Malureanu, L., Baker, D.J., Abraham, S.C. and van Deursen, J.M. (2007). Bub1 mediates cell death in response to chromosome missegregation and acts to suppress spontaneous tumorigenesis. *The Journal of Cell Biology*, 179 (2), 255–67. Available from <https://doi.org/10.1083/jcb.200706015> [Accessed 14 August 2020].

Jinek, M., Chylinski, K., Fonfara, I., Hauer, M., Doudna, J.A. and Charpentier, E. (2012). A programmable dual-RNA-guided DNA endonuclease in adaptive bacterial immunity. *Science*, 337 (6096), 816–21. Available from <https://doi.org/10.1126/science.1225829> [Accessed 10 September 2020].

Jinek, M., East, A., Cheng, A., Lin, S., Ma, E. and Doudna, J. (2013). RNA-programmed genome editing in human cells. *eLife*, 2, e00471. Available from <https://doi.org/10.7554/eLife.00471> [Accessed 4 April 2020].

JJ Yunis, A.S. (1984). Constitutive Fragile Sites and Cancer. *Science*, 226 (4679), 1199–1204 [Accessed 1 September 2020].

Johnson, B.A. and Blackwell, T.K. (2002). Multiple tristetraprolin sequence domains

required to induce apoptosis and modulate responses to TNF α through distinct pathways. *Oncogene*, 21 (27), 4237–4246. Available from <https://doi.org/10.1038/sj.onc.1205526> [Accessed 21 June 2020].

Johnson, B.A., Geha, M. and Blackwell, T.K. (2000). Similar but distinct effects of the tristetraprolin/TIS11 immediate-early proteins on cell survival. *Oncogene*, 19 (13), 1657–1664. Available from <https://doi.org/10.1038/sj.onc.1203474> [Accessed 10 August 2020].

Johnson, B.A., Stehn, J.R., Yaffe, M.B. and Blackwell, T.K. (2002). Cytoplasmic localization of tristetraprolin involves 14-3-3-dependent and independent mechanisms. *The Journal of Biological Chemistry*, 277 (20), 18029–36. Available from <https://doi.org/10.1074/jbc.M110465200> [Accessed 25 July 2020].

Jossen, R. and Bermejo, R. (2013). The DNA damage checkpoint response to replication stress: A Game of Forks. *Frontiers in Genetics*, 4, 26. Available from <https://doi.org/10.3389/fgene.2013.00026> [Accessed 25 September 2020].

Kai, M. (2016). Roles of RNA-binding proteins in DNA damage response. *International Journal of Molecular Sciences*, 17 (3), 1–9. Available from <https://doi.org/10.3390/ijms17030310> [Accessed 2 August 2020].

Kanda, T., Sullivan, K.F. and Wahl, G.M. (1998). Histone-GFP fusion protein enables sensitive analysis of chromosome dynamics in living mammalian cells. *Current Biology*, 8 (7), 377–385. Available from [https://doi.org/10.1016/S0960-9822\(98\)70156-3](https://doi.org/10.1016/S0960-9822(98)70156-3).

Karagiannis, T.C. and El-Osta, A. (2004). DNA damage repair and transcription. *Cellular and Molecular Life Sciences*, 61 (17), 2137–2147. Available from <https://doi.org/10.1007/s00018-004-4174-0> [Accessed 25 September 2020].

Kastan, M.B., Zhan, Q., el-Deiry, W.S., Carrier, F., Jacks, T., Walsh, W. V, Plunkett, B.S., Vogelstein, B. and Fornace, A.J. (1992). A mammalian cell cycle checkpoint pathway utilizing p53 and GADD45 is defective in ataxia-telangiectasia. *Cell*, 71 (4), 587–97. Available from [https://doi.org/10.1016/0092-8674\(92\)90593-2](https://doi.org/10.1016/0092-8674(92)90593-2) [Accessed 18 August 2020].

Kechavarzi, B. and Janga, S.C. (2014). Dissecting the expression landscape of RNA-binding proteins in human cancers. *Genome Biology*, 15 (1), R14. Available from <https://doi.org/10.1186/gb-2014-15-1-r14> [Accessed 16 July 2020].

Kedersha, N. and Anderson, P. (2002). Stress granules: sites of mRNA triage that regulate mRNA stability and translatability. *Biochemical Society Transactions*, 30 (6), 963–969. Available from <https://doi.org/10.1042/bst0300963> [Accessed 26 July 2020].

Kedersha, N., Stoecklin, G., Ayodele, M., Yacono, P., Lykke-Andersen, J., Fritzler, M.J., Scheuner, D., Kaufman, R.J., Golan, D.E. and Anderson, P. (2005). Stress granules and processing bodies are dynamically linked sites of mRNP remodeling. *The Journal of Cell Biology*, 169 (6), 871–884. Available from <https://doi.org/10.1083/jcb.200502088> [Accessed 26 July 2020].

Keene, J.D. (2007). RNA regulons: Coordination of post-transcriptional events. *Nature Reviews Genetics*, 8 (7), 533–543. Available from <https://doi.org/10.1038/nrg2111>.

Khabar, K.S.A. (2017). Hallmarks of cancer and AU-rich elements. *Wiley Interdisciplinary Reviews: RNA*, 8 (1), e1368. Available from <https://doi.org/10.1002/wrna.1368> [Accessed 23 July 2020].

Khong, A., Matheny, T., Jain, S., Mitchell, S.F., Wheeler, J.R. and Parker, R. (2017). The Stress Granule Transcriptome Reveals Principles of mRNA Accumulation in Stress Granules. *Molecular Cell*, 68 (4), 808-820.e5. Available from <https://doi.org/10.1016/j.molcel.2017.10.015> [Accessed 26 July 2020].

Kim, C.W., Kim, H.K., Vo, M.-T., Lee, H.H., Kim, H.J., Min, Y.J., Cho, W.J. and Park, J.W. (2010). Tristetraprolin controls the stability of cIAP2 mRNA through binding to the 3'UTR of cIAP2 mRNA. *Biochemical and Biophysical Research Communications*, 400 (1), 46–52. Available from <https://doi.org/10.1016/j.bbrc.2010.07.136> [Accessed 4 September 2020].

Kim, H.H., Abdelmohsen, K. and Gorospe, M. (2010). Regulation of HuR by DNA damage response Kinases. *Journal of Nucleic Acids*, 2010, 981487. Available from <https://doi.org/10.4061/2010/981487> [Accessed 21 August 2020].

Kim, H.J., Kim, N.C., Wang, Y.-D., Scarborough, E.A., Moore, J., Diaz, Z., MacLea,

K.S., Freibaum, B., Li, S., Molliex, A., Kanagaraj, A.P., Carter, R., Boylan, K.B., Wojtas, A.M., Rademakers, R., Pinkus, J.L., Greenberg, S.A., Trojanowski, J.Q., Traynor, B.J., Smith, B.N., Topp, S., Gkazi, A.-S., Miller, J., Shaw, C.E., Kottlors, M., Kirschner, J., Pestronk, A., Li, Y.R., Ford, A.F., Gitler, A.D., Benatar, M., King, O.D., Kimonis, V.E., Ross, E.D., Weihl, C.C., Shorter, J. and Taylor, J.P. (2013). Mutations in prion-like domains in hnRNPA2B1 and hnRNPA1 cause multisystem proteinopathy and ALS. *Nature*, 495 (7442), 467–73. Available from <https://doi.org/10.1038/nature11922> [Accessed 15 July 2020].

Koike-Yusa, H., Li, Y., Tan, E.-P., Velasco-Herrera, M.D.C. and Yusa, K. (2014). Genome-wide recessive genetic screening in mammalian cells with a lentiviral CRISPR-guide RNA library. *Nature Biotechnology*, 32 (3), 267–73. Available from <https://doi.org/10.1038/nbt.2800> [Accessed 11 September 2020].

Kolas, N.K., Chapman, J.R., Nakada, S., Ylanko, J., Chahwan, R., Sweeney, F.D., Panier, S., Mendez, M., Wildenhain, J., Thomson, T.M., Pelletier, L., Jackson, S.P. and Durocher, D. (2007). Orchestration of the DNA-damage response by the RNF8 ubiquitin ligase. *Science*, 318 (5856), 1637–40. Available from <https://doi.org/10.1126/science.1150034> [Accessed 18 August 2020].

Komeno, Y., Huang, Y.-J., Qiu, J., Lin, L., Xu, Y., Zhou, Y., Chen, L., Monterroza, D.D., Li, H., DeKolver, R.C., Yan, M., Fu, X.-D., Zhang, D.-E., Komeno, C.Y., Y-j, H., X-d, F. and D-e, Z. (2015). SRSF2 Is Essential for Hematopoiesis, and Its Myelodysplastic Syndrome-Related Mutations Dysregulate Alternative Pre-mRNA Splicing Downloaded from. *Mol Cell Biol*, 35, 3071–3082. Available from <https://doi.org/10.1128/MCB.00202-15> [Accessed 16 July 2020].

Kondo, M., Noguchi, A., Matsuura, Y., Shimada, M., Yokota, N. and Kawahara, H. (2018). Novel phosphorelay-dependent control of ZFP36L1 protein during the cell cycle. *Biochemical and Biophysical Research Communications*, 501 (2), 387–393. Available from <https://doi.org/10.1016/j.bbrc.2018.04.212> [Accessed 23 August 2020].

Kops, G.J.P.L., Weaver, B.A.A. and Cleveland, D.W. (2005). On the road to cancer: Aneuploidy and the mitotic checkpoint. *Nature Reviews Cancer*, 5 (10), 773–785. Available from <https://doi.org/10.1038/nrc1714> [Accessed 3 July 2020].

Kotsantis, P., Petermann, E. and Boulton, S.J. (2018). Mechanisms of oncogene-induced replication stress: Jigsaw falling into place. *Cancer Discovery*, 8 (5), 537–555. Available from <https://doi.org/10.1158/2159-8290.CD-17-1461> [Accessed 15 July 2020].

Kremer, E.J., Pritchard, M., Lynch, M., Yu, S., Holman, K., Baker, E., Warren, S.T., Schlessinger, D., Sutherland, G.R. and Richards, R.I. (1991). Mapping of DNA instability at the fragile X to a trinucleotide repeat sequence p(CCG)_n. *Science*, 252 (5013), 1711–1714. Available from <https://doi.org/10.1126/science.1675488> [Accessed 29 July 2020].

Kumagai, A., Lee, J., Yoo, H.Y. and Dunphy, W.G. (2006). TopBP1 activates the ATR-ATRIP complex. *Cell*, 124 (5), 943–55. Available from <https://doi.org/10.1016/j.cell.2005.12.041> [Accessed 18 August 2020].

Kundu, J.K. and Surh, Y.J. (2008). Inflammation: Gearing the journey to cancer. *Mutation Research - Reviews in Mutation Research*, 659 (2008), 15–30. Available from <https://doi.org/10.1016/j.mrrev.2008.03.002> [Accessed 4 July 2020].

Labib, K. and De Piccoli, G. (2011). Surviving chromosome replication: the many roles of the S-phase checkpoint pathway. *Philosophical transactions of the Royal Society of London. Series B, Biological sciences*, 366 (1584), 3554–61. Available from <https://doi.org/10.1098/rstb.2011.0071> [Accessed 16 August 2020].

Lai, W.S. and Blackshear, P.J. (2001). Interactions of CCCH zinc finger proteins with mRNA: tristetraprolin-mediated AU-rich element-dependent mRNA degradation can occur in the absence of a poly(A) tail. *The Journal of Biological Chemistry*, 276 (25), 23144–54. Available from <https://doi.org/10.1074/jbc.M100680200> [Accessed 4 August 2020].

Lai, W.S., Stumpo, D.J. and Blackshear, P.J. (1990). Rapid insulin-stimulated accumulation of an mRNA encoding a proline-rich protein. *Journal of Biological Chemistry*, 265 (27), 16556–16563 [Accessed 5 July 2020].

Lai, W.S., Carballo, E., Strum, J.R., Kennington, E.A., Phillips, R.S. and Blackshear, P.J. (1999). Evidence that tristetraprolin binds to AU-rich elements and promotes the

deadenylation and destabilization of tumor necrosis factor alpha mRNA. *Molecular and Cellular Biology*, 19 (6), 4311–23. Available from <https://doi.org/10.1128/mcb.19.6.4311> [Accessed 22 July 2020].

Lai, W.S., Carballo, E., Thorn, J.M., Kennington, E.A. and Blackshear, P.J. (2000). Interactions of CCCH Zinc Finger Proteins with mRNA building of tristetraprolin-related zinc finger proteins to AU-rich elements and destabilisation of mRNA. *The Journal of Biological Chemistry*, 273(23), 17827-17837. Available from <https://doi.org/10.1074/jbc.M001696200> [Accessed 21 July 2020].

Lai, W.S., Kennington, E.A. and Blackshear, P.J. (2002). Interactions of CCCH Zinc Finger Proteins with mRNA non-binding Tristetraprolin mutants exert an inhibitory effect on degradation of au-rich element-containing mRNAs. *The Journal of Biochemistry*, 277 (11), 9606–9613. Available from <https://doi.org/10.1074/jbc.M110395200> [Accessed 21 July 2020].

Lai, W.S., Kennington, E.A. and Blackshear, P.J. (2003). Tristetraprolin and its family members can promote the cell-free deadenylation of AU-rich element-containing mRNAs by poly(A) ribonuclease. *Molecular and Cellular Biology*, 23 (11), 3798–812. Available from <https://doi.org/10.1128/mcb.23.11.3798-3812.2003> [Accessed 23 July 2020].

Lai, W.S., Carrick, D.M. and Blackshear, P.J. (2005). Influence of Nonameric AU-rich Tristetraprolin-binding Sites on mRNA Deadenylation and Turnover. *Journal of Biological Chemistry*, 280 (40), 34365-77. Available from <https://doi.org/10.1074/jbc.M506757200> [Accessed 22 July 2020].

Lai, W.S., Stumpo, D.J., Kennington, E.A., Burkholder, A.B., Ward, J.M., Fargo, D.L. and Blackshear, P.J. (2013). Life without TTP: Apparent absence of an important anti-inflammatory protein in birds. *American Journal of Physiology - Regulatory Integrative and Comparative Physiology*, 305 (7), 689–700. Available from <https://doi.org/10.1152/ajpregu.00310.2013> [Accessed 7 July 2020].

Lai, W.S., Perera, L., Hicks, S.N. and Blackshear, P.J. (2013). Mutational and structural analysis of the tandem zinc finger domain of tristetraprolin. *Journal of Biological Chemistry*, 289 (1), 565–580. Available from

<https://doi.org/10.1074/jbc.M113.466326> [Accessed 21 June 2020].

Leach, F.S., Nicolaides, N.C., Papadopoulos, N., Liu, B., Jen, J., Parsons, R., Peltomäki, P., Sistonen, P., Aaltonen, L.A. and Nyström-Lahti, M. (1993). Mutations of a mutS homolog in hereditary nonpolyposis colorectal cancer. *Cell*, 75 (6), 1215–25. Available from [https://doi.org/10.1016/0092-8674\(93\)90330-s](https://doi.org/10.1016/0092-8674(93)90330-s) [Accessed 13 August 2020].

Lee, D.Y. and Clayton, D.A. (1998). Initiation of mitochondrial DNA replication by transcription and R-loop processing. *The Journal of Biological Chemistry*, 273 (46), 30614–21. Available from <https://doi.org/10.1074/jbc.273.46.30614> [Accessed 27 August 2020].

Lee, H.H., Vo, M.-T., Kim, H.J., Lee, U.H., Kim, C.W., Kim, H.K., Ko, M.S., Lee, W.H., Cha, S.J., Min, Y.J., Choi, D.H., Suh, H.S., Lee, B.J., Park, J.W. and Cho, W.J. (2010). Stability of the LATS2 Tumor Suppressor Gene Is Regulated by Tristetraprolin. *Journal of Biological Chemistry*, 285 (23), 17329–17337. Available from <https://doi.org/10.1074/JBC.M109.094235> [Accessed 30 July 2020].

Lee, H.H., Yoon, N.A., Vo, M.-T., Kim, C.W., Woo, J.M., Cha, H.J., Cho, Y.W., Lee, B.J., Cho, W.J. and Park, J.W. (2012). Tristetraprolin down-regulates IL-17 through mRNA destabilization. *FEBS letters*, 586 (1), 41–6. Available from <https://doi.org/10.1016/j.febslet.2011.11.021> [Accessed 28 July 2020].

Lee, H.H., Lee, S.-R. and Leem, S.-H. (2014). Tristetraprolin Regulates Prostate Cancer Cell Growth Through Suppression of E2F1. *Journal of Microbiology and Biotechnology*, 24 (2), 287–294. Available from <https://doi.org/10.4014/jmb.1309.09070> [Accessed 4 September 2020].

Lee, J.-H. and Paull, T.T. (2005). ATM activation by DNA double-strand breaks through the Mre11-Rad50-Nbs1 complex. *Science*, 308 (5721), 551–4. Available from <https://doi.org/10.1126/science.1108297> [Accessed 18 August 2020].

Lee, S.K., Kim, S.B., Kim, J.S., Moon, C.H., Han, M.S., Lee, B.J., Chung, D.K., Min, Y.J., Park, J.H., Choi, D.H., Cho, H.R., Park, S.K. and Park, J.W. (2005). Butyrate response factor 1 enhances cisplatin sensitivity in human head and neck squamous

cell carcinoma cell lines. *International Journal of Cancer*, 117 (1), 32–40. Available from <https://doi.org/10.1002/ijc.21133> [Accessed 10 August 2020].

Lee, T.H., Choi, J.Y., Park, J.M. and Kang, T.H. (2020). Posttranscriptional control of the replication stress response via TTP-mediated Claspin mRNA stabilization. *Oncogene*, 39 (16), 3245–3257. Available from <https://doi.org/10.1038/s41388-020-1220-9> [Accessed 5 July 2020].

Leman, A.R. and Noguchi, E. (2013). The replication fork: Understanding the eukaryotic replication machinery and the challenges to genome duplication. *Genes*, 4 (1), 1-32. Available from <https://doi.org/10.3390/genes4010001> [Accessed 23 June 2020].

Letessier, A., Millot, G.A., Koundrioukoff, S., Lachagès, A.M., Vogt, N., Hansen, R.S., Malfoy, B., Brison, O. and Debatisse, M. (2011). Cell-type-specific replication initiation programs set fragility of the FRA3B fragile site. *Nature*, 470 (7332), 120–124. Available from <https://doi.org/10.1038/nature09745> [Accessed 8 July 2020].

Li, G.-M. (2008). Mechanisms and functions of DNA mismatch repair. *Cell Research*, 18 (1), 85–98. Available from <https://doi.org/10.1038/cr.2007.115> [Accessed 24 August 2020].

Li, X. and Manley, J.L. (2005). Inactivation of the SR protein splicing factor ASF/SF2 results in genomic instability. *Cell*, 122 (3), 365–78. Available from <https://doi.org/10.1016/j.cell.2005.06.008> [Accessed 27 August 2020].

Liang, J., Lei, T., Song, Y., Yanes, N., Qi, Y. and Fu, M. (2009). RNA-destabilizing factor tristetraprolin negatively regulates NF-kappaB signaling. *The Journal of Biological Chemistry*, 284 (43), 29383–90. Available from <https://doi.org/10.1074/jbc.M109.024745> [Accessed 8 September 2020].

Limbo, O., Chahwan, C., Yamada, Y., de Bruin, R.A.M., Wittenberg, C. and Russell, P. (2007). Ctp1 is a cell-cycle-regulated protein that functions with Mre11 complex to control double-strand break repair by homologous recombination. *Molecular Cell*, 28 (1), 134–46. Available from <https://doi.org/10.1016/j.molcel.2007.09.009> [Accessed 21 August 2020].

Lin, N.-Y., Lin, C.-T., Chen, Y.-L. and Chang, C.-J. (2007). Regulation of tristetraproline during differentiation of 3T3-L1 preadipocytes. *FEBS Journal*, 274 (3), 867–878. Available from <https://doi.org/10.1111/j.1742-4658.2007.05632.x> [Accessed 28 July 2020].

Lin, R.-J., Huang, C.-H., Liu, P.-C., Lin, I.-C., Huang, Y.-L., Chen, A.-Y., Chiu, H.-P., Shih, S.-R., Lin, L.-H., Lien, S.-P., Yen, L.-C. and Liao, C.-L. (2020). Zinc finger protein ZFP36L1 inhibits influenza A virus through translational repression by targeting HA, M and NS RNA transcripts. *Nucleic Acids Research*, 48 (13), 7371–7384. Available from <https://doi.org/10.1093/nar/gkaa458> [Accessed 23 July 2020].

Liu, C., Zhang, L., Liu, H. and Cheng, K. (2017). Delivery strategies of the CRISPR-Cas9 gene-editing system for therapeutic applications. *Journal of controlled release : official journal of the Controlled Release Society*, 266, 17–26. Available from <https://doi.org/10.1016/j.jconrel.2017.09.012> [Accessed 8 October 2020].

Liu, S., Bekker-Jensen, S., Mailand, N., Lukas, C., Bartek, J. and Lukas, J. (2006). Claspin operates downstream of TopBP1 to direct ATR signaling towards Chk1 activation. *Molecular and Cellular Biology*, 26 (16), 6056–64. Available from <https://doi.org/10.1128/MCB.00492-06> [Accessed 18 August 2020].

Liu, S., Opiyo, S.O., Manthey, K., Glanzer, J.G., Ashley, A.K., Amerin, C., Troksa, K., Shrivastav, M., Nickoloff, J.A. and Oakley, G.G. (2012). Distinct roles for DNA-PK, ATM and ATR in RPA phosphorylation and checkpoint activation in response to replication stress. *Nucleic Acids Research*, 40 (21), 10780–94. Available from <https://doi.org/10.1093/nar/gks849> [Accessed 25 September 2020].

Liu, X., Li, F., Huang, Q., Zhang, Z., Zhou, L., Deng, Y., Zhou, M., Fleenor, D.E., Wang, H., Kastan, M.B. and Li, C.-Y. (2017). Self-inflicted DNA double-strand breaks sustain tumorigenicity and stemness of cancer cells. *Cell Research*, 27 (6), 764–783. Available from <https://doi.org/10.1038/cr.2017.41> [Accessed 17 August 2020].

Loh, X.-Y., Sun, Q.-Y., Ding, L.-W., Mayakonda, A., Venkatachalam, N., Yeo, M.-S., Silva, T.C., Xiao, J.-F., Doan, N.B., Said, J.W., Ran, X.-B., Zhou, S.-Q., Dakle, P., Shyamsunder, P., Koh, A.P.-F., Huang, R.Y.-J., Berman, B.P., Tan, S.-Y., Yang, H., Lin, D.-C. and Koeffler, H.P. (2020). RNA-Binding Protein ZFP36L1 Suppresses

Hypoxia and Cell-Cycle Signaling. *Cancer Research*, 80 (2), 219–233. Available from <https://doi.org/10.1158/0008-5472.CAN-18-2796> [Accessed 8 August 2020].

López-Contreras, A.J. and Fernandez-Capetillo, O. (2010). The ATR barrier to replication-born DNA damage. *DNA repair*, 9 (12), 1249–55. Available from <https://doi.org/10.1016/j.dnarep.2010.09.012> [Accessed 16 August 2020].

Lu, D., Searles, M.A. and Klug, A. (2003). Crystal structure of a zinc-finger-RNA complex reveals two modes of molecular recognition. *Nature*, 426 (6962), 96–100. Available from <https://doi.org/10.1038/nature02088> [Accessed 1 July 2020].

Lukas, C., Savic, V., Bekker-Jensen, S., Doil, C., Neumann, B., Pedersen, R.S., Grøhfte, M., Chan, K.L., Hickson, I.D., Bartek, J. and Lukas, J. (2011). 53BP1 nuclear bodies form around DNA lesions generated by mitotic transmission of chromosomes under replication stress. *Nature Cell Biology*, 13 (3), 243–253. Available from <https://doi.org/10.1038/ncb2201> [Accessed 17 July 2020].

Lukong, K.E., Chang, K. wei, Khandjian, E.W. and Richard, S. (2008). RNA-binding proteins in human genetic disease. *Trends in Genetics*, 24 (8), 416–425. Available from <https://doi.org/10.1016/j.tig.2008.05.004> [Accessed 27 July 2020].

Lunde, B.M., Moore, C. and Varani, G. (2007). RNA-binding proteins: modular design for efficient function. *Nature reviews. Molecular Cell Biology*, 8 (6), 479–90. Available from <https://doi.org/10.1038/nrm2178> [Accessed 13 July 2020].

Lykke-Andersen, J. and Wagner, E. (2005). Recruitment and activation of mRNA decay enzymes by two ARE-mediated decay activation domains in the proteins TTP and BRF-1. *Genes & Development*, 19 (3), 351–61. Available from <https://doi.org/10.1101/gad.1282305> [Accessed 23 July 2020].

Ma, K., Qiu, L., Mrasek, K., Zhang, J., Liehr, T., Quintana, L.G. and Li, Z. (2012). Common fragile sites: genomic hotspots of DNA damage and carcinogenesis. *International Journal of Molecular Sciences*, 13 (9), 11974–99. Available from <https://doi.org/10.3390/ijms130911974> [Accessed 15 October 2020].

Maccaroni, K., Balzano, E., Mirimao, F., Giunta, S. and Pelliccia, F. (2020). Impaired replication timing promotes tissue-specific expression of common fragile sites. *Genes*,

11 (3), 326. Available from <https://doi.org/10.3390/genes11030326> [Accessed 13 September 2020].

MacDougall, C.A., Byun, T.S., Van, C., Yee, M. and Cimprich, K.A. (2007). The structural determinants of checkpoint activation. *Genes & Development*, 21 (8), 898–903. Available from <https://doi.org/10.1101/gad.1522607> [Accessed 16 August 2020].

Macheret, M. and Halazonetis, T.D. (2015). DNA replication stress as a hallmark of cancer. *Annual Review of Pathology: Mechanisms of Disease*, 10, 425–448. Available from <https://doi.org/10.1146/annurev-pathol-012414-040424>.

Mackintosh, C. (2004). Dynamic interactions between 14-3-3 proteins and phosphoproteins regulate diverse cellular processes. *The Biochemical Journal*, 381 (Pt 2), 329–42. Available from <https://doi.org/10.1042/BJ20031332> [Accessed 24 July 2020].

Maclean, KN., McKay, IA., and Bustin, SA. (1998). Differential effects of sodium butyrate on the transcription of the human TIS11 family of early-response genes in colorectal cancer cells. *British Journal of Biomedical Science*, 55 (3), 184–191. Available from <https://europepmc.org/article/med/10367403> [Accessed 19 December 2020].

Madireddy, A., Kosiyatrakul, S.T., Boisvert, R.A., Herrera-Moyano, E., García-Rubio, M.L., Gerhardt, J., Vuono, E.A., Owen, N., Yan, Z., Olson, S., Aguilera, A., Howlett, N.G. and Schildkraut, C.L. (2016). FANCD2 Facilitates Replication through Common Fragile Sites. *Molecular Cell*, 64 (2), 388–404. Available from <https://doi.org/10.1016/j.molcel.2016.09.017> [Accessed 13 October 2020].

Mah, L.-J., El-Osta, A. and Karagiannis, T.C. (2010). γ H2AX: a sensitive molecular marker of DNA damage and repair. *Leukemia*, 24 (4), 679–686. Available from <https://doi.org/10.1038/leu.2010.6> [Accessed 25 September 2020].

Mahat, D.B., Brennan-Laun, S.E., Fialcowitz-White, E.J., Kishor, A., Ross, C.R., Pozharskaya, T., Rawn, J.D., Blackshear, P.J., Hassel, B.A. and Wilson, G.M. (2012). Coordinated expression of tristetraprolin post-transcriptionally attenuates mitogenic induction of the oncogenic ser/thr kinase Pim-1. *PLoS ONE*, 7(3), e33194. Available

from <https://doi.org/10.1371/journal.pone.0033194> [Accessed 25 August 2020].

Maher, R.L., Branagan, A.M. and Morrical, S.W. (2011). Coordination of DNA replication and recombination activities in the maintenance of genome stability. *Journal of Cellular Biochemistry*, 112 (10), 2672–82. Available from <https://doi.org/10.1002/jcb.23211> [Accessed 21 August 2020].

Mahtani, K.R., Brook, M., Dean, J.L., Sully, G., Saklatvala, J. and Clark, A.R. (2001). Mitogen-activated protein kinase p38 controls the expression and posttranslational modification of tristetraprolin, a regulator of tumor necrosis factor alpha mRNA stability. *Molecular and Cellular Biology*, 21 (19), 6461–9. Available from <https://doi.org/10.1128/mcb.21.9.6461-6469.2001> [Accessed 24 July 2020].

Mailand, N., Bekker-Jensen, S., Fastrup, H., Melander, F., Bartek, J., Lukas, C. and Lukas, J. (2007). RNF8 ubiquitylates histones at DNA double-strand breaks and promotes assembly of repair proteins. *Cell*, 131 (5), 887–900. Available from <https://doi.org/10.1016/j.cell.2007.09.040> [Accessed 18 August 2020].

Maitra, S., Chou, C.-F., Lubber, C.A., Lee, K.-Y., Mann, M. and Chen, C.-Y. (2008). The AU-rich element mRNA decay-promoting activity of BRF1 is regulated by mitogen-activated protein kinase-activated protein kinase 2. *RNA*, 14 (5), 950–9. Available from <https://doi.org/10.1261/rna.983708> [Accessed 24 July 2020].

Maizels, N. (2005). Immunoglobulin Gene Diversification. *Annual Review of Genetics*, 39 (1), 23–46. Available from <https://doi.org/10.1146/annurev.genet.39.073003.110544> [Accessed 13 August 2020].

Makarova, K.S., Haft, D.H., Barrangou, R., Brouns, S.J.J., Mojica, F.J.M., Wolf, Y.I., Yakunin, A.F., Oost, J. Van Der and Koonin, E. V. (2011). Evolution and classification of the CRISPR–Cas systems. *Nature*, 9 (6), 467–478. Available from <https://doi.org/10.1038/nrmicro2577>.

Mali, P., Yang, L., Esvelt, K.M., Aach, J., Guell, M., DiCarlo, J.E., Norville, J.E. and Church, G.M. (2013). RNA-guided human genome engineering via Cas9. *Science*, 339 (6121), 823–6. Available from <https://doi.org/10.1126/science.1232033>

[Accessed 10 September 2020].

Mantovani, A., Allavena, P., Sica, A. and Balkwill, F. (2008). Cancer-related inflammation. *Nature*, 454 (7203), 436–444. Available from <https://doi.org/10.1038/nature07205>.

Marderosian, M., Sharma, A., Funk, A.P., Vartanian, R., Masri, J., Jo, O.D. and Gera, J.F. (2006). Tristetraprolin regulates Cyclin D1 and c-Myc mRNA stability in response to rapamycin in an Akt-dependent manner via p38 MAPK signaling. *Oncogene*, 25 (47), 6277–6290. Available from <https://doi.org/10.1038/sj.onc.1209645> [Accessed 28 July 2020].

Maréchal, A. and Zou, L. (2013). DNA damage sensing by the ATM and ATR kinases. *Cold Spring Harbor Perspectives in Biology*, 5 (9), 1–18. Available from <https://doi.org/10.1101/cshperspect.a012716>.

Maréchal, A., Li, J.-M., Ji, X.Y., Wu, C.-S., Yazinski, S.A., Nguyen, H.D., Liu, S., Jiménez, A.E., Jin, J. and Zou, L. (2014). PRP19 Transforms into a Sensor of RPA-ssDNA after DNA Damage and Drives ATR Activation via a Ubiquitin-Mediated Circuitry. *Molecular Cell*, 53 (2), 235-246. Available from <https://doi.org/10.1016/J.MOLCEL.2013.11.002> [Accessed 24 August 2020].

Martincorena, I., Raine, K.M., Gerstung, M., Dawson, K.J., Haase, K., Van Loo, P., Davies, H., Stratton, M.R. and Campbell, P.J. (2017). Universal Patterns of Selection in Cancer and Somatic Tissues. *Cell*, 171 (5), 1029-1041.e21. Available from <https://doi.org/10.1016/j.cell.2017.09.042> [Accessed 20 September 2020].

Martínez-Calle, N., Pascual, M., Ordoñez, R., Enériz, E.S.J., Kulis, M., Miranda, E., Guruceaga, E., Segura, V., Larráyo, M.J., Bellosillo, B., Calasanz, M.J., Besses, C., Rifón, J., Martín-Subero, J.I., Agirre, X. and Prosper, F. (2019). Epigenomic profiling of myelofibrosis reveals widespread DNA methylation changes in enhancer elements and ZFP36L1 as a potential tumor suppressor gene that is epigenetically regulated. *Haematologica*, 104 (8), 1572-1579. Available from <https://doi.org/10.3324/haematol.2018.204917> [Accessed 13 August 2020].

Mastrocola, A.S., Kim, S.H., Trinh, A.T., Rodenkirch, L.A. and Tibbetts, R.S. (2013).

The RNA-binding protein fused in sarcoma (FUS) functions downstream of poly(ADP-ribose) polymerase (PARP) in response to DNA damage. *The Journal of Biological Chemistry*, 288 (34), 24731–41. Available from <https://doi.org/10.1074/jbc.M113.497974> [Accessed 24 August 2020].

Masuda, K., Abdelmohsen, K., Kim, M.M., Srikantan, S., Lee, E.K., Tominaga, K., Selimyan, R., Martindale, J.L., Yang, X., Lehmann, E., Zhang, Y., Becker, K.G., Wang, J.-Y., Kim, H.H. and Gorospe, M. (2011). Global dissociation of HuR-mRNA complexes promotes cell survival after ionizing radiation. *The EMBO Journal*, 30 (6), 1040–53. Available from <https://doi.org/10.1038/emboj.2011.24> [Accessed 23 August 2020].

Matsuoka, S., Rotman, G., Ogawa, A., Shiloh, Y., Tamai, K. and Elledge, S.J. (2000). Ataxia telangiectasia-mutated phosphorylates Chk2 in vivo and in vitro. *Proceedings of the National Academy of Sciences of the United States of America*, 97 (19), 10389–94. Available from <https://doi.org/10.1073/pnas.190030497> [Accessed 18 August 2020].

Matsuoka, S., Ballif, B.A., Smogorzewska, A., McDonald, E.R., Hurov, K.E., Luo, J., Bakalarski, C.E., Zhao, Z., Solimini, N., Lerenthal, Y., Shiloh, Y., Gygi, S.P. and Elledge, S.J. (2007). ATM and ATR Substrate Analysis Reveals Extensive Protein Networks Responsive to DNA Damage. *Science*, 316 (5828), 1160–1166. Available from <https://doi.org/10.1126/SCIENCE.1140321> [Accessed 25 August 2020].

Matsuura, Y., Noguchi, A., Sakai, S., Yokota, N. and Kawahara, H. (2020). Nuclear accumulation of ZFP36L1 is cell cycle-dependent and determined by a C-terminal serine-rich cluster. *The Journal of Biochemistry*, 168 (5), 477–489. Available from <https://doi.org/10.1093/jb/mvaa072> [Accessed 30 July 2020].

Mazan-Mamczarz, K., Galbán, S., López de Silanes, I., Martindale, J.L., Atasoy, U., Keene, J.D. and Gorospe, M. (2003). RNA-binding protein HuR enhances p53 translation in response to ultraviolet light irradiation. *Proceedings of the National Academy of Sciences of the United States of America*, 100 (14), 8354–9. Available from <https://doi.org/10.1073/pnas.1432104100> [Accessed 23 August 2020].

Mazan-Mamczarz, K., Hagner, P.R., Zhang, Y., Dai, B., Lehmann, E., Becker, K.G.,

Keene, J.D., Gorospe, M., Liu, Z. and Gartenhaus, R.B. (2011). ATM regulates a DNA damage response posttranscriptional RNA operon in lymphocytes. *Blood*, 117 (8), 2441-50. Available from <https://doi.org/10.1182/BLOOD-2010-09-310987> [Accessed 23 August 2020].

McCorkle, J.R., Leonard, M.K., Kraner, S.D., Blalock, E.M., Deqin, M., Zimmer, S.G. and Kaetzel, D.M. (2014). The Metastasis Suppressor NME1 Regulates Expression of Genes Linked to Metastasis and Patient Outcome in Melanoma and Breast Carcinoma. *Cancer Genomics & Proteomics*, 11 (4), 175-194. Available from <https://www.ncbi.nlm.nih.gov/pmc/articles/PMC4409327/> [Accessed 20 December 2020].

Melchionna, R., Chen, X.-B., Blasina, A. and McGowan, C.H. (2000). Threonine 68 is required for radiation-induced phosphorylation and activation of Cds1. *Nature Cell Biology*, 2 (10), 762–765. Available from <https://doi.org/10.1038/35036406> [Accessed 18 August 2020].

Meselson, M. and Stahl, F.W. (1958). The Replication of DNA in *Escherichia coli*. *Proceedings of the National Academy of Sciences of the United States of America*, 44 (7), 671–82. Available from <https://doi.org/10.1073/pnas.44.7.671> [Accessed 14 August 2020].

Michel, L.S., Liberal, V., Chatterjee, A., Kirchwegger, R., Pasche, B., Gerald, W., Dobles, M., Sorger, P.K., Murty, V. V and Benezra, R. (2001). MAD2 haplo-insufficiency causes premature anaphase and chromosome instability in mammalian cells. *Nature*, 409 (6818), 355–9. Available from <https://doi.org/10.1038/35053094> [Accessed 14 August 2020].

Milke, L., Schulz, K., Weigert, A., Sha, W., Schmid, T. and Brüne, B. (2013). Depletion of tristetraprolin in breast cancer cells increases interleukin-16 expression and promotes tumor infiltration with monocytes/macrophages. *Carcinogenesis*, 34 (4), 850–7. Available from <https://doi.org/10.1093/carcin/bgs387> [Accessed 4 September 2020].

Mimitou, E.P. and Symington, L.S. (2009). Nucleases and helicases take center stage in homologous recombination. *Trends in Biochemical Sciences*, 34 (5), 264–72.

Available from <https://doi.org/10.1016/j.tibs.2009.01.010> [Accessed 21 August 2020].

Minocherhomji, S., Ying, S., Bjerregaard, V.A., Bursomanno, S., Aleliunaite, A., Wu, W., Mankouri, H.W., Shen, H., Liu, Y. and Hickson, I.D. (2015). Replication stress activates DNA repair synthesis in mitosis. *Nature*, 528 (7581), 286–290. Available from <https://doi.org/10.1038/nature16139> [Accessed 10 August 2020].

Mirza-Aghazadeh-Attari, M., Mohammadzadeh, A., Yousefi, B., Mihanfar, A., Karimian, A. and Majidinia, M. (2019). 53BP1: A key player of DNA damage response with critical functions in cancer. *DNA Repair*, 73, 110–119. Available from <https://doi.org/10.1016/J.DNAREP.2018.11.008> [Accessed 27 September 2020].

Montecucco, A. and Biamonti, G. (2013). Pre-mRNA processing factors meet the DNA damage response. *Frontiers in Genetics*, 4, 102. Available from <https://doi.org/10.3389/fgene.2013.00102> [Accessed 23 August 2020].

Montorsi, L., Guizzetti, F., Alecci, C., Caporali, A., Martello, A., Atene, C.G., Parenti, S., Pizzini, S., Zanovello, P., Bortoluzzi, S., Ferrari, S., Grande, A. and Zanocco-Marani, T. (2016). Loss of ZFP36 expression in colorectal cancer correlates to wnt/ β -catenin activity and enhances epithelial-to-mesenchymal transition through upregulation of ZEB1, SOX9 and MACC1. *Oncotarget*, 7 (37), 59144–59157. Available from <https://doi.org/10.18632/oncotarget.10828> [Accessed 11 August 2020].

Morgan, B.R., Deveau, L.M. and Massi, F. (2015). Probing the Structural and Dynamical Effects of the Charged Residues of the TZF Domain of TIS11d. *Biophysj*, 108, 1503–1515. Available from <https://doi.org/10.1016/j.bpj.2015.01.039> [Accessed 21 July 2020].

Moumen, A., Magill, C., Dry, K. and Jackson, S.P. (2013). ATM-dependent phosphorylation of heterogeneous nuclear ribonucleoprotein K promotes p53 transcriptional activation in response to DNA damage. *Cell Cycle*, 12 (4), 698–704. Available from <https://doi.org/10.4161/cc.23592> [Accessed 25 August 2020].

Moyer, S.E., Lewis, P.W. and Botchan, M.R. (2006). Isolation of the Cdc45/Mcm2–7/GINS (CMG) complex, a candidate for the eukaryotic DNA replication fork helicase. *Proceedings of the National Academy of Sciences*, 103 (27), 10236–10241. Available

from <https://doi.org/10.1073/PNAS.0602400103> [Accessed 23 December 2020].

Moynahan, M.E., Pierce, A.J. and Jasin, M. (2001). BRCA2 is required for homology-directed repair of chromosomal breaks. *Molecular Cell*, 7 (2), 263–72. Available from [https://doi.org/10.1016/s1097-2765\(01\)00174-5](https://doi.org/10.1016/s1097-2765(01)00174-5) [Accessed 21 August 2020].

Mukherjee, N., Jacobs, N.C., Hafner, M., Kennington, E.A., Nusbaum, J.D., Tuschl, T., Blackshear, P.J. and Ohler, U. (2014). Global target mRNA specification and regulation by the RNA-binding protein ZFP36. *Genome Biology*, 15 (1), R12. Available from <https://doi.org/10.1186/gb-2014-15-1-r12> [Accessed 4 September 2020].

Müller-Mcnicoll, M. and Neugebauer, K.M. (2013). How cells get the message: Dynamic assembly and function of mRNA-protein complexes. *Nature Reviews Genetics*, 14 (4), 275–287. Available from <https://doi.org/10.1038/nrg3434> [Accessed 15 July 2020].

Murata, T., Yoshino, Y., Morita, N. and Kaneda, N. (2002). Identification of nuclear import and export signals within the structure of the zinc finger protein TIS11. *Biochemical and Biophysical Research Communications*, 293 (4), 1242–1247. Available from [https://doi.org/10.1016/S0006-291X\(02\)00363-7](https://doi.org/10.1016/S0006-291X(02)00363-7) [Accessed 25 July 2020].

Murphy, J. and Norton, J. (1990). Cell-type-specific early response gene expression during plasmacytoid differentiation of human B lymphocytic leukemia cells. *BBA - Gene Structure and Expression*, 1049 (3), 261–271. Available from [https://doi.org/10.1016/0167-4781\(90\)90096-K](https://doi.org/10.1016/0167-4781(90)90096-K) [Accessed 3 August 2020].

Murphy, J.J., Baou, M. and Jewell, A. (2009). TIS11 family proteins and their roles in posttranscriptional gene regulation. *Journal of Biomedicine and Biotechnology*, 2009. Available from <https://doi.org/10.1155/2009/634520> [Accessed 12 July 2020].

Naim, V. and Rosselli, F. (2009). The FANCD1 pathway and BLM collaborate during mitosis to prevent micro-nucleation and chromosome abnormalities. *Nature Cell Biology*, 11 (6), 761–768. Available from <https://doi.org/10.1038/ncb1883> [Accessed 19 August 2020].

Nam, E.A. and Cortez, D. (2011). ATR signalling: more than meeting at the fork. *The*

Biochemical Journal, 436 (3), 527–36. Available from <https://doi.org/10.1042/BJ20102162> [Accessed 16 August 2020].

Nasir, A., Norton, J.D., Baou, M., Zekavati, A., Bijlmakers, M.J., Thompson, S. and Murphy, J.J. (2012). ZFP36L1 Negatively Regulates Plasmacytoid Differentiation of BCL1 Cells by Targeting BLIMP1 mRNA. *PLoS ONE*, 7 (12), e52187. Available from <https://doi.org/10.1371/journal.pone.0052187> [Accessed 19 July 2020].

Negrini, S., Gorgoulis, V.G. and Halazonetis, T.D. (2010). Genomic instability an evolving hallmark of cancer. *Nature Reviews Molecular Cell Biology*, 11 (3), 220–228. Available from <https://doi.org/10.1038/nrm2858> [Accessed 21 August 2020].

Neufeld, G., Cohen, T., Gengrinovitch, S. and Poltorak, Z. (1999). Vascular endothelial growth factor (VEGF) and its receptors. *The FASEB Journal*, 13 (1), 9–22. Available from <https://doi.org/10.1096/fasebj.13.1.9> [Accessed 10 August 2020].

Newman, R., McHugh, J. and Turner, M. (2016). RNA binding proteins as regulators of immune cell biology. *Clinical and Experimental Immunology*, 183 (1), 37–49. Available from <https://doi.org/10.1111/cei.12684> [Accessed 16 July 2020].

Newman, R., Ahlfors, H., Saveliev, A., Galloway, A., Hodson, D.J., Williams, R., Besra, G.S., Cook, C.N., Cunningham, A.F., Bell, S.E. and Turner, M. (2017). Maintenance of the marginal zone B cell compartment specifically requires the RNA-binding protein ZFP36L1. *Nature Immunology*, 18 (6), 683–693. Available from <https://doi.org/10.1038/ni.3724> [Accessed 15 July 2020].

Nick McElhinny, S.A., Gordenin, D.A., Stith, C.M., Burgers, P.M.J. and Kunkel, T.A. (2008). Division of labor at the eukaryotic replication fork. *Molecular Cell*, 30 (2), 137–44. Available from <https://doi.org/10.1016/j.molcel.2008.02.022> [Accessed 15 August 2020].

Nie, X.F., Maclean, K.N., Kumar, V., McKay, I.A. and Bustin, S.A. (1995). ERF-2, the human homologue of the murine Tis11d early response gene. *Gene*, 152 (2), 285–286. Available from [https://doi.org/10.1016/0378-1119\(94\)00696-P](https://doi.org/10.1016/0378-1119(94)00696-P) [Accessed 12 July 2020].

Nielsen, C.F., Huttner, D., Bizard, A.H., Hirano, S., Li, T.-N., Palmai-Pallag, T.,

Bjerregaard, V.A., Liu, Y., Nigg, E.A., Wang, L.H.-C. and Hickson, I.D. (2015). PICH promotes sister chromatid disjunction and co-operates with topoisomerase II in mitosis. *Nature Communications*, 6 (1), 8962. Available from <https://doi.org/10.1038/ncomms9962> [Accessed 19 September 2020].

Nik-Zainal, S., Davies, H., Staaf, J., Ramakrishna, M., Glodzik, D., Zou, X., Martincorena, I., Alexandrov, L.B., Martin, S., Wedge, D.C., Van Loo, P., Ju, Y.S., Smid, M., Brinkman, A.B., Morganella, S., Aure, M.R., Lingjærde, O.C., Langerød, A., Ringnér, M., Ahn, S.-M., Boyault, S., Brock, J.E., Broeks, A., Butler, A., Desmedt, C., Dirix, L., Dronov, S., Fatima, A., Foekens, J.A., Gerstung, M., Hooijer, G.K.J., Jang, S.J., Jones, D.R., Kim, H.-Y., King, T.A., Krishnamurthy, S., Lee, H.J., Lee, J.-Y., Li, Y., McLaren, S., Menzies, A., Mustonen, V., O'Meara, S., Pauporté, I., Pivot, X., Purdie, C.A., Raine, K., Ramakrishnan, K., Rodríguez-González, F.G., Romieu, G., Sieuwerts, A.M., Simpson, P.T., Shepherd, R., Stebbings, L., Stefansson, O.A., Teague, J., Tommasi, S., Treilleux, I., Van den Eynden, G.G., Vermeulen, P., Vincent-Salomon, A., Yates, L., Caldas, C., Veer, L. van't, Tutt, A., Knappskog, S., Tan, B.K.T., Jonkers, J., Borg, Å., Ueno, N.T., Sotiriou, C., Viari, A., Futreal, P.A., Campbell, P.J., Span, P.N., Van Laere, S., Lakhani, S.R., Eyfjord, J.E., Thompson, A.M., Birney, E., Stunnenberg, H.G., van de Vijver, M.J., Martens, J.W.M., Børresen-Dale, A.-L., Richardson, A.L., Kong, G., Thomas, G. and Stratton, M.R. (2016). Landscape of somatic mutations in 560 breast cancer whole-genome sequences. *Nature*, 534 (7605), 47–54. Available from <https://doi.org/10.1038/nature17676> [Accessed 2 July 2020].

Ning, Z.-Q., Norton, J.D., Li, J. and Murphy, J.J. (1996). Distinct mechanisms for rescue from apoptosis in Ramos human B cells by signaling through CD40 and interleukin-4 receptor: role for inhibition of an early response gene, Berg36. *European Journal of Immunology*, 26 (10), 2356–2363. Available from <https://doi.org/10.1002/eji.1830261013> [Accessed 10 August 2020].

Ning, Z.Q., Norton, J.D., Jin, L.I. and Murphy, J.J. (1997). Distinct mechanisms for rescue from apoptosis in Ramos human B cells by signalling through CD40 and interleukin-4 receptor: Role for inhibition of an early response gene, Berg36. *Biochemical Society Transactions*, 25 (2), 2356–2363. Available from <https://doi.org/10.1042/bst025306s> [Accessed 7 August 2020].

Nishida, K., Kuwano, Y., Nishikawa, T., Masuda, K. and Rokutan, K. (2017). RNA binding proteins and genome integrity. *International Journal of Molecular Sciences*, 18 (7), 3–5. Available from <https://doi.org/10.3390/ijms18071341> [Accessed 21 August 2020].

Nishimasu, H., Ran, F.A., Hsu, P.D., Konermann, S., Shehata, S.I., Dohmae, N., Ishitani, R., Zhang, F. and Nureki, O. (2014). Crystal structure of Cas9 in complex with guide RNA and target DNA. *Cell*, 156 (5), 935–49. Available from <https://doi.org/10.1016/j.cell.2014.02.001> [Accessed 11 September 2020].

Noguchi, A., Adachi, S., Yokota, N., Hatta, T., Natsume, T. and Kawahara, H. (2018). ZFP36L2 is a cell cycle-regulated CCCH protein necessary for DNA lesion-induced S-phase arrest. *Biology open*, 7 (3), bio031575. Available from <https://doi.org/10.1242/bio.031575> [Accessed 5 August 2018].

Ogilvie, R.L., Abelson, M., Hau, H.H., Vlasova, I., Blackshear, P.J. and Bohjanen, P.R. (2005). Tristetraprolin Down-Regulates IL-2 Gene Expression through AU-Rich Element-Mediated mRNA Decay. *The Journal of Immunology*, 174(2), 953-61. Available from <https://www.jimmunol.org/content/jimmunol/174/2/953.full.pdf> [Accessed 28 July 2020].

Ogilvie, R.L., Sternjohn, J.R., Rattenbacher, B., Vlasova, I.A., Williams, D.A., Hau, H.H., Blackshear, P.J. and Bohjanen, P.R. (2009). Tristetraprolin mediates interferon-gamma mRNA decay. *The Journal of Biological Chemistry*, 284 (17), 11216–23. Available from <https://doi.org/10.1074/jbc.M901229200> [Accessed 5 August 2020].

Okazaki, R., Okazaki, T., Sakabe, K., Sugimoto, K., Kainuma, R., Sugino, A. and Iwatsuki, N. (1968). In Vivo Mechanism of DNA Chain Growth. *Cold Spring Harbor Symposia on Quantitative Biology*, 33 (0), 129–143. Available from <https://doi.org/10.1101/SQB.1968.033.01.017> [Accessed 15 August 2020].

Ozeri-Galai, E., Lebofsky, R., Rahat, A., Bester, A.C., Bensimon, A. and Kerem, B. (2011). Failure of Origin Activation in Response to Fork Stalling Leads to Chromosomal Instability at Fragile Sites. *Molecular Cell*, 43 (1), 122–131. Available from <https://doi.org/10.1016/j.molcel.2011.05.019> [Accessed 19 August 2020].

Pabla, N., Huang, S., Mi, Q.-S., Daniel, R. and Dong, Z. (2008). ATR-Chk2 signaling in p53 activation and DNA damage response during cisplatin-induced apoptosis. *The Journal of Biological Chemistry*, 283 (10), 6572–83. Available from <https://doi.org/10.1074/jbc.M707568200> [Accessed 18 August 2020].

Pacek, M. and Walter, J.C. (2004). A requirement for MCM7 and Cdc45 in chromosome unwinding during eukaryotic DNA replication. *The EMBO Journal*, 23 (18), 3667–76. Available from <https://doi.org/10.1038/sj.emboj.7600369> [Accessed 16 August 2020].

Pandiri, I., Chen, Y., Joe, Y., Kim, H.J., Park, J., Chung, H.T. and Park, J.W. (2016). Tristetraprolin mediates the anti-proliferative effects of metformin in breast cancer cells. *Breast Cancer Research and Treatment*, 156 (1), 57–64. Available from <https://doi.org/10.1007/s10549-016-3742-y> [Accessed 4 September 2020].

Papadaki, O., Milatos, S., Grammenoudi, S., Mukherjee, N., Keene, J.D. and Kontoyiannis, D.L. (2009). Control of Thymic T Cell Maturation, Deletion and Egress by the RNA-Binding Protein HuR 1. *The Journal of Immunology*, 182, 6779–6788. Available from <https://doi.org/10.4049/jimmunol.0900377> [Accessed 16 July 2020].

Park, J.-M., Lee, T.-H. and Kang, H. (2018). Roles of Tristetraprolin in Tumorigenesis. *International Journal of Molecular Sciences*, 19 (11), 3384. Available from <https://doi.org/10.3390/ijms19113384> [Accessed 30 July 2020].

Park, S.B., Lee, J.H., Jeong, W.W., Kim, Y.H., Cha, H.J., Joe, Y., Chung, H.T., Cho, W.J., Do, J.W., Lee, B.J., Park, J.W. and Ko, B.K. (2015). TTP mediates cisplatin-induced apoptosis of head and neck cancer cells by down-regulating the expression of *Bcl-2*. *Journal of Chemotherapy*, 27 (3), 174–180. Available from <https://doi.org/10.1179/1973947814Y.0000000234> [Accessed 10 August 2020].

Paronetto, M.P., Miñana, B. and Valcárcel, J. (2011). The Ewing Sarcoma Protein Regulates DNA Damage-Induced Alternative Splicing. *Molecular Cell*, 43 (3), 353–368. Available from <https://doi.org/10.1016/J.MOLCEL.2011.05.035> [Accessed 23 August 2020].

Paulsen, R.D., Soni, D. V., Wollman, R., Hahn, A.T., Yee, M.-C., Guan, A., Hesley,

J.A., Miller, S.C., Cromwell, E.F., Solow-Cordero, D.E., Meyer, T. and Cimprich, K.A. (2009). A Genome-wide siRNA Screen Reveals Diverse Cellular Processes and Pathways that Mediate Genome Stability. *Molecular Cell*, 35 (2), 228–239. Available from <https://doi.org/10.1016/J.MOLCEL.2009.06.021> [Accessed 23 August 2020].

Pereira, B., Billaud, M. and Almeida, R. (2017). RNA-Binding Proteins in Cancer: Old Players and New Actors. *Trends in Cancer*, 3 (7), 506–528. Available from <https://doi.org/10.1016/j.trecan.2017.05.003> [Accessed 23 August 2020].

Phillips, R.S., Ramos, S.B. and Blackshear, P.J. (2002). Members of the Tristetraprolin Family of Tandem CCCH Zinc Finger Proteins Exhibit CRM1-dependent Nucleocytoplasmic Shuttling*. *The Journal of Biological Chemistry*, 277 (13), 11606–11613. Available from <https://doi.org/10.1074/jbc.M111457200> [Accessed 25 July 2020].

Pilch, B., Allemand, E., Facompré, M., Bailly, C., Riou, J.-F., Soret, J. and Tazi, J. (2001). Specific Inhibition of Serine-and Arginine-rich Splicing Factors Phosphorylation, Spliceosome Assembly, and Splicing by the Antitumor Drug NB-506 1. *Cancer Research*, 61(18), 6876-84. Available from <https://cancerres.aacrjournals.org/content/canres/61/18/6876.full.pdf> [Accessed 27 August 2020].

Piruat, J.I. and Aguilera, A.S. (1998). A novel yeast gene, THO2, is involved in RNA pol II transcription and provides new evidence for transcriptional elongation-associated recombination. *The EMBO Journal*, 17(16), 4859-72. Available from <https://www.ncbi.nlm.nih.gov/pmc/articles/PMC1170815/pdf/004859.pdf> [Accessed 27 August 2020].

Planel, S., Salomon, A., Jalinot, P., Feige, J.-J. and Cherradi, N. (2010). A novel concept in antiangiogenic and antitumoral therapy: multitarget destabilization of short-lived mRNAs by the zinc finger protein ZFP36L1. *Oncogene*, 29 (45), 5989–6003. Available from <https://doi.org/10.1038/onc.2010.341> [Accessed 10 August 2020].

Polo, S.E., Blackford, A.N., Chapman, J.R., Baskcomb, L., Gravel, S., Rusch, A., Thomas, A., Blundred, R., Smith, P., Kzhyshkowska, J., Dobner, T., Taylor, A.M.R., Turnell, A.S., Stewart, G.S., Grand, R.J. and Jackson, S.P. (2012). Regulation of DNA-

end resection by hnRNPU-like proteins promotes DNA double-strand break signaling and repair. *Molecular Cell*, 45 (4), 505–16. Available from <https://doi.org/10.1016/j.molcel.2011.12.035> [Accessed 24 August 2020].

Pospisilova, H., Baens, M., Michaux, L., Stul, M., Van Hummelen, P., Van Loo, P., Vermeesch, J., Jarosova, M., Zemanova, Z., Michalova, K., Van den Berghe, I., Alexander, H.D., Hagemeyer, A., Vandenberghe, P., Cools, J., De Wolf-Peeters, C., Marynen, P. and Wlodarska, I. (2007). Interstitial del(14)(q) involving IGH: a novel recurrent aberration in B-NHL. *Leukemia*, 21 (9), 2079–2083. Available from <https://doi.org/10.1038/sj.leu.2404739> [Accessed 21 July 2020].

Povirk, L.F., Zhou, T., Zhou, R., Cowan, M.J. and Yannone, S.M. (2007). Processing of 3'-phosphoglycolate-terminated DNA double strand breaks by Artemis nuclease. *The Journal of Biological Chemistry*, 282 (6), 3547–58. Available from <https://doi.org/10.1074/jbc.M607745200> [Accessed 21 August 2020].

Priestley, P., Baber, J., Lolkema, M.P., Steeghs, N., de Bruijn, E., Shale, C., Duyvesteyn, K., Haidari, S., van Hoeck, A., Onstenk, W., Roepman, P., Voda, M., Bloemendal, H.J., Tjan-Heijnen, V.C.G., van Herpen, C.M.L., Labots, M., Witteveen, P.O., Smit, E.F., Sleijfer, S., Voest, E.E. and Cuppen, E. (2019). Pan-cancer whole-genome analyses of metastatic solid tumours. *Nature*, 575 (7781), 210–216. Available from <https://doi.org/10.1038/s41586-019-1689-y> [Accessed 14 August 2020].

Protter, D.S.W. and Parker, R. (2016). Principles and Properties of Stress Granules. *Trends in Cell Biology*, 26 (9), 668–679. Available from <https://doi.org/10.1016/j.tcb.2016.05.004> [Accessed 26 July 2020].

Pursell, Z.F., Isoz, I., Lundström, E.-B., Johansson, E. and Kunkel, T.A. (2007). Yeast DNA polymerase epsilon participates in leading-strand DNA replication. *Science*, 317 (5834), 127–30. Available from <https://doi.org/10.1126/science.1144067> [Accessed 15 August 2020].

Q, M. and HR, H. (1991). A corrected sequence for the predicted protein from the mitogen-inducible TIS11 primary response gene. *Oncogene*, 6 (7), 1277–1278. Available from <https://europepmc.org/article/med/1861870> [Accessed 20 July 2020].

Q, M. and HR, H. (1995). The yeast homologue YTIS11, of the mammalian TIS11 gene family is a non-essential, glucose repressible gene. *Oncogene*, 10 (3), 487–494. Available from <https://europepmc.org/article/med/7845673> [Accessed 19 July 2020].

Q, M., D, W., T, C. and H, H. (1994). The Drosophila TIS11 homologue encodes a developmentally controlled gene. *Oncogene*, 9 (11), 3329–3334. Available from <https://europepmc.org/article/med/7936658> [Accessed 19 July 2020].

Qian, X., Chen, H., Wu, X., Hu, L., Huang, Q. and Jin, Y. (2017). Interleukin-17 acts as double-edged sword in anti-tumor immunity and tumorigenesis. *Cytokine*, 89, 34–44. Available from <https://doi.org/10.1016/J.CYTO.2015.09.011> [Accessed 9 August 2020].

Ran, F.A., Hsu, P.D., Wright, J., Agarwala, V., Scott, D.A. and Zhang, F. (2013). Genome engineering using the CRISPR-Cas9 system. 8 (11), 2281–2308. Available from <https://doi.org/10.1038/nprot.2013.143> [Accessed 12 April 2020].

Rataj, F., Planel, S., Denis, J., Roelants, C., Filhol, O., Guyon, L., Feige, J.-J. and Cherradi, N. (2019). Targeting AU-rich element-mediated mRNA decay with a truncated active form of the zinc-finger protein TIS11b/BRF1 impairs major hallmarks of mammary tumorigenesis. *Oncogene*, 38 (26), 5174–5190. Available from <https://doi.org/10.1038/s41388-019-0784-8> [Accessed 11 August 2020].

Ratner, H.K., Sampson, T.R. and Weiss, D.S. (2016). Overview of CRISPR-Cas9 Biology. *Cold Spring Harbor protocols*, 2016 (12), pdb.top088849. Available from <https://doi.org/10.1101/pdb.top088849> [Accessed 11 September 2020].

Ray, D., Kazan, H., Chan, E.T., Castillo, L.P., Chaudhry, S., Talukder, S., Blencowe, B.J., Morris, Q. and Hughes, T.R. (2009). Rapid and systematic analysis of the RNA recognition specificities of RNA-binding proteins. *Nature Biotechnology*, 27 (7), 667–670. Available from <https://doi.org/10.1038/nbt.1550> [Accessed 10 July 2020].

Ray, D., Kazan, H., Cook, K.B., Weirauch, M.T., Najafabadi, H.S., Li, X., Gueroussov, S., Abu, M., Zheng, H., Yang, A., Na, H., Irimia, M., Matzat, L.H., Dale, R.K., Smith, S.A., Yarosh, C.A., Kelly, S.M., Nabet, B., Mecnas, D., Li, W., Laishram, R.S., Qiao, M., Lipshitz, H.D., Piano, F., Corbett, A.H., Carstens, R.P., Frey, B.J., Anderson, R.A.,

Lynch, K.W., Penalva, L.O.F., Lei, E.P., Fraser, A.G., Blencowe, B.J., Morris, Q.D. and Hughes, T.R. (2013). A compendium of RNA-binding motifs for decoding gene regulation. *Nature*, 499 (7457), 172–7. Available from <https://doi.org/10.1038/nature12311> [Accessed 13 July 2020].

Redon, C., Pilch, D., Rogakou, E., Sedelnikova, O., Newrock, K. and Bonner, W. (2002). Histone H2A variants H2AX and H2AZ. *Current Opinion in Genetics & Development*, 12 (2), 162–9. Available from [https://doi.org/10.1016/s0959-437x\(02\)00282-4](https://doi.org/10.1016/s0959-437x(02)00282-4) [Accessed 25 September 2020].

Ritchie, K.J., Walsh, S., Sansom, O.J., Henderson, C.J. and Wolf, C.R. (2009). Markedly enhanced colon tumorigenesis in Apc(Min) mice lacking glutathione S-transferase Pi. *Proceedings of the National Academy of Sciences of the United States of America*, 106 (49), 20859–64. Available from <https://doi.org/10.1073/pnas.0911351106> [Accessed 14 August 2020].

Rodgers, K. and McVey, M. (2016). Error-Prone Repair of DNA Double-Strand Breaks. *Journal of Cellular Physiology*, 231 (1), 15–24. Available from <https://doi.org/10.1002/jcp.25053> [Accessed 19 August 2020].

Rodríguez-Rodríguez, D.R., Ramírez-Solís, R., Garza-Elizondo, M.A., Garza-Rodríguez, M.D.L. and Barrera-Saldaña, H.A. (2019). Genome editing: A perspective on the application of CRISPR/Cas9 to study human diseases (Review). *International Journal of Molecular Medicine*, 43 (4), 1559. Available from <https://doi.org/10.3892/IJMM.2019.4112> [Accessed 16 September 2020].

Rogakou, E.P., Pilch, D.R., Orr, A.H., Ivanova, V.S. and Bonner, W.M. (1998). DNA double-stranded breaks induce histone H2AX phosphorylation on serine 139. *The Journal of Biological Chemistry*, 273 (10), 5858–68. Available from <https://doi.org/10.1074/jbc.273.10.5858> [Accessed 18 August 2020].

Rothkamm, K. and Löbrich, M. (2003). Evidence for a lack of DNA double-strand break repair in human cells exposed to very low x-ray doses. *Proceedings of the National Academy of Sciences of the United States of America*, 100 (9), 5057–62. Available from <https://doi.org/10.1073/pnas.0830918100> [Accessed 28 September 2020].

Rounbehler, R.J., Fallahi, M., Yang, C., Steeves, M.A., Li, W., Doherty, J.R., Schaub, F.X., Sanduja, S., Dixon, D.A., Blackshear, P.J. and Cleveland, J.L. (2012). Tristetraprolin impairs myc-induced lymphoma and abolishes the malignant state. *Cell*, 150 (3), 563–74. Available from <https://doi.org/10.1016/j.cell.2012.06.033> [Accessed 30 July 2020].

Rudolph, K.L., Millard, M., Bosenberg, M.W. and DePinho, R.A. (2001). Telomere dysfunction and evolution of intestinal carcinoma in mice and humans. *Nature Genetics*, 28 (2), 155–9. Available from <https://doi.org/10.1038/88871> [Accessed 14 August 2020].

Ruff, P., Donnianni, R.A., Glancy, E. and Oh, J. (2016). RPA Stabilization of Single-Stranded DNA Is Critical for Break-Induced Replication. *Cell Rep.*, 17(12), 3359-68. Available from <https://doi.org/10.1016/j.celrep.2016.12.003> [Accessed 18 October 2020].

Rulten, S.L., Rotheray, A., Green, R.L., Grundy, G.J., Moore, D.A.Q., Gómez-Herreros, F., Hafezparast, M. and Caldecott, K.W. (2014). PARP-1 dependent recruitment of the amyotrophic lateral sclerosis-associated protein FUS/TLS to sites of oxidative DNA damage. *Nucleic Acids Research*, 42 (1), 307–14. Available from <https://doi.org/10.1093/nar/gkt835> [Accessed 24 August 2020].

Saini, Y., Chen, J. and Patial, S. (2020). The Tristetraprolin Family of RNA-Binding Proteins in Cancer : Progress and Future Prospects. *Cancers*, 12(6), 1539. Available from doi: 10.3390/cancers12061539 [Accessed 25 August 2020].

Sakashita, E. and Endo, H. (2010). SR and SR-related proteins redistribute to segregated fibrillar components of nucleoli in a response to DNA damage. *Nucleus*, 1 (4), 367–380. Available from <https://doi.org/10.4161/nucl.1.4.12683> [Accessed 25 August 2020].

Saldivar, J.C., Cortez, D. and Cimprich, K.A. (2017). The essential kinase ATR: ensuring faithful duplication of a challenging genome. *Nature reviews. Molecular Cell Biology*, 18 (10), 622–636. Available from <https://doi.org/10.1038/nrm.2017.67> [Accessed 17 August 2020].

Sanduja, S., Blanco, F.F., Young, L.E., Kaza, V. and Dixon, D.A. (2012). The role of tristetraprolin in cancer and inflammation. *Frontiers in Bioscience (Landmark edition)*, 17, 174–88. Available from <https://doi.org/10.2741/3920> [Accessed 26 July 2020].

Sansregret, L., Vanhaesebroeck, B. and Swanton, C. (2018). Determinants and clinical implications of chromosomal instability in cancer. *Nature Reviews Clinical Oncology*, 15 (3), 139–150. Available from <https://doi.org/10.1038/nrclinonc.2017.198> [Accessed 19 September 2020].

Santos-Pereira, J.M. and Aguilera, A. (2015). R loops: New modulators of genome dynamics and function. *Nature Reviews Genetics*, 16 (10), 583–597. Available from <https://doi.org/10.1038/nrg3961> [Accessed 22 August 2020].

Santos-Pereira, J.M., Herrero, A.B., García-Rubio, M.L., Marín, A., Moreno, S. and Aguilera, A. (2013). The Npl3 hnRNP prevents R-loop-mediated transcription-replication conflicts and genome instability. *Genes & Development*, 27 (22), 2445–58. Available from <https://doi.org/10.1101/gad.229880.113> [Accessed 27 August 2020].

Sartori, A.A., Lukas, C., Coates, J., Mistrik, M., Fu, S., Bartek, J., Baer, R., Lukas, J. and Jackson, S.P. (2007). Human CtIP promotes DNA end resection. *Nature*, 450 (7169), 509–14. Available from <https://doi.org/10.1038/nature06337> [Accessed 21 August 2020].

Saunus, J.M., French, J.D., Edwards, S.L., Beveridge, D.J., Hatchell, E.C., Wagner, S.A., Stein, S.R., Davidson, A., Simpson, K.J., Francis, G.D., Leedman, P.J. and Brown, M.A. (2008). Posttranscriptional Regulation of the Breast Cancer Susceptibility Gene BRCA1 by the RNA Binding Protein HuR. *Cancer Res*, 68 (22), 9469–78. Available from <https://doi.org/10.1158/0008-5472.CAN-08-1159> [Accessed 23 August 2020].

Sawaoka, H., Dixon, D.A., Oates, J.A. and Boutaud, O. (2003). Tristetraprolin binds to the 3'-untranslated region of cyclooxygenase-2 mRNA. A polyadenylation variant in a cancer cell line lacks the binding site. *The Journal of Biological Chemistry*, 278 (16), 13928–35. Available from <https://doi.org/10.1074/jbc.M300016200> [Accessed 30 July 2020].

Schichl, Y.M., Resch, U., Hofer-Warbinek, R. and de Martin, R. (2009). Tristetraprolin impairs NF-kappaB/p65 nuclear translocation. *The Journal of Biological Chemistry*, 284 (43), 29571–81. Available from <https://doi.org/10.1074/jbc.M109.031237> [Accessed 8 September 2020].

Schmidlin, M., Lu, M., Leuenberger, S.A., Stoecklin, G., Mallaun, M., Gross, B., Gherzi, R., Hess, D., Hemmings, B.A. and Moroni, C. (2004). The ARE-dependent mRNA-destabilizing activity of BRF1 is regulated by protein kinase B. *The EMBO Journal*, 23 (24), 4760–9. Available from <https://doi.org/10.1038/sj.emboj.7600477> [Accessed 24 July 2020].

Scott, S.P. and Pandita, T.K. (2006). The cellular control of DNA double-strand breaks. *Journal of Cellular Biochemistry*, 99 (6), 1463–75. Available from <https://doi.org/10.1002/jcb.21067> [Accessed 17 August 2020].

Selmi, T., Martello, A., Vignudelli, T., Ferrari, E., Grande, A., Gemelli, C., Salomoni, P., Ferrari, S. and Zanocco-Marani, T. (2012). ZFP36 expression impairs glioblastoma cell lines viability and invasiveness by targeting multiple signal transduction pathways. *Cell Cycle*, 11 (10), 1977–87. Available from <https://doi.org/10.4161/cc.20309> [Accessed 4 September 2020].

Shalem, O., Sanjana, N.E., Hartenian, E., Shi, X., Scott, D.A., Mikkelsen, T., Heckl, D., Ebert, B.L., Root, D.E., Doench, J.G. and Zhang, F. (2014). Genome-scale CRISPR-Cas9 knockout screening in human cells. *Science*, 343 (6166), 84–87. Available from <https://doi.org/10.1126/science.1247005> [Accessed 11 September 2020].

Shen, S.S. and Ro, J.Y. (2006). DNA damage response: An important anticancer barrier in early human tumorigenesis. *Advances in Anatomic Pathology*, 13 (4), 199. Available from <https://doi.org/10.1097/00125480-200607000-00010> [Accessed 11 July 2020].

Shen, Z., Chakraborty, A., Jain, A., Giri, S., Ha, T., Prasanth, K. V and Prasanth, S.G. (2012). Dynamic association of ORCA with prereplicative complex components regulates DNA replication initiation. *Molecular and Cellular Biology*, 32 (15), 3107–20. Available from <https://doi.org/10.1128/MCB.00362-12> [Accessed 15 August 2020].

Sheu, Y.-J. and Stillman, B. (2006). Cdc7-Dbf4 Phosphorylates MCM Proteins via a Docking Site-Mediated Mechanism to Promote S Phase Progression. *Molecular Cell*, 24 (1), 101–113. Available from <https://doi.org/10.1016/J.MOLCEL.2006.07.033> [Accessed 15 August 2020].

Sheu, Y.-J. and Stillman, B. (2010). The Dbf4–Cdc7 kinase promotes S phase by alleviating an inhibitory activity in Mcm4. *Nature*, 463 (7277), 113–117. Available from <https://doi.org/10.1038/nature08647> [Accessed 15 August 2020].

Shin, K.-H., Kim, Reuben H, Kang, M.K., Kim, Roy H, Kim, S.G., Lim, P.K., Yochim, J.M., Baluda, M.A. and Park, N.-H. (2007). p53 promotes the fidelity of DNA end-joining activity by, in part, enhancing the expression of heterogeneous nuclear ribonucleoprotein G. *DNA repair*, 6 (6), 830–40. Available from <https://doi.org/10.1016/j.dnarep.2007.01.013> [Accessed 23 August 2020].

Skourti-Stathaki, K., Proudfoot, N.J. and Gromak, N. (2011). Human senataxin resolves RNA/DNA hybrids formed at transcriptional pause sites to promote Xrn2-dependent termination. *Molecular Cell*, 42 (6), 794–805. Available from <https://doi.org/10.1016/j.molcel.2011.04.026> [Accessed 27 August 2020].

Smith, D.I., Zhu, Y., McAvoy, S. and Kuhn, R. (2006). Common fragile sites, extremely large genes, neural development and cancer. *Cancer Letters*, 232 (1), 48–57. Available from <https://doi.org/10.1016/j.canlet.2005.06.049> [Accessed 13 September 2020].

Sollier, J., Stork, C.T., García-Rubio, M.L., Paulsen, R.D., Aguilera, A. and Cimprich, K.A. (2014). Transcription-coupled nucleotide excision repair factors promote R-loop-induced genome instability. *Molecular Cell*, 56 (6), 777–85. Available from <https://doi.org/10.1016/j.molcel.2014.10.020> [Accessed 27 August 2020].

Son, Y.-O., Kim, H.-E., Choi, W.-S., Chun, C.-H. and Chun, J.-S. (2019). RNA-binding protein ZFP36L1 regulates osteoarthritis by modulating members of the heat shock protein 70 family. *Nature Communications*, 10 (1), 77. Available from <https://doi.org/10.1038/s41467-018-08035-7> [Accessed 23 July 2020].

Soniat, M.M., Myler, L.R., Kuo, H.C., Paull, T.T. and Finkelstein, I.J. (2019). RPA

Phosphorylation Inhibits DNA Resection. *Molecular Cell*, 75 (1), 145-153.e5. Available from <https://doi.org/10.1016/j.molcel.2019.05.005> [Accessed 12 August 2020].

Sternberg, S.H. and Doudna, J.A. (2015). Expanding the Biologist's Toolkit with CRISPR-Cas9. *Molecular Cell*, 58 (4), 568–574. Available from <https://doi.org/10.1016/j.molcel.2015.02.032> [Accessed 2 June 2020].

Stewart, G.S., Panier, S., Townsend, K., Al-Hakim, A.K., Kolas, N.K., Miller, E.S., Nakada, S., Ylanko, J., Olivarius, S., Mendez, M., Oldreive, C., Wildenhain, J., Tagliaferro, A., Pelletier, L., Taubenheim, N., Durandy, A., Byrd, P.J., Stankovic, T., Taylor, A.M.R. and Durocher, D. (2009). The RIDDLE Syndrome Protein Mediates a Ubiquitin-Dependent Signaling Cascade at Sites of DNA Damage. *Cell*, 136 (3), 420–434. Available from <https://doi.org/10.1016/J.CELL.2008.12.042> [Accessed 18 August 2020].

Stoecklin, G., Ming, X.-F., Looser, R. and Moroni, C. (2000). Somatic mRNA Turnover Mutants Implicate Tristetraprolin in the Interleukin-3 mRNA Degradation Pathway. *Molecular Cell Biology*, 20(11), 3753-63. Available from <https://www.ncbi.nlm.nih.gov/pmc/articles/PMC85689/pdf/mb003753.pdf> [Accessed 28 July 2020].

Stoecklin, G., Stoeckle, P., Lu, M., Muehlemann, O. and Moroni, C. (2001). Cellular mutants define a common mRNA degradation pathway targeting cytokine AU-rich elements. *RNA*, 7 (11), 1578–1588. Available from DOI: 10.1017.S1355838201011074 [Accessed 9 July 2020].

Stoecklin, G., Gross, B., Ming, X.F. and Moroni, C. (2003). A novel mechanism of tumor suppression by destabilizing AU-rich growth factor mRNA. *Oncogene*, 22 (23), 3554–3561. Available from <https://doi.org/10.1038/sj.onc.1206418> [Accessed 8 July 2020].

Stoecklin, G., Stubbs, T., Kedersha, N., Wax, S., Rigby, W.F., Blackwell, T.K. and Anderson, P. (2004). MK2-induced tristetraprolin:14-3-3 complexes prevent stress granule association and ARE-mRNA decay. *The EMBO Journal*, 23, 1313–1324. Available from <https://doi.org/10.1038/sj.emboj.7600163> [Accessed 24 July 2020].

Stoecklin, G., Tenenbaum, S.A., Mayo, T., Chittur, S. V, George, A.D., Baroni, T.E., Blackshear, P.J. and Anderson, P. (2008). Genome-wide Analysis Identifies Interleukin-10 mRNA as Target of Tristetraprolin. *The Journal of Biological Chemistry*, 283(17), 1189-99. Available from <https://doi.org/10.1074/jbc.M709657200> [Accessed 28 July 2020].

Strässer, K., Masuda, S., Mason, P., Pfannstiel, J., Oppizzi, M., Rodriguez-Navarro, S., Rondón, A.G., Aguilera, A., Struhl, K., Reed, R. and Hurt, E. (2002). TREX is a conserved complex coupling transcription with messenger RNA export. *Nature*, 417 (6886), 304–8. Available from <https://doi.org/10.1038/nature746> [Accessed 27 August 2020].

Stucki, M., Clapperton, J.A., Mohammad, D., Yaffe, M.B., Smerdon, S.J. and Jackson, S.P. (2005). MDC1 directly binds phosphorylated histone H2AX to regulate cellular responses to DNA double-strand breaks. *Cell*, 123 (7), 1213–1226. Available from <https://doi.org/10.1016/j.cell.2005.09.038> [Accessed 29 July 2020].

Stumpo, D.J., Byrd, N.A., Phillips, R.S., Ghosh, S., Maronpot, R.R., Castranio, T., Meyers, E.N., Mishina, Y. and Blackshear, P.J. (2004). Chorioallantoic fusion defects and embryonic lethality resulting from disruption of Zfp36L1, a gene encoding a CCCH tandem zinc finger protein of the Tristetraprolin family. *Molecular and Cellular Biology*, 24 (14), 6445–55. Available from <https://doi.org/10.1128/MCB.24.14.6445-6455.2004> [Accessed 5 August 2020].

Stumpo, D.J., Broxmeyer, H.E., Ward, T., Cooper, S., Hangoc, G., Chung, Y.J., Shelley, W.C., Richfield, E.K., Ray, M.K., Yoder, M.C., Aplan, P.D. and Blackshear, P.J. (2009). Targeted disruption of Zfp36l2, encoding a CCCH tandem zinc finger RNA-binding protein, results in defective hematopoiesis. *Blood*, 114 (12), 2401–2410. Available from <https://doi.org/10.1182/blood-2009-04-214619> [Accessed 5 August 2020].

Suk, F.-M., Chang, C.-C., Lin, R.-J., Lin, S.-Y., Liu, S.-C., Jau, C.-F. and Liang, Y.-C. (2018). ZFP36L1 and ZFP36L2 inhibit cell proliferation in a cyclin D-dependent and p53-independent manner. *Scientific Reports*, 8 (1), 2742. Available from <https://doi.org/10.1038/s41598-018-21160-z> [Accessed 28 June 2020].

Sun, L., Stoecklin, G., Van Way, S., Hinkovska-Galcheva, V., Guo, R.-F., Anderson, P. and Shanley, T.P. (2007). Tristetraprolin (TTP)-14-3-3 complex formation protects TTP from dephosphorylation by protein phosphatase 2a and stabilizes tumor necrosis factor- α mRNA. *The Journal of Biological Chemistry*, 282 (6), 3766–77. Available from <https://doi.org/10.1074/jbc.M607347200> [Accessed 3 September 2020].

Sung, P. and Robberson, D.L. (1995). DNA Strand Exchange Mediated by a RAD51-ssDNA Nucleoprotein Filament with Polarity Opposite to That of RecA. *Cell*, 82(3), 453-61. Available from [https://www.cell.com/cell/pdf/0092-8674\(95\)90434-4.pdf?_returnURL=https%3A%2F%2Flinkinghub.elsevier.com%2Fretrieve%2Fpii%2F0092867495904344%3Fshowall%3Dtrue](https://www.cell.com/cell/pdf/0092-8674(95)90434-4.pdf?_returnURL=https%3A%2F%2Flinkinghub.elsevier.com%2Fretrieve%2Fpii%2F0092867495904344%3Fshowall%3Dtrue) [Accessed 21 August 2020].

Sutherland, G.R., Baker, E. and Richards, R.I. (1998). Fragile sites still breaking. *Trends in Genetics*, 14 (12), 501–506. Available from [https://doi.org/10.1016/S0168-9525\(98\)01628-X](https://doi.org/10.1016/S0168-9525(98)01628-X) [Accessed 5 January 2021].

Tarsounas, M., Davies, A.A. and West, S.C. (2004). RAD51 localization and activation following DNA damage. *Philosophical transactions of the Royal Society of London. Series B, Biological sciences*, 359 (1441), 87–93. Available from <https://doi.org/10.1098/rstb.2003.1368> [Accessed 21 August 2020].

Taylor, G.A., Thompson, M.J., Lai, W.S. and Blackshear, P.J. (1995). Phosphorylation of Tristetraprolin, a Potential Zinc Finger Transcription Factor, by Mitogen Stimulation in Intact Cells and by Mitogen-activated Protein Kinase *in Vitro*. *Journal of Biological Chemistry*, 270 (22), 13341–13347. Available from <https://doi.org/10.1074/jbc.270.22.13341> [Accessed 25 July 2020].

Taylor, G.A., Carballo, E., Lee, D.M., Lai, W.S., Thompson, M.J., Patel, D.D., Schenkman, D.I., Gilkeson, G.S., Broxmeyer, H.E., Haynes, B.F. and Blackshear, P.J. (1996). A pathogenetic role for TNF α in the syndrome of cachexia, arthritis, and autoimmunity resulting from tristetraprolin (TTP) deficiency. *Immunity*, 4 (5), 445–454. Available from [https://doi.org/10.1016/S1074-7613\(00\)80411-2](https://doi.org/10.1016/S1074-7613(00)80411-2) [Accessed 27 June 2020].

Taylor, G.A., Thompson, M.J., Lai, W.S. and Blackshear, P.J. (1996). Mitogens stimulate the rapid nuclear to cytosolic translocation of tristetraprolin, a potential zinc-

finger transcription factor. *Molecular Endocrinology*, 10 (2), 140–146. Available from <https://doi.org/10.1210/mend.10.2.8825554> [Accessed 25 July 2020].

Terradas, M., Martín, M., Tusell, L. and Genescà, A. (2009). DNA lesions sequestered in micronuclei induce a local defective-damage response. *DNA Repair*, 8 (10), 1225–1234. Available from <https://doi.org/10.1016/j.dnarep.2009.07.004> [Accessed 4 May 2020].

Thomas, M., White, R.L. and Davis, R.W. (1976). Hybridization of RNA to double-stranded DNA: Formation of R-loops (gene isolation/gene mapping/electron microscopy/restriction endonucleases). *PNAS*, 73(7), 2294-8. Available from <https://www.ncbi.nlm.nih.gov/pmc/articles/PMC430535/pdf/pnas00037-0133.pdf> [Accessed 27 August 2020].

Tiwari, A., Jones, O.A. and Chan, K.-L. (2018). 53BP1 can limit sister-chromatid rupture and rearrangements driven by a distinct ultrafine DNA bridging-breakage process. *Nature Communications*, 9(1), 677. Available from <https://doi.org/10.1038/s41467-018-03098-y> [Accessed 14 May 2020].

Tomasetti, C. and Vogelstein, B. (2015). Cancer etiology. Variation in cancer risk among tissues can be explained by the number of stem cell divisions. *Science*, 347 (6217), 78–81. Available from <https://doi.org/10.1126/science.1260825> [Accessed 12 August 2020].

Trenz, K., Smith, E., Smith, S. and Costanzo, V. (2006). ATM and ATR promote Mre11 dependent restart of collapsed replication forks and prevent accumulation of DNA breaks. *The EMBO Journal*, 25 (8), 1764–74. Available from <https://doi.org/10.1038/sj.emboj.7601045> [Accessed 16 August 2020].

Tudor, C., Marchese, F.P., Hitti, E., Aubareda, A., Rawlinson, L., Gaestel, M., Blackshear, P.J., Clark, A.R., Saklatvala, J. and Dean, J.L.E. (2009). The p38 MAPK pathway inhibits tristetraproline-directed decay of interleukin-10 and pro-inflammatory mediator mRNAs in murine macrophages. *FEBS Letters*, 583 (12), 1933–1938. Available from <https://doi.org/10.1016/j.febslet.2009.04.039> [Accessed 28 July 2020].

Tuduri, S., Crabbé, L., Conti, C., Tourrière, H., Holtgreve-Grez, H., Jauch, A.,

Pantesco, V., De Vos, J., Thomas, A., Theillet, C., Pommier, Y., Tazi, J., Coquelle, A. and Pasero, P. (2009). Topoisomerase I suppresses genomic instability by preventing interference between replication and transcription. *Nature Cell Biology*, 11 (11), 1315–24. Available from <https://doi.org/10.1038/ncb1984> [Accessed 27 August 2020].

Turner, M. and Hodson, D. (2012). Regulation of lymphocyte development and function by RNA-binding proteins. *Current Opinion in Immunology*, 24 (2), 160–165. Available from <https://doi.org/10.1016/j.coi.2012.01.011> [Accessed 21 July 2020].

Twyffels, L., Wauquier, C., Soin, R., Decaestecker, C., Gueydan, C. and Kruys, V. (2013). A Masked PY-NLS in Drosophila TIS11 and Its Mammalian Homolog Tristetraprolin. *PLoS ONE*, 8 (8), e71686. Available from <https://doi.org/10.1371/journal.pone.0071686> [Accessed 29 July 2020].

Uematsu, N., Weterings, E., Yano, K., Morotomi-Yano, K., Jakob, B., Taucher-Scholz, G., Mari, P.-O., van Gent, D.C., Chen, B.P.C. and Chen, D.J. (2007). Autophosphorylation of DNA-PKCS regulates its dynamics at DNA double-strand breaks. *The Journal of Cell Biology*, 177 (2), 219–29. Available from <https://doi.org/10.1083/jcb.200608077> [Accessed 21 August 2020].

Upadhyay, R., Sanduja, S., Kaza, V. and Dixon, D.A. (2013). Genetic Polymorphisms in RNA Binding Proteins Contribute to Breast Cancer Survival. *International Journal of Cancer*, 132 (3), E128-38. Available from <https://doi.org/10.1002/ijc.27789> [Accessed 21 July 2020].

Uziel, T., Lerenthal, Y., Moyal, L., Andegeko, Y., Mittelman, L. and Shiloh, Y. (2003). Requirement of the MRN complex for ATM activation by DNA damage. *The EMBO Journal*, 22 (20), 5612–21. Available from <https://doi.org/10.1093/emboj/cdg541> [Accessed 18 August 2020].

Van Nostrand, E.L., Freese, P., Pratt, G.A., Wang, X., Wei, X., Xiao, R., Blue, S.M., Dominguez, D., Cody, N.A.L., Olson, S., Sundararaman, B., Zhan, L., Bazile, C., Philip, L., Bouvrette, B., Chen, J., Duff, M.O., Garcia, K.E., Gelboin-Burkhart, C., Hochman, A., Lambert, N.J., Li, H., Nguyen, T.B., Palden, T., Rabano, I., Sathe, S., Stanton, R., Bergalet, J., Zhou, B., Su, A., Wang, R., Yee, B.A., Louie, A.L., Aigner, S., Fu, X.-D., Lecuyer, E., Burge, C.B., Graveley, B.R. and Yeo, G.W. (2017). A Large-

Scale Binding and Functional Map of Human RNA Binding Proteins. *Nature*, 583 (7818), 711-719. Available from <https://doi.org/10.1101/179648> [Accessed 16 July 2020].

Van Tubergen, E.A., Banerjee, R., Liu, M., Vander Broek, R., Light, E., Kuo, S., Feinberg, S.E., Willis, A.L., Wolf, G., Carey, T., Bradford, C., Prince, M., Worden, F.P., Kirkwood, K.L. and D'Silva, N.J. (2013). Inactivation or loss of TTP promotes invasion in head and neck cancer via transcript stabilization and secretion of MMP9, MMP2, and IL-6. *Clinical Cancer Research : an official journal of the American Association for Cancer Research*, 19 (5), 1169–79. Available from <https://doi.org/10.1158/1078-0432.CCR-12-2927> [Accessed 11 August 2020].

Varga, T. and Aplan, P.D. (2005). Chromosomal aberrations induced by double strand DNA breaks. *DNA Repair*, 4 (9), 1038. Available from <https://doi.org/10.1016/J.DNAREP.2005.05.004> [Accessed 23 December 2020].

Varnum, B.C., Ma, Q., Chi, T., Fletcher, B. and Herschmanl, H.R. (1991). The TISli Primary Response Gene Is a Member of a Gene Family That Encodes Proteins with a Highly Conserved Sequence Containing an Unusual Cys-His Repeat. *Molecular Cell Biology*, 11(3), 1754-8. Available from <https://www.ncbi.nlm.nih.gov/pmc/articles/PMC369492/pdf/molcellb00166-0580.pdf> [Accessed 20 July 2020].

Vassin, V.M., Anantha, R.W., Sokolova, E., Kanner, S. and Borowiec, J.A. (2009). Human RPA phosphorylation by ATR stimulates DNA synthesis and prevents ssDNA accumulation during DNA-replication stress. *Journal of Cell Science*, 122 (22), 4070–4080. Available from <https://doi.org/10.1242/jcs.053702> [Accessed 11 August 2020].

Vesela, E., Chroma, K., Turi, Z. and Mistrik, M. (2017). Common chemical inductors of replication stress: Focus on cell-based studies. *Biomolecules*, 7 (1). Available from <https://doi.org/10.3390/biom7010019> [Accessed 13 July 2020].

Vignudelli, T., Selmi, T., Martello, A., Parenti, S., Grande, A., Gemelli, C., Zanocco-Marani, T. and Ferrari, S. (2010). ZFP36L1 negatively regulates erythroid differentiation of CD34+ hematopoietic stem cells by interfering with the Stat5b pathway. *Molecular Biology of the Cell*, 21 (19), 3340–51. Available from

<https://doi.org/10.1091/mbc.E10-01-0040> [Accessed 22 July 2020].

Vilas, C.K., Emery, L.E., Denchi, E.L. and Miller, K.M. (2018). Caught with One's Zinc Fingers in the Genome Integrity Cookie Jar. *Trends in Genetics*, 34 (4), 313–325. Available from <https://doi.org/10.1016/j.tig.2017.12.011> [Accessed 1 September 2020].

Vogel, K.U., Bell, L.S., Galloway, A., Ahlfors, H. and Turner, M. (2016). The RNA-Binding Proteins Zfp36l1 and Zfp36l2 Enforce the Thymic β -Selection Checkpoint by Limiting DNA Damage Response Signaling and Cell Cycle Progression. *The Journal of Immunology*, 197 (7), 2673–2685. Available from <https://doi.org/10.4049/jimmunol.1600854> [Accessed 11 September 2020].

Wang, H., Ding, N., Guo, J., Xia, J. and Ruan, Y. (2016). Dysregulation of TTP and HuR plays an important role in cancers. *Tumor Biology*, 37 (11), 14451–14461. Available from <https://doi.org/10.1007/s13277-016-5397-z> [Accessed 8 August 2020].

Wang, T., Wei, J.J., Sabatini, D.M. and Lander, E.S. (2014). Genetic screens in human cells using the CRISPR-Cas9 system. *Science*, 343 (6166), 80–4. Available from <https://doi.org/10.1126/science.1246981> [Accessed 11 September 2020].

Wang, W., Furneaux, H., Cheng, H., Caldwell, M.C., Hutter, D., Liu, Y., Holbrook, N. and Gorospe, M. (2000). HuR regulates p21 mRNA stabilization by UV light. *Molecular and Cellular Biology*, 20 (3), 760–9. Available from <https://doi.org/10.1128/mcb.20.3.760-769.2000> [Accessed 23 August 2020].

Wei, Z.-R., Liang, C., Feng, D., Cheng, Y.-J., Wang, W.-M., Yang, D.-J., Wang, Y.-X. and Cai, Q.-P. (2016). Low tristetraprolin expression promotes cell proliferation and predicts poor patients outcome in pancreatic cancer. *Oncotarget*, 7 (14), 17737–50. Available from <https://doi.org/10.18632/oncotarget.7397> [Accessed 4 September 2020].

Wilhelm, T., Olziersky, A.-M., Harry, D., De Sousa, F., Vassal, H., Eskat, A. and Meraldi, P. (2019). Mild replication stress causes chromosome mis-segregation via premature centriole disengagement. *Nature Communications*, 10 (1), 3585. Available from <https://doi.org/10.1038/s41467-019-11584-0> [Accessed 30 April 2020].

Wood, A.J., Lo, T.-W., Zeitler, B., Pickle, C.S., Ralston, E.J., Lee, A.H., Amora, R., Miller, J.C., Leung, E., Meng, X., Zhang, L., Rebar, E.J., Gregory, P.D., Urnov, F.D. and Meyer, B.J. (2011). Targeted genome editing across species using ZFNs and TALENs. *Science*, 333 (6040), 307. Available from <https://doi.org/10.1126/science.1207773> [Accessed 10 September 2020].

Woodward, A.M., Göhler, T., Luciani, M.G., Oehlmann, M., Ge, X., Gartner, A., Jackson, D.A. and Blow, J.J. (2006). Excess Mcm2-7 license dormant origins of replication that can be used under conditions of replicative stress. *The Journal of Cell Biology*, 173 (5), 673–83. Available from <https://doi.org/10.1083/jcb.200602108> [Accessed 16 August 2020].

Worthington, M.T., Pelo, J.W., Sachedina, M.A., Applegate, J.L., Arseneau, K.O. and Pizarro, T.T. (2002). RNA Binding Properties of the AU-rich Element-binding Recombinant Nup475/TIS11/Tristetraprolin Protein. *Journal of Biological Chemistry*, 277(50), 48558-64. Available from <https://doi.org/10.1074/jbc.M206505200> [Accessed 22 July 2020].

Wu, X., Scott, D.A., Kriz, A.J., Chiu, A.C., Hsu, P.D., Dadon, D.B., Cheng, A.W., Trevino, A.E., Konermann, S., Chen, S., Jaenisch, R., Zhang, F. and Sharp, P.A. (2014). Genome-wide binding of the CRISPR endonuclease Cas9 in mammalian cells. *Nature Biotechnology*, 32 (7), 670–6. Available from <https://doi.org/10.1038/nbt.2889> [Accessed 11 September 2020].

Wyman, C. and Kanaar, R. (2006). DNA double-strand break repair: all's well that ends well. *Annual Review of Genetics*, 40, 363–83. Available from <https://doi.org/10.1146/annurev.genet.40.110405.090451> [Accessed 11 September 2020].

Xu, B., Sun, Z., Liu, Z., Guo, H., Liu, Q., Jiang, H., Zou, Y., Gong, Y., Tischfield, J.A. and Shao, C. (2011a). Replication stress induces micronuclei comprising of aggregated DNA double-strand breaks. *PLoS ONE*, 6 (4), e18618. Available from <https://doi.org/10.1371/journal.pone.0018618> [Accessed 13 June 2020].

Xu, L., Ning, H., Gu, L., Wang, Q., Lu, W., Peng, H., Cui, W., Ying, B., Ross, C.R., Wilson, G.M., Wei, L., Wold, W.S.M., Liu, J., Xu, L., Ning, H., Gu, L., Wang, Q., Lu,

W., Peng, H., Cui, W., Ying, B., Ross, C.R., Wilson, G.M., Wei, L., Wold, W.S.M. and Liu, J. (2015). Tristetraprolin induces cell cycle arrest in breast tumor cells through targeting AP-1/c-Jun and NF- κ B pathway. *Oncotarget*, 6 (39), 41679–41691. Available from <https://doi.org/10.18632/oncotarget.6149> [Accessed 9 August 2020].

Yamamoto, N., Jiang, P., Yang, M., Xu, M., Yamauchi, K., Tsuchiya, H., Tomita, K., Wahl, G.M., Moossa, A.R. and Hoffman, R.M. (2004). Cancer Research. *Cancer Res.*, 50 (9), 2808–2817. Available from <https://doi.org/10.1158/0008-5472.can-04-0643> [Accessed 29 December 2020].

Yang, B., Kang, H., Fung, A., Zhao, H., Wang, T. and Ma, D. (2014). The Role of Interleukin 17 in Tumour Proliferation, Angiogenesis, and Metastasis. *Mediators Inflammation*, 2014, 623759. Available from <https://doi.org/10.1155/2014/623759> [Accessed 9 August 2020].

Yang, H., Li, Q., Fan, J., Holloman, W.K. and Pavletich, N.P. (2005). The BRCA2 homologue Brh2 nucleates RAD51 filament formation at a dsDNA-ssDNA junction. *Nature*, 433 (7026), 653–7. Available from <https://doi.org/10.1038/nature03234> [Accessed 21 August 2020].

Yoon, N.A., Jo, H.G., Lee, U.H., Park, J.H., Yoon, J.E., Ryu, J., Kang, S.S., Min, Y.J., Ju, S.-A., Seo, E.H., Huh, I.Y., Lee, B.J., Park, J.W., Cho, W.J., Yoon, N.A., Jo, H.G., Lee, U.H., Park, J.H., Yoon, J.E., Ryu, J., Kang, S.S., Min, Y.J., Ju, S.-A., Seo, E.H., Huh, I.Y., Lee, B.J., Park, J.W. and Cho, W.J. (2016). Tristetraprolin suppresses the EMT through the down-regulation of Twist1 and Snail1 in cancer cells. *Oncotarget*, 7 (8), 8931–8943. Available from <https://doi.org/10.18632/oncotarget.7094> [Accessed 11 August 2020].

Youn, J.-Y., Dunham, W.H., Hong, S.J., Knight, J.D.R., Bashkurov, M., Chen, G.I., Bagci, H., Rathod, B., MacLeod, G., Eng, S.W.M., Angers, S., Morris, Q., Fabian, M., Côté, J.-F. and Gingras, A.-C. (2018). High-Density Proximity Mapping Reveals the Subcellular Organization of mRNA-Associated Granules and Bodies. *Molecular Cell*, 69 (3), 517-532.e11. Available from <https://doi.org/10.1016/j.molcel.2017.12.020> [Accessed 26 July 2020].

Young, L.E., Sanduja, S., Bemis-Standoli, K., Pena, E.A., Price, R.L. and Dixon, D.A.

(2009). The mRNA binding proteins HuR and tristetraprolin regulate cyclooxygenase 2 expression during colon carcinogenesis. *Gastroenterology*, 136 (5), 1669–79. Available from <https://doi.org/10.1053/j.gastro.2009.01.010> [Accessed 4 September 2020].

Yuan, J., Krämer, A., Matthes, Y., Yan, R., Spänkuch, B., Gätje, R., Knecht, R., Kaufmann, M. and Strebhardt, K. (2006). Stable gene silencing of cyclin B1 in tumor cells increases susceptibility to taxol and leads to growth arrest in vivo. *Oncogene*, 25 (12), 1753–62. Available from <https://doi.org/10.1038/sj.onc.1209202> [Accessed 30 July 2020].

Zekavati, A., Nasir, A., Alcaraz, A., Aldrovandi, M., Marsh, P., Norton, J.D. and Murphy, J.J. (2014). Post-transcriptional regulation of BCL2 mRNA by the RNA-binding protein ZFP36L1 in malignant B cells. *PLoS One*, 9 (7). e102625. Available from <https://doi.org/10.1371/journal.pone.0102625>.

Zeman, M.K. and Cimprich, K.A. (2014). Causes and consequences of replication stress. *Nature Cell Biology*, 16(1), 2-9. Available from <https://doi.org/10.1038/ncb2897> [Accessed 10 June 2020].

Zhang, J., Cho, S.-J., Shu, L., Yan, W., Guerrero, T., Kent, M., Skorpinski, K., Chen, H. and Chen, X. (2011). Translational repression of p53 by RNPC1, a p53 target overexpressed in lymphomas. *Genes & Development*, 25 (14), 1528–43. Available from <https://doi.org/10.1101/gad.2069311> [Accessed 23 August 2020].

Zhang, N., Kaur, R., Akhter, S. and Legerski, R.J. (2009). Cdc5L interacts with ATR and is required for the S-phase cell-cycle checkpoint. *EMBO Reports*, 10 (9), 1029–35. Available from <https://doi.org/10.1038/embor.2009.122> [Accessed 24 August 2020].

Zhao, W., Liu, M., D'Silva, N.J. and Kirkwood, K.L. (2011). Tristetraprolin regulates interleukin-6 expression through p38 MAPK-dependent affinity changes with mRNA 3' untranslated region. *Journal of Interferon & Cytokine research : the official journal of the International Society for Interferon and Cytokine Research*, 31 (8), 629–37. Available from <https://doi.org/10.1089/jir.2010.0154> [Accessed 5 August 2020].

Zou, L. and Elledge, S.J. (2003). Sensing DNA damage through ATRIP recognition of RPA-ssDNA complexes. *Science*, 300 (5625), 1542–8. Available from <https://doi.org/10.1126/science.1083430> [Accessed 16 August 2020].

Zou, Y., Liu, Y., Wu, X. and Shell, S.M. (2006). Functions of human replication protein A (RPA): from DNA replication to DNA damage and stress responses. *Journal of Cellular Physiology*, 208 (2), 267–73. Available from <https://doi.org/10.1002/jcp.20622> [Accessed 8 June 2020].